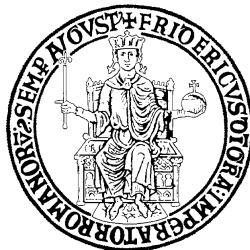# UNIVERSITY OF NAPOLI FEDERICO II

Doctorate School in Molecular Medicine

Doctorate Program in
Genetics and Molecular Medicine
Coordinator: Prof. Lucio Nitsch
XXVII Cycle

"Characterization of Twist1 transcriptional targets in thyroid cancer cells"

Francesca Maria Orlandella

Napoli 2015

"Characterization of Twist1 transcriptional targets in thyroid cancer cells"

TABLE OF CONTENTS

LIST OF PUBLICATIONS

This dissertation is based upon the following publications:

I. Di Maro G, **Orlandella FM**, Bencivenga TC, Salerno P, Ugolini C, Basolo F, Maestro R, Salvatore G. Identification of targets of Twist1 transcription factor in thyroid cancer cells. J Clin Endocrinol Metab. 2014 Sep;99(9):E1617-26. doi: 10.1210/jc.2013-3799. Epub 2014 May 21. PubMed PMID: 24848707.

II. Di Maro G, Salerno P, Unger K, **Orlandella FM**, Monaco M, Chiappetta G, Thomas G, Oczko-Wojciechowska M, Masullo M, Jarzab B, Santoro M, Salvatore G. Anterior gradient protein 2 promotes survival, migration and invasion of papillary thyroid carcinoma cells. Mol Cancer. 2014 Jun 30;13:160. doi: 10.1186/1476-4598-13-160. PubMed PMID: 24976026; PubMed Central PMCID: PMC4094684.

III. **Orlandella FM** et al. Twist1-miR-584-TUSC2 pathway protects thyroid cancer cells from apoptosis. (Manuscript in preparation).

ABBREVIATIONS

AKT	v-akt murine thymoma viral oncogene
ALK	Anaplastic lymphoma kinase
ATC	Anaplastic thyroid carcinoma
bHLH	Basic helix-loop-helix
BRAF	B-type RAF
CBP	CREB-binding protein
CCDC6	Coiled-coil domain containing gene 6
CREB	cAMP-response element binding protein
CTNNB1	Catenin Beta 1 (cadherin-associated protein)
DMEM	Dulbecco's modified Eagle's medium
DMSO	Dimethyl sulfoxide
dNTPs	Deoxyribonucleoside triphosphates
ECM	Extracellular matrix
EGFR	Epidermal growth factor receptor
EMT	Epithelial mesenchymal transition
FBS	Fetal bovine serum
FDA	Food and drug administration
FNA	Fine needle aspiration
FTC	Follicular thyroid carcinoma
GDNF	Glial-derived neurotrophic factor
GFRα	GDNF family receptor alpha
HDAC	Histone deacetylases
IC_{50}	50% growth-inhibitory concentration
IDH1	Isocitrate dehydrogenase 1
mAb	Monoclonal antibodies
MAPK	Mitogen-activated protein kinase
miRNA	MicroRNA
mRNA	RNA messenger
NcoA4	Nuclear receptor co-activator gene 4
NF-Kb	Nuclear factor-kappaB
NLS	Nuclear localization signal
NT	Normal thyroid
NTRK1	Neurotrophic tyrosine kinase receptor type 1
PCAF	P300/CBP associated factor
PDC	Poorly differentiated carcinoma
PI3KCA	Phosphatidylinositol-3 kinase catalytic domain
PPARγ	Peroxisome proliferation activated receptor
PTC	Papillary thyroid carcinoma
PTEN	Phosphatase and tensin homolog
RAI	Radioactive iodine therapy
RET	Rearranged during transfection
RTK	Tyrosine kinase receptors

SCS	Saethre-Chotzen syndrome
siRNA	Small interference RNA
TAM	Tumor associated macrophages
TCGA	The Cancer Genome Atlas
TERT	Telomerase Reverse Transcriptase
TSP-1	Thrombospondin-1
UTR	Untranslated regions
WHO	World Health Organization
WT	Wild type

ABSTRACT

Follicular cell derived thyroid carcinoma comprise a heterogeneous group of cancers with different clinical and morphological characteristics. Anaplastic thyroid carcinomas (ATC) represent less than 5% of all thyroid cancers but are responsible for more than 50% of thyroid cancer mortality, with a mean survival time from diagnosis of ~3–6 months. ATC is characterized by local invasion, distant metastasis, chemo and radio-resistance. We showed that ~ 50% of ATCs up-regulated Twist1 with respect to normal thyroids as well as to poorly and well-differentiated thyroid carcinomas. Twist1 is a highly conserved basic helix-loop-helix transcription factor that plays an important role in the development and progression of human cancer. Knockdown of Twist1 by RNA interference in ATC cells reduced cell migration and invasion and increased sensitivity to apoptosis. The ectopic expression of Twist1 in papillary thyroid carcinoma cells (TPC) induced resistance to apoptosis and increased cell migration and invasion.

In this dissertation, we have investigated the molecular mechanisms by which Twist1 exerts its biological effect in thyroid cancer cells. To this aim, we analyzed gene expression profiles of thyroid cancer cells ectopically expressing Twist1 in comparison to vector control cells. According to gene expression profile, the top functions enriched in TPC-Twist1 cells were: cellular movement, cellular growth and proliferation, cell death and survival. Silencing of the top ten up-regulated genes reduced viability of TPC-Twist1 and CAL62 cells. Silencing of COL1A1, KRT7, PDZK1 induced also cell death. Silencing of HS6ST2, THRB, ID4, RHOB, and PDZK1IP, also impaired migration and invasion of TPC-Twist1 cells. Chromatin immunoprecipitation showed that Twist1 directly binds the promoter of the ten up-regulated genes. q-RT-PCR on thyroid cancer samples showed that HS6ST2, COL1A1, F2RL1, LEPREL1, PDZK1 and PDZK1IP1 are over-expressed in thyroid carcinoma samples compared to normal thyroids.

More recently we have conducted a miRNome expression profile of TPC-Twist1 cells in comparison to control. We identified a set of miRNA potentially regulated by Twist1. We then focused on miR-584 up-regulated by Twist1 in TPC cells. We showed that miR-584 is up-regulated in ATCs respect to normal thyroids and papillary thyroid carcinomas. The ectopic expression of miR-584 protected TPC cells from apoptosis induced by Doxorubicin and Staurosporine. Finally, we showed that miR-584 targets TUSC2 (tumor suppressor candidate 2).

Thus, we have identified a set of mRNA and miRNA that mediates Twist1 biological effects in thyroid cancer cells. Transcription factors as Twist1 are generally believed to be difficult to target due to nuclear localization and lack of a specific groove for tight binding of a small molecule inhibitor. Thus, downstream targets of Twist1 could be more realistic for therapeutic intervention.

1. BACKGROUND

1.1 Thyroid tumors

1.1.1 Morphological and clinical features of follicular cell derived thyroid tumors

Thyroid cancer is a common type of endocrine malignancy and its incidence has been steadily increasing worldwide (Jung et al. 2014). The enhanced incidence is limited to the papillary type of thyroid cancer (Pellegriti et al. 2013) and it is believed to result from increased access to high-resolution imaging (particularly ultrasonography) and increased use of fine needle aspiration (FNA) biopsy of small nodules, as well as progressively decreasing stringency of histopathologic criteria applied to the diagnosis of papillary cancer during the past 10-15 years (Howlader et al. 2012).

There are several histological types and subtypes of thyroid cancer with different cellular origins, characteristics and prognoses. The vast majority of thyroid tumors arise from thyroid follicular epithelial cells, whereas ~3-5% of cancers originate from parafollicular or C cells (Xing 2013). The follicular cell-derived cancers (~95% of cases) are further subdivided into well-differentiated papillary (PTC) carcinoma and follicular carcinoma (FTC), poorly differentiated carcinoma (PDC) and anaplastic (undifferentiated) carcinoma (ATC). Less-differentiated thyroid cancers (PDC and ATC) can develop *de novo* or through a stepwise dedifferentiation of papillary and follicular carcinomas (Figure 1) (Pitoia et al. 2013).
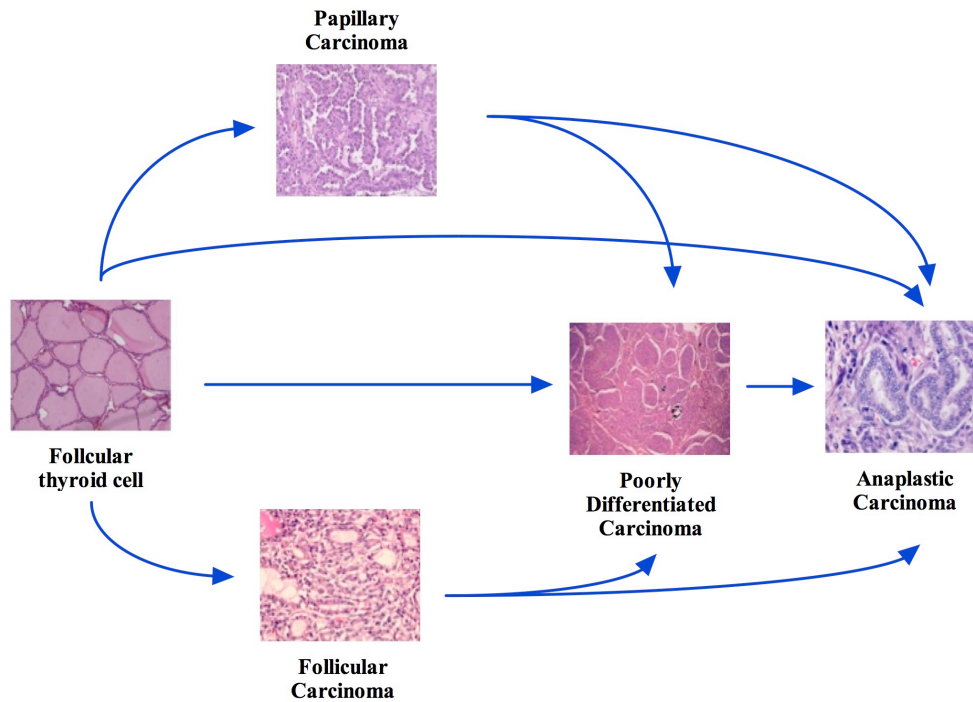
Figure 1. Model of thyroid multi-step carcinogenesis. Scheme of step-wise dedifferentiation of follicular cell-derived thyroid carcinoma with underlined main histological features.

PTCs comprise ~75-85% of all thyroid cancers and represent the most common pediatric thyroid malignancy. Most PTCs in adults occur in patients between 20 and 50 year of age and it is more frequent in women than men (Nikiforov and Nikiforova 2011). Multifocality, lymphatic or local spreading and lymph node metastases are frequent features of PTC whereas distant metastases are relatively uncommon (Omur and Baran 2014). The overall 5 and 10-year survival rates of PTCs are ~98% and 95%, respectively (Jemal et al. 2010). Current treatment involves surgery and radioactive iodine (RAI) therapy (which exploits thyroid follicular cells' avidity for iodine) (Gruber et al. 2015).

FTC is second most common thyroid malignancy and accounts for ~10–15% of thyroid cancer. It mostly affects 40-60 years old patients and it is rare in children (Kondo et al. 2006). FTCs are defined by the World Health Organization (WHO) as malignant epithelial tumors with evidence of follicular cell differentiation but lacking the diagnostic nuclear features of PTC (Najafian et al. 2015). Most of the tumors are encapsulated, consequently are characterized by absence of vascular or capsular invasion and propensity for metastasis via the blood stream.

PDCs (~5% of cases), both morphologically and prognostically, occupy

an intermediate position between differentiated (follicular and papillary) and undifferentiated thyroid carcinomas (Patel et al. 2014). In addition to nodal metastases, patients may also present evidence of distant metastatic disease. Diagnostic criteria for PDC include the presence of a solid-trabecular-insular pattern of growth, absence of the nuclear features typical of PTC and the presence of at least one of these features: convoluted nuclei, high mitotic rate, and tumor necrosis (Volante et al. 2010) (Figure 1).

ATC constitutes less than 5% of thyroid malignancies but it accounts for more than half of the deaths for thyroid cancer, with a mortality rate that is over 90% and a mean survival of ~3-6 months after the diagnosis (Smallridge 2012). ATC is defined by the WHO as a highly malignant tumor completely or partially composed of undifferentiated cells that retain features indicative of an epithelial origin. It usually affects elderly people, with a mean age in the mid-70s and shows a female predominance (Ragazzi et al. 2014). All ATCs are considered stage IV, indeed, ~20–50% of patients present with distant metastases, most often pulmonary, and another 25% develop new metastasis during the rapid course of the disease (Nucera et al. 2011). Benefits obtained from chemotherapy and radiation therapy remain only marginal and there are no alternative treatments yet (Deshpande et al. 2013). The histological categories of these tumors are sarcomatoid and epithelioid-squamoid. Common features to all patterns of ATC are hypercellularity, large foci of necrosis, marked invasiveness, and angiotropism with a tendency to infiltrate medium-sized veins and arteries, replacing their muscular wall. ATCs with sarcomatoid appearance are characterized by spindle cells and giant cells and are the most frequent patterns seen in ATC. In fact, spindle and giant cells have been found, alone or in combination, in ~50% of cases. On the contrary, ATCs with epithelioid-squamoid appearance are histologically less heterogeneous than sarcomatoid tumors. They are characterized by polygonal cells with a clearly epithelial appearance, growing in solid nests, intermingled by desmoplastic stroma. On the other hand, ATC tissues contain tumor-associated macrophages (TAM), which may represent up to 50% of the nucleated cells and show elongated thin ramified cytoplasmic extensions (Hèbrant et al. 2014). A relationship between the increased densities of TAM type M2 and decreased survival was reported in thyroid cancer patients (Caillou et al. 2011).

1.1.2 Genetic alterations in follicular cell derived thyroid tumors

Similar to other cancer types, thyroid cancer initiation and progression occurs through a gradual accumulation of various genetic and epigenetic alterations, including activating and inactivating somatic mutation, alteration in gene expression patterns, microRNA (miRNA) deregulation and aberrant gene methylation (Nikiforov and Nikiforova 2011) (Table 1).

Table 1- Types of follicular cell derived thyroid cancer and their mutational profiles (modified from Nikiforov and Nikiforova 2011).

Characteristics	PTC	FTC	PDC	ATC
Prevalence (%)	~75-85	~10-15	~5	<5
Typical route of spread	Local lymph-node metastases	Hematogenous metastases (to bone and lung)	Invasive local growth, lymph-node and hematogenous metastases	Invasive local growth, lymph-node and hematogenous metastases
10-year survival rate (%)	~95-98	~90-95	~50	< 10
Common mutations (prevalence, %)	BRAF (> 60) RAS (~ 13) RET/PTC (~ 7) NTRK (~ 1) TERT (< 9) IDH1 (~ 20)	RAS (~ 30-45) PAX8/PPARγ (~ 30-45) PIK3CA (~ 5-15) PTEN (< 10)	RAS (~ 20-40) TP53 (~ 20-30) BRAF (~ 10-20) CTNNB1 (~ 25) PIK3CA (~ 5-10) AKT1 (~ 5-10)	TP53 (~ 70-80) CTNNB1 (~ 60-65) RAS (~ 20-30) BRAF (~ 20-40) PIK3CA (~ 15-25) PTEN (~ 10-20) AKT1 (~ 5-10) IDH1 (~ 10-30) ALK (~ 10)

Genetic alterations in PTC

Most mutations in PTC involve members of the mitogen-activated protein kinase (MAPK) pathway: the tyrosine kinase receptor RET (REarranged during Transfection), NTRK1 (neurotrophic receptor-tyrosine kinase) and intracellular signal transducers BRAF and RAS (Table 1) (Kondo et al. 2006). These mutations are typically mutually exclusive, occur in ~70% of PTC cases and are associated with particular clinical, histopatological and biological characteristics.

The RET proto-oncogene, which is located on chromosome 10q11.2, was first identified in 1985 (Takahashi et al. 1985). It encodes a tyrosine kinase receptor consisting of an extracellular domain with a ligand binding site, a transmembrane domain and an intracellular tyrosine kinase domain. RET is activated by interaction with a multicomponent complex that includes a soluble ligand family, the glial cell line-derived neurotrotrophic factors (GDNF). Ligand binding results in receptor dimerization leading to autophosphorylation

of the protein on tyrosine residues and initiation of the signaling cascade. RET-PTC is a chromosomal rearrangement found in PTC and occurs as a consequence of genetic recombination between the tyrosine kinase domain of the RET gene located on the 3' and 5'terminal of various partner genes (Santoro et al. 1994). The rearrangement results in ligand independent dimerization and constitutive tyrosine kinase activity of RET which leads to chronic stimulation of MAPK signaling. Based on the partner genes, at least ten different types of RET/PTC rearrangements have been identified. Of these, the most common types in PTC are RET/PTC1 and RET/PTC3. The partner genes for RET/PTC1 and RET/PTC3 are the coiled-coil domains containing gene 6 (CCDC6) and the nuclear receptor co-activator gene 4 (NcoA4) respectively (Santoro et al. 2000). RET rearrangements are found in ~10-20% of PTCs; in particular, RET/PTC1 is more frequently associated with classic PTCs and with the diffuse sclerosing variant; conversely, RET/PTC3 is more common in the solid variant and in PTCs associated to ionizing radiations (Thomas et al. 1999).

Chromosomal rearrangements involving another neurotrophic tyrosine kinase receptor (NTRK1) also occur in PTC. The NTRK1 gene resides on chromosome 1q22 and can be fused to at least three different partner genes located on the same or different chromosomes (Miranda et al. 1994). The prevalence of NTRK rearrangements is ~3-5% of PTC (Greco et al. 2004).

Point mutations in H-RAS, K-RAS, and N-RAS are uncommon in classic papillary thyroid carcinomas with an overall frequency of less than 10% (Cancer Genome Atlas Research Network 2014).

BRAF, a member of the RAF protein family (ARAF, BRAF, CRAF), is a serine threonine-kinase. There is a direct association between BRAF mutation and aggressive clinical outcomes such as invasion, metastasis and relapse of PTC. Several studies demonstrated a close association between BRAF mutation and dedifferentiation of PTC (Holderfield et al. 2014). In thyroid cancer, BRAF can be activated by point mutations, small in-frame deletions or insertions or by chromosomal rearrangement. The most common oncogenic mutation in BRAF is thymine to adenine transversion at position 1799 (T1799A) resulting in the substitution of valine by glutamate at residue 600 (V600E) (Soares et al. 2003). This mutation causes constitutive activation of BRAF kinase and induction of the MAPK signaling pathway. In small percentages of PTC, K601E point mutation and small deletions or insertion around codon 600 are also observed (Murugan et al. 2011). BRAF mutations are uncommon in radiation-induced PTCs; however, Ciampi and coworkers have reported a rearrangement via paracentric inversion of chromosome 7q resulting in AKAP9-BRAF fusion (Ciampi et al. 2005).

Single nucleotide change in the promoter region of TERT are found in ~9% of PTC. The change generate de novo consensus binding motifs for MAPK-dependent ETS (E-twenty-six) transcription factors and is strongly associated with an increased risk of mortality (Melo et al. 2015).

Novel fusions, including PAX8/PPARγ, ETV6/NTRK3 and

RBPMS/NTRK3 rearrangements, were discovered with low frequency in classical PTC. These fusions are more prevalent in radiation-induced thyroid cancers but have lower prevalence in sporadic PTC (Ricarte-Filho et al. 2013).

Recently, The Cancer Genome Atlas (TCGA) has deposited the analysis results of ~500 thyroid cancer genomes only from PTC patients. These analyses provide a more detailed, multidimensional genomic characterization of thyroid cancer genomes. The TCGA identified novel driver alterations including EIF1AX, PPM1D and CHEK2 in PTC. The EIF1AX gene codes for a protein that is required for the transfer of methionyl-tRNA molecules to ribosomes in order to initiate protein translation. Mutations in EIF1AX, that in most cases target the N-terminal domain of the protein, as occur in PTC, have been previously reported in other tumors (Martin et al. 2013). Newly identified mutations in PPM1D, CHEK2, as well as genes that encode for components of the DNA-damage response pathway, were enriched in samples from patients with high risk PTC and occurred concomitantly with MAPK driver mutations (Cancer Genome Atlas Research Network 2014).

Genetic alterations in FTC

FTCs may develop trough at least two different pathways involving RAS or PPARγ (peroxisome proliferation activated receptor). Mutations in RAS gene family have been detected in up to 50% of follicular adenomas and carcinomas. Nikiforova and coworkers reported that among RAS-positive carcinomas, N-RAS codon 61 mutation is the most common in FTC (Nikiforova 2003). PAX8/ PPARγ rearrangement leads to the fusion between a portion of the PAX8 gene, which encodes a paired domain transcription factor, and the PPARγ gene. The fusion results in strong over-expression of the chimeric PAX8/PPARγ protein. RAS mutations and PAX8/PPARγ rearrangements represent distinct pathogenetic pathways in the development of follicular thyroid carcinomas (Eberhardt et al. 2010).

Genetic alterations in PDC

PDCs have genetic features intermediate between well-differentiated and ATC consistent with the hypothesis of a multi-step model of thyroid carcinogenesis (Tallini 2011) (Figure 1). Similar to well-differentiated thyroid carcinomas, RAS point mutations occur in ~20-40% of PDCs (Volante et al. 2010). Similar to ATC, PDC features in some cases mutations in exon 5-9 of TP53 (~20-30%) or in PIK3CA and its downstream effector AKT or point mutation in exon 3 of CTNNB1 (Catenin-cadherin-associated protein Beta 1) (Ricarte-Filho et al. 2013). Approximately 10-20% of PDC harbor BRAF mutation, particularly those samples with morphological evidence of pre-existing PTC (Begum et al. 2004). A small number of PDC express rearranged tyrosine kinase genes such as RET/PTC or NTRK1, however there is no association with unfavorable clinico-pathological features or decreased

survival (Santoro et al. 2006) (Table 1).

Genetic alterations in ATC

To date, a considerable number of genetic mutations have been identified in ATC (Lee et al. 2013).

Mutations in the components of the principal oncogenic pathways (i.e. MAPK, PI3K, WNT) have been described to occur with high frequency in ATC. RAS mutations are detected in ATCs, with variable frequency ranging from ~20 to 40% of cases (Ragazzi et al. 2014). RAS mutations correlate with aggressiveness and/or poor prognosis (Milosevic et al. 2014). In contrast, RET/PTC rearrangements are rarely found in ATCs (Lee et al. 2013). The BRAF V600E mutation occurs in ~38% of ATC (Vanden Borre et al. 2014), and recent reports indicate that BRAF V600E alters ATC tumor microenvironment through extracellular matrix (ECM) protein such as thrombospondin-1 (TSP-1) and ECM receptors (ie, integrins) (Duquette et al. 2013; Gandolfi et al. 2014).

Gain of function mutations in the PIK3CA (phosphatidylinositol-4, 5-bisphosphate 3-kinase, catalytic subunit alpha) gene are also common in ATC (Charles et al. 2014). Amplification of the PIK3CA genomic locus in 3q26.3 is found in ~40% of ATC suggesting that alteration of the PI3K pathway plays a pivotal role in the pathogenesis of ATCs (Xing 2013). Importantly, the over-activation of the PI3K-AKT pathway can be induced by PTEN inactivation, including PTEN promoter methylation, deletion, or point mutations that occur in ~10–20% of ATC (Nucera et al. 2011).

Somatic mutations in the promoter of the TERT (Telomerase Reverse Transcriptase) gene have been described as highly recurrent in different types of cancer including ATC (Shi et al. 2015). Intriguingly, TERT promoter mutations seem to occur prevalently in those tumors harboring mutated BRAF or RAS, suggesting that TERT alteration is acquired later during tumor development and may provide a functional advance to BRAF or RAS driven tumors by enabling acquisition of additional genetic defects leading to disease progression (Liu et al. 2014).

WNT pathway appears also to play a relevant function in ATC development. Mutations in CTNNB1 gene leading to a constitutively active WNT-signaling have been reported in ~25–60% of ATCs (Kunstman et al. 2015). CTNNB1 is a major component of the E-cadherin cell-cell adhesion complexes and a role of this protein in the epithelial-mesenchymal transition process has been demonstrated (Lamouille et al. 2014).

Although the mutation prevalence is not high, mutations in the gene for isocitrate dehydrogenase 1 (IDH1) have been recently identified in ATC (Hemerly et al. 2010) (Table 1).

In ~11% of ATC patients, a mutation in anaplastic lymphoma kinase (ALK), a tyrosine kinase receptor involved with the activation of both the MAPK and PI3K-AKT pathways, is observed. Specifically, two point

mutations have been identified (ALK L1198F and ALK G1201E) that result in increased tyrosine kinase activity (Murugan and Xing, 2011). Also several rearrangements involving ALK gene were found in ATC. The most common of these involves a fusion between ALK and the striatin (STRN) gene, which is the result of a complex rearrangement involving the short arm of chromosome 2. STRN-ALK leads to constitutive activation of ALK kinase, which is able to transform cells in vitro and to induce tumor formation in nude mice. In addition STRN-ALK did not overlap with other known driver mutations in these tumors (Kelly et al. 2014).

Recently, several novel mutations not previously described in ATC were observed including mTOR, NF1 or ERBB2; some of these are particularly intriguing because have been targeted previously by pharmaceuticals currently in clinical or experimental use (Kunstman et al. 2015).

More than 50% of ATCs have been reported to carry loss of function mutations in the p53 gene. As well, the over-expression of p53, which may reflect altered function of the protein in the absence of mutation, has been frequently observed in ATC (Pita et al 2014).

ATCs are characterized by a higher number of chromosomal alterations with respect to well-differentiated and poorly differentiated thyroid cancer. Liu and colleagues observed that genes coding for tyrosine kinase receptors (RTK) like EGFR, PDGFR, VEGFR, KIT, and MET are frequently amplified in thyroid cancer and in particular in the ATC histotype (Liu et al. 2008). Many of the genes with copy number gains are known to be proto-oncogenes so that they may be play an important role in ATC tumorigenesis.

Wreesman and colleagues observed several chromosomal abnormalities that were common to both well-differentiated and undifferentiated thyroid cancer (like gain of 5p15, 5q11– 13, 19p, and 19q and loss of 8p) and that could represent early event in the genesis of these tumors. Furthermore, they found alterations like gain in 3p13-14, loss of 5q11– 31, and gain in 11q13 that were exclusive of the genome of ATC and that may represent late genetic events driving the transformation of a preexisting thyroid cancer into the aggressive ATC histotype (Wreesman et al. 2002).

Intriguingly, the chromosomal regions affected by the alterations were extremely heterogeneous, suggesting the existence of a high-grade genetic inter-neoplastic diversity in ATC (Ragazzi et al. 2014). This observation implies that the high-grade genomic instability in ATCs is a side effect of the loss of restraining mechanisms of cell proliferation rather than being the cause of tumor progression. Indeed, a number of mitotic proteins involved in cell cycle checkpoints or engaged in chromosome assembly and segregation are deranged in ATCs (Isham et al. 2013; Pita et al. 2014). These include the three members of the Aurora kinase family. Aurora kinases are implicated in several aspects of chromosome segregation and cytokinesis. Expression of all Aurora kinases, in particular of Aurora A, is strongly induced in ATC cells and its over-expression induces centrosome amplification and increases the oncogenic function of RAS (Tatsuka et al. 2005). Moreover, evidences exist of a negative

cross-talk between Aurora A kinase and p53 (Liu et al. 2004). Inhibitors of Aurora kinases, alone or in combination with other drugs, showed an important anticancer effect in preclinical models of ATCs indicating this approach as a possible therapeutic strategy for ATCs treatment (Baldini et al. 2014; Granata et al. 2013).

Epigenetic changes of tumor-associated genes have been found in ATC. Schagdarsurengin and colleagues analyzed the methylation pattern of 17 gene promoters in ATC, included those involved in DNA damage avoidance and repair (MGMT, GSTP1), apoptosis (DAPK, UCHL1), cell cycle control (p16, RB), and regulation of thyrocyte function and growth (TSHR). Among these genes, they found that TSHR, MGMT, UCHL1, p16, and DAPK were frequently methylated in ATC (Schagdarsurengin et al. 2006).

PTEN methylation was found in ATC and was closely associated with the activating mutations in the PI3K/AKT pathway (Milosevic et al. 2014) (Table1).

Additionally, Rodríguez-Rodero and colleagues observed that four oncogenes (INSL4, DPPA2, TCL1B and NOTCH4) are frequently regulated by hypomethylation in ATC (Rodríguez-Rodero et al. 2013).

EZH2, member of the polycomb family of proteins, is a histone lysine-methyl-transferase and is over-expressed in ATC. EZH2 is essential for the regulation of cell proliferation and differentiation. When EZH2 is over-expressed, histone methylation is altered, silencing the PAX8 gene and leading to an aggressive phenotype (Catalano et al. 2012).

Finally, histone deacetylation plays a role in ATC pathogenesis. Most ATC tumors show over-expression of histone deacetylases (HDACs). Less acetylation of histones leads to an altered expression of proteins involved in the regulation of cell cycle and proliferation (Lin et al. 2013).

1.1.3 Aberrant expression of miRNAs in thyroid cancers

MicroRNAs (miRNA) are small (19–25 nucleotides) noncoding RNA molecules that typically function as negative regulators of the expression of protein-encoding genes (Bartel 2009). miRNAs regulate major processes as development, apoptosis, cell proliferation, immune response, and hematopoiesis; they also may act as tumor suppressor genes and oncogenes (Di Leva et al. 2014). Mature miRNAs regulate gene expression through translational inhibition (accounting for ~16%) or mRNA degradation (accounting for ~84%) by annealing to complementary sequences in mRNA 3'untranslated regions (UTRs) (Djuranovic et al. 2011). Each miRNA is predicted to repress the expression of thousands of mRNAs, and in turn, each mRNA can be targeted by several hundred different miRNAs (Di Leva et al 2014). The production of miRNAs follows a canonical multistep process that starts in the nucleus and ends in the cytoplasm and is composed of three main events: cropping, nuclear export, and dicing (Figure 2) (Shen and Hung 2015).
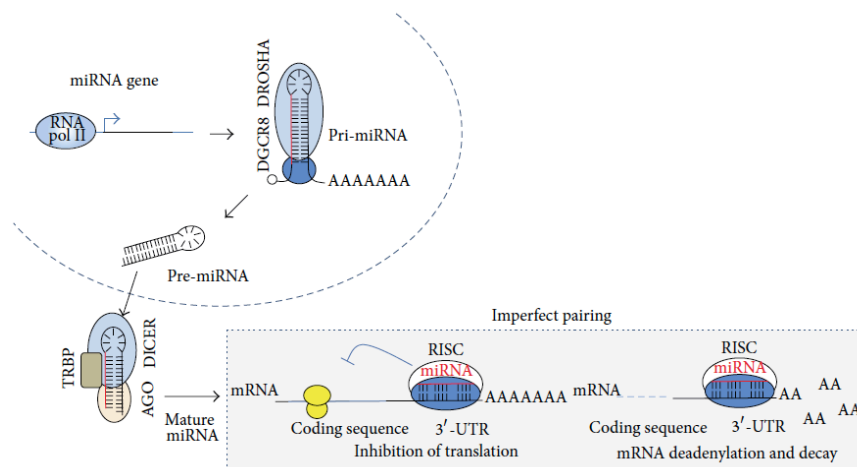
Figure 2: Biogenesis of miRNA. Transcription of miRNA by RNA polymerase II yields a long primary transcript (pri-miRNA) that contains a cap 5' and poly-A tail. The complex DROSHA/DGCR8 cleaves pri-miRNA and gives rise to an miRNA precursor (pre-miRNA) that is exported to the cytoplasm and further processed by DICER endonuclease. A miRNA duplex associates with the RISC complex and retains the mature strand of miRNA. This complex directs imperfect binding to 3'UTR region of target mRNA, leading to a reduction in protein levels via translation blockage and mRNA deadenylation and decay (modified from Di Leva 2014).

Recent data suggests that miRNA deregulation could be a crucial event in thyroid carcinogenesis.

Deregulated expression of several miRNAs in PTC was found to correlate with certain genetic lesions. For example, the expression of miR-187 is enhanced in samples of PTC leading the RET/PTC rearrangement (Nikiforova et al. 2008); also the up-regulation of miR-128a, -128b, -139 and -200a strongly correlates with RET/PTC rearrangement (Cahill et al. 2006). miR -221 and -222 are over-expressed in BRAF-mutated and RAS-mutated PTC. In addition, the miRNA profile is often associated with some clinical features of PTC: a microarray analysis revealed up-regulation of miR-31, -146b -155, -221 and -222 in aggressive versus non-aggressive PTCs (Yip et al. 2011). In particular, deregulated expression of miR-146b, miR-221 and miR-222 may be the crucial component for initiation and development of PTC. The putative target of these miRNAs was suspected to be c-KIT, as a tyrosine kinase receptor that plays an important role in cell growth and differentiation (Yip et al. 2011). Very few miRNAs have been found to be down-regulated in PTC versus normal thyroid tissue. miR-1 is one of the most consistently and drastically down-regulated miRNAs in PTC. Its expression is also decreased in tissue from FTC and ATC, irrespective of the degree of malignancy, suggesting a role of miR-1 down-regulation in early stages of thyroid carcinogenesis. miR-1 targets the chemokine receptor CXCR4 and its ligand CXCL12, and have a critical role in tumor metastasis (Leone et al. 2011). Moreover, miR-1 down-regulation contributes to the EMT by modulating protein levels of the zinc finger protein SNAI2 (also known as SLUG), which is a transcriptional repressor of E-cadherin and a known EMT inducer (Tominaga et al. 2013).

Mancikova and colleagues identified miRNA expression profile specific for follicular thyroid tumors. FTC showed a notable over-expression of several members of miR-515 family, and down-regulation of miR-1247. They also observed the up-regulation of miR-96, -182, and -183 in both follicular adenomas and follicular carcinomas (Mancikova et al. 2015). Recently, the expression level of miR-192, -197, -328 and -346 has been reported to be decreased in FTC compared to normal thyroid. These miRNAs are evidently specifically associated with FTC (Faam et al. 2015).

Specific miRNAs are reduced in thyroid cancer, such as the let-7 family, but other miRNAs, such as the miR-200 and miR- 30 families, are exclusively down-regulated in ATC, indicating that the latter miRNAs may play a role in the acquisition of more aggressive tumor characteristics.

The miR-200 family was recently identified as a suppressor of EMT promoting ZEB degradation and thus suggested to interfere with metastasis by sustaining an epithelial character of tissues. The miR-200 family was found decreased in ATC and the expression of these miRNAs in mesenchymal ATC-derived cells reduced their invasive potential and induced mesenchymal–epithelial transition (MET) by regulating the expression of MET marker proteins (Braun et al. 2010). An important transcriptional activator of miR-200

is p53 (Hermeking et al. 2012).

Down-regulation of the miR-30 family is observed in metastasis compared to the primary tumor suggesting a role in aggressive disease. The group of Hébrant demonstrated, by *in situ* hybridization, aberrant expression of miR-30e in ATC where miR-30 modulated vimentin expression (Hébrant et al. 2014). Furthermore, down-regulation of miR-30 de-represses the expression of EZH2, an important component of the polycomb repressive complex 2 (PRC2) that regulates chromatin condensation and is frequently over-expressed in ATC (Esposito et al. 2012). Another important cellular process regulated by the miR-30 family is autophagy through targeting the key autophagy-promoting protein, Beclin1. In ATC, miR-30d restoration sensitizes cancer cells to cisplatin treatment by repressing Beclin1 (Zhang et al 2014) (Table 2).

Family genes of let-7 are located on different chromosomes and are abundantly expressed in a normal thyroid gland. Deregulation of let-7 is observed in several types of cancer; in particular, in well-differentiated thyroid cancer (PTC and FTC), but a marked decrease in the expression of let-7 family is also observed in ATC (Catalano et al. 2012).

Common miRNAs such as miR-146, -221, -222, and -17-92 are up-regulated in aggressive ATC and in well-differentiated thyroid cancer, indicating that reinforced expression of these miRNAs is important in maintaining the oncogenic process (Table 2).

The miR-17-92 cluster is located on chromosome 13 and transcribes a polycistron that yields seven different mature miRNAs. High levels of miR-17-92 components are expressed in ATC and their inhibition leads to the recovery of PTEN protein levels and resulted in a pronounced apoptosis through activation of caspase-3 and caspase-9 (Takakura et al. 2008). Furthermore, a key target of miR17-5p and miR-17-3p is TIMP-3, an important inhibitor of metalloproteinase activation (Catalano et al. 2012).

miR-146a and -146b are over-expressed in ATC (Pacifico et al. 2010). miR-146a/b are transcribed by two independent genes located on chromosomes 5 and 10, respectively, and either regulated by the transcription factor NF-kB, usually over-activated in ATC. Increased plasma circulating levels of miR-146b can be detected also in PTC before surgery and correlate with tumor aggressiveness and poor prognosis (Lee et al. 2013) (Table 2).

miR-221 and miR-222 over-expression is detected in differentiated (PTC and FTC) (Pallante et al. 2014) and ATC cells (Jikuzono et al. 2013) (Table 2) and it is associated with poor clinical-pathological features of cancer. miR-222 increased circulating plasma level is associated with the presence of the BRAF mutation and recurrent PTC (Lee et al. 2013). Both miR-221 and -222 also influence cell proliferation by targeting the p27kip1 protein, a key regulator of cell cycle progression (Visone et al. 2007). Ectopic expression of miR-221 in cancer cells results in a robust increase in anchorage-independent growth in soft-agar medium (Pallante et al. 2014), pointing to a role for this cluster of miRNAs in the process of invasion and cell migration (Table 2).

Table 2. Validated targets for deregulated miRNAs in ATC.

miRNAs	Validates targets			Cellular processes
Down-regulated miRs	miR-200 family	ZEB1	ZEB2	β-Catenin	EMT and proliferation
	miR-30 family	Beclin1	EZH2	VIM	Autophagy, Chromatin condensation and EMT
	miR-7 family	RAS	HMGA2	LIN28	Proliferation, Histone modification and stemness
	miR-25 family	EZH2	BIM	KLF4	Chromatin condensation and apoptosis
	miR-125 family	MMP1	HMGA2	LIN28A	Invasion, Histone modification and stemness
Up-regulated miRs	miR- 221, -222	P27	RECK	PTEN	Cell cycle, growth, and invasion
	miR-17-92 cluster	P21	TIMP3	PTEN	Cell growth and invasion
	miR -146a; -146b	NF-kB	THRB	SMAD4	Cell differentiation, proliferation, and invasion

1.1.4 Targeted therapy for thyroid carcinomas

The majority of well-differentiated thyroid carcinomas (papillary and follicular) are characterized by good prognosis and good response to surgery and radioiodine therapy. Nevertheless, ~10% of differentiated carcinomas recur and become resistant to all therapies.

The majority of patients with ATC die from aggressive local regional disease, primarily from upper airway respiratory failure. For this reason, aggressive local therapy is indicated in all patients who can tolerate it. Although rarely possible, complete surgical resection gives the best chance of long-term control and improved survival. In fact, surgical de-bulking of local tumor, combined with external beam radiation therapy and chemotherapy as neoadjuvant (before surgery) or adjuvant (after surgery) therapy, may prevent death from local airway obstruction and as best may slight prolong survival (Taccaliti et al. 2012). Investigational clinical trials in phase I or in phase II are actually in running and they include multi-kinase inhibitor, anti-angiogenetic drugs, histone deacetylase and mTOR inhibitors drugs.

Tyrosine-kinase inhibitor. The last decade has seen advances in the understanding of the molecular basis of thyroid cancer, leading to the application of new pharmacological treatments with inhibitors of kinases (Marotta et al. 2013). The BRAF inhibitor vemurafenib (PLX4032) improves survival among patients with metastatic melanoma, and suppresses growth of BRAF-mutated human ATC in a mouse model (Rosove et al. 2013). The beneficial effect of BRAF inhibition in ATC with activating BRAF mutations has been recently reported (Salerno et al. 2010). Sorafenib and Imatinib are a broad-spectrum tyrosine-kinase inhibitor (TKI), that demonstrated an acceptable response rate in pre-treated ATC patients (Thomas et al. 2014; Savvides et al. 2014). Pazopanib, another TKI, similarly to Sorafenib has been tested also in ATC in the context of a phase II trial demonstrating minimal single-agent clinical activity (Bible et al. 2012).

Anti-angiogenetic agents. A common feature of thyroid cancers is their markedly increased vascularization, with an elevated expression of the vascular endothelial growth factor (VEGF) compared with normal thyroid tissue. VEGF levels are correlated with stage, tumor size, extra-thyroidal invasion, and distant metastases (Bauer et al. 2003). On the basis of these findings, several drugs targeting angiogenesis have been evaluated against ATC. Combretastatin A4 (CA4), a vascular disrupting agent which blocks the tumor directed blood flow altering the neovasculature morphology, has shown to produce a trend toward a significant overall survival improvement in ATC patients (Sosa et al. 2012). Axitinib, a VEGFR2 inhibitor, showed therapeutic efficacy only in one of two patients with ATC (Cohen et al. 2014).

Histone deacetylase inhibitors. Histone deacetylase inhibitors are a promising class of antineoplastic agents that induce cell differentiation, cell cycle arrest, and apoptosis through hyperacetylation of histones, with the potential to enhance the cytotoxicity of drugs such as doxorubicin (Smith and

Nucera 2015). Preclinical studies have shown that valproic acid, a potent anti-convulsant agent, is able to enhance the activity of Doxorubicin in cell lines derived from ATC alone or in combination with other drugs (Smith and Nucera 2015).

mTOR inhibitors. More recently inhibition of mTOR has been taken into account for clinical trials (Fury et al. 2013). Everolimus, an inhibitor of the mammalian target of rapamycin (mTOR), is effective in treating tumors harboring alterations in the mTOR pathway. Wagle and colleagues identified potential genomic mechanisms of exquisite sensitivity and acquired resistance to everolimus by performing whole-exome sequencing on the pre-treatment and drug-resistant tumors. Nonsense mutation in TSC2, a negative regulator of mTOR, results in sensitivity to mTOR inhibition in some cancer, whereas the mechanism of acquired resistance to everolimus was identified as a mutation in mTOR that causes resistance to allosteric mTOR inhibition by preventing the binding of the drug to the protein (Wagle et al. 2014).

Nevertheless, the effectively right strategy of therapy may be a multi disciplinary approach based on a radical surgery followed by adjuvant chemo and target therapy and external beam radiotherapy. Early integration of all the available strategy is the only way to face this poor prognosis disease (Perri et al. 2014).

1.2 The transcription factor Twist1

1.2.1 Molecular structures of the Twist1 gene and protein

Little is known about the molecular events that lead from the highly curable differentiated tumors to the very aggressive ATC. Through, a cDNA microarray analysis on different thyroid tumors in comparison to normal thyroids, we have isolated Twist1 transcription factor as a gene up-regulated in ATC (Salvatore et al. 2007).

Twist1 was first identified in *Drosophila* (D-Twist) as a gene involved in the early development of the mesoderm and during gastrulation promoting the N-cadherin expression (Puisieux et al. 2006). *Drosophila* embryos lacking the Twist1 gene failed to gastrulate normally, produced no mesoderm and died at the end of embryogenesis with a 'twisted' appearance. D-Twist is able to form homodimers and does not need to form heterodimers for DNA binding (Šošić et al. 2003).

Two Twist genes exist in vertebrates, well conserved during evolution, Twist1 and Twist2 (formerly Dermo-1). The Twist proteins display a high degree of sequence similarity in their C-terminal portion, including the bHLH and 'Twist-box' domains, but are more divergent in their N-terminal portion. While Twist1 has a glycine-abundant region in the N-terminal side, Twist2 does not have it (Bialek et al. 2004). Once expressed, Twist1 and Twist2 may function either as transcriptional activators or repressors, through both direct and indirect mechanisms. Both proteins have been associated with the differentiation of cells like muscle, cartilage and osteogenic cells. Mutations in Twist2 are associated with the Setleis Syndrome, an inherited developmental disorder characterized by bilateral temporal marks (Tukel et al. 2010). Twist1 gene mutations cause Saethre-Chotzen syndrome (SCS), an autosomal dominant inheritance disease characterized by a broad spectrum of malformations including short stature, craniosynostoses, ptosis (El Ghouzzi et al. 1997).

Human Twist1 gene maps on chromosome 7q21.2 and contains two exons and one intron (Wang et al. 1997). The first exon contains an ATG site followed by an open reading frame encoding 202 amino-acid residues. The open reading frame is followed by a 45-bp untranslated portion in exon 1, a 536-bp intron and a second untranslated exon with two potential polyadenylation sites that are 65 and 415 bp from the 5′ end of exon 2 (Figure 3A).
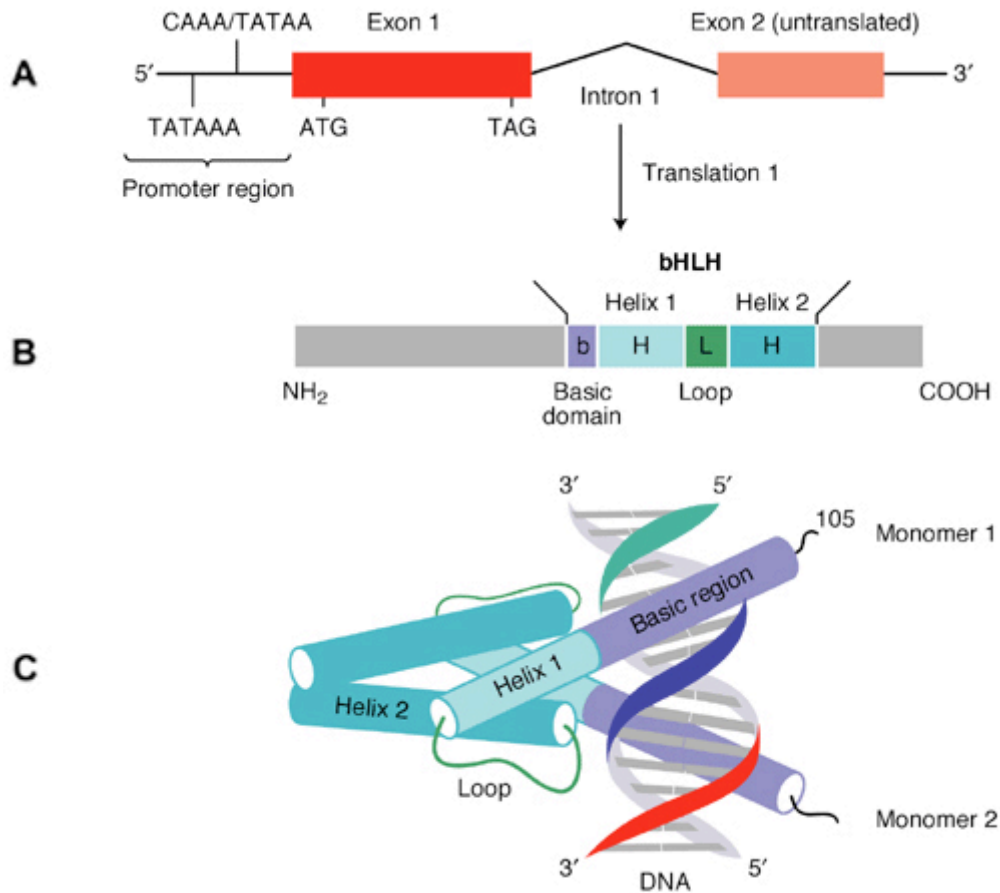
Figure 3. Structure of human Twist1. **A.** The human-Twist1 gene comprises two exons separated by a unique intron. **B.** The human-Twist1 protein is 202 amino acids presenting a basic helix-loop-helix (bHLH) domain. **C.** Interaction of dimers of Twist1 with DNA (modified from Bonaventure and El Ghouzzi 2003).

The molecular mass calculated from the amino-acid sequence of human Twist1 is ~21 kDa, with a theoretical isoelectric point of ~9.6. The protein contains relatively more polar amino-acid residues in the region close to the NH2-terminus and more non-polar residues at the COOH-terminus where the bHLH (basic helix–loop–helix) domain is located (Qin et al. 2012).

Twist1 is a transcription factor that belongs to the bHLH family (Thisse et al. 1987). The bHLH domains of Twist1 show a very high degree of conservation among a broad range of species. Structurally, bHLH proteins are characterized by the presence of a conserved domain containing a stretch of basic amino acids adjacent to two amphipathic α-helices separated by an inter-helical loop (Figure 3B). The α-helices mediate the interaction of this protein with a second bHLH factor, leading to the formation of a dimer that binds to 5'-CANNTG-3' hexanucleotide sequence known as the E-box. The traditional classification categorizes the bHLH family into three subfamilies: class A,

class B and class C (Murre et al. 1989). The proteins in class A, which include E12, E47, HEB, E2-2 and are ubiquitously expressed in mammalian cells. Class B comprises bHLH proteins that have relative specificity in tissue expression and form dimers with class A molecules for binding to E-boxes. Class C molecules, consisting of the Myc proteins, do not form heterodimers with either class A or class B proteins. The Twist family, which has relative tissue specificity and forms heterodimers with E12 and E47, falls into class B (Castanon and Baylies 2002).

Twist box, also known as 'WR motif' (the tryptophan and arginine motif), is located between 20 and 55 amino acids COOH-terminal to the bHLH region and it is highly conserved among vertebrates (Figure 4). It has been demonstrated that the Twist box is required for the transactivation function of Twist1, and genetic mutations in the Twist box domain are associated with SCS of human patients (Puisieux et al. 2006). Recently it was demonstrated that through the Twist box, Twist1 binds and inhibits p53, suggesting that the Twist box is essential for inhibition exerted by Twist1 on other transcription factors (Piccinin et al. 2012).

Twist1 functions as a transcription factor in the cell nucleus. There are two nuclear localization signal (NLS) sequences, 37RKRR40 and 73KRGKK77, in the human Twist1 protein (Figure 3). In the nucleus, N-terminus of Twist1 can interact with p300, cAMP-response element binding protein (CREB), CREB-binding protein (CBP) and p300/CBP associated factor (PCAF) (Figure 3), resulting in inhibition of the acetyltransferase activities of these histone remodeling enzymes (Hamamori et al. 1999). Since histone acetylation is usually coupled with transcriptional activation, the inhibition of p300, CBP and PCAF activities by Twist1 should repress gene expressions. Finally, the C-terminus of Twist1 interacts with the DNA-binding domain of Runx2 to repress Runx2 function (Figure 3). Runx2 is a necessary transcription factor for osteoblast differentiation. These findings suggest that Twist1 may function as transcriptional activators or repressor, through both direct and indirect mechanisms recruiting other transcription factors such as MEF2, MyoD, RUNX1-2, CEBP-a and NF-kB (Figure 3) (Puisieux et al. 2006).

Regulation of protein stability is an important way to control Twist1 function. The most characterized post-translational modification of Twist1 its phosphorylation on serine68 (S68) by p38, JNK and ERK1/2 MAPKs; and this phosphorylation prevents Twist1 protein from ubiquitination-mediated degradation (Hong et al. 2011). In addition, p62 (autophagy adaptor protein) has been shown to bind Twist1 protein and inhibit its degradation; p62-dependent Twist1 stabilization, following autophagy inhibition, promotes tumor cell growth and metastasis (Qiang et al. 2014). Conversely, a recent study has shown that the ectopic expression of death effector domaincontaining DNA-binding protein (DEDD) in metastatic breast cancer cells induces autophagy and increases degradation of Snail and Twist1 through the autophagy-lysosome degradation system (Lv et al. 2012). Twist1 stability is also regulated at the post-trascriptional level through phosphorylation on Ser42

by AKT. AKT phosphorylation of Twist1 Ser42 has also been shown to confer cell death resistance to DNA damage through inhibition of a p53-dependent pathway (Xue et al. 2012).

Among the bHLH proteins, Twist1 proteins are unique in their ability to form functional homo- and heterodimers. Twist1 can heterodimerize with different transcription factors. Partner choice could also be regulated by the phosphorylation state of specific threonine (Thr 125) and serine (Ser 127) residues (TQS motif) that are conserved in the first α-helix of the HLH domain of Twist1 protein. The phosphorylation state is determined by protein kinase A (PKA) and C (PKC) (Firulli et al. 2003). Gajula et al. for the first time described also the requirement of the PI3K-AKT-mTOR pathway for phosphorylation of TQS motif, which is required for the pro-metastatic functions of Twist1 in prostate cancer cells (Gajula et al. 2015).
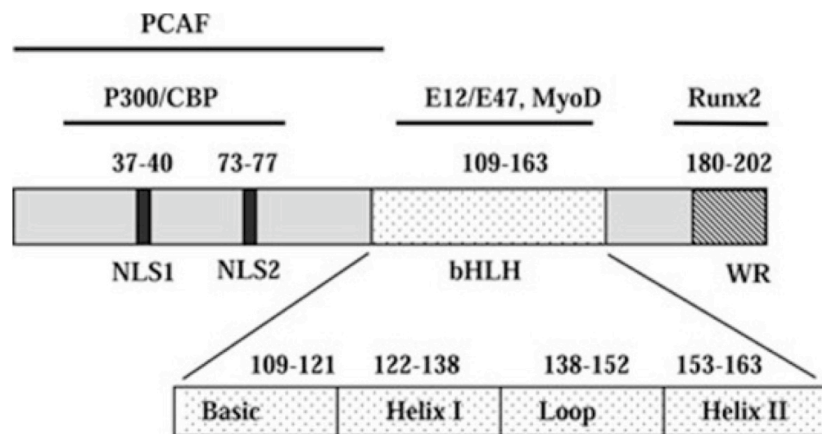
Figure 3 Molecular structure of the human Twist1 protein. The number of amino-acid residues for each structural domain is indicated. The regions that interact with other proteins are also indicated by solid lines. NLS1 and NLS2, nuclear localization signal sequences 1 and 2; bHLH, basic helix-loop-helix domain; WR, the tryptophan (W) and arginine (R) motif; CBP, cAMP-response element binding protein (CREB)-binding protein; PCAF, p300/CBP-associated factor, Runx2, Runt-related transcription factor; E12/E47, a bHLH transcription factor that forms dimer with Twist1; MyoD, a bHLH transcription factor that regulates muscle differentiation (modified from Qin 2012).

1.2.2 Physiological functions of Twist1 protein

Twist1 was originally identified in *Drosophila* as a zygotic developmental gene crucial for the establishment of the ventral furrow, a prerequisite for the development of all mesoderm-derived internal organs (Thisse et al. 1987).

In mice, Twist1 haploinsufficiency produces viable offspring but leads to abnormal craniofacial structures and polydactyly in the hind limb, a phenotype reminiscent to the dominantly inherited SCS in humans where Twist1 is mutated (Bourgeois et al. 1998). Twist1$^{-/-}$ mice undergo normal gastrulation but die at E10.5-11. Twist1, therefore, acts after mesoderm specification in vertebrates, but remains essential in mesoderm differentiation including muscle, cartilage and osteogenic cell lineages. Twist1$^{-/-}$ mice also present a significant increase in apoptotic cells, especially in the developing sclerotome (Chen and Behringer 1995). This cell death could reflect Twist1 anti-apoptotic properties as Twist1 proteins also behave as key regulators of the p53 onco-suppressive protein and as major effectors of the NF-kB survival pathway (Maestro et al. 1999). The lethality of the Twist1 knockout mouse led to the development of a Cre-mediated conditional knockout mouse to help study the regulatory functions of Twist1 post-neural crest cell migration (Bildsoe et al. 2009).

The expression profile of Twist1 during human embryogenesis is lacking. After birth, Twist1 is expressed in the adult stem cells of the mesenchyme (Qin et al. 2011). Ectopic expression of Twist1 in human bone marrow-derived mesenchymal stromal/stem cells (MSC) was found to maintain an immature stromal phenotype, to inhibit their osteo-chondrogenic potential and conversely to increase their adipocyte potential, strengthening their role in cell fate determination (Patterson et al. 2011). Twist1 expression was originally defined as being restricted to mesoderm-derived tissues including placenta, heart and skeletal muscles (Wang et al. 1997), presumably in precursor cells. Recently, the protein was found to be additionally expressed in brown fat and to be essential for its function in adaptative thermogenesis, a process that consists of metabolizing fat as heat (Dobrian et al. 2012). Twist1 behaves as a negative regulator of the PGC1-a transcription factor, the key regulator of the entire program of thermogenesis, by scaffolding together PGC1-a with a class II histone deacetylase to silent its target genes. Twist1 depletion is sufficient to provide a remarkable obesity-resistant phenotype, elevated oxygen consumption and mitochondrial biogenesis linking for the first time Twist1 to cell metabolism (Patterson et al. 2011). Twist1 expression was not observed in human epithelial cells, although its mRNA was detected in both fetal and adult human skin fibroblasts (Wang et al. 1997).

1.2.3 Twist1 expression in cancers

Twist1 plays an important role in development and progression of different types of cancer (Wushou et al. 2015).

Up-regulation of Twist1 expression is frequently reported in breast cancer and indicates advanced tumor stage and poor overall survival (Lim et al. 2015). Moreover, Twist1 is also responsible for the hormone resistance in breast cancer cells (Vesuna et al. 2012). In particular, Twist1 is responsible for the loss of estrogen receptor (ER) activity, which contributes to the generation of hormone-resistant. Studies showed that the hyper-methylation of specific genes is a common feature of breast carcinomas and Twist1 is one of these genes (Dumont et al. 2008).

Twist1 over-expression is associated with another gynecological cancer, i.e. epithelial ovarian cancer. In epithelial ovarian carcinomas Twist1 expression was significantly increased in response to the chemotherapy and was associated with increased migration of the cells (Du et al. 2014).

Twist1 is a critical regulator of prostate cancer cell growth and is a prognostic marker of high-grade prostate cancer (Raatikainen et al. 2015). High expression of Twist1 is closely associated with more aggressive behaviors of hepatocellular carcinoma (HCC) (Zhang et al. 2015). Different studies have reported that the over-expression of Twist1 is also associated with gastric carcinoma, colon-rectal carcinoma and esophageal squamous carcinoma (Qin et al. 2012). Co-expression of Twist1 with hypoxia-inducible factor-1 alpha (HIF1-α) and Snail is an important prognostic predictor in patients with non-small cell lung cancer and it is associated with mesenchymal phenotype (Liu et al. 2015).

1.2.4 Mechanisms of Twist1 reactivation in human cancers

The mechanisms leading to the aberrant reactivation of Twist1 appear to be various and complex. Up-regulation of Twist1 or its promoter methylation is reported in brain cancer, head and neck cancer (Ou et al. 2008). Like carcinomas, Twist1 is also over-expressed in chronic myeloid leukemia (CML) patients and in other hematological malignancies (Merindol et al. 2014).

Twist1 is activated by a variety of signal transduction pathway, including AKT, STAT3, MAPK, RAS and WNT signaling. It was demonstrated that STAT3 bind to Twist1 promoter activating the transcription. The activity of STAT3 depends of its phosphorylation state (Zhao et al. 2015). Co-expression of Tyr705 p-STAT3 and Twist1 within the nucleus was observed in late-state tumors (Cheng et al. 2008). The epidermal growth factor (EGF) is able to increase the RNA and protein levels of Twist1 in EGFR- expressing cells via STAT3 activation (Cho et al. 2014).

Stress conditions seem to control both the physiological and aberrant expression of Twist1. Hypoxic conditions are similarly defined as potent inducers of Twist1 expression in cancer cells thereby promoting cell dissemination to less hostile environment. Consistently, up-regulation of Twist1 by HIF1α during hypoxic conditions has significant implications in tumor invasion and angiogenesis (Du et al. 2015; Yang et al. 2008).

Other results indicated that over-expression of Sox12, a member of SYR-related HMG box (SOX) family proteins, induced invasion and metastasis by trans-activating Twist1 expression in hepatocellular carcinoma (HCC). Co-expression of Sox12 and Twist1 were significantly correlated with loss of tumor encapsulation, microvascular invasion and a higher tumor-nodule-metastasis and indicated poor prognosis in human HCC (Huang et al. 2015).

It was reported that also YB1 (Y box-binding protein I) is able to modulate Twist1 expression. The DNA/RNA binding protein YB1 was found to suppress cap-dependent initiation of growth promoting mRNAs and enhances the cap-independent translation initiation of EMT-inducing mRNA including Twist1, thereby promoting growth arrest and cell dissemination (Evdokimova et al. 2009).

Recent data support that hyper-methylation of Twist1 promoter may represent an alternative mechanism for its regulation and influence the EMT in colorectal cancer (Galván et al. 2015).

Epstein-Barr virus (EBV)-associated nasopharyngeal carcinoma is highly metastatic compared to other head and neck tumors. A study showed that the principal EBV oncoprotein, latent membrane protein 1 (LMP1), up-regulates Twist1 to induce EMT, suggesting the contribution of Twist1 induction by the human viral oncoprotein LMP1 to the highly metastatic nature of nasopharyngeal carcinoma (Horikawa et al. 2007).

Moreover, it was describes that Twist1 form a negative loop with inflammatory cytokines, as Twist1 are transcriptionally induced by NF-kB and in turn bind to the TNFα (Tumor Necrosis Factor α) and IL1β promoters blocking NF-kB

transcriptional activity (Šošić et al. 2003). In a recent paper it was also demonstrated that HMGA2 (high mobility group A2) protein in association with Smad complex directly associate with A:T rich sequences and promote transcription from the Twist1 promoter (Tan et al. 2012).

miRNAs are endogenous small non-coding RNA that regulate gene expression post-transcriptionally by modulating mRNA translation or stability. The mammalian Twist1 3'UTRs are highly conserved and contain a number of potential regulatory elements including miRNA target sites. Recently, it was reported that Twist1 is regulated by miR- 145a-5p, miR-151-5p and miR-337-3p. All of the miRNAs shown to repress Twist1 expression are involved both in embryonic development and cancer (Nairismägi et al. 2013).

1.3.5 Downstream effects of Twist1 in human cancers

Twist1 plays an important role in several processes involved in cancer progression i.e. cromosomal instability, angiogenesis, invadopodia formation, extravasation and metastasis. Twist1 also protects cancer cell from apoptotic cell death. In addiction, Twist1 is responsible for the stemness of cancer cells and the generation of drug resistance.

Epithelial- to-mesenchymal transition

A crucial mechanism by which tumor cells enhance their invasive capacity is the dissolution of intercellular adhesions and the acquisition of a more motile mesenchymal phenotype as part of an epithelial- to-mesenchymal transition (EMT) (Hanahan and Weinberg 2011). EMT is a critical mechanism of migration and invasion during development and in the case of cancer cells is a mechanism of increased invasion, metastasis, and resistance to chemotherapy. A hallmark of EMT is the functional loss of the protein E-cadherin encoded by the CDH1 gene (De Craene and Berx 2013). Twist1 has been identified as a master regulator of EMT (Ansieau et al. 2010).

In accordance with its important role in EMT, it was demonstrated that Twist1 directly down-regulates the epithelial marker E-cadherin and on the other hand up-regulates the mesenchymal marker N-cadherin (Vesuna et al. 2008). In particular, there is a positive correlation among ZEB1, ZEB2 (E-cadherin repressors) and Twist1 expression, suggesting the collaboration between these proteins to increase the E-cadherin suppression (Neves et al. 2010). Moreover, it has been demonstrated that Twist1 can interact with MTA2, RbAp46, Mi-2 and HDAC2, all these proteins bind to the NuRD complex and are necessary to repress E-Cadherin expression and promote cancer cell EMT and metastasis. Twist1 can interact with RAS or ErbB2 proteins to induce EMT (Ansieau et al. 2008). Recent data demonstrated that miR-520d-5p promotes a decrease of Twist1, resulting in restoration of E-Cadherin expression, which in turn results in reduced cellular motility and invasiveness (Tsukerman et al. 2014).

Recent data support an oncogenic feed-forward loop in which cytoplasmic p27 promotes EMT and tumor metastasis via STAT3-mediated Twist1 up-regulation in breast and bladder models (Zhao et al. 2015).

In addition, Twist1 activated the integrin α5 promoter by interacting with and activating the transcription factor AP-1 (Nam et al. 2015). Integrin α5, a fibronectin receptor, is an important mesenchymal marker; its up-regulation is required for EMT induction in transformed mammary epithelial cells and in melanoma cells (Qian et al. 2005). Recently, the group of Wang reported that SOX5 promotes EMT and cell invasion via regulation of Twist1 expression in hepatocellular carcinoma (Wang et al. 2015). SOX5 is one member of the SOX family of transcription factors that play important roles in the regulation of embryonic development in various types of cancers (Schanze et al. 2013).

Suppression of apoptosis

Various studies have shown that Twist1 protein negatively regulate the p53 pathway at many steps, including p53 stabilization, post-translational modifications, DNA binding and trans-activation potential (Pinho et al. 2011).

Mechanistic investigations revealed that Twist1 exerts its negative effect on p53 protein by reducing the expression of the p14ARF tumor suppressor. Moreover, Twist1 binds to the C-terminal of p53 through the Twist box and facilitates its MDM2-mediated degradation (Piccinin et al. 2012). In addition to interfering with p53, Twist1 is positively associated with anti-apoptotic protein Bcl-2. Twist1 and Bcl-2 are usually co-expressed in cancer patients in hypoxic condition (Zhao et al. 2012). Other results indicated that Twist1 and T-bet induce expression of miR-148a. miR-148a regulates expression of the pro-apoptotic gene Bim, resulting in a decreased Bim/Bcl2 ratio and, thus, leading to inhibition of apoptosis (Haftmann et al. 2015).

Stemness of cancer cells

Recent studies show that the stem cell properties induced by EMT was one of reasons for the dismal outcome of ATC (Jung et al. 2015). Beside the role of Twist1 in inducing EMT, it was demonstrated that its over-expression can promote the formation of cancer stem cells (CSCs) phenotype in breast cancer cells, which have the ability of self-renew and resistance to the chemotherapy. Notably, Twist1 directly up-regulates Bmi1, a polycomb-group protein that maintains stem cell self-renewal and is frequently over-expressed in human cancers (Wu et al. 2011). Anticancer molecule, sulforaphane (SNF), can eliminate CSC characteristics in pancreatic CSCs and inhibition of Twist1 expression is one of the mechanisms behind this property of SFN (Srivastava et al. 2011). Recent data show that SATB1 (Special AT-rich sequence-binding protein1) participates in the maintenance of breast cancer stem cells through regulation of the Notch signaling pathway, which promotes up-regulation of Twist1 (Sun et al. 2014). Twist1 directly represses CD24 expression through the E-box element to increase CD44$^+$/CD24^{-low} cancer stem-like cell population in breast cancer cells (Venusa et al. 2009).

Interestingly, recent data provide that persistent activity of Twist1 inhibits stem-cell-like properties and the outgrowth of disseminated cancer cells into macroscopic metastases, while transient Twist1 activation primes a subset of mammary epithelial cells with stem-cell-like properties, which only emerge and stably persist following Twist1 deactivation promoting all steps of the metastatic cascade (Schmidt et al. 2015).

Angiogenesis

Angiogenesis is the physiological process involved in the growth of new blood vessels from preexisting vessels, which is a critical event for cancer

metastasis. Twist1 has demonstrated its ability to develop angiogenesis and this effect may be through the induction of VEGF-C and VEGFR-3 expression in supraglottis carcinomas and in hepatocellular carcinoma (Lu et al. 2011).

Recent data show that Twist1 recruits stromal macrophages through CCL2 induction to promote angiogenesis and tumor progression (Low-Marchelli et al. 2013).

Moreover, Twist1 directly activated the cell adhesion protein periostin (POSTN), involved in cancer metastasis (Oshima et al. 2002). Twist1 induces also PDGFRα (Platelet-derived Growth Factor Receptor α) expression, which in turn activates Src, to promote invadopodia formation. Invadopodia are specialized membrane protrusions for extracellular matrix degradation (Eckert et al. 2011). In addition, Twist1 can promote cancer cell invasion and metastasis also by repressing the expression of TIMP1 a key inhibitor of MMPs (metalloproteinase) (Okamura et al. 2009).

Inflammation

In addition to its role in embryogenesis, Twist1 has been found to be a key regulator in the development of hematopoietic cells and in inflammatory processes (Merindol et al. 2014). Šošić et al. first observed that Twist1 regulates cytokine signaling by establishing a negative feedback loop that represses the NF-kB-dependent cytokine pathway (Šošić et al. 2003). Sharif et al. then reported the interaction between Type I interferons (IFNs), Twist1, NF-kB. IFNs are pleiotropic cytokines and have immune regulatory functions by controlling the production of pro-inflammatory cytokines. They found that IFNs suppressed the production of TNFα through the regulation of the expression of the receptor tyrosine kinase Axl and downstream induction of Twist1 (Sharif et al. 2006). Moreover, Twist1 negatively regulates NF-kB-dependent cytokine production through the regulation of miR-199a, which subsequently inhibits IKKβ and therefore NF-kB activity (Yin et al. 2010). Moreover, Twist1 also plays an important role in regulating the function and differentiation of immune cells, particularly T helper 1 (Th1) cells (Niesner et al. 2008). Pham et al. showed that Twist1 decreased IFN-γ production in Th1 cells by impairing the activity of the Th1 transcription factor network T-bet, STAT4, and Runx3. In a subsequent study, they showed that Twist1 was a key component of a STAT3-induced feedback loop that controls IL6 signaling (Pham et al. 2013).

Drug resistance

Chemoresistance is a major limitation on the successful treatment of all types of cancers. Emerging evidence suggests that Twist1 can cause drug resistance or decrease sensitivity to chemotherapy agents. In details, Twist1 is responsible for the generation of resistance against chemotherapeutic drug Taxol, once considered one of the most effective anticancer drugs against

many types of human cancers including bladder, ovarian and prostate cancer; in Cisplatin and Doxorubicin-resistant tumor cells, Twist1 is over-expressed and by targeting YB-1, acts synergistically enhancing cell growth, invasion, motility and drug resistance (Shiota et al. 2008). Moreover, Twist1 up-regulation, likely induced by NF-kB, was associated with an impaired chemotherapeutic-induced programmed cell death (Pham et al. 2007). Finally, Twist1 suppression increases etoposide drug response in mouse fibroblast (Hosono et al. 2007).
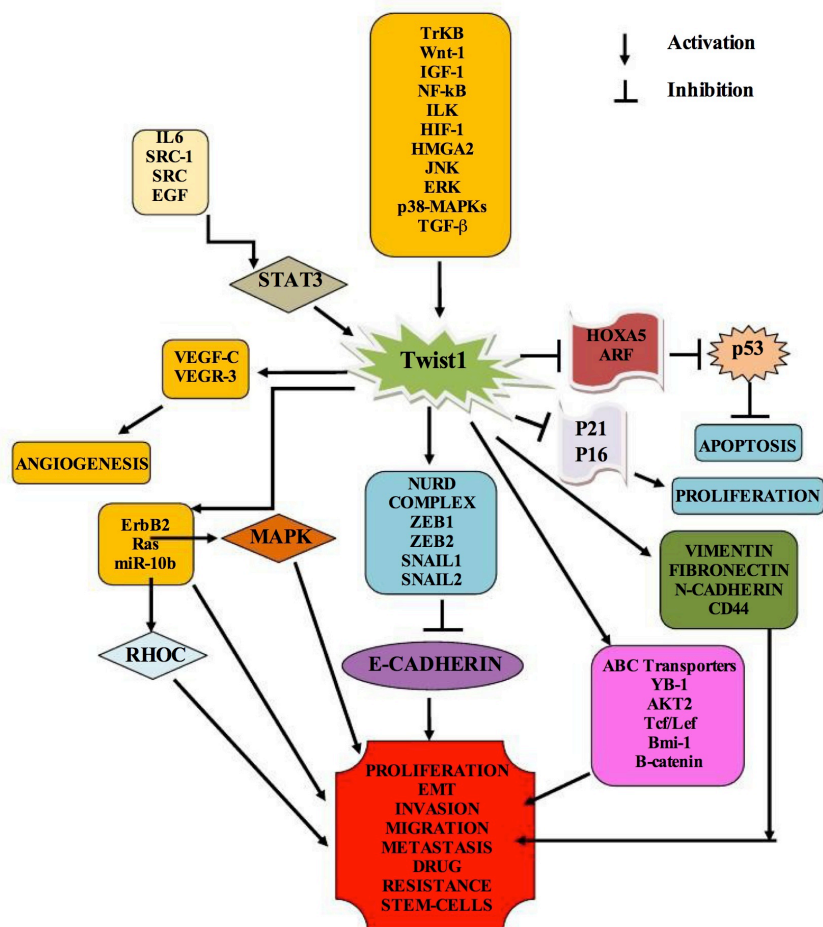
Figure 5: Twist1 signaling. The interaction of Twist1 with different proteins and mechanisms by which could acts to promote several cellular reactions as apoptosis, proliferation, EMT, invasion, migration, metastasis, drug resistance and stem-cells development is shown (modified from Je, 2013).

2. AIMS OF THE STUDY

The aim of this study was to identify transcriptional targets that mediate Twist1 biological effects in thyroid cancer cells.
The specific aims were as follow:

1. Identification of mRNA targets of Twist1 in thyroid cancer cells and analysis of the functional consequences of silencing of top up-regulated genes on cell proliferation, survival, migration and invasion.

2. Identification of miRNA targets of Twist1 in thyroid cancer cells. In particular, we focused on miR-584 induced by Twist1. We investigated the role of miR-584 ectopic expression (in TPC negative cells) and of miR-584 knockdown (in TPC-Twist1 cells) on cell proliferation, migration, invasion and resistance to apoptosis.

Besides Twist1 studies, another project developed during my PhD program regarded also the identification of Anterior gradient protein 2 (AGR2), as a novel marker of PTC. We showed that AGR2 is up-regulated in PTC and is involved in thyroid cancer cells survival, migration and invasion and in protection from endoplasmatic reticulum stress (attached manuscript II).

3. MATERIALS AND METHODS

3.1 Reagents

Staurosporine and Doxorubicin were obtained from Sigma-Aldrich (St. Louis, MO).

3.2 Cell lines

The human papillary thyroid cancer cells, TPC-1 (named TPC) were obtained from M. Nagao (Carcinogenesis Division, National Cancer Center Research Institute, Tokyo, Japan). The TPC cell line was identified on the basis of the unique presence of the RET/PTC1 rearrangement. CAL62 was purchased from DSMZ (Deutsche Sammlung von Mikroorganismen und Zellkulturen GmbH, Germany). CAL62 cells were DNA profiled by short tandem repeats analysis in 2009 and shown to be unique and identical with those reported in Schweppe et al (Schweppe et al. 2008). The TPC-Twist1 cell lines (mp1, mp2, and Cl2) and the CAL62 shTwist1 cells were generated and characterized as described in Salerno et al, 2011 (Salerno et al. 2011). The thyroid cancer cell lines were grown in DMEM (Dulbecco's Modified Eagle Medium, Invitrogen) containing 10% FBS (fetal bovine serum), L-glutamine and penicillin/streptomycin (Invitrogen, Carlsbad, CA, USA).

3.3 Tissue samples

Tumors and normal thyroid tissue samples for immunohistochemical analysis, RNA extraction and quantitative RT-PCR were retrieved from the files of the Department of Surgery, University of Pisa (Italy). Case selection was based on the histological findings and on the availability of adequate material for RNA extraction. PDC were defined as malignant tumors of follicular cells displaying predominant solid/trabecular/insular growth patterns, high grade features such as mitoses (more than three to five mitoses x10 high power field) and/or necrosis and convoluted nuclei, with or without concurrent differentiated components of the follicular or papillary type. ATC were defined as tumors displaying admixtures of spindle, pleomorphic giant, and epithelioid cells; high mitotic activity; extensive coagulative necrosis with irregular borders; and infiltration of vascular walls often accompanied by obliteration of the vascular lumina. Processing of samples and of patient information proceeded in agreement with review board-approved protocols.

3.4 Immunohistochemistry

Formalin-fixed and paraffin-embedded 3- to 5 μm-thick tumor sections were deparaffinized, placed in a solution of absolute methanol and 0.3% hydrogen peroxide for 30 min, and treated with blocking serum for 20 min. The slides of tumor sections were incubated with a rabbit polyclonal antibody against TUSC2 (Proteintech, Chicago, USA) and processed according to standard procedures. Cases were scored as positive when unequivocal brown staining was observed in the nuclei of tumor cells. Immunoreactivity was expressed as the percentage of positively stained cells and scored in four intensity categories (-, no staining; +, low/weak; ++ moderate; +++, high/ intense).

3.5 Microarray analysis

Total RNA from TPC-Twist1 cells (Twist1 mp1, Twist1 mp2, Twist1 Cl2) and pcDNA control cells was transcribed into cDNA using Superscript RT (Invitrogen, Carlsbad, CA, USA), in the presence of T7-oligo (dT) 24 primer, deoxyribonucleoside triphosphates (dNTPs), and T7 RNA polymerase promoter (Invitrogen, Carlsbad, CA, USA). An in vitro transcription reaction was then performed to generate biotinylated cRNA which, after fragmentation, was used in a hybridization assay on Affymetrix U133 plus 2.0 GeneChip microarrays, according to manufacturer's protocol (GeneChip 3' ivt Express Kit, Affymetrix). Normalization was performed by global scaling and analysis of differential expression was performed by Microarray Suite software 5.0 (Affymetrix).

miRNome array was performed using the TaqMan LDA cards. The TaqMan Array Human MicroRNA Card Set v3.0 consist of two card set containing a total of 384 TaqMan MicroRNA Assays per card.

Both screening were conducted at Aarhus Biotechnology (Aarhus, Denmark). The final results were imported into Microsoft Excel (Microsoft).

3.6 Network and gene ontology analysis

For functional analysis, the set of input genes (158 up-regulated and 221 down-regulated genes) were uploaded into the Ingenuity Pathway Analysis (IPA) online tool (Ingenuity System Inc, www.ingenuity.com). IPA is a system that transforms large data sets into a group of relevant networks biological processes, and pathways, containing direct or indirect relationships between genes based on known interactions in the literature and in the experimental studies. IPA computes a score for each biological process according to the fit of the user's set of significant genes. The score indicates the likelihood of the

genes in a biological process from the Ingenuity knowledge base being found together due to random chance.

3.7 RNA extraction, cDNA synthesis, and quantitative real-time PCR

RNA was isolated using the mirVana^{TM} miRNA Isolation Kit (Ambion, Austin, TX, USA) according to the manufacturer's instructions. The purity and quantity of RNA were assessed using the NanoDrop spectrophotometer (Thermo Scientific, Wilmington, DE, USA). The quality of the RNAs was verified by the 2100 Bioanalyzer (Agilent Techonologies, Waldbronn, Germany). Only samples with RNA integrity number (RIN) value > 7 were used for further analysis.

miRNA expression levels were measured using specific primers and probes (Thermo Scientific, Waltham, MA, USA). Briefly, for miRNA detection, 10 ng of total RNA were reverse transcribed using a miRNA Reverse Transcription Kit (Thermo Scientific, Waltham, MA, USA), followed by amplification using a TaqMan Universal Master Mix II (Thermo Scientific, Waltham, MA, USA). U6 snRNA was used as an endogenous control.

mRNA expression levels were measured by quantitative PCR assay, using the Universal ProbeLibray Set, Human (Roche, Basel, Switzerland). PCR reactions were performed in triplicate and fold changes were calculated with the formula: $2^{-(sample\ 1\ \Delta Ct\ -\ sample\ 2\ \Delta Ct)}$, where ΔCt is the difference between the amplification fluorescent thresholds of the mRNA of interest and the mRNA of RNA polymerase 2 used as an internal reference. The primers used were reported the attached manuscript II.

mRNA expression levels of TUSC2 and β-Actin were measured by quantitative PCR assay, using specific primers and probes and TaqMan Universal PCR Master Mix (Thermo Scientific, Waltham, MA, USA).

3.8 RNA silencing

TPC-Twist1 and CAL62 cells were transfected with the specific small interfering RNAs (siRNAs) (QIAGEN) in 6-well plates in triplicate. siRNA and the protocol of transfection are described in the attached manuscript I.

3.9 Cell Proliferation Assays

$5x10^{4}$ cells were plated in a 6-well. Cells were kept in DMEM supplemented with 10% fetal bovine serum. The day after plating, compounds were added. To estimate IC50 value, cells were counted after 24 or 48 hours with TC10^{TM} Automated Cell Counter (Biorad, Richmond, VA, USA).

3.10 Transwell and Collagen Cell Migration Assay, Collagen Cell Invasion Assay, Transendothelial Cell Migration Assay

The procedures to perform these experiments are described in detail in the attached manuscript I.

3.11 Chromatin immunoprecipitation assay

Chromatin samples were processed for chromatin immunoprecipitation (ChIP) as reported in detail in the attached manuscript I. All quantitative ChIP data were derived from at least three independent experiments, and for each experiment, q-RT-PCR was performed in triplicate. The GAPDH promoter amplicon was used as a negative control.

3.12 miR-584 transfection

The miR-584 precursor construct expressing pre-miR-584, pEP-has-miR-584 and the corresponding empty vector were purchased at Cell Biolabs (San Diego, USA).

For miRNA inhibition, hsa-miR-584 inhibitor and control vector were purchased at GeneCopoeia (Nivelles, Belgium).

The day of transfection, $1x10^5$ cells were incubated with 50 nmol/ml of plasmid (pEP-has-miR-584 or hsa-miR-584 inhibitor) or with their respective control and transfected using Lipofectamine 2000 (Invitrogen, Carlsbad, CA, USA) according to the manufacturer's instructions. Mass population was selected in Puromicyn (1 mg/ml) 48h after transfection and analyzed for miR-584 expression.

3.13 Wound Closure Assay and Matrigel Invasion assay

A wound was induced on the confluent monolayer cells by scraping a gap using a micropipette tip after 48h of transfection with specific siRNA. Photographs were taken at 10 X magnification using phase-contrast microscopy immediately after wound incision and 24h later. Pixel densities in the wound areas was measured using the Cell^a software (Olympus Biosystem Gmb) and expressed as percentage of wound closure where 100 % is the value obtained at 24h for control cells.

Cell invasion was examined using a reconstituted extracellular matrix (Matrigel, BD Biosciences, San Jose, CA). The cell suspension (1 x 10^5 cells per well) was resuspended in serum free culture medium (100 μl) and loaded onto the upper chamber of transwell cell culture chambers on a prehydrated polycarbonate membrane filter of 8-μm pore size (Costar, Cambridge, MA)

coated with 35 μg of Matrigel (BD Biosciences, San Jose, CA). The lower chamber was filled with 2.5% medium (500 μl). After 24-h incubation at 37°C, non-migrating cells on the upper side of the filter were wiped-off. Invading cells were stained and quantified at OD 570 nm after color extraction, in triplicate.

3.14 Protein studies

Immunoblotting was carried out according to standard procedures. TUSC2 (1538-1AP) antibody was from Proteintech (Chicago, IL, USA), monoclonal anti-α-Tubulin antibody was from Sigma-Aldrich (St. Louis, MO); Secondary anti-mouse and anti-rabbit antibodies coupled to horseradish peroxidase were from Santa Cruz Biotechnology.

3.15 Luciferase Assay

TPC miR-584 cells were seeded into a 96-well plate (10^3 cells per well) and cultured for 24 hours. The pLightswitch 3'UTR reporter gene plasmid (pLightswitch-TUSC2-3'UTR or pLightswitch-Empty-3'UTR) were transfected into the cells using the FuGENE Transfection Reagent (Roche, Basel, Switzerland) according to the manufacturer's protocol. Luciferase activity was measured 24 hours after transfection using the LightSwitch Luciferase Assay reagent (SwitchGear Genomics, CA) according to the manufacturer's protocol.
The primers used to generate the mutant pLuc TUSC2-3'UTR del were:
TUSC2-3'UTR del forward 5'- GGGACTGTTCACCACCTTGT- 3'
TUSC2-3'UTR del reverse 5'- CCCAAGCCATTTCCCACATT-3'.

3.16 Statistical analysis

Data are presented as mean ± SD. Two-tailed paired Student's t test (normal distributions and equal variances) was used for statistical analysis. Differences were significant when $P < 0.05$. Statistical analyses were carried out using the GraphPad InStat software program version 3.1a (San Diego, CA).

4. RESULTS

4.1 Identification of mRNA targets of Twist1

4.1.1 mRNA expression profile of TPC-Twist1 cells

We used cDNA microarrays to characterize the gene expression profile of ATC compared with PTC and normal thyroid tissue samples. Among the genes differentially expressed in undifferentiated *vs* differentiated samples, we isolated the transcription factor Twist1 as a gene up-regulated in ATC cells (Salvatore et al. 2007). We showed that ~50% of ATCs up-regulated Twist1, both at mRNA and protein level, compared to normal thyroids as well as to well-differentiated and poorly-differentiated thyroid carcinoma. Silencing of Twist1, by RNA interference, impaired cell migration and invasion in the ATC cell lines CAL62 and increased sensitivity to apoptosis. On the contrary, ectopic expression of Twist1 in the papillary thyroid cancer cells (TPC) induced resistance to apoptosis and increased cell migration and invasion (Salerno et al. 2011).

Despite the growing literature on the role of Twist1 in cancer progression, through which target genes Twist1 exerts its functions remains elusive. In this dissertation we aim to identify transcriptional targets of Twist1.

Thus, we analyzed gene expression profiles of TPC-Twist1 in comparison with control cells (TPC-pcDNA). Total RNA extracted from three TPC-Twist1 stable transfectants (mp1, mp2, and Cl2) and vector control cells was analyzed using human Genome U133 Plus 2.0 Array GeneChips (Affymetrix) containing > 47 000 gene transcripts. We sorted only the genes that were changed in all three Twist1 transfectants compared with vector control cells. We found 158 genes up-regulated and 221 down-regulated by ~ 1.5-fold in TPC-Twist1 cells compared with control cells (data are described in detail in the attached manuscript I). Consistent with the role of Twist1 in ATC, the top three molecular and cellular bio functions enriched in TPC-Twist1 cells were: i) cellular movement, ii) cellular growth and proliferation, iii) cell death and survival. In details 53.6% of the genes (203 of 379) belonged to cellular movement, cellular growth and proliferation, and cell death and survival, 17.6% (67 of 379) belonged to other top categories involved mainly to cancer (cellular assembly and organization; cellular function and maintenance), and 28.7% (109 of 379) were not classified (Figure 6). There wasn't any difference in the distribution in the different groups among up-regulated and down-regulated genes (data not shown).
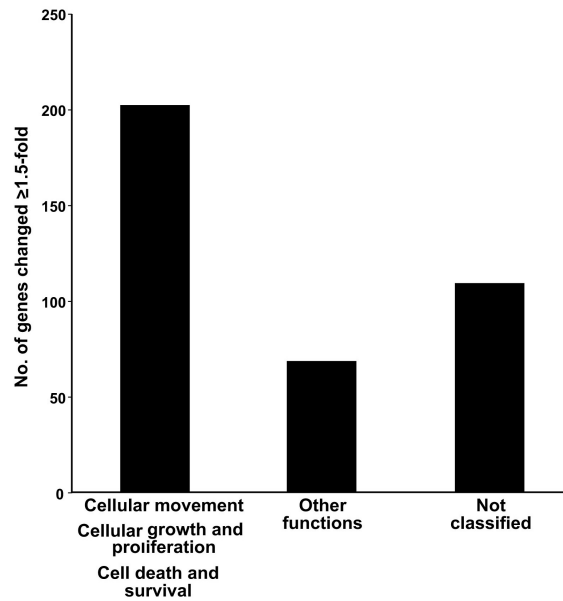
Figure 6. **Graphic representation of Twist1 target genes classified by Ingenuity Pathways Analysis.** The number of the genes is reported on y axis.

We performed q-RT-PCR of the top 16 up-regulated genes in the cell lines used in the screening in comparison with vector control cells. As shown in Figure 7, q-RT-PCR confirmed the microarray screening, albeit with some variability in the different Twist1 clones.
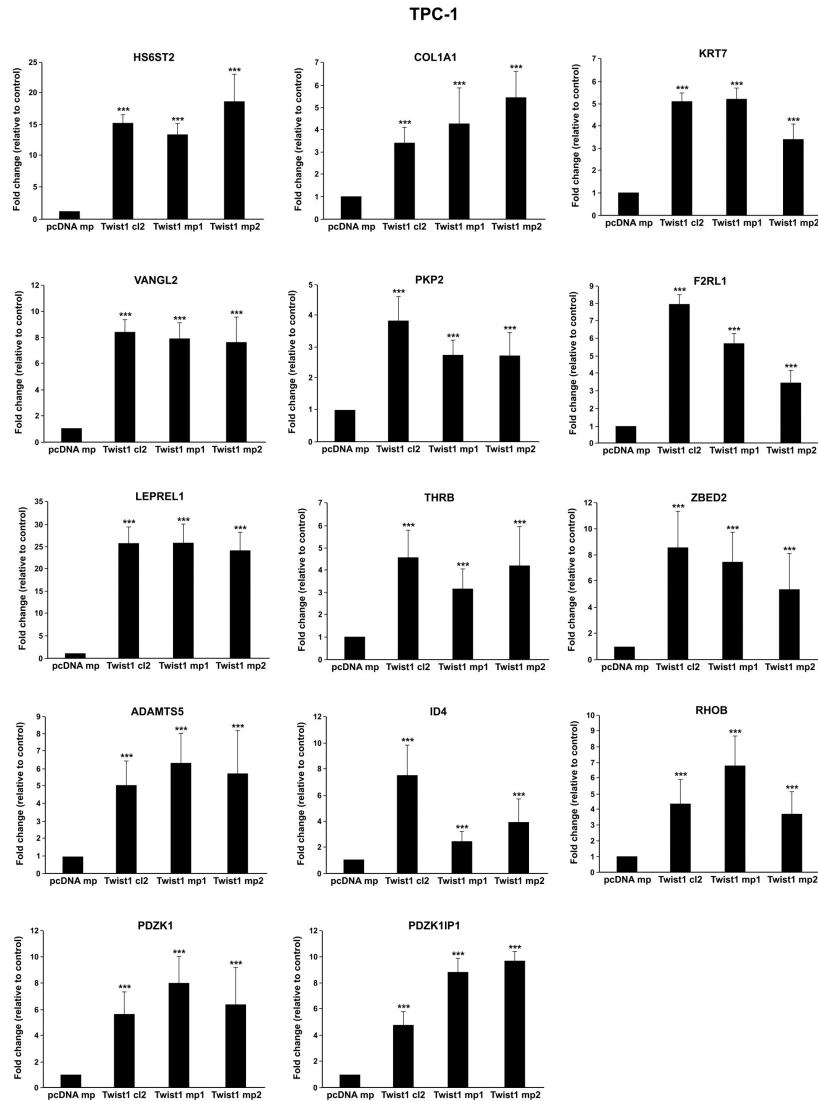
Figure 7. Expression levels of Twist1 targets in TPC transfected cells. q-RT-PCR of the indicated genes in TPC-Twist1 cells in comparison to vector control cells (pcDNA mp). Values represent the average of triplicate experiments ± standard deviations. Asterisks indicate p < 0.001 (***).

To confirm that Twist1 transcriptionally regulates the identified genes, we studied whether silencing of Twist1 affected their expression levels. Thus, we performed q-RT-PCR of the top up-regulated genes in the CAL62 (ATC) cell line stably transfected with shTwist1 plasmid. The CAL62 cell line presents a high endogenous level of Twist1 (Salerno et al. 2011), and in CAL62-shTwist1 cells, Twist1 mRNA was down-regulated ~2-fold (Salerno et al. 2011). Transfection of CAL62 with a Twist1 short hairpin RNA blunted expression of up-regulated genes with respect to the control cell (data not shown, see attached manuscript I).

4.1.2 Silencing of Twist1-upregulated genes in TPC-Twist1 and in CAL62 cells impairs cell viability

Ten of the top up-regulated genes (~70%) belong to the categories cellular movement, cellular growth and proliferation and cell death and survival. Focusing on these genes (Table 3), TPC-Twist1 and CAL62 cells were transiently transfected with siRNAs for HS6ST2, COL1A1, KRT7, F2RL1, LEPREL1, THRB, ID4, RHOB, PDZK1, PDZK1IP1, or a scrambled siRNA and examined at 48 and 72 hours after transfection for cell viability using a trypan blue assay.

Table 3. List of top 10 up-regulated genes by Twist1 in TPC cells.

Gene	Fold change	Molecular and Cellular Bio function
HS6ST2	10.28	Cellular growth and proliferation
COL1A1	7.22	Cellular growth and proliferation, cell death and survival, cellular movement
KRT7	5.56	Cellular growth and proliferation, cellular movement
F2RL1	5.31	Cellular growth and proliferation, cell death and survival, cellular movement
LEPREL1	4.99	Cellular growth and proliferation
THRB	4.88	Cellular growth and proliferation, cellular movement
ID4	4.33	Cellular growth and proliferation cell death and survival
RHOB	4.13	Cellular growth and proliferation cell death and survival, cellular movement
PDZK1	3.99	Cellular growth and proliferation cell death and survival
PDZK1IP1	2.90	Cellular growth and proliferation

As shown in Figure 8, transient silencing of all 10 genes decreased cell number in TPC-Twist1 (Figure 8A) and in CAL62 (Figure 8B) cells at different time points. Silencing of COL1A1, KRT7, and PDZK1 also increased the cell death rate (in particular at 72 hours after transfection).
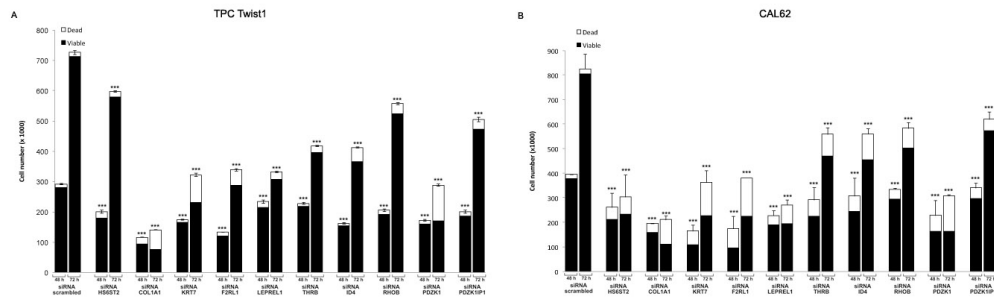
Figure 8. Silencing of the top up-regulated genes impairs cell viability. TPC-Twist1 and CAL62 cell lines were transfected with the indicated siRNAs or scrambled siRNA; after 48 and 72 hours, cells were collected by trypsinization, stained for 10 minutes with trypan blue, and counted; black bars represent the viable cells, and white bars represent the dead cells.

As a control, transfection of the 10 siRNAs efficiently down-regulated the specific genes, albeit with some variability (data not shown, see attached manuscript I).

4.1.3 Silencing of HS6ST2, THRB, ID4, RHOB, and PDZK1IP1 in TPC-Twist1 and in CAL62 cells impairs cell migration and invasion

Twist1 increases the migration ability of TPC cells, whereas Twist1 knockdown in CAL62 cells decreases cell migration (Salerno et al. 2011). We selected HS6ST2, THRB, ID4, RHOB and PDZK1IP1 because silencing of these genes affected the cell viability to a lower extent than silencing of other target genes and, thus there were a sufficient number of surviving cells available for further analysis (Figures 8A and B). A scraped wound was introduced on the confluent monolayer of TPC-Twist1 and CAL62 cells transfected with specific siRNAs or scrambled siRNA, and the cell migration into the wound was monitored after 24 hours. TPC-Twist1 and CAL62 cells transfected with the scrambled control efficiently migrated into the wound; by contrast, cells transfected with HS6ST2, THRB, ID4, RHOB, and PDZK1IP1 siRNAs displayed reduced migrating ability. This phenomenon was particularly evident with siRNA of RHOB or PDZK1IP1 (Figure 9A).

To better characterize this effect, we performed a Transwell migration assay. As shown in Figure 9B silencing of HS6ST2, THRB, ID4, RHOB, and PDZK1IP1 reduced the number of migrated cells in the Transwell.

Twist1 increased (~ 2-fold) the ability of TPC cells to migrate into Collagen I matrix whereas Twist1 knockdown in CAL62 cells decreased cell migration into Collagen I matrix (data not shown, see attached manuscript I). Thus, we asked whether silencing of HS6ST2, THRB, ID4, RHOB and

PDZK1IP1 affected this ability. As shown in Figure 9C, TPC-Twist1 and CAL62 cells transfected with HS6ST2, THRB, ID4, RHOB and PDZK1IP1 siRNA presented a decreased ability to migrate into Collagen I matrix compared with siRNA scrambled transfected cells
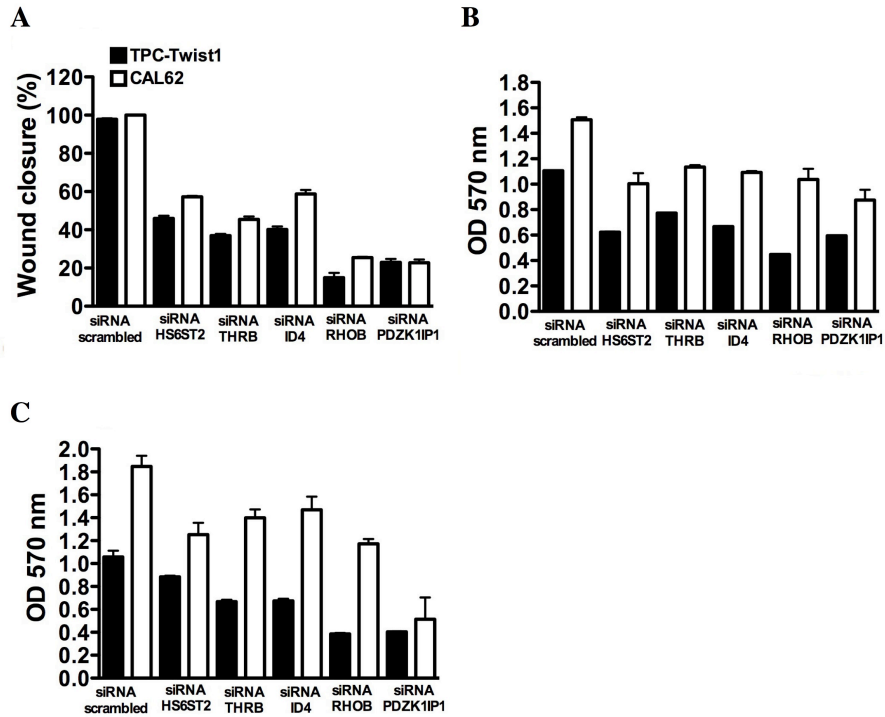
Figure 9. Silencing of the indicated genes reduces the migration ability of TPC-Twist1 and CAL62 cells. A. Cells were transfected with specific siRNAs, and 48 hours after transfection, scratch wounds were inflicted on the confluent cell monolayer. After 24 hours, cells were photographed. Wound closure was measured by calculating pixel densities in the wound area and expressed as percentage of wound closure of triplicate areas ±SDs. **B.** TPC-Twist and CAL62 cells were transfected with specific siRNAs or scrambled control, and 48 hours after transfection, cells were seeded in the upper chambers of Transwells, allowed to migrate. Migration ability is expressed as absorbance at OD 570 nm. Values represent the average of triplicate experiments ±SDs. **C.** TPC-Twist1 and CAL62 transfected cells were seeded onto the insert coated with Collagen I, left to migrate. Migration ability in Collagen I is expressed as absorbance at OD 570 nm. Values represent the average of triplicate experiments ±SDs.

We evaluated cell invasion in Collagen I matrix. Silencing of HS6ST2, THRB, ID4, RHOB and PDZK1IP1 reduced this ability compared with cells transfected with scrambled siRNA (Figure 10A). We, then, evaluated cell invasion in Matrigel matrix. Twist1 increased the invasion ability of TPC cells ~5-fold in Matrigel, whereas Twist1 knockdown in CAL62 cells decreased cell invasion in Matrigel (Salerno et al. 2011). TPC-Twist1 and CAL62 cells transfected with HS6ST2, THRB, ID4, RHOB and PDZK1IP1 siRNA presented a reduced ability to invade Matrigel compared with siRNA scrambled transfected cells. In particular, the silencing of RHOB and PDZK1IP1 induced a reduction of ~86% and ~84% in TPC-Twist1 and of ~ 59% and ~ 56% in CAL62 cells respectively, of invasion ability assessed by counting the number of invaded cells in 3 different fields (Figure 10B).

Finally, we studied the cell ability to penetrate into the endothelium by a trans-endothelial cell migration assay. TPC-Twist1 cells presented an increased ability to migrate through endothelial cells compared with control cells, whereas CAL62 shTwist1 presented a reduced ability to migrate through endothelial cells compared with control (data not shown, see attached manuscript I). As shown in Figure 10C, TPC-Twist1 and CAL62 cells transfected with HS6ST2, THRB, ID4, RHOB, and PDZK1IP1 siRNA presented a decrease in the trans-endothelial cell migration ability compared with cells transfected with scrambled siRNA.
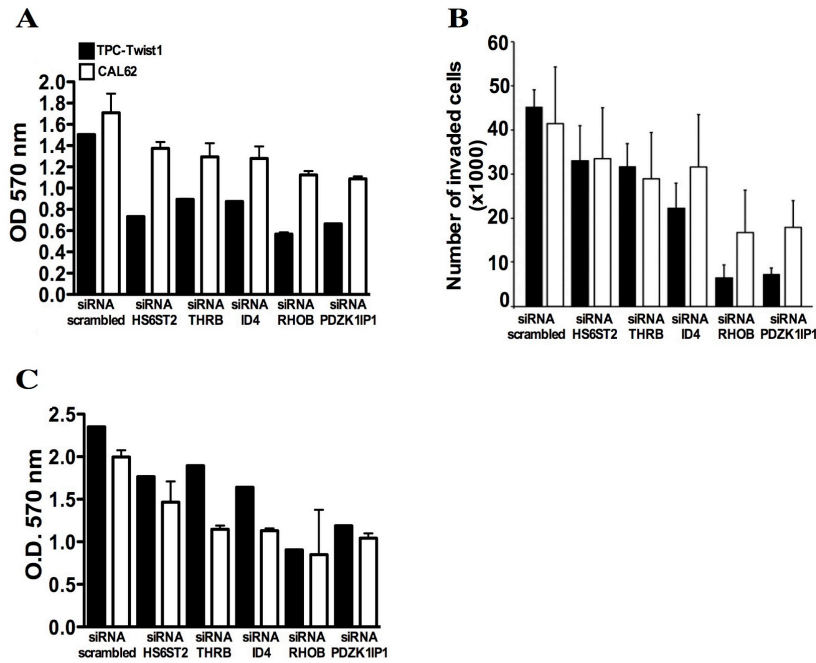
Figure 10. Silencing of the indicated genes reduces the invasion ability of TPC-Twist1 and CAL62 cells. A. TPC-Twist1 and CAL62 transfected cells were seeded in the upper chamber of Transwells coated with Collagen I matrix and incubated for 24 hours (TPC-Twist1) or 48 hours (CAL62). The invasive ability in Collagen I is expressed as absorbance at OD 570 nm. **B.** TPC-Twist1 and CAL62 transfected cells were seeded in the upper chambers of Transwells coated with Matrigel and incubated; the upper surface of the filter was wiped clean and cells on the lower surface were stained and counted. The invasive ability in Matrigel matrix is expressed as number of invaded cells. **C.** TPC-Twist1 and CAL62 transfected cells were seeded on a confluent monolayer of endothelial human umbilical vein endothelial cells (HUVECs) and left to migrate. Migration ability through HUVECs is expressed as absorbance at OD 570 nm. Values represent the average of triplicate experiments ±SDs.

4.1.4 Twist1 directly binds the promoter of target genes

To formally prove that the identified genes are direct Twist1 targets, we verified whether Twist1 binds to their promoters. Consensus binding sites for Twist1 are represented by an E-box (5'-CANNTG-3') sequence motif (Qin et al. 2012). In the promoter of all 10 up-regulated genes, we found several E-box sequences (Figure 11).
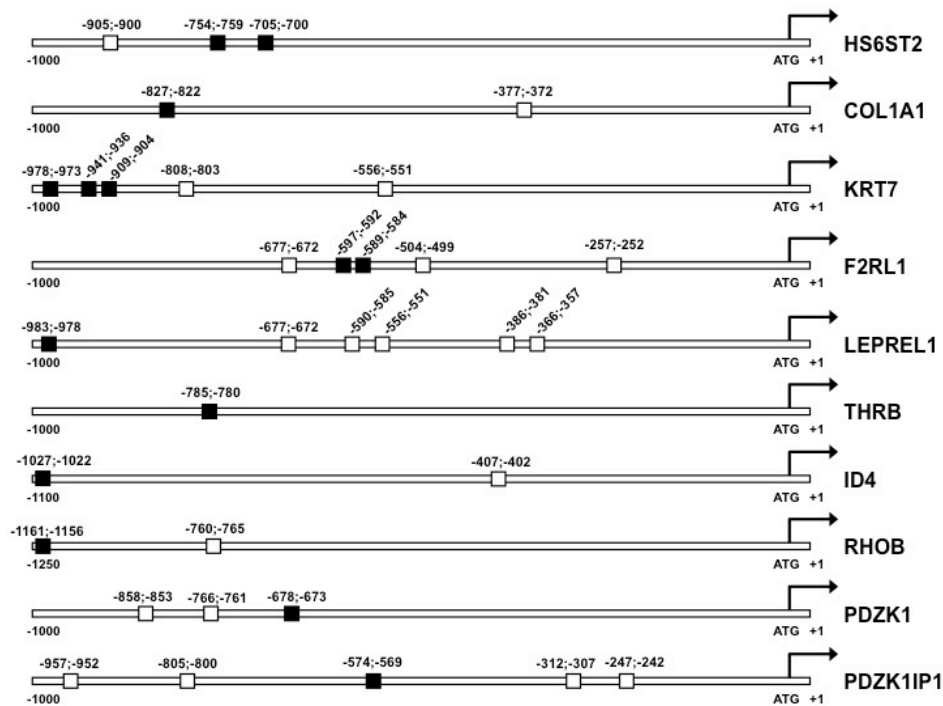
Figure 11. **Twist1 directly binds the promoter of the indicated genes.** Schematic representation of the E-box consensus sequences (CANNTG) in the promoter regions of the top ten up-regulated genes. In black are reported the E-box amplified in ChIP assay.

Thus, DNA-chromatin complexes from TPC-pcDNA and TPC-Twist1 were subjected to immunoprecipitation (IP) with Twist1 antibody or with control antibody (IgG1). As shown in Figure 12, promoter regions of all 10 up-regulated genes were significantly enriched by Twist1 IP in TPC-Twist1 cells compared with TPC-pcDNA cells. Conversely, no amplification was observed with anti-IgG precipitates and when primers for the GAPDH promoter were used. This corroborates the notion that the top up-regulated genes are direct Twist1 targets.
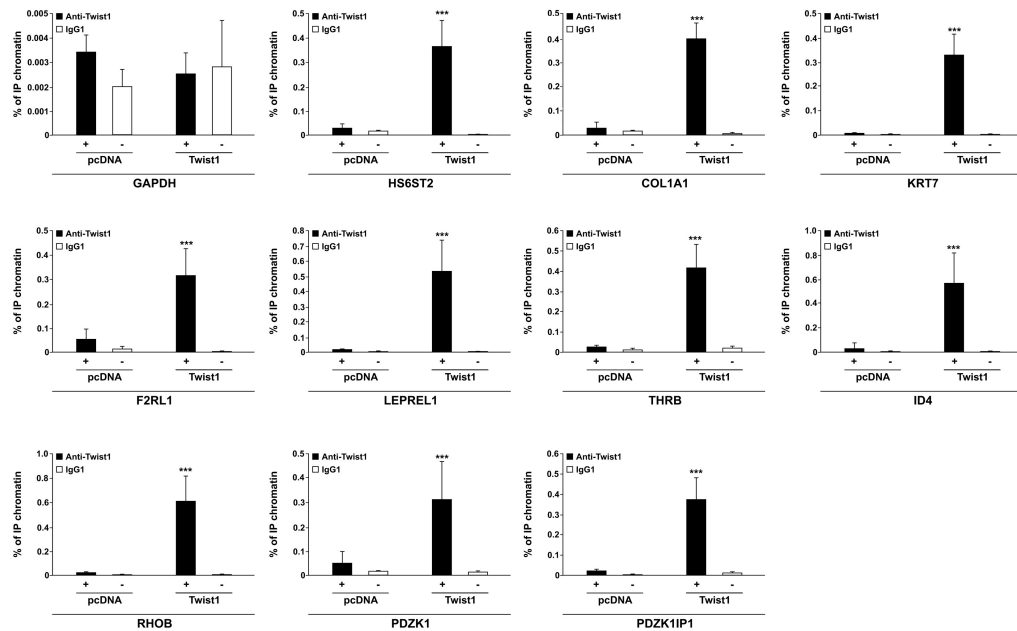
Figure 12. Twist1 directly binds the promoter of target genes. ChIP assay followed by q-RT-PCR was performed on TPC-Twist1 and TPC-pcDNA cells. Equal amounts of proteins were subjected to IP with anti-Twist1 antibody or IgG1 antibody, as indicated. The GAPDH promoter amplicon was used as a negative control. Columns represent the average of 3 independent experiments ±SDs.

4.1.5 Twist1 target genes are over-expressed in PTC, PDC, and ATC samples

Finally, to assess the role of the identified Twist1 targets in thyroid carcinogenesis we performed a q-RT-PCR on a set of normal thyroid (n = 9), PTC (n = 9), PDC (n = 8), and ATC (n = 12) samples. As shown in Figure 13, HS6ST2, COL1A1, F2RL1, LEPREL1, PDZK1, and PDZK1IP1 are differentially over-expressed in PTC, PDC, and ATC samples. The expression levels of KRT7, THRB, ID4, and RHOB were not significantly altered in thyroid carcinomas compared with normal thyroid samples (not shown). To verify these data at the protein level, we performed immunohistochemistry studies for leprecan-like 1 (LEPREL1) in a panel of normal thyroid (n = 27), PTC (n = 19), and ATC (n = 40) samples. LEPREL1 is over-expressed in 26% of PTC (5 of 19) and in 67% of ATC (27 of 40) samples in comparison with normal thyroids (attached manuscript I).
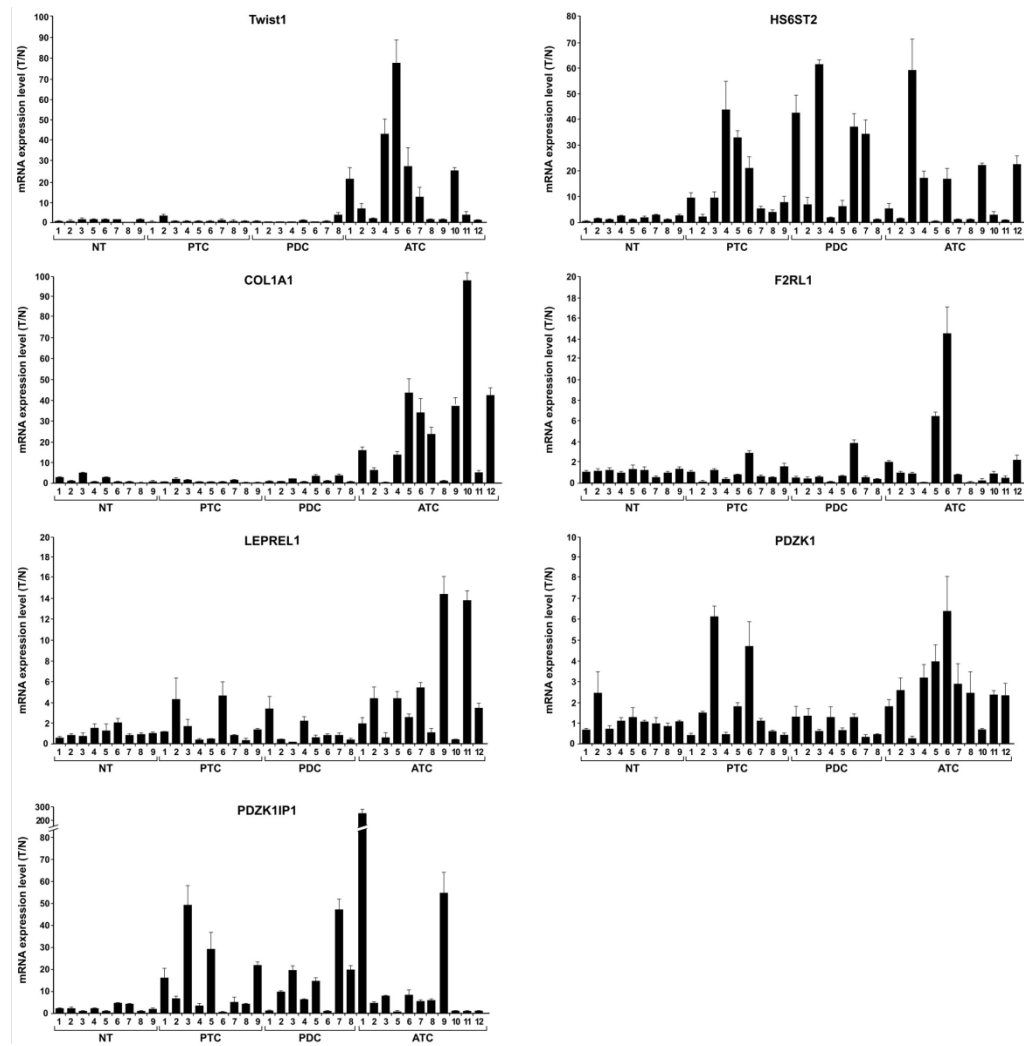
Figure 13. Expression of Twist1 targets in thyroid tissue samples. q-RT-PCR of the indicated genes in normal thyroids (NT) (n = 9), PTC (n = 9), PDC (n = 8), and ATC (n = 12) snap-frozen tissues. The expression levels of genes in each sample were measured by comparing its fluorescence threshold with the average fluorescence threshold of the NT samples. The average results of triplicate samples are plotted ± SDs.

4.2 Identification of Twist1 target miRNAs

4.2.1 miRNome profiles of TPC-Twist1 cells

Recently, deregulation of miRNAs has been implicated in tumorigenesis and cancer progression. Deregulation of miRNA expression is also detected in thyroid cancer (Fuziwara et al. 2014). Twist1 regulated miRNA are poorly characterized thus to further dissect the molecular mechanisms through which Twist1 exerts its biological effects in thyroid cancers cells we aimed to identify Twist1 regulated miRNAs. We screened the miRNome profiles of TPC-Twist1 cells (mp1, mp2 and Cl2) in comparison to control (TPC pcDNA). Fifty-one miRNAs (14 up-regulated and 37 down-regulated) were differentially expressed in all the three TPC-Twist1 cells clones by more than 2 fold compared to vector control (Tables 4 and 5).

Table 4. miRNAs up-regulated in TPC-Twist1 cells.

miRNA	pcDNA	Twist1 mp1		Twist1 mp2		Twist1 Cl2	
	Ct	Ct	Fold Change	Ct	Fold Change	Ct	Fold Change
hsa-mir-597	38.4	32.1	81.4	31.9	92.9	32.0	89.3
hsa-mir-29b-2*	38.8	32.9	61.6	32.6	74.7	32.5	78.1
hsa-mir-145	35.4	30.8	24.2	32.3	8.4	31.3	17.2
hsa-mir-584	38.5	35.1	10.1	31.6	116.9	32.4	68.2
hsa-mir-30c-2*	35.9	32.6	10.0	32.3	12	29.6	78.5
hsa-mir-519b-3p	38.2	35.2	7.9	36.4	3.3	34.9	9.8
hsa-mir-133a	37.1	34.2	7.2	35	4.1	37.2	1.1
hsa-mir-101	37	34.3	6.6	34.7	4.9	34.1	7.5
hsa-mir-501-5p	35.2	32.8	5.2	30.9	19	32.7	5.6
hsa-mir-650	35.3	33.5	3.6	34.5	1.8	34	2.5
hsa-mir-639	35.8	34.3	2.8	33.8	3.9	33.7	4.3
hsa-mir-190b	33.6	32.1	2.7	32.4	2.2	31.5	4.4
hsa-mir-500	31.4	30	2.7	30.3	2.2	29.4	3.9
hsa-mir-99a*	32.5	31.4	2.1	29.3	9	30.6	3.6

Table 5. miRNAs down-regulated in TPC-Twist1 cells.

miRNA	pcDNA Ct	Twist1 mp1 Ct	Twist1 mp1 Fold Change	Twist1 mp2 Ct	Twist1 mp2 Fold Change	Twist1 Cl2 Ct	Twist1 Cl2 Fold Change
hsa-mir-326	33.6	38	21.3	37.5	14.6	und	
hsa-mir-124	34.2	38	14.2	34.7	1.4	36.1	3.7
hsa-mir-604	35.8	39.5	12.3	und		36.2	1.2
hsa-mir-222*	34.6	38	10.5	35.6	2	38.9	19.8
hsa-mir-190	33.5	36.9	10.1	34.3	1.7	34.3	1.8
hsa-mir-519a	31.2	34.3	9.2	31.2	1	32.2	2.1
hsa-mir-770-5p	35.6	38.8	9.2	37.2	3.1	37.6	3.9
hsa-mir-576-3p	33.4	36.1	6.6	33.8	1.3	33.8	1.4
hsa-mir-202	32.4	34.9	5.5	33.6	2.4	34.1	3.2
hsa-mir-301b	33.1	35.5	5.3	33.2	1	34.1	2
hsa-mir-449a	36.0	33.6	5.3	35.1	2	34.7	2.6
hsa-mir-551b*	31.5	33.8	4.9	32.9	2.8	34.6	8.6
hsa-mir-15b*	28.9	31.2	4.9	30.1	2.3	29.9	2.1
hsa-mir-30d*	33.2	35.4	4.6	37.0	14.1	33.9	1.6
hsa-mir-20a*	32.0	34.1	4.2	32.0	1.0	35.4	10.4
hsa-mir-572	31.3	33.3	4.0	32.5	2.3	31.1	1.2
hsa-mir-148b*	32.0	33.9	3.7	34.0	3.9	32.6	1.5
hsa-mir-363	35.7	37.6	3.7	38.9	9.0	Und	
hsa-mir-200c	29.4	31.3	3.6	30.4	2.0	32.8	10.1
hsa-mir-100*	30.5	32.3	3.6	31.8	2.4	33.2	6.6
hsa-mir-301a	30.8	32.7	3.6	31.4	1.5	34.9	17.3
hsa-mir-331-5p	31.8	33.6	3.5	33.7	3.8	33.2	2.6
hsa-mir-215	29.5	31.2	3.5	30.2	1.7	33.1	12.8
hsa-mir-639	34.2	36.0	3.4	34.1	1.1	33.3	1.9
hsa-mir-206	31.7	33.4	3.3	32.6	1.9	31.9	1.2
hsa-mir-572	31.0	32.7	3.2	31.4	1.3	31.6	1.6
hsa-mir-622	33.3	34.8	3.0	34.3	2.0	35.9	6.4
hsa-mir-432*	29.1	30.6	2.7	29.8	1.6	30.5	2.6
hsa-mir-505	31.4	32.8	2.7	31.6	1.2	32.8	2.7
hsa-mir-26a-1*	31.0	32.4	2.7	31.4	1.3	31.0	1.0
hsa-mir-888	37.0	38.3	2.5	37.8	1.8	38.5	2.9
hsa-mir-135b	26.0	27.2	2.3	25.8	1.1	28.2	4.5
hsa-mir-194	27.6	28.7	2.3	28.3	1.6	29.6	4.1
hsa-mir-636	31.6	32.7	2.2	31.7	1.1	32.2	1.6
hsa-mir-340	29.6	30.7	2.1	31.0	2.5	30.7	2.1
hsa-mir-218	30.4	31.4	2.1	30.7	1.3	32.4	4.1
hsa-mir-184	31.9	32.9	2.1	33.7	3.6	36.4	22.8

Initially, we verified the microarray results by q-RT-PCR of the 10 top (5 up and 5 down) changed miRNAs in TPC-Twist1 cells in comparison to control. We confirmed ~80% of the deregulated miRNAs (Figure 14). The expression of miR-124 and miR-190 did not change in TPC-Twist1 cells respect to control cells (data not shown).
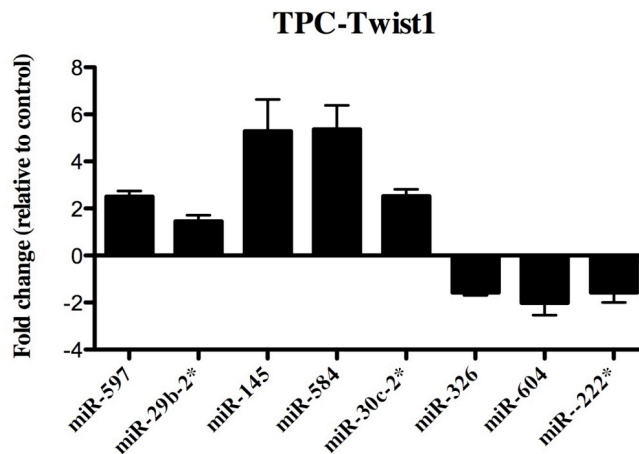
Figure 14. Relative expression levels of the indicated miRNAs in TPC-Twist1 cells. Quantitative-RT-PCR of the indicated miRNAs in TPC-Twist1 cells in comparison to vector control cells. Samples were normalized using U6 snRNA measurement. Average results of three independent experiments were reported and expressed as fold change compared to control cells ± SD.

4.2.2 miR-584 is up-regulated in ATC samples

We then focused on miR-584 because it was one of the most up-regulated in TPC-Twist1 cells respect to the control cells and because its role in cancer is poorly studied.

We measured miR-584 by q-RT-PCR on total RNA extracted from 7 normal thyroid (NT), 6 papillary thyroid carcinoma (PTC), and 5 anaplastic thyroid carcinoma (ATC) tissues samples. As illustrated in Figure 15, all ATC samples showed a significant higher expression of miR-584 compared to normal thyroid and PTC samples, with a fold change values ranging from 2 to 7 fold.
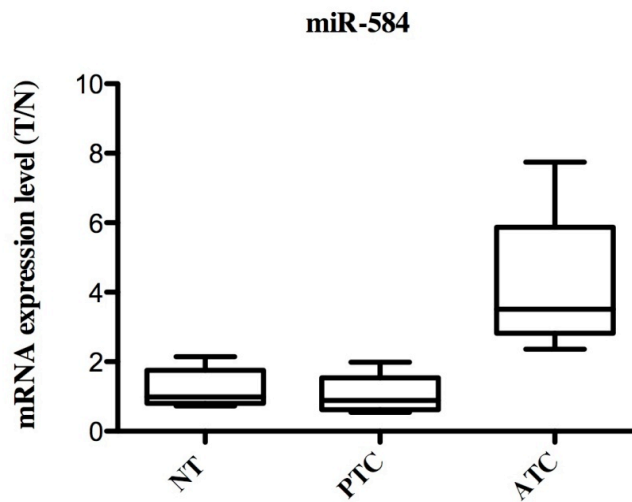
miR-584

Figure 15. Expression of miR-584 in thyroid tissue samples. Quantitative RT-PCR analysis of miR-584 in normal thyroid (NT), PTC, and ATC snap-frozen tissue samples. The level of miR-584 in each sample was measured by comparing its fluorescence threshold with the average fluorescence threshold of the NT samples. The average results of triplicate samples are plotted.

4.2.3 Ectopic expression of miR-584 protects TPC cells from apoptosis

We previously showed that Twist1 sustains the invasive and motile phenotype of ATC cells (Salerno et al. 2011). Therefore, we investigated whether miR-584 could be, at least partially, responsible for these effects.

To these aim, TPC cells, which have low endogenous level of miR-584, were stably transfected with the precursor of miR-584 or with the empty vector (null) as control. Quantitive-RT-PCR confirmed that miR-584 was increased in a selected mass population of TPC-transfected cells compared to control cells (Figure 16).

TPC
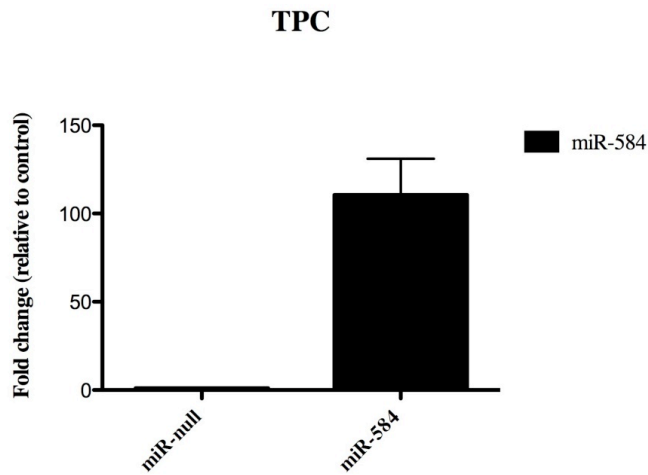
Figure 16. miR-584 expression level was measured by q-RT-PCR in TPC cells after stable transfection. Results are reported as fold change in comparison with the control. Values represent the average of triplicate experiments ± SDs.

We performed a wound-closure assay, by introducing a scraped wound on a confluent monolayer of TPC miR-584 or control cells and cell migration into the wound was monitored after 12 and 24 hours. As shown in Figure 17A, miR-584 over-expression did not affect the motility rate of TPC cells, indeed after 24 hours both cell lines equally closed the wound. Moreover, we performed a Matrigel invasion assay, TPC miR-584 and control cells were seeded into the top chamber of Transwells and their ability to invade into the matrix were evaluated after 24 hours. No difference in cell invasion ability was observed in TPC miR-584 cells compared with control (Figure 17B). Finally, we asked whether miR-584 forced expression affects cell proliferation rate. TPC cells, with or without miR-584, were seeded at a density of 5×10^4 cells and counted every 24 hours for 96 hours. Four days after plating, TPC miR-584 cells were 8.6×10^5 while TPC miR-null were 8.4×10^5. Thus miR-584 forced expression did not affect cellular proliferation (Figure 17C).

A
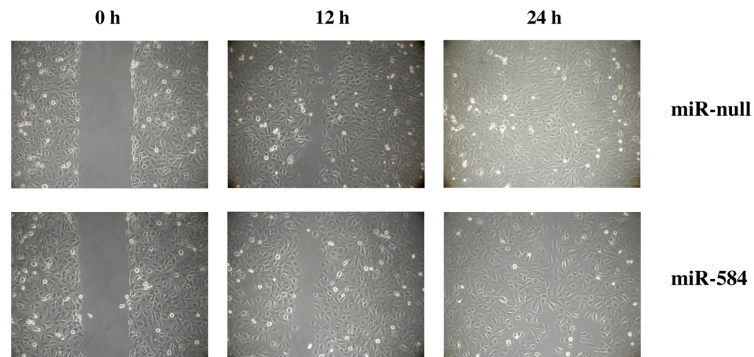
B
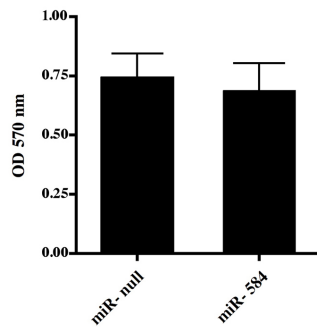
C
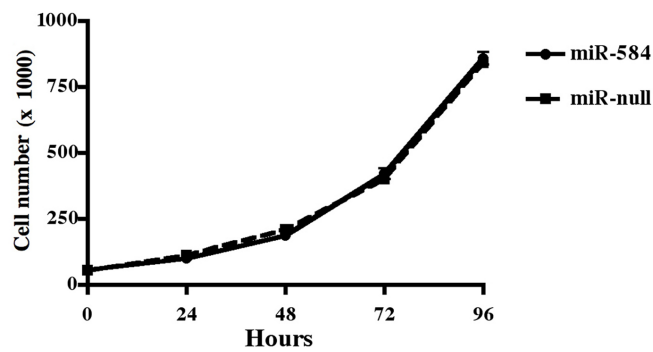
Figure 17. Effects of miR-584 expression in TPC cells on cell migration, invasion and proliferation. A. Scratch wounds were inflicted at confluent cell monolayer and after 12 and 24h cells were photographed. **B.** TPC miR-584 and TPC miR-null were seeded in upper chamber of Transwells and allowed to migrate for 24h; migration ability was expressed as absorbance at OD 570 nm. **C.** TPC miR-584 and TPC miR-null cells were plated and counted at different time points. Values represent the average of triplicate experiments. Values represent the average of triplicate experiments ± standard deviations.

Then, we investigated whether over-expression of miR-584 affects sensitivity to apoptosis, since Twist1 is an anti-apoptotic factor.

To this purpose, we used two different inducers of apoptosis Doxorubicin and Staurosporine. TPC miR-584 and control cells were treated with different doses of Doxorubicin (ranging from 10 nM to 3000 nM) or Staurosporine (ranging from 20 nM to 1500 nM) and counted after 48 and 24 hours, respectively. The growth-inhibitory concentration 50% (IC_{50}) of Doxorubicin in TPC miR-null cells was 8.9 nM while in TPC miR-584 cells was 48 nM (Figure 18A). Similarly, miR-584 expression induced a reduction of sensitivity to Staurosporine in TPC cells, with an IC_{50} of 123 nM in TPC miR-null cells and of 334 nM in TPC miR-584 cells (Figure 18B).
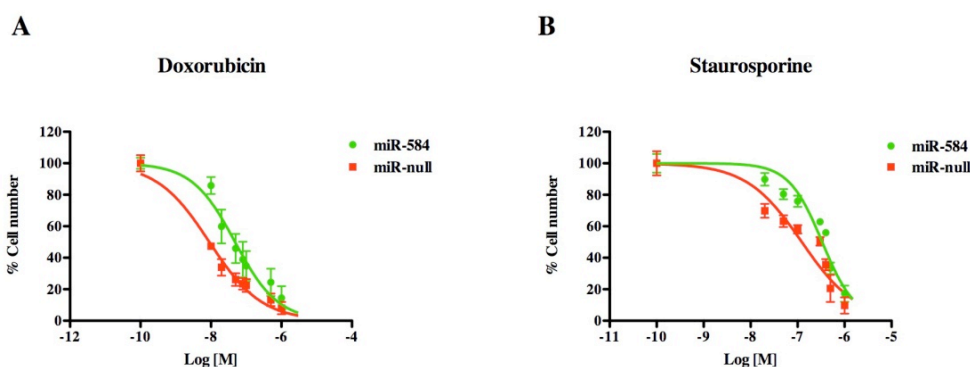
Figure 18. IC_{50} of Doxorubicin (A) and Staurosporine (B) in TPC cells transfected with or without miR-584. A. TPC-transfected cells were treated with increasing concentrations of Doxorubicin and counted 48 hours after treatment. B) TPC-transfected cells were treated with increasing concentrations of Staurosporine and counted 24 hours after treatment. Average of three independent experiments ± SD were represented. IC_{50} values were calculated with Prism software.

4.2.4 Silencing of miR-584 in TPC-Twist1 cells induces apoptosis

Furthermore, we silenced miR-584 in TPC-Twist1 cells by using a vector containing an Anti-miR-584, a chemically modified single-stranded nucleic acid, designed to specifically bind and inhibit endogenous miRNAs molecules. After antibiotic selection, cells were screened by q-RT-PCR for miR-584 expression. A mass population (TPC-Twist1 Anti-miR-584) with a miR-584 knockdown of ~50% was used for further study (Figure 19).
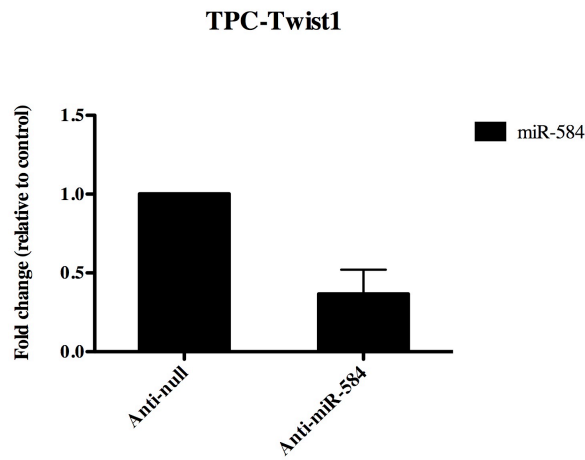
TPC-Twist1

Figure 19. Silencing of miR-584 TPC-Twist1 cells. q-RT-PCR of miR-584 in TPC-Twist1 cells transfected with Anti-miR-584 or a empty vector (Anti-null) are shown. The expression levels of miR-584 were normalized to those of U6 snRNA. Values represent the average of triplicate experiments ± SDs.

Initially, we evaluated in these cell lines proliferation, migration and invasion. As shown in Figures 20A, B and C, silencing of miR-584 did not affect cell proliferation, invasion and migration in TPC-Twist1 Anti-miR-584 cell in comparison to control cells.
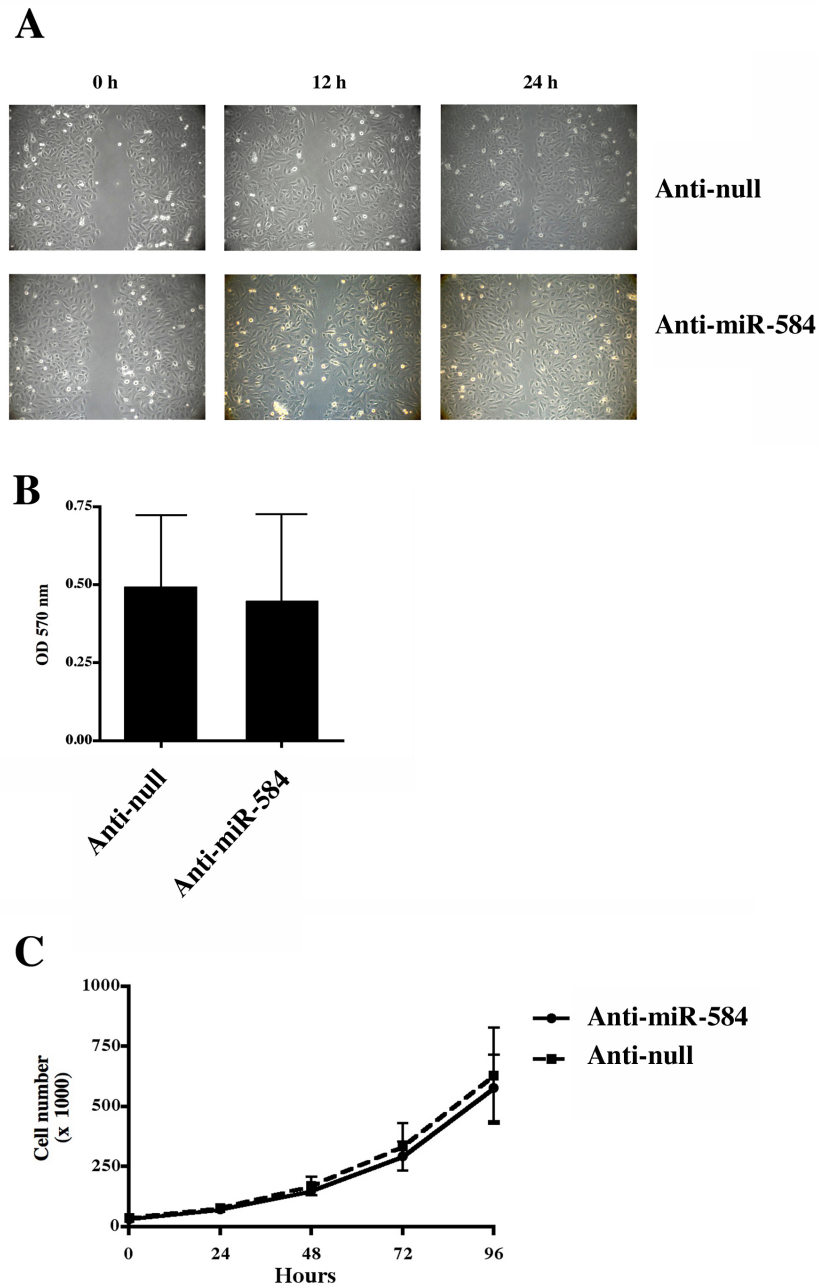
Figure 20. Effects of miR-584 silencing in TPC-Twist1 cells on cell migration, invasion and proliferation. A. A scratch wounds were inflicted at confluent cell monolayer and after 12 and 24h cells were photographed. **B**. TPC-Twist1 Anti-miR-584 and control cells were seeded in upper chamber of transwells and allowed to migrate for 24h; migration ability was expressed as absorbance at OD 570 nm. Values represent the average of triplicate experiments ± standard deviations. **C.** TPC-Twist1 Anti-miR-584 and TPC-Twist1 Anti-miR-null cells were plated and counted at different time points. Values represent the average of triplicate experiments.

Then, we treated TPC-Twist1 Anti-miR-584 and control cells with different doses of Doxorubicin and Staurosporine (Figures 21A and B). The IC_{50} for Doxorubicin was 4.9 nM in TPC-Twist1 Anti-miR-584, whereas in TPC-Twist1 transfected with control was 14.2 nM. Similarly, Staurosporine showed an IC_{50} of 101.8 nM and 23.2 nM in TPC-Twist1 Anti-miR-584 and in TPC-Twist1 Anti-null respectively (Figure 21). All together, these data suggested that miR-584 contributes in Twist1 induced resistance to apoptosis.
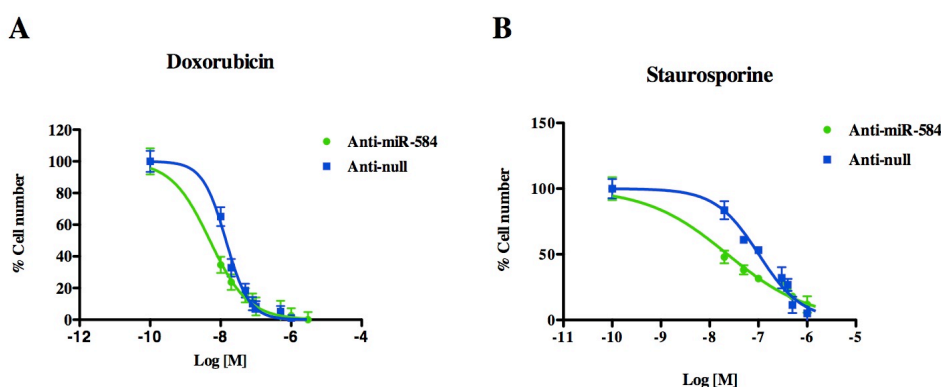
Figure 21. The sensitivity to apoptosis is increased in TPC-Twist1 cells after miR-584 silencing. A-B. The cells were treated with increasing doses of Doxorubicin or Staurosporine and counted after 48 and 24 hours, respectively. The 50% growth-inhibitory concentration (IC_{50}) is shown: values represent the average of three independent experiments ± SD.

4.2.5 miR-584 targets TUSC2

We then searched putative targets of miR-584 by using five different bioinformatics programs (Targetscan, Pictar, DianaLab, miRDB and Miranda). Among the ~200 targets predicted by all five programs, TUSC2 (tumor suppressor candidate 2, also named FUS1) was of particular interest because of its involvement in apoptosis and chemosensitivity (Li et al. 2014; Deng et al. 2008) in according with our observed effects of miR-584 in TPC cells and with the role of Twist1.

The 3'UTR of TUSC2 is highly conserved across different species, strongly suggesting that it plays an important role in regulating TUSC2 expression. In the 3'UTR of TUSC2 there is sequence of complementarity with miR-584 (Figure 22).

```
3'    gagucaggguccgUUUGGUAUu     5'       hsa-miR-584
                | |  | | | | | |
5'    agaaaggagggaaAAACCAUAa     3'       3'UTR - TUSC2
```
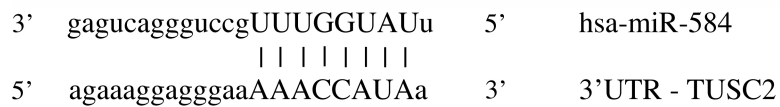
Figure 22. Predicted duplex formation between human TUSC2-3'UTR and miR-584.

We further evaluated the expression of TUSC2, both at mRNA and protein level, in TPC transfected with miR-584 and control. As shown in Figure 23A, TUSC2 protein level was decreased of ~2-fold in TPC miR-584 cells respect to control cells. Further, TUSC2 mRNA decreased upon miR-584 over-expression (Figure 23B) suggesting that miR-584 could act both by reducing translation and by accelerating mRNA degradation of TUSC2.

A

B
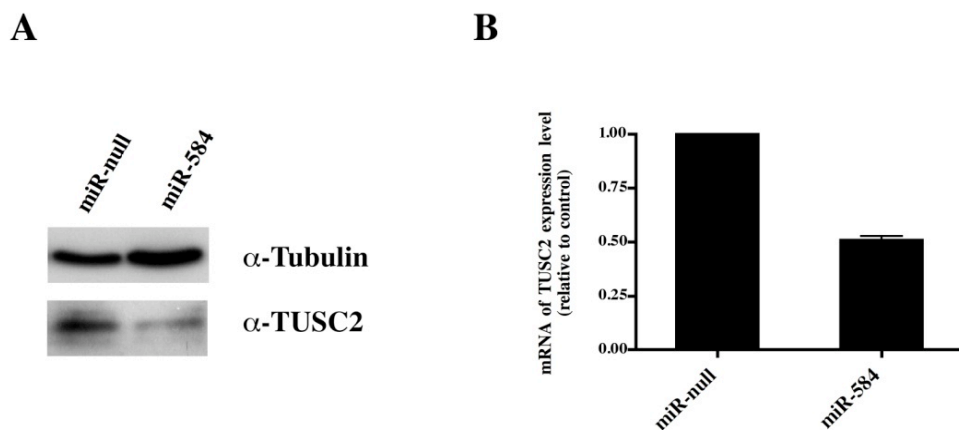
Figure 23. miR-584 suppresses TUSC2 in TPC cells. A. Immunoblotting of TUSC2 and α-Tubulin in TPC miR-584 or control cells. **B.** q-RT-PCR of TUSC2 in TPC cells transfected with miR-584 or empty vector; data were normalized to the level of RNAPol mRNA and assuming that the value of TPC transfected with a empty vector is equal to 1.

We also evaluated the expression of TUSC2 in TPC-Twist1 cells transfected with Anti-miR-584 or control by q-RT-PCR and Western blot. As shown in Figures 24, A and B, TUSC2 was increased, both at mRNA and protein level in miR-584 silenced cells.
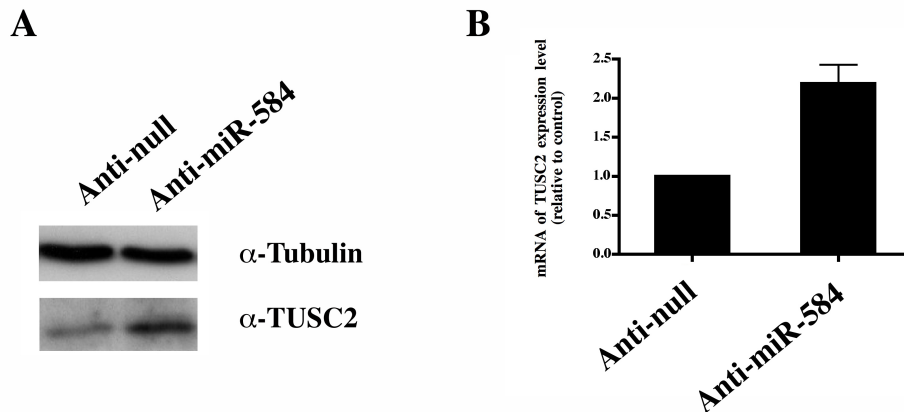
Figure 24. Silencing of miR-584 induced an increased of TUSC2 expression in TPC Twist1 cells. A. Immunoblotting of TUSC2 and α-Tubulin in TPC miR-584 and in TPC-Twist1 Anti miR-584 or control cells, respectively. **B**. q-RT-PCR of TUSC2 in TPC-Twist1 Anti miR-584 and in control cells ; data were normalized to the level of RNAPol mRNA.

To further verify whether TUSC2 is a direct target of miR-584, we generated a vector containing a synthetic luciferase reporter gene fused with the 3'UTR sequence of TUSC2, driven by a constitutive promoter. A mutant version of this plasmid, where the 8 nucleotides of 3'UTR of TUSC2 complementary to miR-584 were deleted, was also generated and used as control (Figure 25A). TPC miR-584 and TPC miR-null cells were transiently transfected with the plasmids and luciferase activity was measured 24 hours after transfection. miR-584 over-expression induced a significant reduction in luciferase activity compared with control cells. No change of luciferase activity was observed in TPC miR-584 cells, transfected with the deletion mutant reporter plasmids. These data demonstrates that miR-584 binds to the 3'UTR sequence of TUSC2 mRNA, damping its expression (Figure 25B).

A

3'   gagucaggguccgUUUGGUAUu   5'   hsa-miR-584

| | | | | | | |

5'   agaaaggagggaaAAACCAUAa   3'   3'UTR - TUSC2 del
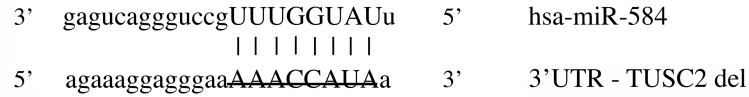
B
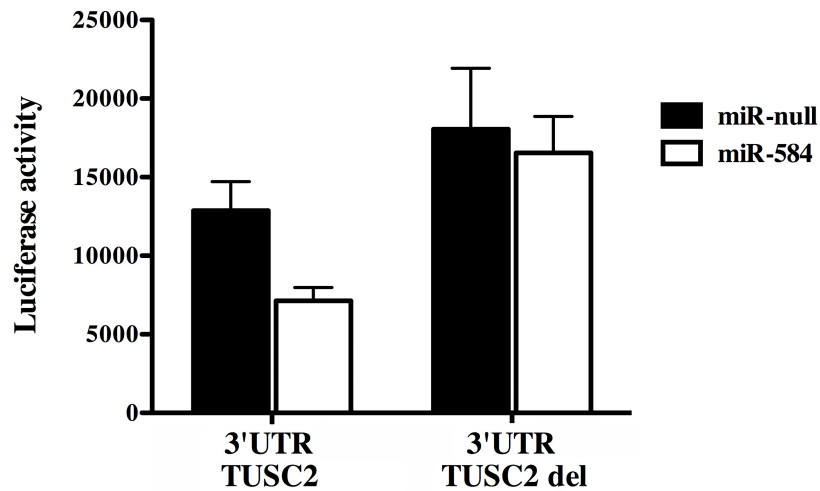
Figure 25. TUSC2 is a direct target of miR-584. A. Sequence of miR-584 binding site deleted within the TUSC2 3'UTR. **B.** Luciferase activity of wild-type (TUSC2-3'UTR) or delete (TUSC2-3'UTR del) TUSC2-3'UTR reporter gene in TPC cells stably transfected with miR-584, or empty vector. Luciferase activity was normalized on that a co-transfected β-actin-reporter.

4.2.6 TUSC2 is down-regulated in human thyroid tumors

Finally, we evaluated by immunohistochemistry the expression level of TUSC2 protein in a panel of human thyroid carcinoma tissues, including 37 normal thyroids (NT), 20 PTCs, 9 PDCs and 40 ATCs. As reported in Table 6, all normal thyroids examined showed TUSC2 positivity, with ~60% of samples showing strong TUSC2 staining (+++). On the contrary TUSC2 was undetectable in all PDC and ATC samples. An intermediated positivity of staining was seen in PTC, suggesting a correlation between TUSC2 down-regulation and tumor progression (Table 6). A representative image of TUSC2 staining is shown in Figure 26.

Table 6: TUSC2 expression in thyroid samples (n = 106).

TUSC2	NT (N = 37)	PTC (N = 20)	PDC (N = 9)	ATC (N = 40)
+++	22 (59.5%)	-	-	-
++	11 (29.8%)	1 (5%)	-	-
+	4 (10.8%)	4 (20%)	-	1 (2.5%)
Negative	-	15 (75%)	9 (100%)	39 (97.5%)

+: ≥ 5 – ≤ 25% of positive cells; ++: > 25 – <60% of positive cells; +++: ≥ 60% of positive cells. Percentage of positive samples respect to each group was reported in parenthesis.
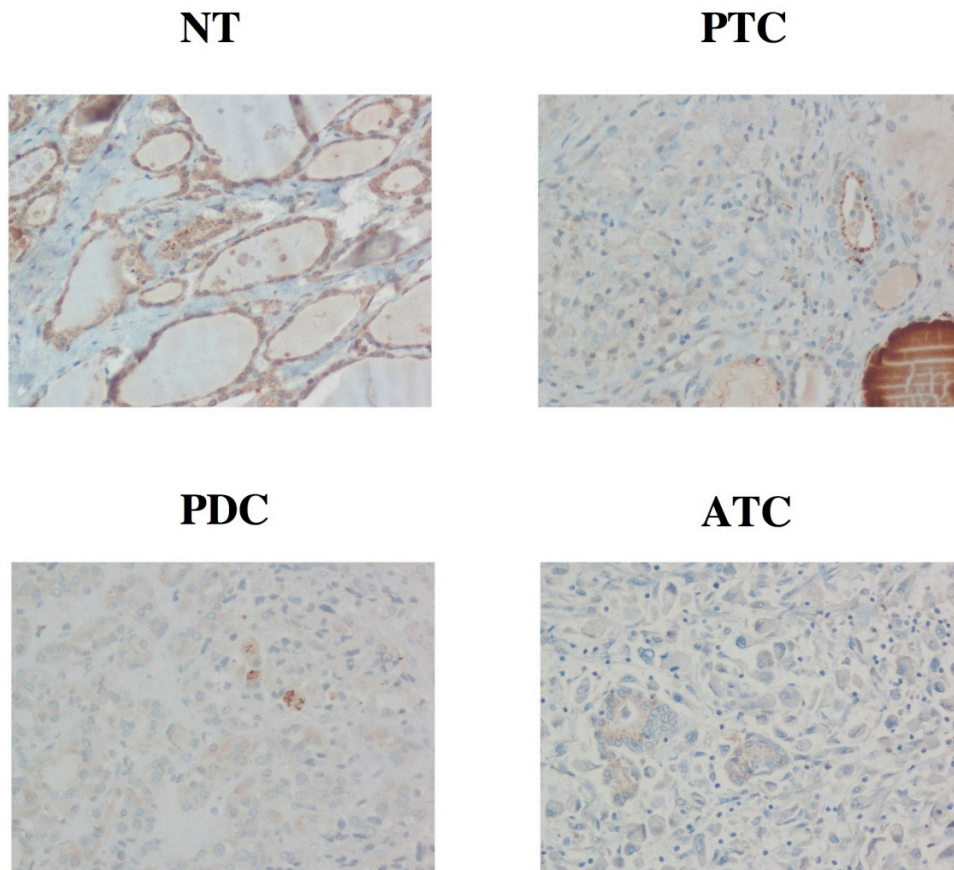
Figure 26. Expression of TUSC2 in thyroid tissue samples. Immunohistochemical analysis of TUSC2 protein expression in normal and malignant thyroid tissues. Representative histological sections from NT (20 X magnification), classical PTC (20 X magnification), PDC (20 X magnification), and ATC (20 X and magnification) stained with an anti-TUSC2 antibody are shown.

5. DISCUSSION

Anaplastic thyroid cancer (ATC) is the most lethal histotype of thyroid cancer, responsible for more than one-third of thyroid cancer-related deaths. The fast-growing nature of this type of cancer and its refractoriness to radioiodine treatment limit the efficacy of therapeutic interventions.

Previously, we have demonstrated that Twist1 transcription factor is up-regulated, both at mRNA and protein level, in approximately 50% of ATC. Twist1 plays a pleiotropic role in determining the ATC phenotype affecting cell migration, invasion and resistance to apoptosis (Salerno et al. 2011).

This dissertation is focused on unraveling the molecular mechanisms responsible for Twist1 biological effects in thyroid cancer cells. To achieve this goal, we have analyzed mRNA and miRNA expression profile of TPC cells over-expressing Twist1 protein.

mRNA signature in TPC-Twist1 cells was enriched for genes involved in invasion, migration and apoptosis consistent with the role of Twist1 in anaplastic thyroid cancer cells. We focused on the up-regulated genes because more is known about the role of Twist1 as transcriptional activator. The top up-regulated genes by more than 4-fold studied were: HS6ST2, COL1A1, KRT7, F2RL1, LEPREL1, THRB, ID4, RHOB, PDZK1, and PDZK1IP1.

Chromatin immunoprecipitation provides evidence that these genes are direct transcriptional targets of Twist1. Herein, we also demonstrated that HS6ST2, COL1A1, F2RL1, LEPREL1, PDZK1, and PDZK1IP1 are over-expressed in ATC. Moreover, immunohistochemistry analysis showed that LEPREL1 was over-expressed in 67% of ATC and in 26% of PTC cases. In the same dataset, Twist1 was over-expressed in 62% of ATC and in 0% of PTC samples. Interestingly, many of the identified Twist1 targets are over-expressed also in PTC where Twist1 is negative (Figure 13). It is possible that other factors regulate the identified target genes in Twist1 negative samples. Furthermore, we have performed a gene expression profile in TPC-Twist1 cells that, although express high levels of Twist1, are a cell line and thus could be not representative of thyroid cancer complexity.

Heparan sulfate 6-O-sulfotransferase 2 (HS6ST2) is an enzyme that attaches sulfate groups to glucosamine residues in heparan sulfate. Heparan sulfate proteoglycans are ubiquitous components of the cell surface, extracellular matrix, and basement membranes and interact with various ligands to influence cell growth, differentiation, adhesion, and migration (Song et al. 2011). Importantly, it was recently reported that the specific inhibition of HS6ST2 by heparin and a high-molecular-weight *Escherichia coli* K5-derived heparin-like polysaccharide (K5-NSOS) efficiently reduced osteolytic lesion area and metastatic tumor burden in a mouse model of breast cancer bone metastasis (Pollari et al. 2012).

LEPREL1 encodes a member of the prolyl 3-hydroxylase subfamily of 2-

oxo-glutarate-dependent dioxygenases. These enzymes play a critical role in collagen chain assembly, stability, and cross-linking by catalyzing post-translational 3-hydroxylation of proline residues (Fernandes et al. 2011). Hypoxia-inducible factor 1 activates the transcription of collagen prolyl hydroxylases (Gilkes et al. 2013). Of note, Twist1 is a downstream target of hypoxia-inducible factor 1 (Yang et al. 2008). Noteworthy, an ethyl 3,4-dihydroxybenzoate, a prolyl hydroxylase inhibitor, decreased tumor fibrosis and metastasis in a mouse model of breast cancer (Gilkes et al. 2013). During cancer progression, increased deposition of collagens can occur within and near the primary tumors, and it is associated with a poor outcome due to increased local invasion and distant metastasis (Conklin et al. 2011). Straightened and aligned collagen fibers in tumor samples are predictive of patient mortality, presumably because collagen fibers provide directional cues that dictate cell morphology and promote cell migration as well as induce stiffness, which promotes tissue tension to enhance cancer progression (Provenzano et al. 2006).

Indeed, in TPC-Twist1 cells, we found up-regulated COL1A1 (7.2 ± 1.4), COL4A1 (2.0 ± 0.05), COL18A1 (1.7 ± 0.1), COL4A2 (1.5 ± 0.2) (data are described in the manuscript I). These results are in agreement with Hébrant and colleagues (Hébrant et al. 2012) who demonstrated that one of the clusters that differentiated ATC *vs* PTC is composed of genes involved in calcification and fibrosis processes.

PDZK1IP1, also known as membrane-associated protein 17 (MAP17), is a small 17-kDa non-glycosylated membrane protein over-expressed in a great variety of human carcinomas. Immunohistochemical analysis of PDZK1IP1 shows that over-expression of the protein strongly correlates with tumor progression (Birrane et al. 2013). The increased malignant cell behavior induced by PDZK1IP1 is associated with an increase in reactive oxygen species production, and the treatment of PDZK1IP1-expressing cells with antioxidants resulted in a reduction in the tumorigenic properties of these cells (Cancero et al. 2012; Birrane et al. 2013).

Coagulation factor II (thrombin) receptor-like 1 (F2RL1), also known as protease-activated receptor 2 (PAR2), is a member of the large family of 7-transmembrane- region receptors that couple to guanosine nucleotide- binding proteins and is a key signaling component for proteases in vascular biology and tumor progression (Schaffner et al. 2012). PAR2 is involved in tissue factor (TF) signaling pathway and plays a crucial role in tumor growth. TF forms a catalytic enzyme complex with coagulation factor VIIa, and selective inhibition of TF-factor VIIa-PAR2 signaling using a monoclonal antibody was shown to reduce breast tumor growth. Consistent with the hypothesis that F2RL1 mediated signaling contributes to tumor growth in breast cancer, mice lacking F2RL1 exhibited reduced tumor growth in a model of spontaneous mammary tumors (Versteeg et al. 2008).

Thus, we have identified a set of novel direct transcriptional targets of Twist1. The identified targets could be important to mediate Twist1 biological

effects also in other malignancies such as breast and prostate carcinoma and sarcoma where Twist1 is over-expressed (Ansieau et al. 2010). All the genes identified are potential targets for cancer therapy. Indeed, HS6ST2 and LEPREL1 are enzymes, whereas PDZK1IP1 and F2RL1 are membrane proteins and thus targetable by small molecules or monoclonal antibodies respectively (Imai et al. 2006).

Recently, deregulation of microRNAs (miRNAs), a class of small endogenous RNAs that regulated the protein expression, has been implicated in tumorigenesis and cancer progression. A large body of evidence shows that human tumors are characterized by a global miRNA down-regulation, hence their oncogenic targets are over-expressed enhancing tumor proliferation, invasion and metastasis, what makes this cancers perfect targets for the use of specific miRNA mimetics as therapeutics tools. On the contrary, in human cancer some specific miRNAs are up-regulated with oncogenic potential (oncomiRs) and, thus, they are possible therapeutic targets for inhibition. To date, oncogenic miRNAs can be inhibited by using antisense oligonucleotides, antagomirs, sponges or locked nucleic acid (LNA) constructs (Garzon et al. 2010).

By analyzing the miRNome of human thyroid carcinomas it has been shown up-regulation of miRNAs, such as miR-146b, miR-221, and miR-222, in ATC and also in differentiated thyroid cancer (papillary and follicular), indicating that these miRNAs' over-expression is essential in maintaining tumorigenesis. However, specific miRNAs are down-regulated in ATC, such as those of the miR-200 and miR-30 families, which are important negative regulators of cell migration, invasion, and epithelial-to-mesenchymal transition (EMT) (Braun et al. 2010; Visone et al. 2007).

To unravel miRNA regulated by Twist1, we have explored miRNA expression profile of TPC-Twist1 protein, using a miRNACHIP microarray. We found 51 miRNAs changed (14 up-regulated, Table 4, and 37 down-regulated, Table 5) by more than 2 fold in TPC-Twist1 cells in comparison to control.

We searched in our array miRNA that were previously reported to be deregulated in ATC samples. TPC-Twist1 cells down-regulated with respect to control miR-148b (Table 5). The paper of Braun and the paper of Visone, reported a down-regulation of this miRNA in ATC samples in comparison to normal thyroid. Interestingly, miR-148b is also down-regulated in aggressive breast and lung tumors, in which it is a major coordinator of malignancy influencing invasion, survival to anoikis, extravasation, metastasis formation, and chemotherapy response (Cimino et al. 2013).

In addition, also miR-301a and miR-301b, down-regulated in several microarray of ATC samples (Braun et al. 2010), were decreased in our array (Table 5).

We found a significant decrease in miR-200c in TPC-Twist1 cells compared to control (Table 5). miR-200 family is involved in EMT and tumor invasion and was found to be down-regulated in ATC but not in PTC and FTC.

Restoration of miR-200 family members in ATC cells reduced their invasive potential and inhibited EMT (Braun et al. 2010).

miR-15b targets directly the expression of BMI1; interestingly, BMI1 cooperates with Twist1 in repressing E-cadherin and promoting EMT. miR-15b was down-regulated in TPC-Twist1 cells respect to control cells (Table 5).

Despite the general reduction of miRNA expression levels in cancers, several miRNAs are up-regulated; some of them play oncogenic role (Di Leva et al. 2014). Among Twist1 induced miRNAs, miR-584 was found to be one of the most up-regulated, showing a ~ 6-fold increase in TPC-Twist1 cells with respect to the control cells. The human miR-584 is located within the chromosome 5q32. miR-584 promoter displays 13 consensus binding sites for Twist1 (E-boxes), therefore we are currently performing chromatin immunoprecipitation to formally prove that Twist1 direct regulates its expression.

Quantitative-RT-PCR was performed to evaluate the expression of miR-584 in a panel of normal thyroid, PTC and ATC samples. All undifferentiated samples showed a statistically significant higher expression of miR-584 compared to normal thyroid and PTC samples, suggesting that Twist1 over-expression could induce miR-584 expression also *in vivo*.

To address miR-584 role in thyroid cell biology, we have conducted functional experiments by ectopic transfection of miR-584 in well-differentiated thyroid carcinoma cells (TPC) and by silencing miR-584, through the transfection of Anti-miR-584 plasmid, in TPC-Twist1 cells.

We determined the effects of miR-584 on sensitivity of TPC cells to apoptosis induced by two different agents Doxorubicin and Staurosporine. Doxorubicin elicits its anti-neoplastic activity by binding to DNA and distrusting template functions or by inhibition of topoisomerase II activities, Staurosporine is an inhibitor of protein kinase. Here we showed that miR-584 is involved in resistance to induced apoptosis in thyroid carcinoma cells. On the other hand miR-584 forced expression or silencing did not affect cell proliferation, migration and invasion.

The biological functions of miRNAs are highly dependent on cellular context, which may be due to the differential expression of their targets mRNAs. Accordingly, some miRNAs are oncogenic and up-regulated in one cancer type but are tumor suppressive and down-regulated in another cancer type, consequently, miRNA functions across different contexts and tissues (Di Leva et al. 2014). Consistently miR-584 was found to be down-regulated in other types of neoplasm such as glioma where could suppress cell growth (Wang et al. 2014). Moreover, down-regulation of miR-584 is required for TGF-β-induced cell migration of breast cancer cells (Fils-Aimé et al. 2013).

In agreement with our findings, miR-584 was found up-regulated in a microarray screening of different malignant thyroid tissues compared to benign lesions (Vriens et al. 2011).

miRNAs generally bind to target mRNA through their 3'untranslated regions (UTRs) and recruit the RNA-induced silencing complex, which

mediates the inhibition of translation and the degradation of the respective mRNA. To identify targets of miR-584 we used several computational algorithms based on conservation criteria such as Targetscan, Pictar, DianaLab, miRDB and Miranda. Among targets predicted by all five computational methods, TUSC2 was of particular interest because its role in carcinogenesis. Tumor suppressor candidate 2 (TUSC2), also known as FUS1, is a tumor suppressor gene located on human chromosome 3p21.3, a region in which deficient gene expression is frequently seen in lung cancer (Lerman et al. 2000). Indeed, a reduction or complete loss of TUSC2 expression was found in 82% of non–small-cell lung cancer cell lines and in 100% of small-cell lung cancer cell lines studied and was associated with significantly worse overall survival (Deng et al. 2008). Genes in the 3p21.3 region are associated with cell differentiation, cell proliferation, ion exchange and transportation, apoptosis, and cell death (Ji et al. 2005). Over-expression of TUSC2 significantly inhibits tumor growth and progression in mouse models and TUSC2 knockout mice show an increased frequency of spontaneous cancers (Ivanova et al. 2007).

The 3'UTR of TUSC2 is highly conserved, strongly suggesting that it plays an important role in regulating TUSC2 expression (Du et al. 2009). Here, we show that miR-584 directly interacts with the 3′-untranslated region (3'UTR) of TUSC2, leading to down-regulation of protein expression. In fact, deletion of this site renders the reporter construct insensitive to miR-584 expression.

We are currently verifying if TUSC2 revert the biological effects induced by miR-584 to further prove that TUSC2 is a miR-584 target.

In this dissertation, we demonstrated that TUSC2 was down-regulated not only in ATC but also in PTC and PDC samples where Twist1 and miR-584 are not expressed. These suggest that other mechanism could modulate the expression of TUSC2 in PTC and PDC samples. Notably, loss or reduced TUSC2 expression could be caused by various mechanisms. For example, allelic loss of the 3p21.3 chromosomal region containing TUSC2 is the major cause of loss or reduction of TUSC2 expression in lung cancer (Prudkin et al. 2008). One mechanism regulating TUSC2 expression and function has already been shown by Uno et al. who showed that loss of myristoylation of TUSC2 protein causes it to be rapidly degraded and removes its ability to suppress tumor growth (Uno et al. 2004).

Preclinical studies in human lung cancer cell lines identified the intrinsic apoptosis pathway as a mediator of cell death following forced expression of TUSC2 (Ji et al. 2008; Deng et al. 2007). To translate these finding into clinical applications for molecular cancer therapy, a novel TUSC2-expressing nanoparticle has been developed for treating patients with lung cancer. Nanoparticles have been reported to deliver drugs and siRNA to tumors in humans. Lu and coworkers first showed, in phase I of clinical trial, the ability of systemic administration of genes via this DC nanoparticle vector to efficiently deliver therapeutic tumor suppressor genes, to suppress metastasis growth and to prolong survival. In particular, they observed major changes in

gene expression in the intrinsic pro-apoptotic pathway in the tumor following DC-TUSC2 treatment (Lu et al. 2012). Thus, the low level of side effects after repeated DC administrations is very encouraging suggesting that DC-TUSC2 may be combined with small molecule targeted drugs at an effective dose. They observed major changes in gene expression in the intrinsic pro-apoptotic pathway in the tumor following DC-TUSC2 treatment.

Benefits obtained from chemotherapy and radiation therapy of ATC remains only marginal and there are no alternative treatments yet, therefore new therapeutic approaches are needed. To date several approaches are suggested: silencing of one or more miRNA up-regulated in tumor cells (i.e. miR-584), may be an interesting approach to treat the ATC patients, but, of course, it raises the question of cell specificity.

Here we showed that miR-584 enables thyroid cancer cells to acquire resistance to chemotherapeutics induced apoptosis. Further experiments are on going in our laboratory to characterize the molecular mechanisms of resistance to apoptosis induced by miR-584.

Over-expression of miR-584 inhibits synthesis of the TUSC2 protein by targeting the 3'UTR of TUSC2. Importantly, TUSC2 is progressively down-regulated in PTC, PDC and ATC tissues suggesting that TUSC2 is also likely to be involved in thyroid cancer progression, with implications for TUSC2 targeting as a rational therapeutic strategy in ATC.

6. CONCLUSIONS

Anaplastic thyroid carcinoma (ATC) is the least common but the most lethal type of thyroid cancers. We previously showed that Twist1 transcription factor plays a pleiotropic role in determining malignant features of the anaplastic phenotype. In this dissertation, we aimed to identify transcriptional targets of Twist1 because they could be more realistic for therapeutic intervention. Here, we have identified a set of mRNA and miRNA regulated by Twist1, which mediates the biological effects of Twist1 in thyroid carcinoma cells. Consistent with the biological functions of Twist1 in ATC, mRNA targets of Twist1 affected cellular movement, cellular growth and proliferation and cell death and survival. Further, we identified a set of miRNA potentially regulated by Twist1. We focused on miR-584 and showed that is up-regulated in ATCs respect to normal thyroids as well as to poorly and well differentiated thyroid carcinomas. The ectopic expression of miR-584 enables thyroid cancer cells to acquire resistance to apoptosis. Finally, we have identified among the putative mRNA targets of miR-584, TUSC2 tumor suppressor.

7. ACKNOWLEDGEMENTS

8. REFERENCES

- Ansieau S, Bastid J, Doreau A, Morel AP, Bouchet BP, Thomas C, Fauvet F, Puisieux I, Doglioni C, Piccinin S, Maestro R, Voeltzel T, Selmi A, Valsesia-Wittmann S, Caron de Fromentel C, Puisieux A. Induction of EMT by twist proteins as a collateral effect of tumor-promoting inactivation of premature senescence. Cancer Cell 2008 (a); 14: 79-89.
- Ansieau S, Morel AP, Hinkal G, Bastid J, Puisieux A. TWISTing an embryonic transcription factor into an oncoprotein. Oncogene 2010 3; 29(22):3173-84.
- Baldini E, D'Armiento M, Ulisse S. A new aurora in anaplastic thyroid cancer therapy. Int J Endocrinol. 2014;2014:816430. doi: 10.1155/2014/816430. Epub 2014 Jul 1. Review. PubMed PMID: 25097550; PubMed Central PMCID: PMC4106108.
- Bartel DP. MicroRNAs: target recognition and regulatory functions. Cell. 2009 Jan 23;136(2):215-33. doi: 10.1016/j.cell.2009.01.002. Review. PubMed PMID:19167326; PubMed Central PMCID: PMC3794896.
- Bauer AJ, Patel A, Terrell R, Doniparthi K, Saji M, Ringel M, Tuttle RM, Francis GL. Systemic administration of vascular endothelial growth factor monoclonal antibody reduces the growth of papillary thyroid carcinoma in a nude mouse model. Ann Clin Lab Sci. 2003 Spring;33(2):192-9. PubMed PMID: 12817624.
- Begum S, Rosenbaum E, Henrique R, Cohen Y, Sidransky D, Westra WH. BRAF mutations in anaplastic thyroid carcinoma: implications for tumor origin, diagnosis and treatment. Mod Pathol. 2004; 17(11): 1359-63.
- Bialek P, Kern B, Yang X, Schrock M, Sosic D, Hong N, Wu H, Yu K,Ornitz DM, Olson EN, Justice MJ, Karsenty G. A twist code determines the onset of osteoblast differentiation. Dev Cell 2004; 6: 423-35.
- Bible KC, Suman VJ, Menefee ME, Smallridge RC, Molina JR, Maples WJ, Karlin NJ, Traynor AM, Kumar P, Goh BC, Lim WT, Bossou AR, Isham CR, Bieber C, Burton JK, Harris P, Erlichman C; Mayo Phase 2 Consortium; Mayo Clinic Endocrine Malignances Disease Oriented Group. A multiinstitutional phase 2 trial of pazopanib monotherapy in advanced anaplastic thyroid cancer. J Clin Endocrinol Metab. 2012 Sep;97(9):3179-84. Epub 2012 Jul 6. PubMed PMID: 22774206.
- Bildsoe H, Loebel DA, Jones VJ, Chen YT, Behringer RR, Tam PP. Requirement for Twist1 in frontonasal and skull vault development in the mouse embryo. Dev Biol. 2009 15; 331 (2):176-88.
- Birrane G, Mulvaney EP, Pal R, Kinsella BT, Kocher O. Molecular Analysis of the Prostacyclin Receptor's Interaction with the PDZ1

Domain of Its Adaptor Protein PDZK1. PLoS One. 2013;8 (2): e53819.

- Bourgeois P, Bolcato-Bellemin AL, Danse JM, Bloch-Zupan A, Yoshiba K, Stoetzel C, Perrin-Schmitt F. The variable expressivity and incomplete penetrance of the twist-null heterozygous mouse phenotype resemble those of human Saethre-Chotzen syndrome. Hum Mol Genet. 1998 (6): 945-57.
- Braun J, Hoang-Vu C, Dralle H, Hüttelmaier S. Downregulation of microRNAs directs the EMT and invasive potential of anaplastic thyroid carcinomas. Oncogene. 2010 Jul 22;29(29):4237-44. doi: 10.1038/onc.2010.169. Epub 2010 May 24. PubMed PMID: 20498632.
- Braun J, Hoang-Vu C, Dralle H, Hüttelmaier S. Downregulation of microRNAs directs the EMT and invasive potential of anaplastic thyroid carcinomas.Oncogene. 2010 Jul 22;29(29):4237-44. doi: 10.1038/onc.2010.169. Epub 2010 May 24. PubMed PMID: 20498632.
- Cahill S, Smyth P, Finn SP, Denning K, Flavin R, O'Regan EM, Li J, Potratz A, Guenther SM, Henfrey R, O'Leary JJ, Sheils O. Effect of ret/PTC 1 rearrangement on transcription and post-transcriptional regulation in a papillary thyroid carcinoma model. Mol Cancer. 2006 Dec 11;5:70. PubMed PMID: 17156473; PubMed Central PMCID: PMC1713250.
- Caillou B, Talbot M, Weyemi U, Pioche-Durieu C, Al Ghuzlan A, Bidart JM, Chouaib S, Schlumberger M, Dupuy C. Tumor-associated macrophages (TAMs) form an interconnected cellular supportive network in anaplastic thyroid carcinoma. PLoS One. 2011;6(7):e22567. doi: 10.1371/journal.pone.0022567. Epub 2011 Jul 21.PubMed PMID: 21811634; PubMed Central PMCID: PMC3141071.
- Cancer Genome Atlas Research Network. Integrated genomic characterization of papillary thyroid carcinoma. Cell. 2014 Oct 23;159(3):676-90. doi:10.1016/j.cell.2014.09.050. PubMed PMID: 25417114; PubMed Central PMCID:PMC4243044.
- Castanon I, Baylies MK. A Twist in fate: evolutionary comparison of Twist structure and function. Gene. 2002 Apr 3;287(1-2):11-22. Review. PubMed PMID: 11992718.
- Catalano MG, Fortunati N, Boccuzzi G. Epigenetics modifications and therapeutic prospects in human thyroid cancer. Front Endocrinol. 2012 Mar 19;3:40. doi: 10.3389/fendo.2012.00040. eCollection 2012. PubMed PMID: 22649419; PubMed Central PMCID: PMC3355953.
- Charles RP, Silva J, Iezza G, Phillips WA, McMahon M. Activating BRAF and PIK3CA mutations cooperate to promote anaplastic thyroid carcinogenesis. Mol Cancer Res. 2014 Jul;12(7):979-86. doi: 10.1158/1541-7786.MCR-14-0158-T. Epub 2014 Apr 25. PubMed PMID: 24770869.
- Chen ZF, Behringer RR. Twist is required in head mesenchyme for cranial neural tube morphogenesis. Genes Dev 1995; 9: 686-99.
- Cheng GZ, Zhang W, Wang LH. Regulation of cancer cell survival,

migration, and invasion by Twist: AKT2 comes to interplay. Cancer Res. 2008 Feb 15;68(4):957-60.doi: 10.1158/0008-5472.CAN-07-5067. Review. PubMed PMID: 18281467.

- Cho KH, Choi MJ, Jeong KJ, Kim JJ, Hwang MH, Shin SC, Park CG, Lee HY. A ROS/STAT3/HIF-1α signaling cascade mediates EGF-induced TWIST1 expression and prostate cancer cell invasion. Prostate. 2014 May;74(5):528-36. doi: 10.1002/pros.22776. PubMed PMID: 24435707.

- Ciampi R, Knauf JA, Rabes HM, Fagin JA, Nikiforov YE. BRAF kinase activation via chromosomal rearrangement in radiation-induced and sporadic thyroid cancer. Cell Cycle. 2005 Apr;4(4):547-8. Epub 2005 Apr 24. Review. PubMed PMID: 15753649.

- Cimino D, De Pittà C, Orso F, Zampini M, Casara S, Penna E, Quaglino E, Forni M, Damasco C, Pinatel E, Ponzone R, Romualdi C, Brisken C, De Bortoli M, Biglia N, Provero P, Lanfranchi G, Taverna D. miR148b is a major coordinator of breast cancer progression in a relapse-associated microRNA signature by targeting ITGA5, ROCK1, PIK3CA, NRAS, and CSF1. FASEB J. 2013 Mar;27(3):1223-35. doi: 10.1096/fj.12-214692. Epub 2012 Dec 11. PubMed PMID: 23233531.

- Cohen EE, Tortorici M, Kim S, Ingrosso A, Pithavala YK, Bycott P. A Phase II trial of axitinib in patients with various histologic subtypes of advanced thyroid cancer: long-term outcomes and pharmacokinetic/ pharmacodynamic analyses. Cancer Chemother Pharmacol. 2014 Dec;74(6):1261-70. doi:10.1007/s00280-014-2604-8. Epub 2014 Oct 15. PubMed PMID: 25315258.

- Conklin MW, Eickhoff JC, Riching KM, Pehlke CA, Eliceiri KW, Provenzano PP, Friedl A, Keely PJ. Aligned collagen is a prognostic signature for survival in human breast carcinoma. Am J Pathol. 2011 Mar;178(3):1221-32. doi: 10.1016/j.ajpath.2010.11.076. PubMed PMID: 21356373.

- De Craene B, Berx G. Regulatory networks defining EMT during cancer initiation and progression. Nat Rev Cancer. 2013 Feb;13(2):97-110. doi: 10.1038/nrc3447. Review. PubMed PMID: 23344542.

- Deng WG, Wu G, Ueda K, Xu K, Roth JA, Ji L. Enhancement of antitumor activity of cisplatin in human lung cancer cells by tumor suppressor FUS1. Cancer Gene Ther. 2008 Jan;15(1):29-39. Epub 2007 Sep 7. PubMed PMID: 17828283.

- Deshpande HA, Roman S, Sosa JA. New targeted therapies and other advances in the management of anaplastic thyroid cancer. Curr Opin Oncol. 2013 Jan;25(1):44-9. doi: 10.1097/CCO.0b 013e32835a448c. Review. PubMed PMID: 23159847.

- Di Leva G, Garofalo M, Croce CM. MicroRNAs in cancer. Annu Rev Pathol.2014;9:287-314. doi: 10.1146/annurev-pathol-012513-104715. Epub 2013 Sep 25.Review. PubMed PMID: 24079833; PubMed Central PMCID: PMC4009396.

- Djuranovic S, Nahvi A, Green R. A parsimonious model for gene regulation by miRNAs. Science. 2011 Feb 4;331(6017):550-3. doi: 10.1126/science.1191138.Review. PubMed PMID: 21292970; PubMed Central PMCID: PMC3955125.
- Dobrian AD. A tale with a Twist: a developmental gene with potential relevance for metabolic dysfunction and inflammation in adipose tissue. Front Endocrinol (Lausanne). 2012; 3:108.
- Du J, Sun B, Zhao X, Gu Q, Dong X, Mo J, Sun T, Wang J, Sun R, Liu Y. Hypoxia promotes vasculogenic mimicry formation by inducing epithelial-mesenchymal transition in ovarian carcinoma. Gynecol Oncol. 2014 Jun;133(3):575-83. doi: 10.1016/j.ygyno.2014.02.034. Epub 2014 Feb 28. PubMed PMID: 24589413.
- Dumont N, Wilson MB, Crawford YG, Reynolds PA, Sigaroudinia M, Tlsty TD. Sustained induction of epithelial to mesenchymal transition activates DNA methylation of genes silenced in basal-like breast cancers. Proc Natl Acad Sci U S A. 2008 Sep 30;105(39):14867-72. doi: 10.1073/pnas.0807146105. Epub 2008 Sep 19. PubMed PMID: 18806226.
- Duquette M, Sadow PM, Lawler J, Nucera C. Thrombospondin-1 Silencing Down-Regulates Integrin Expression Levels in Human Anaplastic Thyroid Cancer Cells with BRAF(V600E): New Insights in the Host Tissue Adaptation and Homeostasis of Tumor Microenvironment. 2013 Dec 2;4:189. doi: 10.3389/fendo.2013.00189. eCollection 2013. PubMed PMID: 24348463.
- Eberhardt NL, Grebe SK, McIver B, Reddi HV. The role of the PAX8/PPARgamma fusion oncogene in the pathogenesis of follicular thyroid cancer. Mol Cell Endocrinol. 2010; 321(1):50-6.
- Eckert MA, Lwin TM, Chang AT, Kim J, Danis E, Ohno-Machado L, Yang J. Twist1-induced invadopodia formation promotes tumor metastasis. Cancer Cell. 2011; 19(3): 372-86.
- El Ghouzzi V, Le Merrier M, Perrin-Schmitt F, Lajeunie E, Benit P, Renier D et al. Mutations of the TWIST gene in the Saethre- Chotzen syndrome. Nat Genet 1997; 15: 42-46.
- Esposito F, Tornincasa M, Pallante P, Federico A, Borbone E, Pierantoni GM, Fusco A. Down-regulation of the miR-25 and miR-30d contributes to the development of anaplastic thyroid carcinoma targeting the polycomb protein EZH2. J Clin Endocrinol Metab. 2012 May;97(5):E710-8. doi: 10.1210/jc.2011-3068. Epub 2012 Mar 7. PubMed PMID: 22399519.
- Evdokimova V, Tognon C, Ng T, Ruzanov P, Melnyk N, Fink D, Sorokin A, Ovchinnikov LP, Davicioni E, Triche TJ, Sorensen PH. Translational activation of snail1 and other developmentally regulated transcription factors by YB-1 promotes an epithelial-mesenchymal transition. Cancer Cell. 2009;15(5):402-15.
- Faam B, Ghaffari MA, Ghadiri A, Azizi F. Epigenetic modifications in

human thyroid cancer. Biomed Rep. 2015 Jan;3(1):3-8. PubMed PMID: 25469237.

- Fernandes RJ, Farnand AW, Traeger GR, Weis MA, Eyre DR. A role for prolyl 3-hydroxylase 2 in post-translational modification of fibril-forming collagens. J Biol Chem. 2011; 286(35):30662-9.

- Fils-Aimé N, Dai M, Guo J, El-Mousawi M, Kahramangil B, Neel JC, Lebrun JJ. MicroRNA-584 and the protein phosphatase and actin regulator 1 (PHACTR1), a new signaling route through which transforming growth factor-β Mediates the migration and actin dynamics of breast cancer cells. J Biol Chem. 2013Apr26;288(17):11807-23. doi: 10.1074/jbc.M112.430934. Epub 2013 Mar 11. PubMed PMID:23479725,

- Firulli BA, Howard MJ, McDaid JR, McIlreavey L, Dionne KM, Centonze VE, Cserjesi P, Virshup DM, Firulli AB. PKA, PKC, and the protein 60 phosphatase 2A influence HAND factor function: a mechanism for tissuespecific transcriptional regulation. Mol Cell; 12(5): 1225-37.

- Fury MG, Sherman E, Haque S, Korte S, Lisa D, Shen R, Wu N, Pfister D. A phase I study of daily everolimus plus low-dose weekly cisplatin for patients with advanced solid tumors. Cancer Chemother Pharmacol. 2012 Mar;69(3):591-8. doi: 10.1007/s00280-011-1734-5. Epub 2011 Sep 13. PubMed PMID: 21913034.

- Gajula RP, Chettiar ST, Williams RD, Nugent K, Kato Y, Wang H, Malek R, Taparra K, Cades J, Annadanam A, Yoon AR, Fertig E, Firulli BA, Mazzacurati L, Burns TF, Firulli AB, An SS, Tran PT. Structure-Function Studies of the b HLH Phosphorylation Domain of TWIST1 in ProstateCancerCells. Neoplasia.2015Jan;17(1):16-31.doi: 10.1016/j.neo. 2014.10.009. PubMed PMID: 25622896;

- Galvan JA, Helbling M, Koelzer VH, Tschan MP, Berger MD, Hädrich M, Schnüriger B, Karamitopoulou E, Dawson H, Inderbitzin D, Lugli A, Zlobec I. TWIST1 and TWIST2 promoter methylation and protein expression in tumor stroma influence the epithelial-mesenchymal transition-like tumor budding phenotype in colorectal cancer. Oncotarget. 2015 Jan 20;6(2):874-85. PubMed PMID: 25528769.

- Gandolfi G, Sancisi V, Piana S, Ciarrocchi A. Time to re-consider the meaning of BRAF V600E mutation in papillary thyroid carcinoma. Int J Cancer. 2014 May 15.doi: 10.1002/ijc.28976. PubMed PMID: 24828987.

- Gilkes DM, Chaturvedi P, Bajpai S, Wong CC, Wei H, Pitcairn S, Hubbi ME, Wirtz D, Semenza GL. Collagen prolyl hydroxylases are essential for breast cancer metastasis. Cancer Res. 2013 Jun 1;73(11):3285-96. doi:10.1158/0008-5472.CAN-12-3963. Epub 2013 Mar 28. PubMed PMID: 23539444.

- Granata R, Locati L, Licitra L. Therapeutic strategies in the management of patients with metastatic anaplastic thyroid cancer:

review of the current literature. Curr Opin Oncol. 2013 May;25(3):224-8. doi: 10.1097/CCO.0b013e32835ff44b. Review. PubMed PMID: 23493194.

- Greco A, Roccato E, Pierotti MA. TRK oncogenes in papillary thyroid carcinoma. Cancer Treat Res. 2004;122:207-19. Review. PubMed PMID: 16209047.

- Gruber JJ, Colevas AD. Differentiated Thyroid Cancer: Focus on Emerging Treatments for Radioactive Iodine-Refractory Patients. Oncologist. 2015 Feb;20(2):113-126. Epub 2015 Jan 23. Review. PubMed PMID: 25616432.

- Haftmann C, Stittrich AB, Zimmermann J, Fang Z, Hradilkova K, Bardua M, Westendorf K, Heinz GA, Riedel R, Zimmel D, Rajewsky N, Jäck HM, Radbruch A, Mashreghi MF. miR-148a is upregulated by Twist1 and T-bet and promotes Th1-cell survival by regulating the proapoptotic gene Bim. Eur J Immunol. 2014 Dec 8. doi: 10.1002/eji.201444633.

- Hamamori Y, Sartorelli V, Ogryzko V, Puri PL, Wu HY, Wang JY, Nakatani Y, Kedes L. Regulation of histone acetyltransferases p300 and PCAF by the bHLH protein twist and adenoviral oncoprotein E1A. Cell. 1999 Feb 5;96(3):405-13. PubMed PMID: 10025406.

- Hanahan D, Weinberg RA. Hallmarks of cancer: the next generation. Cell. 2011 Mar 4;144(5):646-74. doi: 10.1016/j.cell.2011.02.013. Review. PubMed PMID: 21376230.

- Hébrant A, Dom G, Dewaele M, Andry G, Trésallet C, Leteurtre E, Dumont JE, Maenhaut C. mRNA expression in papillary and anaplastic thyroid carcinoma:molecular anatomy of a killing switch. PLoS One. 2012;7(10):e37807. doi:10.1371/journal.pone.0037807. Epub 2012 Oct 24. PubMed PMID: 23115614.

- Hébrant A, Floor S, Saiselet M, Antoniou A, Desbuleux A, Snyers B, La C, de Saint Aubain N, Leteurtre E, Andry G, Maenhaut C. miRNA expression in anaplastic thyroid carcinomas. PLoS One. 2014 Aug 25;9(8):e103871. doi: 10.1371/journal.pone.0103871. eCollection 2014. PubMed PMID: 25153510; PubMed Central PMCID: PMC4143225.

- Hemerly JP, Bastos AU, Cerutti JM. Identification of several novel non-p.R132 IDH1 variants in thyroid carcinomas. Eur J Endocrinol 2010;163:747-755.

- Hermeking H. MicroRNAs in the p53 network: micromanagement of tumour suppression. Nat Rev Cancer. 2012 Sep;12(9):613-26. doi: 10.1038/nrc3318. Epub 2012 Aug 17. Review. PubMed PMID: 22898542.

- Holderfield M, Deuker MM, McCormick F, McMahon M. Targeting RAF kinases for cancer therapy: BRAF-mutated melanoma and beyond. Nat Rev Cancer. 2014 Jul;14(7):455-67. doi: 10.1038/nrc3760. Review. PubMed PMID: 24957944; PubMed Central PMCID:

PMC4250230.

- Hong J, Zhou J, Fu J, He T, Qin J, Wang L, Liao L, Xu J. Phosphorylation of serine 68 of Twist1 by MAPKs stabilizes Twist1 protein and promotes breast cancer cell invasiveness. Cancer Res. 2011; 71(11): 3980-90.

- Horikawa T, Yang J, Kondo S, Yoshizaki T, Joab I, Furukawa M, Pagano JS. Twist and epithelial-mesenchymal transition are induced by the EBV oncoprotein latent membrane protein 1 and are associated with metastatic nasopharyngeal carcinoma. Cancer Res. 2007 67(5): 1970-8.

- Hosono S, Kajiyama H, Terauchi M, Shibata K, Ino K, Nawa A, Kikkawa F. Expression of Twist increases the risk for recurrence and for poor survival in epithelial ovarian carcinoma patients. Br J Cancer. 2007 Jan 29;96(2):314-20. Epub 2007 Jan 9. PubMed PMID: 17211477.

- Howlader, N. et al. SEER Cancer Statistics Review 1975–2009 (Vintage 2009 Populations). National Cancer Institute http://seer.cancer.gov/ csr/19752009pops09 (2012).

- Huang W, Chen Z, Shang X, Tian D, Wang D, Wu K, Fan D, Xia L. Sox12, a direct target of FoxQ1, promotes hepatocellular carcinoma metastasis through up-regulating Twist1 and FGFBP1. Hepatology. 2015 Feb 23. doi: 10.1002/hep.27756. PubMed PMID: 25704764.

- Imai K, Takaoka A. Comparing antibody and small-molecule therapies for cancer. Nat Rev Cancer. 2006;6:714–727.

- Isham CR, Bossou AR, Negron V, Fisher KE, Kumar R, Marlow L, Lingle WL, Smallridge RC, Sherman EJ, Suman VJ, Copland JA, Bible KC. Pazopanib enhances paclitaxel-induced mitotic catastrophe in anaplastic thyroid cancer. Sci Transl Med. 2013 Jan 2;5(166):166ra3. doi: 10.1126/scitranslmed.3004358. PubMed PMID: 23283368.

- Ivanova AV, Ivanov SV, Pascal V, Lumsden JM, Ward JM, Morris N, Tessarolo L, Anderson SK, Lerman MI. Autoimmunity, spontaneous tumourigenesis, and IL-15 insufficiency in mice with a targeted disruption of the tumour suppressor gene Fus1. J Pathol. 2007 Apr;211(5):591-601. PubMed PMID: 17318811.

- Je, Escobar-Cabrera; Lca, Berumen Safe; Ga, García Alcocer. The Role of Transcription Factor TWIST in Cancer Cells. Journal of Genetic Syndromes & Gene Therapy; 2013, Vol. 4.

- Jemal A, Siegel R, Xu J, Ward E. Cancer statistics, 2010. CA Cancer J Clin. 2010 Sep-Oct;60(5):277-300. doi: 10.3322/caac.20073. Epub 2010 Jul 7. Erratum in: CA Cancer J Clin. 2011 Mar-Apr;61(2):133-4. PubMed PMID: 20610543.

- Ji L, Minna J, Roth J (2005) 3p21.3 tumor suppressor cluster: prospects for translational applications. Future Oncol 1: 79–92.

- Jikuzono T, Kawamoto M, Yoshitake H, Kikuchi K, Akasu H, Ishikawa H, Hirokawa M, Miyauchi A, Shimizu K, Takizawa T. The miR-221/222 cluster, miR-10b and miR-92a are highly upregulated in

metastatic minimally invasive follicular thyroid carcinoma. Int J Oncol. 2013 Jun;42(6):1858-68. doi: 10.3892/ijo.2013.1879. Epub 2013 Apr 2. PubMed PMID: 23563786.

- Jung CK, Little MP, Lubin JH, Brenner AV, Wells SA Jr, Sigurdson AJ, Nikiforov YE. The increase in thyroid cancer incidence during the last four decades is accompanied by a high frequency of BRAF mutations and a sharp increase in RAS mutations. J Clin Endocrinol Metab. 2014 Feb;99(2):E276-85. doi: 10.1210/jc.2013-2503. Epub 2013 Nov 18. PubMed PMID: 24248188; PubMed Central PMCID: PMC3913801. 5

- Jung CW, Han KH, Seol H, Park S, Koh JS, Lee SS, Kim MJ, Choi IJ, Myung JK. Expression of cancer stem cell markers and epithelial-mesenchymal transition-related factors in anaplastic thyroid carcinoma. Int J Clin Exp Pathol. 2015 Jan 1;8(1):560-8. PubMed PMID: 25755746.

- Kelly LM, Barila G, Liu P, Evdokimova VN, Trivedi S, Panebianco F, Gandhi M, Carty SE, Hodak SP, Luo J, Dacic S, Yu YP, Nikiforova MN, Ferris RL, Altschuler DL, Nikiforov YE. Identification of the transforming STRN-ALK fusion as a potential therapeutic target in the aggressive forms of thyroid cancer. Proc Natl Acad Sci U S A. 2014 Mar 18;111(11):4233-8. doi: 10.1073/pnas.1321937111. Epub 2014 Feb 3. PubMed PMID: 24613930; PubMed Central MCID: PMC3964116.

- Kimura ET, Nikiforova MN, Zhu Z, KnaufJA, Nikiforov YE, Fagin JA. High prevalence of BRAF mutations in thyroid cancer: genetic evidence for constitutive activation of the RET/PTC-RAS-BRAF signaling pathway in papillary thyroid carcinoma. Cancer Res 2003; 63: 1454-7.

- Kondo T, Ezzat S, Asa SL. Pathogenetic mechanisms in thyroid follicular-cell neoplasia. Nat Rev Cancer. 2006 Apr;6(4):292-306. Review. PubMed PMID: 16557281.

- Kunstman JW, Juhlin CC, Goh G, Brown TC, Stenman A, Healy JM, Rubinstein JC, Choi M, Kiss N, Nelson-Williams C, Mane S, Rimm DL, Prasad ML, Larsson C, Carling T. Characterization of the mutational landscape of anaplastic thyroid cancer via whole-exome sequencing. Hum Mol Genet. 2015 Jan 9. pii: ddu749. PubMed PMID: 25576899.

- Lamouille S, Xu J, Derynck R. Molecular mechanisms of epithelial-mesenchymal transition. Nat Rev Mol Cell Biol. 2014 Mar;15(3):178-96. doi: 10.1038/nrm3758. Review. PubMed PMID: 24556840; PubMed Central PMCID: PMC4240281.

- Lee J, Hwang JA, Lee EK. Recent progress of genome study for anaplasticthyroid cancer. Genomics Inform. 2013 Jun;11(2):68-75. doi: 10.5808/GI.2013.11.2.68. Epub 2013 Jun 30. PubMed PMID: 23843772; PubMed Central PMCID: PMC3704929.

- Leone V, D'Angelo D, Rubio I, de Freitas PM, Federico A, Colamaio M, Pallante P, Medeiros-Neto G, Fusco A. MiR-1 is a tumor suppressor in thyroid carcinogenesis targeting CCND2, CXCR4, and SDF-1alpha. J Clin Endocrinol Metab. 2011 Sep;96(9):E1388-98. doi: 10.1210/jc.2011-0345. Epub 2011 Jul 13. PubMed PMID: 21752897.
- Li L, Yu C, Ren J, Ye S, Ou W, Wang Y, Yang W, Zhong G, Chen X, Shi H, Su X, Chen L, Zhu W. Synergistic effects of eukaryotic coexpression plasmid carrying LKB1 and FUS1 genes on lung cancer in vitro and in vivo. J Cancer Res Clin Oncol. 2014 Jun;140(6):895-907. PubMed PMID: 24659339.
- Lim JC, Koh VC, Tan JS, Tan WJ, Thike AA, Tan PH. Prognostic significance of epithelial-mesenchymal transition proteins Twist and Foxc2 in phyllodes tumours of the breast. Breast Cancer Res Treat. 2015 Feb;150(1):19-29. doi: 10.1007/s10549-015-3296-4. Epub 2015 Feb 13. PubMed PMID: 25677742.
- Lin SF, Lin JD, Chou TC, Huang YY, Wong RJ. Utility of a histone deacetylase inhibitor (PXD101) for thyroid cancer treatment. PLoS One. 2013 Oct 14;8(10):e77684. doi: 10.1371/journal.pone.0077684. eCollection 2013. PubMed PMID: 24155971; PubMed Central PMCID: PMC3796495.
- Liu Q, Kaneko S, Yang L, Feldman RI, Nicosia SV, Chen J, Cheng JQ. Aurora-A abrogation of p53 DNA binding and transactivation activity by phosphorylation of serine 215. J Biol Chem. 2004 Dec 10;279(50):52175-82. Epub 2004 Oct 6. PubMed PMID: 15469940.
- Liu R, Xing M. Diagnostic and prognostic TERT promoter mutations in thyroid fine-needle aspiration biopsy. Endocr Relat Cancer. 2014 Oct;21(5):825-30. doi: 10.1530/ERC-14-0359. Epub 2014 Aug 13. PubMed PMID: 25121551; PubMed Central PMCID: PMC4175020.
- Liu Y, Mayo MW, Xiao A, Hall EH, Amin EB, Kadota K, Adusumilli PS, Jones DR. Loss of BRMS1 promotes a mesenchymal phenotype through NF-kB-dependent regulation of Twist1. Mol Cell Biol. 2015 Jan;35(1):303-17. doi: 10.1128/MCB.00869-14. Epub 2014 Nov 3. PubMed PMID: 25368381.
- Liu Z, Hou P, Ji M, Guan H, Studeman K, Jensen K, Vasko V, El-Naggar AK, Xing M. Highly prevalent genetic alterations in receptor tyrosine kinases and phosphatidylinositol 3-kinase/akt and mitogen-activated protein kinase pathways in anaplastic and follicular thyroid cancers. J Clin Endocrinol Metab. 2008 Aug;93(8):3106-16. doi: 10.1210/jc.2008-0273. Epub 2008 May 20. PubMed PMID: 18492751.
- Low-Marchelli JM, Ardi VC, Vizcarra EA, van Rooijen N, Quigley JP, Yang J.Twist1 induces CCL2 and recruits macrophages to promote angiogenesis. Cancer Res.2013 Jan 15;73(2):662-71. doi: 10.1158/0008-5472.CAN-12-0653. PubMed PMID:23329645; Lu SM, Yu L, Tian JJ, Ma JK, Li JF, Xu W, Wang HB. Twist modulates lymphangiogenesis and correlates with lymph node metastasis in

supraglottic carcinoma. Chin Med J (Engl). 2011 May;124(10):1483-7. PubMed PMID: 21740802.

- Lu C, Stewart DJ, Lee JJ, Ji L, Ramesh R, Jayachandran G, Nunez MI, Wistuba II, Erasmus JJ, Hicks ME, Grimm EA, Reuben JM, Baladandayuthapani V, Templeton NS, McMannis JD, Roth JA. Phase I clinical trial of systemically administered TUSC2(FUS1)-nanoparticles mediating functional gene transfer in humans. PLoS One. 2012;7(4):e34833. doi: 10.1371/journal.pone.0034833. Epub 2012 Apr 25. PubMed PMID: 22558101.

- Lu SM, Yu L, Tian JJ, Ma JK, Li JF, Xu W, Wang HB. Twist modulates lymphangiogenesis and correlates with lymph node metastasis in supraglottic carcinoma. Chin Med J (Engl). 2011 May;124(10):1483-7. PubMed PMID: 21740802.

- Lv Q, Wang W, Xue J, Hua F, Mu R, Lin H, Yan J, Lv X, Chen X, Hu ZW. DEDD interacts with PI3KC3 to activate autophagy and attenuate epithelial-mesenchymal transition in human breast cancer. Cancer Res. 2012 ul1;72(13):3238-50. doi: 10.1158/0008-5472.CAN-11-3832. PubMed PMID: 22719072.

- Maestro R, Dei Tos AP, Hamamori Y, Krasnokutsky S, Sartorelli V, Kedes L, Doglioni C, Beach DH, Hannon GJ. Twist is a potential oncogene that inhibits apoptosis. Genes Dev. 1999 Sep 1;13(17):2207-17.

- Mancikova V, Castelblanco E, Pineiro-Yanez E, Perales-Paton J, de Cubas AA,Inglada-Perez L, Matias-Guiu X, Capel I, Bella M, Lerma E, Riesco-Eizaguirre G,Santisteban P, Maravall F, Mauricio D, Al-Shahrour F, Robledo M. MicroRNAdeep-sequencing reveals master regulators of follicular and papillary thyroidtumors. Mod Pathol. 2015 Feb 27. doi: 10.1038/modpathol.2015.44. PubMed PMID: 25720323.

- Marotta V, Ramundo V, Camera L, Del Prete M, Fonti R, Esposito R, Palmieri G, Salvatore M, Vitale M, Colao A, Faggiano A. Sorafenib in advanced iodine-refractory differentiated thyroid cancer: efficacy, safety and exploratory analysis of role of serum thyroglobulin and FDG-PET. Clin Endocrinol (Oxf). 2013

- Martin M, Maßhöfer L, Temming P, Rahmann S, Metz C, Bornfeld N, van de Nes J, Klein-Hitpass L, Hinnebusch AG, Horsthemke B, Lohmann DR, Zeschnigk M. Exome sequencing identifies recurrent somatic mutations in EIF1AX and SF3B1 in uveal melanoma with disomy 3. Nat Genet. 2013 Aug;45(8):933-6. doi: 10.1038/ng.2674. Epub 2013 Jun 23. PubMed PMID: 23793026; PubMed Central PMCID: PMC4307600.

- Melo M, da Rocha AG, Vinagre J, Sobrinho-Simões M, Soares P. Coexistence of TERT Promoter and BRAF Mutations in Papillary Thyroid Carcinoma: Added Value in Patient Prognosis? J Clin Oncol. 2015 Feb 20;33(6):667-8. doi: 10.1200/JCO.2014.59.4614. Epub 2015 Jan 20. PubMed PMID: 25605839.

- Merindol N, Riquet A, Szablewski V, Eliaou JF, Puisieux A, Bonnefoy N. The emerging role of Twist proteins in hematopoietic cells and hematological malignancies. Blood Cancer J. 2014 Apr 25;4:e206. doi: 10.1038/bcj.2014.22. Erratum in: Blood Cancer J. 2014 Oct;4:e254. PubMed PMID: 24769647; PubMed Central PMCID: PMC4003416.
- Milosevic Z, Pesic M, Stankovic T, Dinic J, Milovanovic Z, Stojsic J, Dzodic R, Tanic N, Bankovic J. Targeting RAS-MAPK-ERK and PI3K-AKT-mTOR signal transduction pathways to chemosensitize anaplastic thyroid carcinoma. Transl Res. 2014 Nov;164(5):411-23. doi:10.1016/j.trsl.2014.06.005. Epub 2014 Jun 23. PubMed PMID: 25016932.
- Miranda C, Minoletti F, Greco A, Sozzi G, Pierotti MA.Refined localization of the human TPR gene to chromosome 1q25 by in situ hybridization.Genomics. 1994; 23(3):714-5.
- Murre C, McCaw PS, Vaessin H, Caudy M, Jan LY, Jan YN, Cabrera CV, Buskin JN, Hauschka SD, Lassar AB, et al. Interactions between heterologous helix-loop-helix proteins generate complexes that bind specifically to a common DNA sequence. Cell. 1989 Aug 11;58(3):537-44. PubMed PMID: 2503252.
- Murugan AK, Xing M. Anaplastic thyroid cancers harbor novel oncogenic mutations of the ALK gene. Cancer Res 2011; 71:4403-4411.
- Nairismägi ML, Füchtbauer A, Labouriau R, Bramsen JB, Füchtbauer EM. The proto-oncogene TWIST1 is regulated by microRNAs. PLoS One. 2013 May 31;8(5):e66070. doi: 10.1371/journal.pone.0066070. Print 2013. PubMed PMID:23741524.
- Najafian A, Olson MT, Schneider EB, Zeiger MA. Clinical Presentation of Patients with a Thyroid Follicular Neoplasm: Are there Preoperative Predictors of Malignancy? Ann Surg Oncol. 2015 Jan 7. PubMed PMID: 25564170.
- Nam EH, Lee Y, Moon B, Lee JW, Kim S. Twist1 and AP-1 cooperatively upregulate integrin α5 expression to induce invasion and the epithelial-mesenchymal transition. Carcinogenesis. 2015 Jan 18. pii: bgv005. PubMed PMID: 25600770.
- Neves R, Scheel C, Weinhold S, Honisch E, Iwaniuk KM, Trompeter HI, Niederacher D, Wernet P, Santourlidis S, Uhrberg M. Role of DNA methylation in miR-200c/141 cluster silencing in invasive breast cancer cells. BMC Res Notes. 2010 Aug 3;3:219. doi: 10.1186/1756-0500-3-219. PubMed PMID: 20682048; PubMed Central PMCID: PMC3161370.
- Niesner U, Albrecht I, Janke M, Doebis C, Loddenkemper C, Lexberg MH, Eulenburg K, Kreher S, Koeck J, Baumgrass R, Bonhagen K, Kamradt T, Enghard P, Humrich JY, Rutz S, Radbruch A. Autoregulation of Th1-mediated inflammation by twist1. J Exp Med. 2008 Aug 4;205(8):1889-901. doi: 10.1084/jem.20072468. Epub 2008

Jul 28. PubMed PMID: 18663125; PubMed Central PMCID: PMC2525589.

- Nikiforov YE, Nikiforova MN. Molecular genetics and diagnosis of thyroid cancer. Nat Rev Endocrinol. 2011 Aug 30;7(10):569-80. doi: 10.1038/nrendo.2011.142. Review. PubMed PMID: 21878896.

- Nikiforova MN, Kimura ET, Gandhi M, Biddinger PW, Knauf JA, Basolo F, Zhu Z, Giannini R, Salvatore G, Fusco A, Santoro M, Fagin JA, Nikiforov YE. BRAF mutations in thyroid tumors are restricted to papillary carcinomas and anaplastic or poorly differentiated carcinomas arising from papillary carcinomas. Journal of Clinical Endocrinology & Metabolism 2003;88:5399–5404.

- Nikiforova MN, Tseng GC, Steward D, Diorio D, Nikiforov YE. MicroRNA expression profiling of thyroid tumors: biological significance and diagnostic utility. J Clin Endocrinol Metab. 2008 May;93(5):1600-8. doi:10.1210/jc.2007-2696. Epub 2008 Feb 12. PubMed PMID: 18270258; PubMed CentralPMCID: PMC2386678.

- Nucera C, Nehs MA, Nagarkatti SS, Sadow PM, Mekel M, Fischer AH, Lin PS, Bollag GE, Lawler J, Hodin RA, Parangi S. Targeting BRAFV600E with PLX4720 displays potent antimigratory and anti-invasive activity in preclinical models of human thyroid cancer. Oncologist. 2011;16(3):296-309. doi: 10.1634/theoncologist.2010-0317. Epub 2011 Feb 25. PubMed PMID: 21355020.

- Okamura H, Yoshida K, Haneji T.Negative regulation of TIMP1 is mediated by transcription factor TWIST1. Int J Oncol. 2009 Jul;35(1):181.

- Omur O, Baran Y. An update on molecular biology of thyroid cancers. Crit Rev Oncol Hematol. 2014 Jun;90(3):233-52. doi: 10.1016/j.critrevonc.2013.12.007. Epub 2013 Dec 18. Review. PubMed PMID: 24405857.

- Oshima A, Tanabe H, Yan T, Lowe GN, Glackin CA, Kudo A. A novel mechanism for the regulation of osteoblast differentiation: transcription of periostin, a member of the fasciclin I family, is regulated by the bHLH transcription factor, twist. J Cell Biochem. 2002;86(4):792-804. PubMed PMID: 12210745.

- Ou DL, Chien HF, Chen CL, Lin TC, Lin LI. Role of Twist in head and neck carcinoma with lymph node metastasis. Anticancer Res. 2008 Mar-Apr;28(2B):1355-9.PubMed PMID: 18505078.

- Pacifico F, Crescenzi E, Mellone S, Iannetti A, Porrino N, Liguoro D, Moscato F, Grieco M, Formisano S, Leonardi A. Nuclear factor-kB contributes to anaplastic thyroid carcinomas through up-regulation of miR-146a. J Clin Endocrinol Metab. 2010 Mar;95(3):1421-30. doi: 10.1210/jc.2009-1128. Epub 2010 Jan 8. PubMed PMID: 20061417.

- Pallante P, Battista S, Pierantoni GM, Fusco A. Deregulation of microRNA expression in thyroid neoplasias. Nat Rev Endocrinol. 2014 Feb;10(2):88-101. doi:10.1038/nrendo.2013.223. Epub 2013 Nov 19.

Review. PubMed PMID: 24247220.

- Patel KN, Shaha AR. Poorly differentiated thyroid cancer. Curr Opin Otolaryngol Head Neck Surg. 2014 Apr;22(2):121-6. doi: 10.1097/MOO.0000000000000037. Review. PubMed PMID: 24492853.

- Pellegriti G, Frasca F, Regalbuto C, Squatrito S, Vigneri R. Worldwide increasing incidence of thyroid cancer: update on epidemiology and risk factors.J Cancer Epidemiol. 2013;2013:965212. doi: 10.1155/2013/965212. Epub 2013 May 7. PubMed PMID: 23737785; PubMed Central PMCID: PMC3664492.

- Perri F, Pezzullo L, Chiofalo MG, Lastoria S, Di Gennaro F, Scarpati GD, Caponigro F. Targeted therapy: A new hope for thyroid carcinomas. Crit Rev Oncol Hematol. 2014 Nov 1. pii: S1040-8428(14)00172-3. doi: 10.1016/j.critrevonc.2014.10.012. Review. PubMed PMID: 25465739.

- Pettersson AT, Mejhert N, Jernås M, Carlsson LM, Dahlman I, Laurencikiene J, Arner P, Rydén M.Twist 1 in human white adipose tissue and obesity. J Clin Endocrinol Metab. 2011; 96(1): 133-41.

- Pham CG, Bubici C, Zazzeroni F, Knabb JR, Papa S, Kuntzen C, Franzoso G. Upregulation of Twist-1 by NF-kappaB blocks cytotoxicity induced by chemotherapeutic drugs. Mol Cell Biol. 2007 Jun;27(11):3920-35. Epub 2007 Apr 2. PubMed PMID: 17403902; PubMed Central PMCID: PMC1900008.

- Pham D, Yu Q, Walline CC, Muthukrishnan R, Blum JS, Kaplan MH. Opposing roles of STAT4 and Dnmt3a in Th1 gene regulation. J Immunol. 2013 Jul 15;191(2):902-11. doi: 10.4049/jimmunol.1203229. Epub 2013 Jun 14. PubMed PMID: 23772023; PubMedCentral PMCID: PMC3703830.

- Piccinin S, Tonin E, Sessa S, Demontis S, Rossi S, Pecciarini L, Zanatta L, Pivetta F, Grizzo A, Sonego M, Rosano C, Dei Tos AP, Doglioni C, Maestro R. A "twist box" code of p53 inactivation: twist box: p53 interaction promotes p53 degradation. Cancer Cell. 2012 Sep 11;22(3):404-15. doi: 10.1016/j.ccr.2012.08.003. PubMed PMID: 22975381.

- Pinho AV, Rooman I, Real FX. p53-dependent regulation of growth, epithelial-mesenchymal transition and stemness in normal pancreatic epithelial cells. Cell Cycle. 2011 Apr 15;10(8):1312-21. Epub 2011 Apr 15. PubMed PMID: 21490434.

- Pita JM, Figueiredo IF, Moura MM, Leite V, Cavaco BM. Cell cycle deregulation and TP53 and RAS mutations are major events in poorly differentiated and undifferentiated thyroid carcinomas. J Clin Endocrinol Metab. 2014 Mar;99(3):E497-507. doi: 10.1210/jc.2013-1512. Epub 2014 Jan 13. PubMed PMID: 24423316.

- Pitoia F, Bueno F, Urciuoli C, Abelleira E, Cross G, Tuttle RM. Outcomes of patients with differentiated thyroid cancer risk-stratified

according to the American thyroid association and Latin American thyroid society risk of recurrence classification systems. Thyroid. 2013 Nov;23(11):1401-7. doi: 10.1089/thy.2013.0011. Epub 2013 Jul 25. PubMed PMID: 23517313. 7

- Pollari S, Käkönen RS, Mohammad KS, Rissanen JP, Halleen JM, Wärri A, Nissinenm L, Pihlavisto M, Marjamäki A, Perälä M, Guise TA, Kallioniemi O, Käkönen SM. Heparin-like polysaccharides reduce osteolytic bone destruction and tumor growth in a mouse model of breast cancer bone metastasis. Mol Cancer Res. 2012 May;10(5):597-604. doi: 10.1158/1541-7786.MCR-11-0482. Epub 2012 Apr 20. PubMed PMID: 22522458.

- Prudkin L, Behrens C, Liu DD, Zhou X, Ozburn NC, Bekele BN, Minna JD, Moran C, Roth JA, Ji L, Wistuba II. Loss and reduction of FUS1 protein expression is a frequent phenomenon in the pathogenesis of lung cancer. Clin Cancer Res. 2008 Jan 1;14(1):41-7. doi: 10.1158/1078-0432.CCR-07-1252. PubMed PMID: 18172250.

- Puisieux A, Valsesia-Wittmann S, Ansieau S. A twist for survival and cancer progression. Br J Cancer. 2006 Jan 16;94(1):13-7. Review. PubMed PMID: 16306876; PubMed Central PMCID: PMC2361066.

- Qian F, Zhang ZC, Wu XF, Li YP, Xu Q. Interaction between integrin alpha(5) and fibronectin is required for metastasis of B16F10 melanoma cells. Biochem Biophys Res Commun. 2005 Aug 12;333(4):1269-75. PubMed PMID: 15979576.

- Qiang L, Zhao B, Ming M, Wang N, He TC, Hwang S, Thorburn A, He YY. Regulation of cell proliferation and migration by p62 through stabilization of Twist1. Proc Natl Acad Sci U S A. 2014 Jun 24;111(25):9241-6. doi: 10.1073/pnas.1322913111.Epub 2014 Jun 9. PubMed PMID: 24927592; PubMed Central PMCID: PMC4078859.

- Qin Q, Xu Y, He T, Qin C, Xu J. Normal and disease-related biological functions of Twist1 and underlying molecular mechanisms. Cell Res. 2012 Jan;22(1):90-106. doi: 10.1038/cr.2011.144. Epub 2011 Aug 30. Review. PubMed PMID: 21876555; PubMed Central PMCID: PMC3351934.

- Raatikainen S, Aaltomaa S, Palvimo JJ, Kärjä V, Soini Y. TWIST overexpression predicts biochemical recurrence-free survival in prostate cancer patients treated with radical prostatectomy. Scand J Urol. 2015 eb;49(1):51-7. doi:10.3109/21681805.2014.909529. Epub 2014 Apr 30. PubMed PMID: 24779451.

- Ragazzi M, Ciarrocchi A, Sancisi V, Gandolfi G, Bisagni A, Piana S. Update on anaplastic thyroid carcinoma: morphological, molecular, and genetic features of the most aggressive thyroid cancer. Int J Endocrinol. 2014;2014:790834. doi:10.1155/2014/790834. Epub 2014 Aug 21. Review. PubMed PMID: 25214840; PubMed Central PMCID: PMC4158294.

- Ricarte-Filho JC, Li S, Garcia-Rendueles ME, Montero-Conde C, Voza

F, Knauf JA, Heguy A, Viale A, Bogdanova T, Thomas GA, Mason CE, Fagin JA. Identification of kinase fusion oncogenes in post-Chernobyl radiation-induced thyroid cancers. J Clin Invest. 2013 Nov;123(11):4935-44. doi: 10.1172/JCI69766. Epub 2013 Oct 25. PubMed PMID: 24135138; PubMed Central PMCID: PMC3809792.

- Rodríguez-Rodero S, Fernández AF, Fernández-Morera JL, Castro-Santos P, Bayon GF, Ferrero C, Urdinguio RG, Gonzalez-Marquez R, Suarez C, Fernández-Vega I,Fresno Forcelledo MF, Martínez-Camblor P, Mancikova V, Castelblanco E, Perez M,Marrón PI, Riesco-Eizaguirre G,Matías-Guiu X, Carnero A, Robledo M, Delgado-Álvarez E, Menéndez-Torre E, Fraga MF. DNA methylation signatures identify biologically distinct thyroid cancer subtypes. J Clin Endocrinol Metab. 2013 Jul;98(7):2811-21. doi:10.1210/jc.2012-3566. Epub 2013 May 10. PubMed PMID: 23666970.
- Rosove MH, Peddi PF, Glaspy JA. BRAF V600E inhibition in anaplastic thyroid cancer. N Engl J Med. 2013 Feb 14;368(7):684-5. doi: 10.1056/NEJMc1215697. PubMed PMID: 23406047.
- Salerno P, De Falco V, Tamburrino A, Nappi TC, Vecchio G, Schweppe RE, Bollag G, Santoro M, Salvatore G. Cytostatic activity of adenosine triphosphate-competitive kinase inhibitors in BRAF mutant thyroid carcinoma cells. J Clin Endocrinol Metab. 2010 Jan;95(1):450-5. doi: 10.1210/jc.2009-0373. Epub 2009 Oct 30. PubMed PMID: 19880792.
- Salerno P, Garcia-Rostan G, Piccinin S, Bencivenga TC, Di Maro G, Doglioni C, Basolo F, Maestro R, Fusco A, Santoro M, Salvatore G. TWIST1 plays a pleiotropic role in determining the anaplastic thyroid cancer phenotype. J Clin Endocrinol Metab. 2011 May;96(5):E772-81. doi: 10.1210/jc.2010-1182. Epub 2011 Mar 9. PubMed PMID: 21389145.
- Salvatore G, Nappi TC, Salerno P, Jiang Y, Garbi C, Ugolini C, Miccoli P, Basolo F, Castellone MD, Cirafici AM, Melillo RM, Fusco A, Bittner ML, Santoro M. A cell proliferation and chromosomal instability signature in anaplastic thyroid carcinoma. Cancer Res 2007; 67(21):10148-58.
- Santoro M, Dathan NA, Berlingieri MT, Borganzone I, Paulin C, Grieco M, Pierotti MA, Vecchio G, Fusco A. Molecular characterization of RET/PTC3; a novel rearranged version of the RET proto-oncogene in human thyroid papillary carcinoma. Oncogene 1994; 9: 509-16.
- Santoro M, Melillo RM, Fusco A. RET/PTC activation in papillary thyroid carcinoma: European Journal of Endocrinology Prize Lecture. Eur J Endocrinol. 2006; 155(5):645-53.
- Santoro M, Thomas GA, Vecchio G, Williams GH, Fusco A, Chiappetta G, Pozcharskaya V, Bogdanova TI, Demidchik EP, Cherstvoy ED, Voscoboinik L, Tronko ND, Carss A, Bunnell H,

Tonnachera M, Parma J, Dumont JE, Keller G, Höfler H, Williams ED. Gene rearrangement and Chernobyl related thyroid cancers. Br J Cancer. 2000; Jan;82(2):315-22. PubMed PMID: 10646883.

- Savvides P, Nagaiah G, Lavertu P, Fu P, Wright JJ, Chapman R, Wasman J, Dowlati A, Remick SC. Phase II trial of sorafenib in patients with advanced anaplastic carcinoma of the thyroid. Thyroid. 2013 May;23(5):600-4. doi:10.1089/thy.2012.0103. Epub 2013 Apr 18. PubMed PMID: 23113752; PubMed Central PMCID: PMC3643255.

- Schaffner F, Yokota N, Ruf W. Tissue factor proangiogenic signaling in cancer progression. Thromb Res. 2012;129(Suppl 1):S127–S131.

- Schagdarsurengin U, Gimm O, Dralle H, Hoang-Vu C, Dammann R. CpG Island methylation of tumor-related promoters occurs preferentially in undifferentiated carcinoma. Thyroid. 2006 Jul;16(7):633-42. PubMed PMID: 16889486.

- Schanze I, Schanze D, Bacino CA, Douzgou S, Kerr B, Zenker M. Haploinsufficiency of SOX5, a member of the SOX (SRY-related HMG-box) family of transcription factors is a cause of intellectual disability. Eur J Med Genet. 2013 Feb;56(2):108-13. doi: 10.1016/j.ejmg.2012.11.001. Epub 2012 Dec 5. PubMed PMID: 23220431.

- Schmidt JM, Panzilius E, Bartsch HS, Irmler M, Beckers J, Kari V, Linnemann JR, Dragoi D, Hirschi B, Kloos UJ, Sass S, Theis F, Kahlert S, Johnsen SA, Sotlar K, Scheel CH. Stem-Cell-like Properties and Epithelial Plasticity Arise as Stable Traits after Transient Twist1 Activation. Cell Rep. 2015 Jan 7. pii: S2211-1247(14)01061-4. doi: 10.1016/j.celrep.2014.12.032. PubMed PMID: 25578726.

- Sharif MN, Sosic D, Rothlin CV, Kelly E, Lemke G, Olson EN, Ivashkiv LB. Twist mediates suppression of inflammation by type I IFNs and Axl. J Exp Med. 2006 Aug 7;203(8):1891-901. Epub 2006 Jul 10. PubMed PMID: 16831897; PubMed Central PMCID:PMC2118370.

- Shen J, Hung MC. Signaling-Mediated Regulation of MicroRNA Processing. Cancer Res. 2015 Mar 1;75(5):783-791. Epub 2015 Feb 6. Review. PubMed PMID: 25660948;PubMed Central PMCID: PMC4348149.

- Shi X, Liu R, Qu S, Zhu G, Bishop J, Liu X, Sun H, Shan Z, Wang E, Luo Y, Yang X, Zhao J, Du J, Teng W, Xing M. Association of TERT Promoter Mutation 1,295,228 C>T with BRAF V600E Mutation, Older Patient Age, and Distant Metastasis in Anaplastic Thyroid Cancer. J Clin Endocrinol Metab. 2015 Jan 13:jc20143606. PubMed PMID: 25584719.

- Shiota M, Izumi H, Onitsuka T, Miyamoto N, Kashiwagi E, Kidani A, Hirano G, Takahashi M, Naito S, Kohno K. Twist and p53 reciprocally regulate target genes via direct interaction. Oncogene 2008. 27: 5543-53.

- Smallridge RC. Approach to the patient with anaplastic thyroid

carcinoma. J Clin Endocrinol Metab. 2012 Aug;97(8):2566-72. doi: 10.1210/jc.2012-1314. PubMed PMID: 22869844; PubMed Central PMCID: PMC3410281.

- Smith N, Nucera C. Personalized therapy in patients with anaplastic thyroid cancer: targeting genetic and epigenetic alterations. J Clin Endocrinol Metab.2015 Jan;100(1):35-42. doi: 10.1210/jc.2014-2803. PubMed PMID: 25347569; PubMed Central PMCID: PMC4283016.
- Soares P, Trovisco V, Rocha AS, et al.: BRAF mutations and Ret/ PTC rearrangements are alternative events in the etiopathogeneses of PTC. Oncogene 2003;32:4578–4580.
- Song K, Li Q, Peng YB, Li J, Ding K, Chen LJ, Shao CH, Zhang LJ, Li P. Silencing of hHS6ST2 inhibits progression of pancreatic cancer through inhibition of Notch signalling. Biochem J 2011; 436:271-82.
- Sosa JA, Balkissoon J, Lu SP, Langecker P, Elisei R, Jarzab B, Bal CS, Marur S, Gramza A, Ondrey F. Thyroidectomy followed by fosbretabulin (CA4P) combination regimen appears to suggest improvement in patient survival in anaplastic thyroid cancer. Surgery. 2012 Dec;152(6):1078-87. doi: 10.1016/j.surg.2012.08.036.Review. PubMed PMID: 23158178.
- Šošić D, Richardson JA, Yu K, Ornitz DM, Olson EN. Twist regulates cytokine gene expression through a negative feedback loop that represses NF-kappaB activity. Cell. 2003 Jan 24;112(2):169-80.
- Srivastava RK, Tang SN, Zhu W, Meeker D, Shankar S. Sulforaphane synergizes with quercetin to inhibit self-renewal capacity of pancreatic cancer stem cells. Front Biosci (Elite Ed). 2011 Jan 1;3:515-28. PubMed PMID: 21196331; PubMed Central PMCID: PMC4080794.
- Sun Z, Zhang C, Zou X, Jiang G, Xu Z, Li W, Xie H. Special AT-rich sequence-binding protein-1 participates in the maintenance of breast cancer stem cells through regulation of the Notch signaling pathway and expression of Snail1 and Twist1. Mol Med Rep. 2015 May;11(5):3235-542. doi: 10.3892/mmr.2015.3192. PubMed PMID: 25586771.
- Taccaliti A, Silvetti F, Palmonella G, Boscaro M. Anaplastic thyroid carcinoma. Front Endocrinol (Lausanne). 2012 Jul 5;3:84. doi: 10.3389/fendo.2012.00084. eCollection 2012. PubMed PMID: 22783225.
- Takahashi M, Ritz J, Cooper GM: Activation of a novel human transforming gene, ret, by DNA rearrangement. Cells 1985;42: 581–588.
- Takakura S, Mitsutake N, Nakashima M, Namba H, Saenko VA, Rogounovitch TI, Nakazawa Y, Hayashi T, Ohtsuru A, Yamashita S. Oncogenic role of miR-17-92 cluster in anaplastic thyroid cancer cells. Cancer Sci. 2008 Jun;99(6):1147-54. doi: 10.1111/j.1349-7006.2008.00800.x. Epub 2008 Apr 21. PubMed PMID: 18429962.
- Tallini G. Poorly differentiated thyroid carcinoma. Are we there yet?

Endocr Pathol. 2011 Dec;22(4):190-4.

- Tan EJ, Thuault S, Caja L, Carletti T, Heldin CH, Moustakas A. Regulation of transcription factor Twist expression by the DNA architectural protein high mobility group A2 during epithelial-to-mesenchymal transition. J Biol Chem. 2012 Mar 2;287(10):7134-45. doi: 10.1074/jbc.M111.291385. Epub 2012 Jan 11. PubMed PMID: 22241470.

- Tatsuka M, Sato S, Kitajima S, Suto S, Kawai H, Miyauchi M, Ogawa I, Maeda M, Ota T, Takata T. Overexpression of Aurora-A potentiates HRAS-mediated oncogenic transformation and is implicated in oral carcinogenesis. Oncogene. 2005 Feb 3;24(6):1122-7. PubMed PMID: 15592510.

- Thisse B, el MM, Perrin-Schmitt F. The twist gene: isolation of a Drosophila zygotic gene necessary for the establishment of dorsoventral pattern. Nucleic Acids Res 1987; 15: 3439-53.

- Thomas GA, Bunnell H, Cook HA, Williams ED, Nerovnya A, CherstvoyED, Tronko ND, Chiappetta G, Viglietto G, Pentimalli F, Salvatore G, Fusco A, Santoro M, Vecchio G. High prevalence of RET/PTC rearrangements in Ukrainian and Belarussian post-Chernobyl thyroid papillary carcinomas: a strong correlation between RET/PTC3 and the solid-follicular variant. J Clin Endocrinol Metab 1999; 84: 4232-8.

- Thomas L, Lai SY, Dong W, Feng L, Dadu R, Regone RM, Cabanillas ME. Sorafenib in metastatic thyroid cancer: a systematic review. Oncologist. 2014 Mar;19(3):251-8. doi: 10.1634/ theoncologist.2013-0362. Epub 2014 Feb 21. Review. PubMed PMID: 24563075; PubMed Central PMCID: PMC3958462.

- Tominaga E, Yuasa K, Shimazaki S, Hijikata T. MicroRNA-1 targets Slug and endows lung cancer A549 cells with epithelial and anti-tumorigenic properties. Exp Cell Res. 2013 Feb 1;319(3):77-88. doi: 10.1016/j.yexcr.2012.10.015. Epub 2012 Nov 7. PubMed PMID: 23142026.

- Tsukerman P, Yamin R, Seidel E, Khawaled S, Schmiedel D, Bar-Mag T, Mandelboim O. MiR-520d-5p directly targets TWIST1 and downregulates the metastamiR miR-10b. Oncotarget. 2014 Dec 15;5(23):12141-50. PubMed PMID: 25426550; PubMed Central PMCID: PMC4323010.

- Tukel T, Šošić D, Al-Gazali LI, Erazo M, Casasnovas J, Franco HL, Richardson JA, Cadilla CL, Desnick RJ. Homozygous nonsense mutations in TWIST2 cause Setleis syndrome. Am J Hum Genet. 2010 Aug 13;87(2):289-96. doi: 10.1016/j.ajhg.2010.07.009. PubMed PMID: 20691403.

- Uno F, Sasaki J, Nishizaki M, Carboni G, Xu K, Atkinson EN, Kondo M, Minna JD, Roth JA, Ji L. Myristoylation of the fus1 protein is required for tumor suppression in human lung cancer cells. Cancer Res.

2004 May 1;64(9):2969-76.PubMed PMID: 15126327.

- Vanden Borre P, Gunda V, McFadden DG, Sadow PM, Varmeh S, Bernasconi M, Parangi S. Combined BRAF(V600E)- and SRC-inhibition induces apoptosis, evokes an immune response and reduces tumor growth in an immunocompetent orthotopic mouse model of anaplastic thyroid cancer. Oncotarget. 2014 Jun 30;5(12):3996-4010. PubMed PMID: 24994118; PubMed Central PMCID: PMC4147301.

- Versteeg HH, Schaffner F, Kerver M, Petersen HH, Ahamed J, Felding-Habermann B, Takada Y, Mueller BM, Ruf W. Inhibition of tissue factor signaling suppresses tumor growth. Blood. 2008 Jan 1;111(1):190-9. Epub 2007 Sep 27. PubMed PMID:17901245.

- Vesuna F, Lisok A, Kimble B, Domek J, Kato Y, van der Groep P, Artemov D, Kowalski J, Carraway H, van Diest P, Raman V. Twist contributes to hormone resistance in breast cancer by downregulating estrogen receptor-α. Oncogene. 2012 Jul 5;31(27):3223-34. doi: 10.1038/onc.2011.483. Epub 2011 Nov 7. PubMed PMID:22056872; PubMed Central PMCID: PMC3276743.

- Vesuna F, van Diest P, Chen JH, Raman V. Twist is a transcriptional repressor of E-cadherin gene expression in breast cancer. Biochem Biophys Res Commun. 2008 Mar 7;367(2):235-41.

- Visone R, Russo L, Pallante P, De Martino I, Ferraro A, Leone V, Borbone E, Petrocca F, Alder H, Croce CM, Fusco A. MicroRNAs (miR)-221 and miR-222, both overexpressed in human thyroid papillary carcinomas, regulate p27Kip1 protein levels and cell cycle. Endocr Relat Cancer. 2007 Sep;14(3):791-8. PubMed PMID:17914108.

- Volante M, Papotti M. Poorly differentiated thyroid carcinoma: 5 years after the 2004 WHO classification of endocrine tumours. Endocr Pathol. 2010 Mar;21(1):1-6. doi: 10.1007/s12022-009-9100-4. PubMed PMID: 19960273.

- Vriens MR, Weng J, Suh I, Huynh N, Guerrero MA, Shen WT, Duh QY, Clark OH, Kebebew E. MicroRNA expression profiling is a potential diagnostic tool for thyroid cancer. Cancer. 2012 Jul 1;118(13):3426-32. doi: 10.1002/cncr.26587. Epub 2011 Oct 17. PubMed PMID: 22006248.

- Wagle N, Grabiner BC, Van Allen EM, Amin-Mansour A, Taylor-Weiner A, Rosenberg M, Gray N, Barletta JA, Guo Y, Swanson SJ, Ruan DT, Hanna GJ, Haddad RI, Getz G, Kwiatkowski DJ, Sabatini DM, Jänne PA, Garraway LA, Lorch JH. Response and acquired resistance to everolimus in anaplastic thyroid cancer. N Engl J Med.2014 Oct 9;371(15):1426-33. doi: 10.1056/NEJMoa1403352. PubMed PMID: 25295501.

- Wang D, Han S, Wang X, Peng R, Li X. SOX5 promotes epithelial-mesenchymal transition and cell invasion via regulation of Twist1 in hepatocellular carcinoma. Med Oncol. 2015 Feb;32(2):461. doi: 10.1007/s12032-014-0461-2. PubMed PMID: 25572815.

- Wang SM, Coljee VW, Pignolo RJ, Rotenberg MO, Cristofalo VJ, Sierra F. Cloning of the human twist gene: its expression is retained in adultmesodermally-derived tissues. Gene. 1997 Mar 10;187(1):83-92.
- Wreesmann VB, Ghossein RA, Patel SG, Harris CP, Schnaser EA, Shaha AR, Tuttle RM, Shah JP, Rao PH, Singh B. Genome-wide appraisal of thyroid cancer progression. Am J Pathol. 2002 Nov;161(5):1549-56. PubMed PMID: 12414503.
- Wu KJ. Direct activation of Bmi1 by Twist1: implications in cancer stemness, epithelial-mesenchymal transition, and clinical significance. Chang Gung Med J. 2011 May-Jun;34(3):229-38. Review. PubMed PMID: 21733352.
- Wushou A, Hou J, Zhao YJ, Shao ZM. Twist-1 up-regulation in carcinoma correlates to poor survival. Int J Mol Sci. 2014 Nov 25;15(12):21621-30. doi: 10.3390/ijms151221621. PubMed PMID: 25429425.
- Xing M. Molecular pathogenesis and mechanisms of thyroid cancer. Nat Rev Cancer. 2013 Mar;13(3):184-99. doi: 10.1038/nrc3431. Review. PubMed PMID: 23429735; PubMed Central PMCID: PMC3791171.
- Xue G, Restuccia DF, Lan Q, Hynx D, Dirnhofer S, Hess D, Rüegg C, Hemmings BA.Akt/PKB-mediated phosphorylation of Twist1 promotes tumor metastasis via mediating cross-talk between PI3K/Akt and TGF-β signaling axes. Cancer Discov. 2012 Mar;2(3):248-59. doi: 10.1158/2159-8290.CD-11-0270. PubMed PMID: 22585995.
- Yang MH, Wu MZ, Chiou SH, Chen PM, Chang SY, Liu CJ, Teng SC, Wu KJ. Direct regulation of TWIST by HIF-1alpha promotes metastasis. Nat Cell Biol. 2008;10(3):295-305.
- Yazlovitskaya EM, Uzhachenko R, Voziyan PA, Yarbrough WG, Ivanova AV. A novel radioprotective function for the mitochondrial tumor suppressor protein Fus1. Cell Death Dis. 2013 Jun 20;4:e687. doi: 10.1038/cddis.2013.212. PubMed PMID:23788044.
- Yin G, Chen R, Alvero AB, Fu HH, Holmberg J, Glackin C, Rutherford T, Mor G. TWISTing stemness, inflammation and proliferation of epithelial ovarian cancer cells through MIR199A2/214. Oncogene. 2010 Jun 17;29(24):3545-53. doi: 10.1038/onc.2010.111. PubMed PMID: 20400975.
- Yip L, Kelly L, Shuai Y, Armstrong MJ, Nikiforov YE, Carty SE, Nikiforova MN. MicroRNA signature distinguishes the degree of aggressiveness of papillary thyroid carcinoma. Ann Surg Oncol. 2011 Jul;18(7):2035-41. doi: 10.1245/s10434-011-1733-0. PubMed PMID: 21537871.
- Zhang C, Guo F, Xu G, Ma J, Shao F. STAT3 cooperates with Twist to mediate epithelial-mesenchymal transition in human hepatocellular carcinoma cells. Oncol Rep. 2015 Apr;33(4):1872-82. doi: 10.3892/or.2015.3783. PubMed PMID: 25653024.

- Zhang Y, Yang WQ, Zhu H, Qian YY, Zhou L, Ren YJ, Ren XC, Zhang L, Liu XP, Liu CG, Ming ZJ, Li B, Chen B, Wang JR, Liu YB, Yang JM. Regulation of autophagy by miR-30d impacts sensitivity of anaplastic thyroid carcinoma to cisplatin. Biochem Pharmacol. 2014 Feb 15;87(4):562-70. doi: 10.1016/j.bcp.2013.12.004. Epub 2013 Dec 15. PubMed PMID: 24345332.
- Zhao D, Besser AH, Wander SA, Sun J, Zhou W, Wang B, Ince T, Durante MA, Guo W, Mills G, Theodorescu D, Slingerland J. Cytoplasmic p27 promotes epithelial-mesenchymal transition and tumor metastasis via STAT3-mediated Twist1 upregulation. Oncogene. 2015 Feb 16. doi: 10.1038/onc.2014.473. PubMed PMID: 25684140.
- Zhao N, Sun BC, Zhao XL, Liu ZY, Sun T, Qiu ZQ, Gu Q, Che N, Dong XY. Coexpression of Bcl-2 with epithelial-mesenchymal transition regulators is a prognostic indicator in hepatocellular carcinoma. Med Oncol. 2012 Dec;29(4):2780-92. doi: 10.1007/s12032-012-0207-y. PubMed PMID: 2246083.

Attached Manuscript # I

Gennaro Di Maro, **Francesca Maria Orlandella,**
Tammaro Claudio Bencivenga, Paolo Salerno, Clara
Ugolini, Fulvio Basolo, Roberta Maestro, and Giuliana
Salvatore

Identification of Targets of Twist1 Transcription Factor in Thyroid Cancer Cells

Gennaro Di Maro, Francesca Maria Orlandella, Tammaro Claudio Bencivenga, Paolo Salerno, Clara Ugolini, Fulvio Basolo, Roberta Maestro, and Giuliana Salvatore

Dipartimento di Medicina Molecolare e Biotecnologie Mediche (G.D.M., F.M.O., T.C.B., P.S.), Università di Napoli "Federico II," Italy 80131; Dipartimento di Area Medica (C.U.), Azienda Ospedaliero-Universitaria Pisana, Pisa, Italy 56126; Dipartimento di Patologia Chirugica, Medica (F.B.), Molecolare e dell'Area Critica dell' Università di Pisa, Italy 56124; Experimental Oncology 1 (R.M.), Centro di Riferimento Oncologico, Aviano, Italy 33081; and Dipartimento di Scienze Motorie e del Benessere (G.S.), Universita' "Parthenope," 80133 Napoli, Italy 80133

Context: Anaplastic thyroid carcinoma (ATC) is one of the most aggressive human tumors. Twist1 is a basic helix-loop-helix transcription factor involved in cancer development and progression. We showed that Twist1 affects thyroid cancer cell survival and motility.

Objective: We aimed to identify Twist1 targets in thyroid cancer cells.

Design: Transcriptional targets of Twist1 were identified by gene expression profiling the TPC-Twist1 cells in comparison with control cells. Functional studies were performed by silencing in TPC-Twist1 and in CAL62 cells the top 10 upregulated genes and by evaluating cell proliferation, survival, migration, and invasion. Chromatin immunoprecipitation was performed to verify direct binding of Twist1 to target genes. Quantitative RT-PCR was applied to study the expression level of Twist1 target genes in human thyroid carcinoma samples.

Results: According to the gene expression profile, the top functions enriched in TPC-Twist1 cells were cellular movement, cellular growth and proliferation, and cell death and survival. Silencing of the top 10 upregulated genes reduced viability of TPC-Twist1 and of CAL62 cells. Silencing of *COL1A1*, *KRT7*, and *PDZK1* also induced cell death. Silencing of *HS6ST2*, *THRB*, *ID4*, *RHOB*, and *PDZK1IP* also impaired migration and invasion of TPC-Twist1 and of CAL62 cells. Chromatin immunoprecipitation showed that Twist1 directly binds the promoter of the top 10 upregulated genes. Quantitative RT-PCR showed that *HS6ST2*, *COL1A1*, *F2RL1*, *LEPREL1*, *PDZK1*, and *PDZK1IP1* are overexpressed in thyroid carcinoma samples compared with normal thyroids.

Conclusions: We identified a set of genes that mediates Twist1 biological effects in thyroid cancer cells. (*J Clin Endocrinol Metab* 99: E1617–E1626, 2014)

Anaplastic thyroid carcinoma (ATC) is one of the most lethal human malignancies. Ninety percent of patients with ATC die within 6 months of diagnosis (1, 2). ATC usually presents as a rapidly expanding tumor mass in the neck, causing hoarseness, breathing difficulties, and dysphagia (3, 4). Current treatments for ATC are aggres- sive and include surgery, chemotherapy, and radiation therapy. However, ATC is resistant to all types of therapy, and disease prognosis has remained unchanged (5–7).

ATC may derive de novo or from preexisting papillary thyroid carcinoma (PTC) or follicular thyroid carcinoma. Many patients do indeed have a history of preexisting

Abbreviations: ATC, anaplastic thyroid carcinoma; ChIP, chromatin immunoprecipitation; F2RL1, coagulation factor II (thrombin) receptor-like 1; HS6ST2, heparan sulfate 6-*O*-sulfotransferase 2; LEPREL1, leprecan-like 1; PAR2, protease-activated receptor 2; PDC, poorly differentiated thyroid carcinoma; PDZK1, PDZ domain containing 1; PDZK1, PDZ domain containing 1; PTC, papillary thyroid carcinoma; qRT-PCR, quantitative RT-PCR; siRNA, small interfering RNA; TF, tissue factor.

well-differentiated thyroid carcinoma or nodular goiters (8–10). Little is known about the molecular events that lead from the highly curable differentiated tumors to ATCs. The main differences between the 2 tumor types bear on the much stronger epithelial to mesenchymal transition (EMT), dedifferentiation, fibrosis, and glycolytic phenotypes shown by the ATC (11). Through a microarray analysis on different thyroid tumors in comparison with normal thyroids, we have isolated Twist1 transcription factor as a gene upregulated in ATC (12, 13).

Twist1 is a highly conserved transcription factor that belongs to the family of basic helix-loop-helix proteins. Twist1 overexpression is associated with many types of aggressive tumors and correlates with poor prognosis and high grade/stage of the tumor (reviewed in Refs. 14 and 15). Twist1 has been identified as a master regulator of epithelial to mesenchymal transition, a critical mechanism used by cancer cells to increase invasion, metastasis, and resistance to chemotherapy (16–18). We showed that approximately 50% of ATCs upregulated Twist1 with respect to normal thyroids as well as to poorly and well-differentiated thyroid carcinoma. Silencing of Twist1, by RNA interference, in ATC cells (CAL62) reduced cell migration and invasion and increased sensitivity to apoptosis. The ectopic expression of Twist1 in papillary thyroid cancer cells (TPC-1) induced resistance to apoptosis and increased cell migration and invasion (13).

Here, we aimed to identify a set of genes that mediates Twist1 biological effects in thyroid cancer cells.

Materials and Methods

Cell lines

The human papillary thyroid cancer cell line TPC-1 (hereafter named TPC), was obtained from M. Nagao (Carcinogenesis Division, National Cancer Center Research Institute, Tokyo, Japan). The TPC cell line was authenticated based on the unique presence of the RET/PTC1 rearrangement. The human anaplastic thyroid cancer cell line CAL62 was purchased from DSMZ (Deutsche Sammlung von Mikroorganismen und Zellkulturen GmbH). CAL62 cells were DNA profiled by short tandem repeat analysis in 2009 and shown to be unique and identical with those reported in Schweppe et al (19). The TPC-Twist1 cell lines (mp1, mp2, and Cl2) and the CAL62 shTwist1 cells were generated and characterized as described in Salerno et al, 2011 (13). TPC and CAL62 cells were grown in DMEM (Dulbecco's Modified Eagle Medium) supplemented with 10% FBS (fetal bovine serum), L-glutamine and penicillin/streptomycin (Invitrogen, Carlsbad, CA). Normal human umbilical vein endothelial cells (HUVEC) were purchased from Lonza (Lonza, Switzerland) and cultured in EBM-2 (Endothelial Cell Basal Medium) medium supplemented with SingleQuot growth supplements (Lonza) up to passage 7.

Microarray analysis, network and gene ontology analysis, RNA extraction, cDNA synthesis, and quantitative real-time PCR, immunohistochemistry, migration and invasion assay, and transendothelial cell migration assay

These studies were performed according to standard procedures. A description is available in Supplemental Methods.

RNA silencing

All functional experiments described hereafter have been performed in TPC-Twist1 mp1 (TPC-Twist1) and in CAL62 cells. TPC-Twist1 and CAL62 cells were transfected with the specific small interfering RNAs (siRNAs) (QIAGEN) in 6-well plates in triplicate. For each transfection, 5 μL of 100μM siRNA was mixed with 20 μL of HiPerFect Transfection reagent (QIAGEN) and 300 μL of Optimem medium (Invitrogen). After 10 minutes of incubation, the transfection mix was delivered to each well and incubated at 37°C for 72 hours. The following specific siRNAs (QIAGEN) were used: siRNA *HS6ST2* (SI04269020), siRNA *COL1A1* (SI04434773), siRNA *KRT7* (SI04339776), siRNA *F2RL1* (SI04435088), siRNA *LEPREL1* (SI04265184), siRNA *THRB* (SI03027535), siRNA *ID4* (SI00445389), siRNA *RHOB* (SI00058912), siRNA *PDZK1* (SI04314723), siRNA *PDZK1IP1* (SI04164587), and AllStars negative control siRNA (SI03650318).

Trypan blue assay

Cells were collected by trypsinization after 48 and 72 hours of transfection, stained for 10 minutes with 0.4% trypan blue (Sigma-Aldrich) according to manufacturer's instructions, and counted in triplicate with TC10 automated cell counter (Bio-Rad).

Wound closure assay

A wound was inflicted on the confluent monolayer cells by scraping a gap using a micropipette tip 48 hours after transfection with specific siRNAs. Photographs were taken at ×10 magnification using phase-contrast microscopy immediately after wound incision and 24 hours later. Pixel densities in the wound areas were measured using the Cell[a] software (Olympus Biosystem GmbH) and expressed as percentage of wound closure, where 100% is the value obtained at 24 hours for control cells.

Chromatin immunoprecipitation assay

Chromatin samples were processed for chromatin immunoprecipitation (ChIP) as reported elsewhere (20). Briefly, TPC-pcDNA and TPC-Twist1 cell lysates were sonicated on ice in a cold room, 30 times for 30 seconds each at maximum settings, to obtain fragments between 0.3 and 1.0 kb. Samples were subjected to IP with anti-Twist1 antibody (Twist2C1a, sc-81417; Santa Cruz Biotechnology, Inc) or control antibody (mouse IgG1 isotype control, clone G3A1, no. 5415; Cell Signaling). For quantitative RT-PCR (qRT-PCR), 2 of 30 μL immunoprecipitated DNA was used. Input DNA values were used to normalize the values from quantitative ChIP samples. Percent input was calculated as $2^{-\Delta Ct} \times 3$, where Ct is cycle threshold and ΔCt is the difference between Ct_{input} and Ct_{cIP}. All quantitative ChIP data were derived from at least 3 independent experiments, and for each experiment, qRT-PCR was performed in triplicate. The *GAPDH* promoter amplicon was used as a negative control. The

sequences of the primers, covering E-box regions, used in ChIP assays are listed in Supplemental Table 1.

Tissue samples

Tumors and normal thyroid tissue samples for RNA extraction and qRT-PCR were retrieved from the files of the Department of Surgery, University of Pisa (Italy). The institutional review boards approved the study protocols. Informed consent was obtained from each subject. Samples were classified according to the diagnostic criteria required for the identification of PTC, poorly differentiated thyroid carcinoma (PDC), and ATC (21).

Statistical analysis

Data are presented as mean ± SD. Two-tailed paired Student's *t* test (normal distributions and equal variances) was used for statistical analysis. Differences were significant when $P <$ .05. Statistical analyses were carried out using the GraphPad InStat software program version 3.1a.

Results

Identification of Twist1 target genes

We analyzed gene expression profiles of TPC-Twist1 cells in comparison with control cells (TPC-pcDNA). Total RNA extracted from 3 TPC-Twist1 stable transfectants (Twist1 mp1, Twist1 mp2, and Twist1 Cl2) and vector control cells was analyzed using human Genome U133 Plus 2.0 Array GeneChips (Affymetrix) containing >47 000 gene transcripts. We sorted only the genes that were changed in all 3 Twist1 transfectants compared with vector control cells. We found 158 genes upregulated (Supplemental Table 2) and 221 downregulated (Supplemental Table 3) by ≥1.5-fold in TPC-Twist1 cells compared with control cells. Ingenuity Pathways Analysis (Ingenuity Systems, www.ingenuity.com) was used to classify Twist1 target genes. Consistent with the biological functions of Twist1 in ATC, the top 3 categories enriched in TPC-Twist1 cells compared with vector control were cellular movement, cellular growth and proliferation, and cell death and survival (Supplemental Figure 1). Other top categories were cancer, reproductive system disease, tissue

development, and tumor morphology. In details 53.6% of the genes (203 of 379) belonged to cellular movement, cellular growth and proliferation, and cell death and survival, 17.6% (67 of 379) belonged to other top categories (mainly to cancer), and 28.7% (109 of 379) were not classified (Supplemental Figure 2). Here we focused on the genes that were upregulated by ≥4-fold; *PDZK1IP1*, although upregulated ~3-fold, was also studied because it is the interacting protein of PDZ domain containing 1 (PDZK1) (22, 23) (Supplemental Table 4).

Expression levels of upregulated genes are affected by Twist1 level

We performed qRT-PCR of the top 16 upregulated genes in the cell lines used in the screening in comparison with vector control cells. As shown in Supplemental Figure 3, qRT-PCR confirmed the microarray screening, albeit with some variability in the different Twist1 clones. We failed to efficiently detect the expression of *MXRA8* and *GFRA1*; thus, these genes were excluded from further study. To confirm that Twist1 transcriptionally regulates the identified genes, we studied whether silencing of Twist1 affected their expression levels. Thus, we performed qRT-PCR of the top 14 upregulated genes in the CAL62 (ATC) cell line stably transfected with shTwist1 plasmid. The CAL62 cell line presents a high endogenous level of Twist1 (13), and in CAL62-shTwist1 cells, Twist1 mRNA was downregulated ~2-fold (13). As shown in Supplemental Figure 4, transfection of CAL62 with a Twist1 short hairpin RNA blunted expression of upregulated genes with respect to the control cell.

Silencing of Twist1-upregulated genes in TPC-Twist1 and in CAL62 cells impairs cell viability

Ten of the top 14 upregulated genes (~70%) belong to the categories cellular movement, cellular growth and proliferation, and cell death and survival. Focusing on these genes (Table 1), TPC-Twist1 and CAL62 cells were transiently transfected with siRNAs for *HS6ST2, COL1A1, KRT7, F2RL1, LEPREL1, THRB, ID4, RHOB, PDZK1*,

Table 1. List of Top 10 Upregulated Genes

Gene	Fold Change	Molecular and Cellular Biofunction
HS6ST2	10.28	Cellular growth and proliferation
COL1A1	7.22	Cellular growth and proliferation, cell death and survival, cellular movement
KRT7	5.56	Cellular growth and proliferation, cellular movement
F2RL1	5.31	Cellular growth and proliferation, cell death and survival, cellular movement
LEPREL1	4.99	Cellular growth and proliferation
THRB	4.88	Cellular growth and proliferation, cellular movement
ID4	4.33	Cellular growth and proliferation, cell death and survival
RHOB	4.13	Cellular growth and proliferation, cell death and Survival, cellular movement
PDZK1	3.99	Cellular growth and proliferation, cell death and survival
PDZK1IP1	2.90	Cellular growth and proliferation

PDZK1IP1, or a scrambled siRNA and examined at 48 and 72 hours after transfection for cell viability using a trypan blue assay. As shown in Figure 1, A and B, transient silencing of all 10 genes decreased cell number in TPC-Twist1 (Figure 1A) and in CAL62 (Figure 1B) cells at different time points ($P < .001$). Silencing of *COL1A1*, *KRT7*, and *PDZK1* also increased the cell death rate (in particular at 72 hours after transfection). As a control, transfection of the 10 siRNAs efficiently downregulated the specific genes, albeit with some variability (Figure 1, C and D).

Silencing of *HS6ST2*, *THRB*, *ID4*, *RHOB*, and *PDZK1IP1* in TPC-Twist1 and in CAL62 cells impairs cell migration

Twist1 increases the migration ability of TPC cells, whereas Twist1 knockdown in CAL62 cells decreases cell migration (13). We selected *HS6ST2*, *THRB*, *ID4*, *RHOB*, and *PDZK1IP1* because silencing of these genes affected the cell viability to a lesser lower extent than silencing of other target genes and, thus there were a sufficient number of surviving cells available for further analysis (Figure 1, A and B). A scraped wound was introduced on the confluent monolayer of TPC-Twist1 and CAL62 cells transfected with specific siRNAs or scrambled siRNA, and the cell migration into the wound was monitored after 24 hours. TPC-Twist1 and CAL62 cells transfected with the scrambled control efficiently migrated into the wound; by contrast, cells transfected with *HS6ST2*, *THRB*, *ID4*, *RHOB*, and *PDZK1IP1* siRNAs displayed reduced migrating ability. This phenomenon was particularly evident with siRNA of *RHOB* or *PDZK1IP1* (Figure 2A).

To better characterize this effect, we performed a Transwell migration assay. As shown in Figure 2, B–D, silencing of *HS6ST2*, *THRB*, *ID4*, *RHOB*, and *PDZK1IP1* reduced the number of migrated cells in the Transwell.

Twist1 increased (~2-fold) the ability of TPC cells to migrate into collagen I matrix (Supplemental Figure 5, A and B), whereas Twist1 knockdown in CAL62 cells decreased cell migration into collagen I matrix (Supplemental Figure 5, C and D) ($P < .001$). Thus, we asked whether
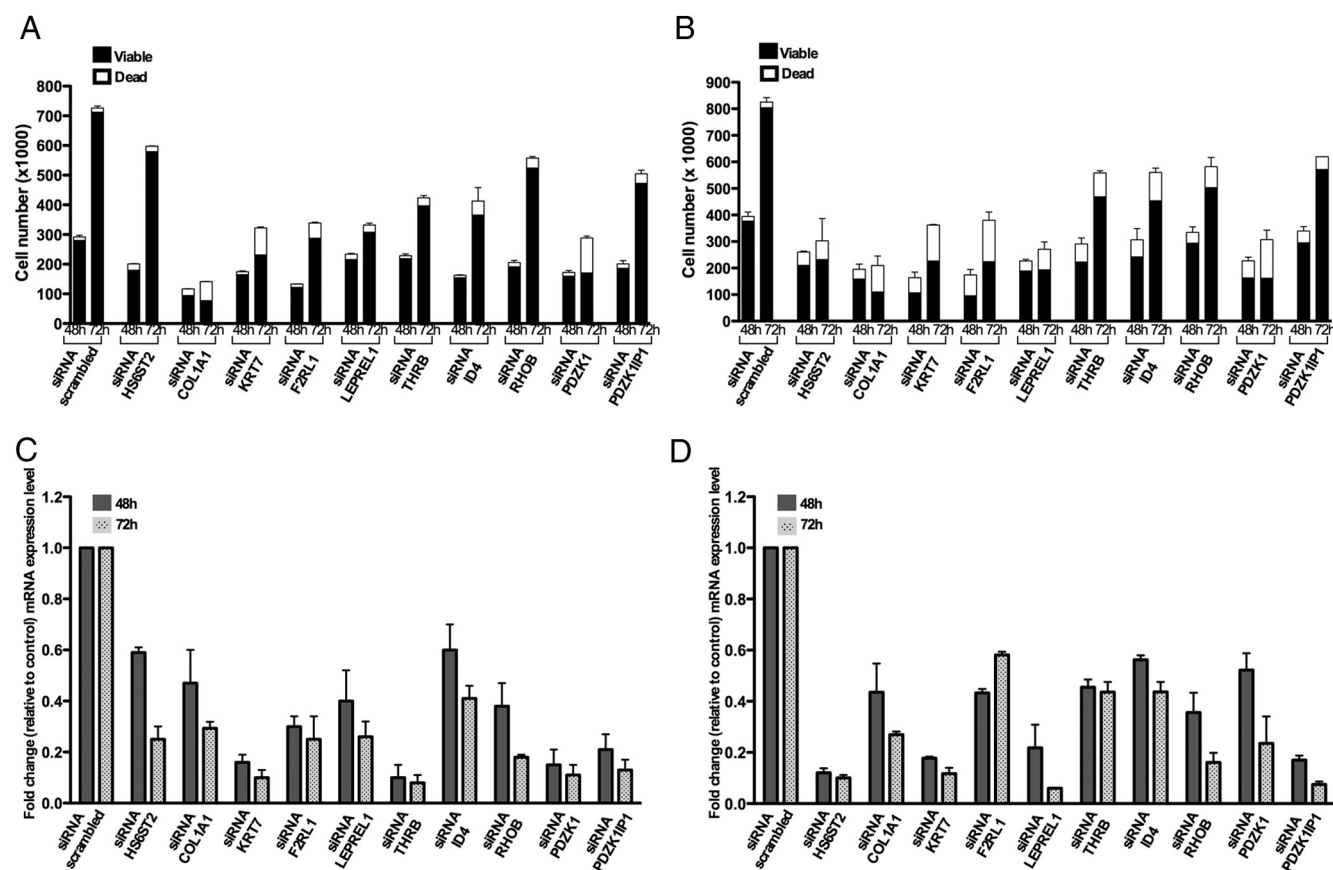
Figure 1. Silencing of the top 10 upregulated genes impairs cell viability. A and B, TPC-Twist1 (A) and CAL62 (B) cells were transfected with the indicated siRNAs or scrambled siRNA; after 48 and 72 hours, cells were collected by trypsinization, stained for 10 minutes with trypan blue, and counted; black bars represent the viable cells, and white bars represent the dead cells. C and D, mRNA expression levels of the indicated genes were measured by qRT-PCR in TPC-Twist1 (C) and in CAL62 (D) cells. Results are reported as fold change in comparison with the scrambled control. Values represent the average of triplicate experiments ± SDs.
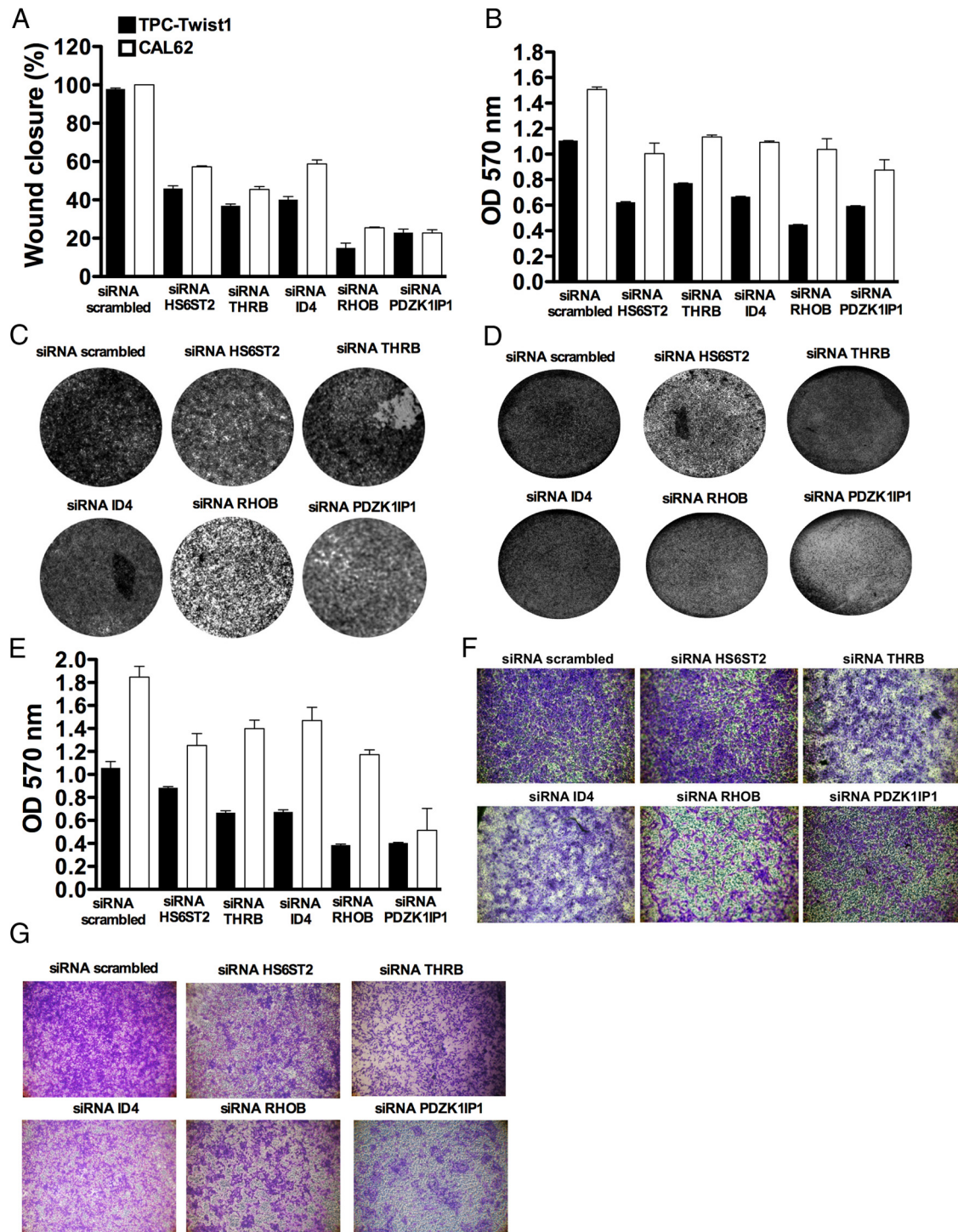
Figure 2. Silencing of the indicated genes reduces the migration ability of TPC-Twist1 and CAL62 cells. A, Cells were transfected with specific siRNAs, and 48 hours after transfection, scratch wounds were inflicted on the confluent cell monolayer. After 24 hours, cells were photographed. Wound closure was measured by calculating pixel densities in the wound area and expressed as percentage of wound closure of triplicate areas ± SDs. B–D, TPC-Twist and CAL62 cells were transfected with specific siRNAs or scrambled control, and 48 hours after transfection, cells were seeded in the upper chambers of Transwells, allowed to migrate, and photographed (C, TPC-Twist1; D, CAL62). Migration ability is expressed as absorbance at OD 570 nm (B). Values represent the average of triplicate experiments ± SDs. E–G, TPC-Twist1 and CAL62 transfected cells were seeded onto the insert coated with collagen I, left to migrate, stained, and photographed (F, TPC-Twist1; G, CAL62). Migration ability in collagen I is expressed as absorbance at OD 570 nm (E). Values represent the average of triplicate experiments ± SDs.

silencing of *HS6ST2*, *THRB*, *ID4*, *RHOB*, and *PDZK1IP1* affected this ability. As shown in Figure 2, E–G, TPC-Twist1 and CAL62 cells transfected with *HS6ST2*, *THRB*, *ID4*, *RHOB*, and *PDZK1IP1* siRNA presented a decreased ability to migrate into Collagen I matrix compared with siRNA scrambled transfected cells ($P < .001$).

Silencing of *HS6ST2*, *THRB*, *ID4*, *RHOB*, and *PDZK1IP1* in TPC-Twist1 and in CAL62 cells impairs cell invasion

We evaluated cell invasion in collagen I matrix. As shown in Supplemental Figure 6, A and B, Twist1 increased the ability of TPC cells to invade the collagen I matrix, whereas Twist1 knockdown in CAL62 cells de-

creased cell migration into collagen I matrix (Supplemental Figure 6, C and D) ($P < .001$). Silencing of *HS6ST2*, *THRB*, *ID4*, *RHOB*, and *PDZK1IP1* reduced this ability compared with cells transfected with scrambled siRNA (Figure 3, A–C). We then evaluated cell invasion in Matrigel matrix. Twist1 increased the invasion ability of TPC cells ~5-fold in Matrigel, whereas Twist1 knockdown in CAL62 cells decreased cell invasion in Matrigel (13). TPC-Twist1 and CAL62 cells transfected with *HS6ST2*, *THRB*, *ID4*, *RHOB*, and *PDZK1IP1* siRNA presented a reduced ability to invade Matrigel compared with siRNA scrambled transfected cells. In particular, the silencing of *RHOB* and *PDZK1IP1* induced a reduction of ~86% and ~84% in TPC-Twist1 and of ~59% and ~56% in CAL62 cells,
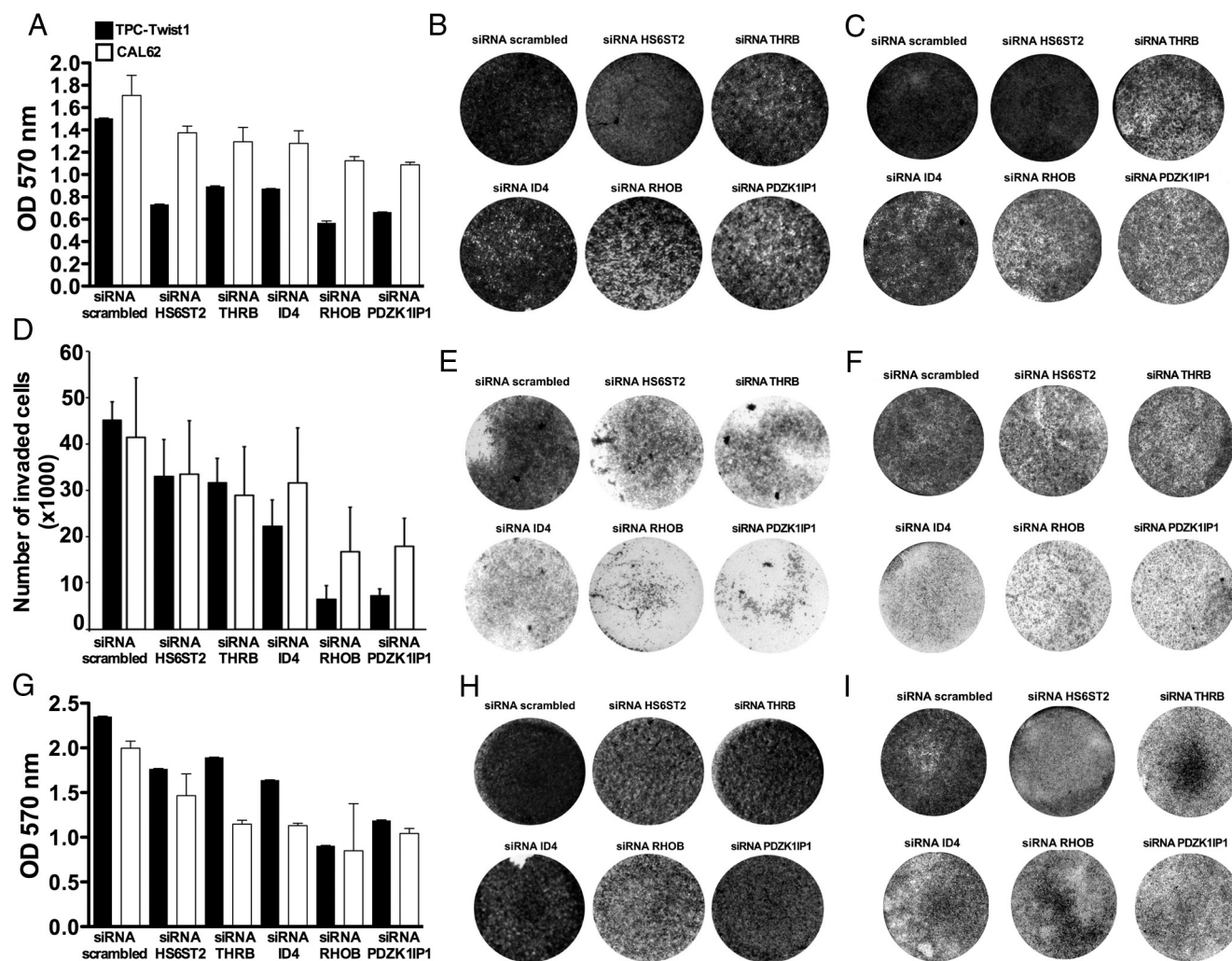
Figure 3. Silencing of the indicated genes reduces the invasion ability of TPC-Twist1 and CAL62 cells. A–C, TPC-Twist1 and CAL62 transfected cells were seeded in the upper chamber of Transwells coated with collagen I matrix and incubated for 24 hours (B, TPC-Twist1) or 48 hours (C, CAL62). The invasive ability in collagen I is expressed as absorbance at OD 570 nm (A). D–F, TPC-Twist1 and CAL62 transfected cells were seeded in the upper chambers of Transwells coated with Matrigel and incubated; the upper surface of the filter was wiped clean and cells on the lower surface were stained, photographed (E, TPC-Twist1; F, CAL62), and counted. The invasive ability in Matrigel matrix is expressed as number of invaded cells (D). G–I, TPC-Twist1 and CAL62 transfected cells were seeded on a confluent monolayer of endothelial human umbilical vein endothelial cells (HUVECs) and left to migrate. Cells were then stained and photographed (H, TPC-Twist1; I, CAL62). Values represent the average of triplicate experiments ± SDs. Migration ability through HUVECs is expressed as absorbance at OD 570 nm (G).

respectively, of invasion ability assessed by counting the number of invaded cells in 3 different fields (Figure 3, D–F) ($P < .001$).

Finally, we studied the cell ability to penetrate into the endothelium (24, 25) by a transendothelial cell migration assay. As shown in Supplemental Figure 7, A and B, TPC-Twist1 cells presented an increased ability to migrate through endothelial cells compared with control cells ($P < .001$), whereas CAL62 shTwist1 presented a reduced ability to migrate through endothelial cells compared with control (Supplemental Figure 7, C and D) ($P < .001$). As shown in Figure 3, G–I, TPC-Twist1 and CAL62 cells transfected with *HS6ST2*, *THRB*, *ID4*, *RHOB*, and *PDZK1IP1* siRNA presented a decrease in the transendothelial cell migration ability compared with cells transfected with scrambled siRNA.

Twist1 directly binds the promoter of target genes

To formally prove that the identified genes are direct Twist1 targets, we verified whether Twist1 binds to their promoters. Consensus binding sites for Twist1 are represented by an E-box (5′-CANNTG-3′) sequence motif (14, 15). In the promoter of all 10 upregulated genes, we found several E-box sequences (Supplemental Figure 8). Thus, DNA-chromatin complexes from TPC-pcDNA and TPC-

Twist1 were subjected to IP with Twist1 antibody or with control antibody (IgG1). As shown in Figure 4, promoter regions of all 10 upregulated genes were significantly enriched by Twist1 IP in TPC-Twist1 cells compared with TPC-pcDNA cells ($P < .001$). Conversely, no amplification was observed with anti-IgG precipitates and when primers for the *GAPDH* promoter were used. This corroborates the notion that the top upregulated genes are direct Twist1 targets.

Twist1 target genes are overexpressed in PTC, PDC, and ATC samples

To assess the role of the identified Twist1 targets in thyroid carcinogenesis we performed a qRT-PCR on a set of normal thyroid (n = 9), PTC (n = 9), PDC (n = 8), and ATC (n = 12) samples. As shown in Figure 5, *HS6ST2*, *COL1A1*, *F2RL1*, *LEPREL1*, *PDZK1*, and *PDZK1IP1* are differentially overexpressed in PTC, PDC, and ATC samples. The expression level of *KRT7*, *THRB*, *ID4*, and *RHOB* was not significantly altered in thyroid carcinomas compared with normal thyroid samples (not shown).

To verify these data at the protein level, we performed immunohistochemistry studies for leprecan-like 1 (LEPREL1) in a panel of normal thyroid (n = 27), PTC (n = 19), and ATC (n = 40) samples. As shown in Supplemental
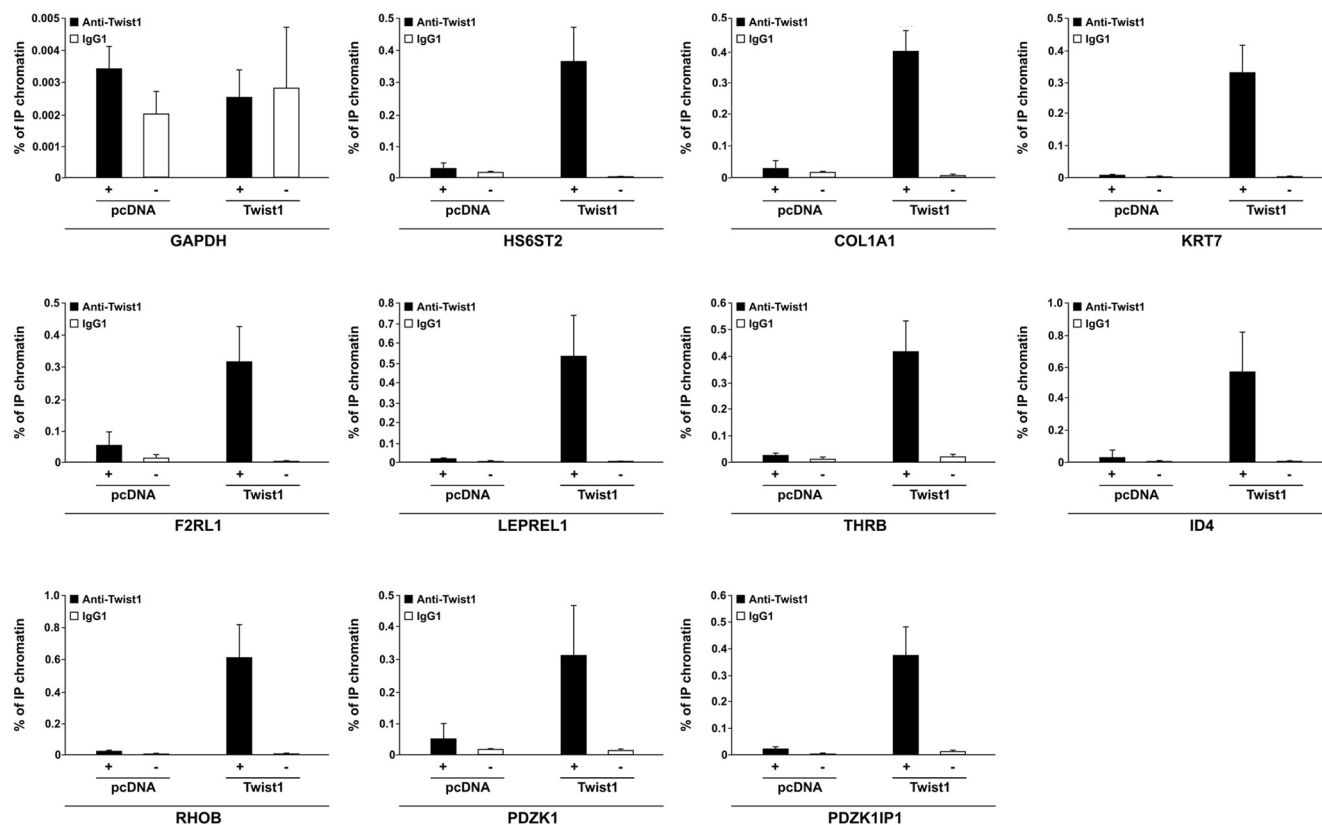
Figure 4. Twist1 directly binds the promoter of target genes. ChIP assay followed by qRT-PCR was performed on TPC-Twist1 and TPC-pcDNA cells. Equal amounts of proteins were subjected to IP with anti-Twist1 antibody or IgG1 antibody, as indicated. The *GAPDH* promoter amplicon was used as a negative control. Columns represent the average of 3 independent experiments ± SDs.
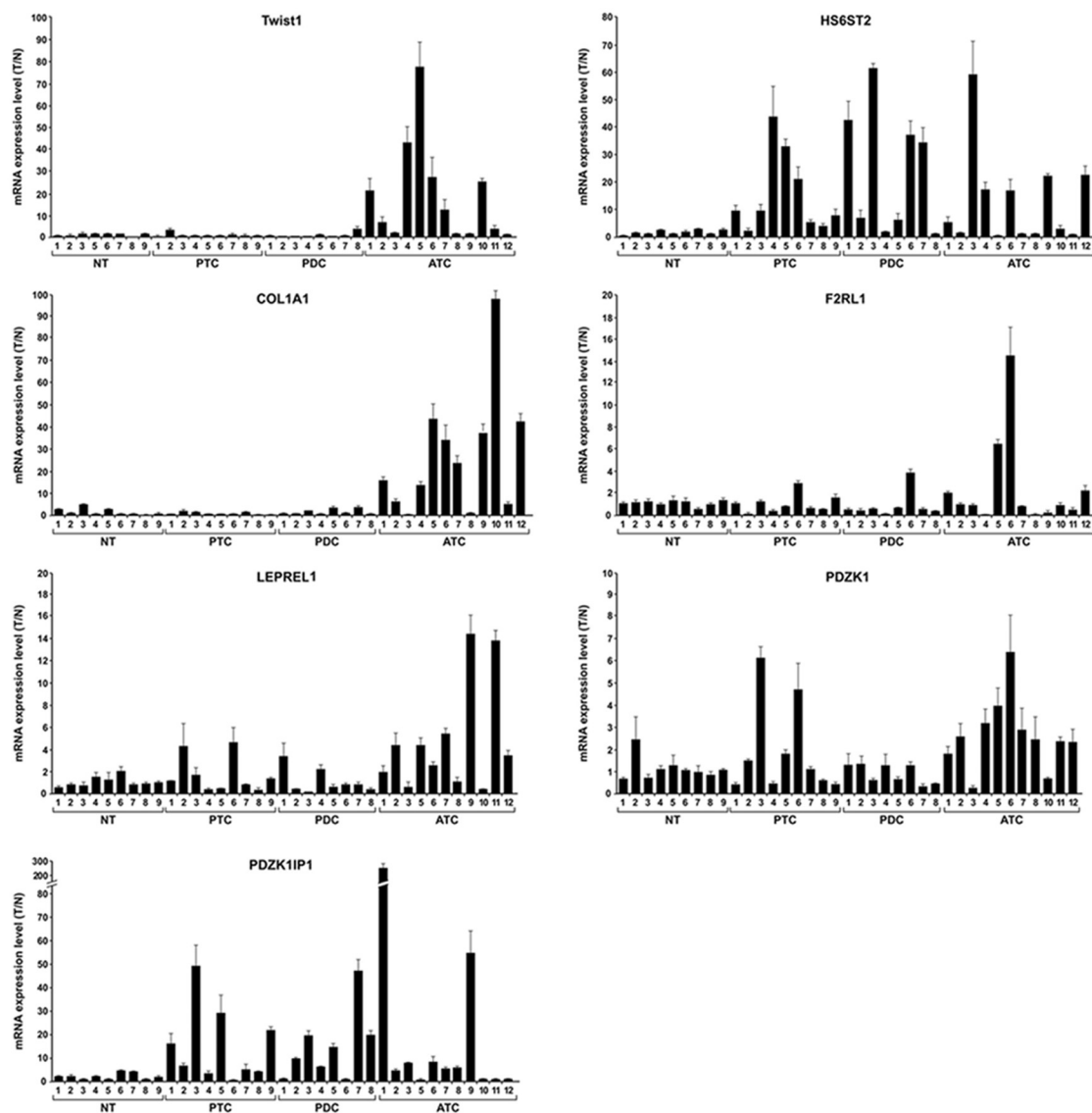
Figure 5. Twist1 targets are upregulated in thyroid carcinoma samples, as shown by qRT-PCR of the indicated genes in normal thyroids (NT) (n = 9), PTC (n = 9), PDC (n = 8), and ATC (n = 12) snap-frozen tissues. The expression levels of genes in each sample were measured by comparing its fluorescence threshold with the average fluorescence threshold of the NT samples. The average results of triplicate samples are plotted ± SDs.

Table 6 and Supplemental Figure 9, LEPREL1 is overexpressed in 26% of PTC (5 of 19) and 67% of ATC (27 of 40) samples in comparison with normal thyroids.

Discussion

Thyroid cancer includes well-differentiated carcinomas with a good prognosis and undifferentiated carcinomas (ATC) that represent one of the most aggressive human cancers and present a dismal prognosis. The molecular players sustaining such aggressive behavior are largely unknown. We have previously demonstrated that Twist1 is upregulated in ATC and that silencing of Twist1 in ATC cells reduces cell migration and invasion and increases sensitivity to apoptosis (13).

Twist1 is a transcription factor capable of directly binding E-box consensus sites (5′-CANNTG-3′) to exert transcriptional effects (14, 15). Despite the growing literature on the role of Twist1 in cancer progression, through which target genes Twist1 exerts its functions remains elusive. Here, we provide evidence that *HS6ST2*, *COL1A1*, *KRT7*, *F2RL1*, *LEPREL1*, *THRB*, *ID4*, *RHOB*, *PDZK1*, and *PDZK1IP1* are direct transcriptional targets of Twist1 with *COL1A1*, *KRT7*, and *PDZK1* mostly mediating Twist1 prosurvival properties, whereas *HS6ST2*, *THRB*, *ID4*, *RHOB*, and *PDZK1IP* are mainly involved in Twist1 promotile effects. Furthermore, we showed that *HS6ST2*, *COL1A1*, *F2RL1*, *LEPREL1*, *PDZK1*, and *PDZK1IP1* were differentially overexpressed in PTC, PDC, and ATC samples.

Heparan sulfate 6-O-sulfotransferase 2 (HS6ST2) is an enzyme that attaches sulfate groups to glucosamine residues in heparan sulfate. Heparan sulfate proteoglycans are ubiquitous components of the cell surface, extracellular matrix, and basement membranes and interact with various ligands to influence cell growth, differentiation, adhesion, and migration (26, 27). Importantly, it was recently reported that the specific inhibition of HS6ST2 by heparin and a high-molecular-weight *Escherichia coli* K5-derived heparin-like polysaccharide (K5-NSOS) efficiently reduced osteolytic lesion area and metastatic tumor burden in a mouse model of breast cancer bone metastasis (26).

LEPREL1 encodes a member of the prolyl 3-hydroxylase subfamily of 2-oxo-glutarate-dependent dioxygenases (28). These enzymes play a critical role in collagen chain assembly, stability, and cross-linking by catalyzing posttranslational 3-hydroxylation of proline residues (29). Hypoxia-inducible factor 1 activates the transcription of collagen prolyl hydroxylases (30). Of note, Twist1 is a downstream target of hypoxia-inducible factor 1 (31). Noteworthy, an ethyl 3,4-dihydroxybenzoate, a prolyl hydroxylase inhibitor, decreased tumor fibrosis and metastasis in a mouse model of breast cancer (30). During cancer progression, increased deposition of collagens can occur within and near the primary tumors, and it is associated with a poor outcome due to increased local invasion and distant metastasis (32). Straightened and aligned collagen fibers in tumor samples are predictive of patient mortality, presumably because collagen fibers provide directional cues that dictate cell morphology and promote cell migration as well as induce stiffness, which promotes tissue tension to enhance cancer progression (33). Indeed, in TPC-Twist1 cells, we found upregulated *COL1A1* (7.2 ± 1.4), *COL4A1* (2.0 ± 0.05), *COL18A1* (1.7 ± 0.1), *COL4A2* (1.5 ± 0.2) (Supplemental Table 2). These results are in agreement with Hébrant and colleagues (11) who demonstrated that one of the clusters that differentiated ATC vs PTC is composed of genes involved in calcification and fibrosis processes.

PDZK1IP1, also known as membrane-associated protein 17 (MAP17), is a small 17-kDa nonglycosylated membrane protein overexpressed in a great variety of human carcinomas (22). Immunohistochemical analysis of PDZK1IP1 shows that overexpression of the protein strongly correlates with tumor progression (22, 23). The increased malignant cell behavior induced by PDZK1IP1 is associated with an increase in reactive oxygen species production, and the treatment of PDZK1IP1-expressing cells with antioxidants resulted in a reduction in the tumorigenic properties of these cells (22, 23).

Coagulation factor II (thrombin) receptor-like 1 (F2RL1), also known as protease-activated receptor 2 (PAR2), is a member of the large family of 7-transmembrane-region receptors that couple to guanosine nucleotide-binding proteins and is a key signaling component for proteases in vascular biology and tumor progression (34). PAR2 is involved in tissue factor (TF) signaling pathway and plays a crucial role in tumor growth. TF forms a catalytic enzyme complex with coagulation factor VIIa, and selective inhibition of TF-factor VIIa-PAR2 signaling using a monoclonal antibody was shown to reduce breast tumor growth (35). Consistent with the hypothesis that F2RL1 mediated signaling contributes to tumor growth in breast cancer, mice lacking F2RL1 exhibited reduced tumor growth in a model of spontaneous mammary tumors (36).

Here, we showed by immunohistochemistry that LEPREL1 was overexpressed in 67% of ATC and in 26% of PTC cases. In the same dataset, Twist1 was overexpressed in 62% of ATC and in 0% of PTC samples. Similarly, many identified Twist1 targets were overexpressed also in PTC where Twist1 is negative (Figure 5). It is possible that other factors regulate the identified target genes in Twist1 negative samples. Furthermore, we have performed a gene expression profile in TPC-Twist1 cells that, although they express high levels of Twist1, are a cell line and thus could be not representative of thyroid cancer complexity.

In conclusion, here we have identified a set of novel direct targets of Twist1. The identified targets could be important to mediate Twist1 biological effects also in other malignancies such as breast and prostate carcinoma and sarcoma where Twist1 is overexpressed (14, 15, 37). All the genes identified are novel transcriptional targets of Twist1 and are potential targets for cancer therapy. Indeed, HS6ST2 and LEPREL1 are enzymes, whereas PDZK1IP1 and F2RL1 are membrane proteins and thus targetable by small molecules or monoclonal antibodies respectively (38).

Identification of genes downstream transcription factors, ie, Twist1, could be important for clinical translation of basic research. Directly inhibiting the transcription factors is currently difficult, as targeting large binding interfaces is not amenable to small-molecule inhibition. Twist1 is generally believed to be difficult to target due to its nuclear localization and lack of a specific groove for tight binding of a small molecule inhibitor. In particular the absence of a clear ligand-binding domain in Twist1 creates a hurdle toward developing inhibitors that can suppress its function. Thus, downstream targets of Twist1 could be more realistic for therapeutic intervention.

Acknowledgments

References

1. **Taccaliti A, Silvetti F, Palmonella G, Boscaro M.** Anaplastic thyroid carcinoma. *Front Endocrinol (Lausanne)*. 2012;3:84.
2. **Smallridge RC, Copland JA.** Anaplastic thyroid carcinoma: pathogenesis and emerging therapies. *Clin Oncol (R Coll Radiol)*. 2010; 22:486–497.
3. **O'Neill JP, Power D, Condron C, Bouchier-Hayes D, Walsh M.** Anaplastic thyroid cancer, tumorigenesis and therapy. *Ir J Med Sci*. 2010;179:9–15.
4. **Smallridge RC.** Approach to the patient with anaplastic thyroid carcinoma. *J Clin Endocrinol Metab*. 2012;8:2566–2572.
5. **Segerhammar I, Larsson C, Nilsson IL, et al.** Anaplastic carcinoma of the thyroid gland: treatment and outcome over 13 years at one institution. *J Surg Oncol*. 2012;106:981–986.
6. **Perri F, Lorenzo GD, Scarpati GD, Buonerba C.** Anaplastic thyroid carcinoma: A comprehensive review of current and future therapeutic options. *World J Clin Oncol*. 2011;2:150–157.
7. **Smallridge RC, Ain KB, Asa SL, et al.** American Thyroid Association guidelines for management of patients with anaplastic thyroid cancer. *Thyroid*. 2012;22:1104–1139.
8. **Kondo T, Ezzat S, Asa SL.** Pathogenetic mechanisms in thyroid follicular-cell neoplasia. *Nat Rev Cancer*. 2006;6:292–306.
9. **Nikiforov YE, Nikiforova MN.** Molecular genetics and diagnosis of thyroid cancer. *Nat Rev Endocrinol*. 2011;7:569–580.
10. **Xing M.** Molecular pathogenesis and mechanisms of thyroid cancer. *Nat Rev Cancer*. 2013;13:184–199.
11. **Hébrant A, Dom G, Dewaele M, et al.** mRNA expression in papillary and anaplastic thyroid carcinoma: molecular anatomy of a killing switch. *PLoS One*. 2012;7:37807.
12. **Salvatore G, Nappi TC, Salerno P, et al.** A cell proliferation and chromosomal instability signature in anaplastic thyroid carcinoma. *Cancer Res*. 2007;67:10148–10158.
13. **Salerno P, Garcia-Rostan G, Piccinin S, et al.** TWIST1 plays a pleiotropic role in determining the anaplastic thyroid cancer phenotype. *J Clin Endocrinol Metab*. 2011;96:772–781.
14. **Qin Q, Xu Y, He T, Qin C, Xu J.** Normal and disease-related biological functions of Twist1 and underlying molecular mechanisms. *Cell Res*. 2012;22:90–106.
15. **Ansieau S, Morel AP, Hinkal G, Bastid J, Puisieux A.** TWISTing an embryonic transcription factor into an oncoprotein. *Oncogene*. 2010;29:3173–3184.
16. **Zheng H, Kang Y.** Multilayer control of the EMT master regulators. *Oncogene*. 2014;33:1755–1763.
17. **Sánchez-Tilló E, Liu Y, de Barrios O, et al.** EMT-activating transcription factors in cancer: beyond EMT and tumor invasiveness. *Cell Mol Life Sci*. 2012;69:3429–3456.
18. **De Craene B, Berx G.** Regulatory networks defining EMT during cancer initiation and progression. *Nat Rev Cancer*. 2013;13:97–110.
19. **Schweppe RE, Klopper JP, Korch C, et al.** Deoxyribonucleic acid profiling analysis of 40 human thyroid cancer cell lines reveals cross-contamination resulting in cell line redundancy and misidentification. *J Clin Endocrinol Metab*. 2008;93:4331–4341.
20. **Pierantoni GM, Rinaldo C, Esposito F, Mottolese M, Soddu S, Fusco A.** High Mobility Group A1 (HMGA1) proteins interact with p53 and inhibit its apoptotic activity [retracted in: *Cell Death Differ*. 2014;21:503]. *Cell Death Differ*. 2006;13:1554–1563.
21. **Hedinger C, Williams ED, Sobin LH.** The WHO histological classification of thyroid tumors: a commentary on the second edition. *Cancer*. 1989;63:908–911.
22. **Carnero A.** MAP17 and the double-edged sword of ROS. *Biochim Biophys Acta*. 2012;1826:44–52.
23. **Birrane G, Mulvaney EP, Pal R, Kinsella BT, Kocher O.** Molecular analysis of the prostacyclin receptor's interaction with the PDZ1 domain of its adaptor protein PDZK1. *PLoS One*. 2013;8:53819.
24. **Chambers AF, Groom AC, MacDonald IC.** Dissemination and growth of cancer cells in metastatic sites. *Nat Rev Cancer*. 2002;2:563–572.
25. **Joosse SA, Pantel K.** Biologic challenges in the detection of circulating tumor cells. *Cancer Res*. 2013;73:8–11.
26. **Pollari S, Käkönen RS, Mohammad KS, et al.** Heparin-like polysaccharides reduce osteolytic bone destruction and tumor growth in a mouse model of breast cancer bone metastasis. *Mol Cancer Res*. 2012;10:597–604.
27. **Song K, Li Q, Peng YB, et al.** Silencing of hHS6ST2 inhibits progression of pancreatic cancer through inhibition of Notch signalling. *Biochem J*. 2011;436:271–282.
28. **Järnum S, Kjellman C, Darabi A, Nilsson I, Edvardsen K, Aman P.** LEPREL1, a novel ER and Golgi resident member of the Leprecan family. *Biochem Biophys Res Commun*. 2004;317:342–351.
29. **Fernandes RJ, Farnand AW, Traeger GR, Weis MA, Eyre DR.** A role for prolyl 3-hydroxylase 2 in post-translational modification of fibril-forming collagens. *J Biol Chem*. 2011;286:30662–30669.
30. **Gilkes DM, Chaturvedi P, Bajpai S, et al.** Collagen prolyl hydroxylases are essential for breast cancer metastasis. *Cancer Res*. 2013; 73:3285–3296.
31. **Yang MH, Wu MZ, Chiou SH, et al.** Direct regulation of TWIST by HIF-1α promotes metastasis. *Nat Cell Biol*. 2008;10:295–305.
32. **Conklin MW, Eickhoff JC, Riching KM, et al.** Aligned collagen is a prognostic signature for survival in human breast carcinoma. *Am J Pathol*. 2011;178:1221–1232.
33. **Provenzano PP, Eliceiri KW, Campbell JM, Inman DR, White JG, Keely PJ.** Collagen reorganization at the tumor-stromal interface facilitates local invasion. *BMC Med*. 2006;4:38.
34. **Schaffner F, Yokota N, Ruf W.** Tissue factor proangiogenic signaling in cancer progression. *Thromb Res*. 2012;129(Suppl 1):S127–S131.
35. **Versteeg HH, Schaffner F, Kerver M, et al.** Inhibition of tissue factor signaling suppresses tumor growth. *Blood*. 2008;111:190–199.
36. **Versteeg HH, Schaffner F, Kerver M, et al.** Protease-activated receptor (PAR) 2, but not PAR1, signaling promotes the development of mammary adenocarcinoma in polyoma middle T mice. *Cancer Res*. 2008;68:7219–7227.
37. **Piccinin S, Tonin E, Sessa S, et al.** A "twist box" code of p53 inactivation: twist box: p53 interaction promotes p53 degradation. *Cancer Cell*. 2012;22:404–415.
38. **Imai K, Takaoka A.** Comparing antibody and small-molecule therapies for cancer. *Nat Rev Cancer*. 2006;6:714–727.

Identification of targets of Twist1 transcription factor in thyroid cancer cells

Gennaro Di Maro[1], Francesca Maria Orlandella[1], Tammaro Claudio Bencivenga[1], Paolo Salerno[1], Clara Ugolini[2], Fulvio Basolo[3], Roberta Maestro[4], Giuliana Salvatore[5]

[1] Dipartimento di Medicina Molecolare e Biotecnologie Mediche, Università di Napoli "Federico II", 80131 Napoli, Italy.

[2] Dipartimento di area medica, Azienda ospedaliero-universitaria pisana, 56126 Pisa, Italy.

[3] Dipartimento di patologia chirugica, medica, molecolare e dell'area critica dell' Università di Pisa, 56124 Pisa, Italy.

[4] Experimental Oncology 1, Centro di Riferimento Oncologico, 33081 Aviano, Italy.

[5] Dipartimento di Scienze Motorie e del Benessere, Universita' "Parthenope", 80133 Napoli, Italy.

Supplemental Informations

Supplemental Methods

Microarray analysis

300 ng of purified total RNA from TPC-Twist1 cells (Twist1 mp1, Twist1 mp2, Twist1 Cl2) and TPC-pcDNA control cells were transcribed into cDNA using Superscript RT (Invitrogen, Carlsbad, CA, USA), in the presence of T7-oligo (dT) 24 primer, deoxyribonucleoside triphosphates (dNTPs), and T7 RNA polymerase promoter (Invitrogen). An *in vitro* transcription reaction was then performed to generate biotinylated cRNA which, after fragmentation, was used in a hybridization assay on Affymetrix U133 plus 2.0 GeneChip microarrays, according to manufacturer's protocol (GeneChip 3' ivt Express Kit, Affymetrix). The screening was conducted at Aarhus Biotechnology (Aarhus, Denmark). Normalization was performed by global scaling and analysis of differential expression was performed by Microarray Suite software 5.0 (Affymetrix). The final results were imported into Microsoft Excel (Microsoft).

Network and gene ontology analysis

The set of input genes (158 up-regulated and 221 down-regulated genes) was uploaded into the Ingenuity Pathway Analysis (IPA) online tool (Ingenuity System Inc, www.ingenuity.com). IPA is a system that transforms large data sets into relevant networks biological processes, and pathways, containing direct or indirect relationships between genes based on known interactions in the literature. IPA computes a score for each biological process according to the fit of the user's

set of significant genes. The score indicates the likelihood of the genes in a biological process to cluster together not due to random chance.

RNA extraction, cDNA synthesis, and quantitative real-time PCR

Total RNA was isolated with the RNeasy Kit (Qiagen, Crawley, West Sussex, UK). The quality and concentration of the RNA was verified by the NanoDrop (Thermo Scientific, Waltham, MA, USA) and by the 2100 Bioanalyzer (Agilent Technologies, Waldbronn, Germany); only samples with RNA integrity number value above 7 were used for further analysis. One µg of total RNA from each sample was reverse-transcribed with the QuantiTect® Reverse Transcription (Qiagen) according to manufacturer's instructions. The expression level of each gene was measured by quantitative PCR assay, using the Universal ProbeLibrary Set, Human (Roche, Basel, Switzerland). PCR reactions were performed in triplicate and fold changes were calculated with the formula: $2^{-(\text{sample 1 }\Delta Ct\ -\ \text{sample 2 }\Delta Ct)}$, where ΔCt is the difference between the amplification fluorescent thresholds of the mRNA of interest and the mRNA of RNA polymerase 2 used as an internal reference. The primers used are listed in Supplemental Table 5.

Migration and Invasion Assay

The migration ability was evaluated with Transwell and Collagen I assay. The TPC-Twist1 (1 × 10^5) and CAL62 cells (5 × 10^4) transfected with specific siRNAs, were resuspended respectively

in serum free and 2.5% serum culture medium and loaded onto the upper well of prehydrated polycarbonate membrane filter of 8 μm pore size (Costar, Cambridge, MA) or on a membrane coated with Collagen I at the bottom side (CytoSelected™ 24-Well Cell Haptotaxis Assay, Cell Biolabs, San Diego, CA). Medium (500 μl) that contained 2.5% serum (TPC-Twist1) or 10% serum (CAL62) was added to the lower well and cells were allowed to migrate for 24h (TPC-Twist1) or for 48h (CAL62) at 37°C. Migrated cells were stained with crystal violet and quantified at OD 570 nm (Model 550 Microplate Reader, Biorad, Hercules, CA, USA).

The invasion ability was evaluated with Matrigel and Collagen I invasion assay. The TPC-Twist1 (1×10^5) and CAL62 cells (5×10^4) transfected with specific siRNAs, were resuspended respectively in serum free and 2.5% serum culture medium and loaded onto the upper well of prehydrated polycarbonate membrane filter of 8 μm pore size coated with 35 μg of reconstituted extracellular matrix (Matrigel, BD Biosciences, San Jose, CA) or on a membrane coated with Collagen I at the upper side (CytoSelected™ 24-Well Cell Invasion assay, Collagen I, Colorimetric Format, Cell Biolabs). Medium (500 μl) that contained 2.5% serum (TPC-Twist1) or 10% serum (CAL62) was added to the lower well and cells were allowed to migrate for 24h (TPC-Twist1) or for 48h at 37°C (CAL62). Invaded cells in Matrigel were fixed with 10% glutaraldehyde solution (Sigma-Aldrich, St. Louis, MO, USA) for 30 minutes, mounted on glass slides and stained with Hoechst (Sigma). Cell invasion in Matrigel was quantified by counting the number of stained nuclei in five individual fields in triplicate. Invaded cells in Collagen I were stained with crystal violet and quantified at OD 570 nm (Model 550 Microplate Reader, Biorad, Hercules, CA, USA).

Transendothelial Cell Migration Assay

QCM™ Tumor Cell Transendothelial Migration Assay was used to analyze the ability of tumor cells to invade the endothelium (Millipore, Billerica, MA, USA). HUVEC (1 x 10^5 cells) were grown to confluence for 48h on cell culture inserts coated with fibronectin and then treated with

20 ng/ml of TNFα for 18h. The TPC-Twist1 (1×10^5 silenced cells suspension) and CAL62 (5×10^4 silenced cells suspension) were resuspended in serum free and in 2.5% serum culture medium (250 µl) respectively, added on the endothelial layer and left to migrate for 24h (TPC-Twist1) or for 48h (CAL62) at 37°C. Media (500 µl) that contained 2.5% serum (TPC-Twist1) or 10% serum (CAL62) was added to the lower well. Migrated cells were stained with Cell Stain Solution (Millipore) and color intensity was measured by OD 570 nm according to the assay instruction.

Immunohistochemistry

The study group included 86 patients who underwent total thyroidectomy at the Department of Surgery of the University of Pisa (Pisa, Italy) from 2010 to 2014.

Hematoxylin-eosin stained sections of 86 patients from the archives of the section of Pathology of University of Pisa were re-evaluated independently by two pathologists (C.U., F.B.). A diagnostic concordance rate of 98% was achieved between the two investigators.

The study group included 40 anaplastic thyroid carcinoma, 19 papillary thyroid carcinoma of classic variant. As control 27 normal tissues from controlateral dissection of adenomas or uninodular goiters were evaluated. Immunohistochemical analysis of Twist1, LEPREL1 expression was performed on formalin-fixed, paraffin-embedded (FFPE) tumor sections using mouse monoclonal anti-human of Twist1 (Twist 2C1a) (Santa Cruz Biotechnology, Inc. Dallas, Texas) and a rabbit polyclonal anti-human LEPREL1 (HPA007890, Sigma-Aldrich S.r.l. Milan,

Italy). Antibodies were optimized for automated slide stainer and sections were stained using the

Benchmarck IHC automated slide stainer (Ventana Medical Systems, Tucson, Az). Staining

>10% of tumor cells was considered positive for LEPREL1 and for Twist1.

Supplemental Table 1: List of the primers used in the ChIP.

Gene	Forward Primer	Reverse Primer
HS6ST2	5'-ggggtagagaagggcgtaaa-3'	5'-cgacttgctatcggagacg-3'
COL1A1	5'-atgtttctcaccctgcacct-3'	5'-gaatcaaatgccttcctcca-3'
KRT7	5'-atgtgtgccattgtgtagcc-3'	5'-ctctgggctctgctgtgct-3'
F2RL1	5'-gccattccatgtcttctttcc-3'	5'-gtagaggcaggtgggcaac-3'
LEPREL1	5'-gtgttaggcgtctggctgtt-3'	5'-agaacctttggaggcaggag-3'
THRB	5'-cttgcagacatcagcagcat-3'	5'-atccaaccatcttcccatga-3'
ID4	5'-tatggtttcggcaaatgtga-3'	5'-tgttcaagaaggcacgttca-3'
RHOB	5'-ctgtccggtaacttcctcca-3'	5'-ggagctggctgtctggag-3'
PDZK1	5'-caaaataacacctggaagctca-3'	5'-caccctcaccaactcctctg-3'
PDZK1IP1	5'-cccagcattagagtcccaga-3'	5'-agcctggcctatttcctgtt-3'
GAPDH	5'-cccaaagtcctcctgtttca-3'	5'-gtcttgaggcctgagctac-3'

Gene Title	Gene Symbol	Fold Change	SD	Chromosomal Location	Cellular Growth and Proliferation	Cell Death and Survival	Cellular Movement	Other functions	Not Classified
				Supplementary Table2: Genes upregulated by Twist1 by ≥1.5 fold					
heparan sulfate 6-O-sulfotransferase 2	HS6ST2	10,28173122	0,351188458	chrXq26.2	X				
collagen, type I, alpha 1	COL1A1	7,222289403	1,410673598	chr17q21.33	X	X	X		
GDNF family receptor alpha 1	GFRA1	6,919557528	0,608276253	chr10q26	X	X	X		
keratin 7	KRT7	5,567294029	0,8326664	chr12q12-q13	X		X		
vang-like 2 (van gogh, Drosophila)	VANGL2	5,480655757	0,305505046	chr1q22-q23				X	
matrix-remodelling associated 8	MXRA8	5,415015976	0,577350269	chr1p36.33				X	
plakophilin 2	PKP2	5,339337988	0,873689495	chr12p11				X	
coagulation factor II (thrombin) receptor-like 1	F2RL1	5,312989839	0,953939201	chr5q13	X	X	X		
leprecan-like 1	LEPREL1	4,994543441	0,472581563	chr3q28	X				
thyroid hormone receptor, beta (erythroblastic leukemia viral (v-erb-a) oncogene homolog 2, avian)	THRB	4,883874803	0,871779789	chr3p24.2	X		X		
zinc finger, BED-type containing 2	ZBED2	4,597610544	0,655743852	chr3q13.13					X
ADAM metallopeptidase with thrombospondin type 1 motif, 5 (aggrecanase-2)	ADAMTS5	4,369317144	0,850490055	chr21q21.3				X	
inhibitor of DNA binding 4, dominant negative helix-loop-helix protein	ID4	4,336721203	0,264575131	chr6p22-p21	X	X			
ras homolog gene family, member B	RHOB	4,135412309	0,611010093	chr2p24	X	X	X		
PDZ domain containing 1	PDZK1	3,993886633	0,550757055	chr1q21	X	X			

Gene	Symbol			Location					
netrin 4	NTN4	3,979515052	0,75055535	chr12q22-q23	X	X	X		
papilin, proteoglycan-like sulfated glycoprotein	PAPLN	3,94748841	0,702376917	chr14q24.2					X
cytochrome P450, family 24, subfamily A, polypeptide 1	CYP24A1	3,895790353	0,971253486	chr20q13	X				
filaggrin	FLG	3,72986228	0,692820323	chr1q21.3				X	
NUAK family, SNF1-like kinase, 2	NUAK2	3,644961964	0,519615242	chr1q32.1		X	X		
coiled-coil domain containing 80	CCDC80	3,585786458	0,86216781	chr3q13.2		X			
transforming growth factor, beta-induced, 68kDa	TGFBI	3,504545129	0,2	chr5q31	X	X	X		
Suppression of tumorigenicity 7 like	ST7L	3,453420992	0,871779789	chr1p13.2	X				
prostaglandin I2 (prostacyclin) synthase	PTGIS	3,43195669	0,776745347	chr20q13.13		X			
transgelin	TAGLN	3,405866218	1,006644591	chr11q23.2			X		
mal, T-cell differentiation protein 2	MAL2	3,381182308	0,519615242	chr8q23					X
EGF-like repeats and discoidin I-like domains 3	EDIL3	3,288688661	0,635085296	chr5q14		X	X		
tumor-associated calcium signal transducer 1	TACSTD1	3,241226113	0,953939201	chr2p21	X		X		
death-associated protein kinase 1	DAPK1	3,211787362	0,6244998	chr9q34.1		X			
LIM and cysteine-rich domains 1	LMCD1	3,202603619	0,461880215	chr3p26-p24				X	
WAS protein family, member 3	WASF3	3,116089412	0,585946528	chr13q12			X		
microphthalmia-associated transcription factor	MITF	2,945811369	0,854400375	chr3p14.2-p14.1	X	X	X		
phospholipase C, beta 4	PLCB4	2,936408568	0,793725393	chr20p12				X	

ADAM metallopeptidase with thrombospondin type 1 motif, 1	ADAMTS1	2,930214545	0,781024968	chr21q21.2	X	X	X		
chromosome 10 open reading frame 65	HOGA1	2,924178087	0,611010093	chr10q24.1					X
PDZK1 interacting protein 1	PDZK1IP1	2,901835211	0,577350269	chr1p33	X				
inositol(myo)-1(or 4)-monophosphatase 2	IMPA2	2,835027268	0,550757055	chr18p11.2					X
doublecortin domain containing 2	DCDC2	2,765568919	0,642910051	chr6p22.1			X		
Cbp/p300-interacting transactivator, with Glu/Asp-rich carboxy-terminal domain, 2	CITED2	2,717517969	0,86216781	chr6q23.3	X	X	X		
homolog of rat pragma of Rnd2	PRAGMIN	2,645044724	0,56862407	chr8p23.1					X
myosin, light chain kinase	MYLK	2,580367042	0,642910051	chr3q21	X	X	X		
thrombospondin 1	THBS1	2,470516694	0,4163332	chr15q15	X	X	X		
Kv channel interacting protein 1	KCNIP1	2,446433025	0,608276253	chr5q35.1		X			
argininosuccinate synthetase 1	ASS1	2,429964151	0,702376917	chr9q34.1				X	
O-6-methylguanine-DNA methyltransferase	MGMT	2,419540831	0,4163332	chr10q26	X	X			
endothelial PAS domain protein 1	EPAS1	2,36398258	0,435889894	chr2p21-p16	X	X	X		
syncoilin, intermediate filament 1	SYNC1	2,361554172	0,585946528	chr1p34.3-p33					X
alpha-kinase 2	ALPK2	2,336479509	0,513160144	chr18q21.31		X			
ring finger 144B	RNF144B	2,28151547	0,503322296	chr6p22.3		X			
apolipoprotein L domain containing 1	APOLD1	2,267236721	0,702376917	chr12p13.1				X	
ribokinase	RBKS	2,2545217	0,404145188	chr2p23.3					X
cystatin E/M	CST6	2,2545217	0,404145188	chr11q13	X		X		
SRY (sex determining region Y)-box 4	SOX4	2,247681135	0,556776436	chr6p22.3	X	X			

Description	Symbol	Value1	Value2	Location	C1	C2	C3	C4	C5
GLIS family zinc finger 3	GLIS3	2,246526787	0,529150262	chr9p24.2				X	
ATPase, class II, type 9A	ATP9A	2,246526787	0,529150262	chr20q13.2					X
melanoma cell adhesion molecule	MCAM	2,24373728	0,519615242	chr11q23.3	X	X	X		
RAB40B, member RAS oncogene family	RAB40B	2,237691725	0,351188458	chr17q25.3					X
growth arrest-specific 6	GAS6	2,216209577	0,251661148	chr13q34	X	X	X		
shroom family member 3	SHROOM3	2,205673738	0,435889894	chr4q21.1				X	
transducin-like enhancer of split 4 (E(sp1) homolog, Drosophila)	TLE4	2,204871835	0,550757055	chr9q21.31	X				
secreted phosphoprotein 1 (osteopontin, bone sialoprotein I, early T-lymphocyte activation 1)	SPP1	2,173953455	0,642910051	chr4q21-q25	X				
immediate early response 5-like	IER5L	2,168360602	0,264575131	chr9q34.11					X
tubulin, alpha 1a	TUBA1A	2,148548898	0,550757055	chr12q12-q14.3		X	X		
uncoupling protein 2 (mitochondrial, proton carrier)	UCP2	2,103543126	0,404145188	chr11q13	X	X	X		
collagen, type IV, alpha 1	COL4A1	2,09569795	0,057735027	chr13q34	X	X	X		
small nuclear RNA activating complex, polypeptide 1, 43kDa	SNAPC1	2,093480906	0,519615242	chr14q22					X
odz, odd Oz/ten-m homolog 2 (Drosophila)	ODZ2	2,057218164	0,550757055	chr5q34-q35.1	X	X			
UDP-glucose ceramide glucosyltransferase	UGCG	2,057218164	0,550757055	chr9q31					X
prickle homolog 1 (Drosophila)	PRICKLE1	2,051577463	0,4	chr12q12	X				
suppressor of cytokine signaling 2	SOCS2	2,004667006	0,550757055	chr12q	X	X	X		
interleukin 11	IL11	2,003204303	0,1	chr19q13.3-q13.4	X	X	X		
tuftelin 1	TUFT1	1,962675136	0,404145188	chr1q21					X

mixed lineage kinase 4	KIAA1804	1,95883413	0,404145188	chr1q42				X	
enabled homolog (Drosophila)	ENAH	1,95855963	0,115470054	chr1q42.12			X		
PRKC, apoptosis, WT1, regulator	PAWR	1,95571516	0,529150262	chr12q21	X	X			
PHD finger protein 17	PHF17	1,951719066	0,37859389	chr4q26-q27		X			
family with sequence similarity 83, member H	FAM83H	1,942631582	0,321455025	chr8q24.3					X
arrestin domain containing 3	ARRDC3	1,941529905	0,5	chr5q14.3	X		X		
Bardet-Biedl syndrome 10	BBS10	1,931443504	0,458257569	chr12q21.2				X	
keratin 80	KRT80	1,914189457	0,4	chr12q13.13					X
transmembrane, prostate androgen induced RNA	TMEPAI	1,90636884	0,360555128	chr20q13.31-q13.33	X	X			
progesterone receptor membrane component 2	PGRMC2	1,903870091	0,360555128	chr4q26					X
myosin, light chain 9, regulatory	MYL9	1,900435804	0,346410162	chr20q11.23	X				
phospholipase C, epsilon 1	PLCE1	1,887667543	0,264575131	chr10q23	X	X			
transducin-like enhancer of split 1 (E(sp1) homolog, Drosophila)	TLE1	1,872534505	0,404145188	chr9q21.32					X
fibroblast growth factor 2 (basic)	FGF2	1,867503395	0,37859389	chr4q26-q27	X	X	X		
RNA binding motif, single stranded interacting protein	RBMS3	1,861009508	0,513160144	chr3p24-p23					X
glutaminase	GLS	1,859225418	0,351188458	chr2q32-q34					X
Zinc finger protein 84	ZNF84	1,851404801	0,305505046	chr12q24.33					X
zinc finger protein 91	ZNF91	1,841776492	0,251661148	chr19p13.1-p12				X	
Rho guanine nucleotide exchange factor (GEF) 5	ARHGEF5	1,836384281	0,2081666	chr7q33-q35				X	
Regulating synaptic membrane exocytosis 2	RIMS2	1,833669061	0,4163332	chr8q22.3				X	

Description	Gene	Value1	Value2	Chromosome					
heterogeneous nuclear ribonucleoprotein A3	HNRPA3	1,831240653	0,404145188	chr2q31.2					X
GLI-Kruppel family member GLI2	GLI2	1,827656868	0,404145188	chr2q14	X	X	X		
LIM domain and actin binding 1	LIMA1	1,817570466	0,351188458	chr12q13	X				
transmembrane emp24 domain trafficking protein 2	TMED2	1,812539356	0,321455025	chr12q24.31				X	
FOS-like antigen 2	FOSL2	1,80210051	0,458257569	chr2p23.3	X	X	X		
hepatitis A virus cellular receptor 1	HAVCR1	1,800121539	0,251661148	chr5q33.2	X				
KIAA0802	KIAA0802	1,798202369	0,458257569	chr18p11.22					X
par-3 partitioning defective 3 homolog (C. elegans)	PARD3	1,797518837	0,230940108	chr10p11.22-p11.21			X		
SMAD family member 7	SMAD7	1,778705022	0,360555128	chr18q21.1	X	X	X		
kalirin, RhoGEF kinase	KALRN	1,778705022	0,360555128	chr3q21.1-q21.2				X	
eukaryotic translation elongation factor 1 alpha 1	EEF1A1	1,776276614	0,346410162	chr6q14.1	X	X			
Cysteine rich transmembrane BMP regulator 1 (chordin-like)	CRIM1	1,776276614	0,346410162	chr2p21	X	X			
protease, serine, 23	PRSS23	1,776276614	0,346410162	chr11q14.1				X	
unc-51-like kinase 2 (C. elegans)	ULK2	1,765837768	0,472581563	chr17p11.2				X	
angiomotin like 2	AMOTL2	1,763571984	0,461880215	chr3q21-q22					X
collagen, type XVIII, alpha 1	COL18A1	1,743890634	0,1	chr21q22.3	X	X	X		
placenta-specific 8	PLAC8	1,743714804	0,404145188	chr4q21.22	X	X			
heat shock 22kDa protein 8	HSPB8	1,724993353	0,288675135	chr12q24.23	X	X			
guanine nucleotide binding protein (G protein), gamma 4	GNG4	1,71843823	0,251661148	chr1q42.3	X				

Description	Gene symbol	Value 1	Value 2	Location	C1	C2	C3	C4	C5
UDP-N-acetyl-alpha-D-galactosamine:polypeptide N-acetylgalactosaminyltransferase 4 (GalNAc-T4)	GALNT4	1,708607945	0,404145188	chr12q21.3-q22				X	
WW and C2 domain containing 1	WWC1	1,707627892	0,152752523	chr5q35.1				X	
heterogeneous nuclear ribonucleoprotein R	HNRNPR	1,702235682	0,057735027	chr1p36.12	X				
F11 receptor	F11R	1,699070132	0,37859389	chr1q21.2-q21.3	X		X		
galectin-related protein	HSPC159	1,69585321	0,351188458	chr2p14					X
Fucosyltransferase 1 (galactoside 2-alpha-L-fucosyltransferase, H blood group)	FUT1	1,69585321	0,351188458	chr19q13.3					X
thioredoxin reductase 2	TXNRD2	1,68141923	0,458257569	chr22q11.21	X	X	X		
KIT ligand	KITLG	1,68141923	0,458257569	chr12q22		X			
dual specificity phosphatase 16	DUSP16	1,677144378	0,230940108	chr12p13			X		
RAB11 family interacting protein 1 (class I)	RAB11FIP1	1,677144378	0,230940108	chr8p11.22				X	
inhibitor of DNA binding 1, dominant negative helix-loop-helix protein	ID1	1,677039394	0,435889894	chr20q11	X	X	X		
family with sequence similarity 115, member A	FAM115A	1,677039394	0,435889894	chr7q35	X	X	X		
cylindromatosis (turban tumor syndrome)	CYLD	1,673793557	0,2081666	chr16q12.1	X	X	X		
B-cell CLL/lymphoma 2	BCL2	1,673793557	0,2081666	chr18q21.33|18q21.3	X	X	X		
cleavage and polyadenylation specific factor 6, 68kDa	CPSF6	1,673793557	0,2081666	chr12q15					X
tumor necrosis factor, alpha-induced protein 2	TNFAIP2	1,66639871	0,4	chr14q32				X	
prenylcysteine oxidase 1	PCYOX1	1,657324683	0,346410162	chr2p13.3	X				

Gene name	Symbol	Value	Score	Location	1	2	3	4	5
NUAK family, SNF1-like kinase, 1	NUAK1	1,648004234	0,3	chr12q23.3		X	X		
armadillo repeat containing, X-linked 3	ARMCX3	1,648004234	0,3	chrXq21.33-q22.2		X	X		
pleiomorphic adenoma gene-like 1	PLAGL1	1,645470844	0,461880215	chr6q24-q25	X	X			
zinc finger protein 395	ZNF395	1,643310043	0,264575131	chr8p21.1		X			
vesicle-associated membrane protein 3 (cellubrevin)	VAMP3	1,643310043	0,264575131	chr1p36.23					X
mitochondrial ribosomal protein L30	MRPL30	1,632499705	0,173205081	chr2q11.2					X
zinc finger protein 260	ZNF260	1,630135968	0,404145188	chr19q13.12					X
myristoylated alanine-rich protein kinase C substrate	MARCKS	1,627107495	0,1	chr6q22.2			X		
Ribosomal protein L37	RPL37	1,624504793	1,05367E-08	chr5p13		X			
phosphoribosyl pyrophosphate synthetase 1	PRPS1	1,611741492	0,305505046	chrXq21.32-q24				X	
nephroblastoma overexpressed gene	NOV	1,600570055	0,230940108	chr8q24.1	X	X	X		
ROD1 regulator of differentiation 1 (S. pombe)	ROD1	1,598665371	0,2081666	chr9q32	X				
programmed cell death 6 interacting protein	PDCD6IP	1,598665371	0,2081666	chr3p22.3		X			
CDC14 cell division cycle 14 homolog B (S. cerevisiae)	CDC14B	1,598665371	0,2081666	chr9q22.33					X
nucleosome assembly protein 1-like 1	NAP1L1	1,596301634	0,4163332	chr12q21.2	X				
zinc finger protein 558	ZNF558	1,593273161	0,152752523	chr19p13.2					X
lysophosphatidylcholine acyltransferase 2	LPCAT2	1,582286993	0,351188458	chr16q12.2				X	
glucosamine (N-acetyl)-6-sulfatase (Sanfilippo disease IIID)	GNS	1,56709682	0,251661148	chr12q14				X	

arginine vasopressin-induced 1	AVPI1	1,56170461	0,2081666	chr10q24.2					X
KIAA1600	KIAA1600	1,557010418	0,152752523	chr10q25.3					X
deleted in liver cancer 1	DLC1	1,554407716	0,115470054	chr8p22	X	X	X		
mex-3 homolog D (C. elegans)	MEX3D	1,548452659	0,360555128	chr19p13.3				X	
dopey family member 2	DOPEY2	1,533262485	0,264575131	chr21q22.2				X	
ubiquitin-conjugating enzyme E2H (UBC8 homolog, yeast)	UBE2H	1,532250111	0,264575131	chr7q32					X
cysteine-rich, angiogenic inducer, 61	CYR61	1,525441868	0,2	chr1p31-p22	X	X	X		
collagen, type IV, alpha 2	COL4A2	1,525441868	0,2	chr13q34	X	X	X		
protein-L-isoaspartate (D-aspartate) O-methyltransferase domain containing 1	PCMTD1	1,518144974	0,1	chr8q11.23					X
keratin 81	KRT81	1,518144974	0,1	chr12q13					X
actin binding LIM protein 1	ABLIM1	1,501693935	0,288675135	chr10q25					X

					Cellular Growth and Proliferation	Cell Death and Survival	Cellular Movement	Other functions	Not Classified
Supplementary Table 3: Genes downregulated by Twist1 by ≥1.5 fold									
Gene Title	**Gene Symbol**	**Fold Change**	**SD**	**Chromosomal Location**					
peroxisomal biogenesis factor 5-like	PEX5L	-32,00209	3,2470499	chr3q26.33				X	
NADPH oxidase, EF-hand calcium binding domain 5	NOX5	-25,62318	2,8219379	chr15q23	X				
hydroxysteroid (11-beta) dehydrogenase 1	HSD11B1	-24,56294	2,2143472	chr1q32-q41	X				
protocadherin 7	PCDH7	-23,26581	2,5716402	chr4p15					X
interleukin 13 receptor, alpha 2	IL13RA2	-23,05602	2,6539279	chrXq13.1-q28	X		X		
granzyme A (granzyme 1, cytotoxic T-lymphocyte-associated serine esterase 3)	GZMA	-19,47463	1,3650397	chr5q11-q12		X			
Rho GTPase activating protein 9	ARHGAP9	-15,03306	1,8556221	chr12q14					X
interleukin 1, beta	IL1B	-13,13285	2,1079216	chr2q14	X	X	X		
hematopoietic cell-specific Lyn substrate 1	HCLS1	-12,83846	2,0256686	chr3q13	X	X	X		
G protein-coupled receptor 65	GPR65	-11,24875	1,4422205	chr14q31-q32.1		X			
FAT tumor suppressor homolog 3 (Drosophila)	FAT3	-9,696294	2,0231988	chr11q14.3					X
solute carrier family 22 (organic cation transporter), member 18 antisense	SLC22A18AS	-9,626603	1,6441817	chr11p15.5					X
BCL2-related protein A1	BCL2A1	-9,266626	1,6623277	chr15q24.3	X	X			
linker for activation of T cells family, member 2	LAT2	-8,215016	1,40119	chr7q11.23	X				
serpin peptidase inhibitor, clade D (heparin cofactor), member 1	SERPIND1	-8,148235	1,6072751	chr22q11.2|22q11.21	X				
heat shock 70kDa protein 1A	HSPA1A	-7,849436	1,473092	chr6p21.3	X	X	X		
myeloma overexpressed gene (in a subset of t(11;14) positive multiple myelomas)	MYEOV	-7,781161	0,6806859	chr11q13				X	
gap junction protein, beta 2, 26kDa	GJB2	-7,678659	1,7039171	chr13q11-q12	X	X	X		
protease, serine, 3 (mesotrypsin)	PRSS3	-7,638278	1,2583057	chr9p11.2			X		
growth hormone receptor	GHR	-7,380771	1,0066446	chr5p13-p12	X	X			
interleukin 1, alpha	IL1A	-7,078349	1,106044	chr2q14	X	X	X		
synaptotagmin-like 3	SYTL3	-6,859925	1,473092	chr6q25.3					X
vanin 1	VNN1	-6,5932	0,9165151	chr6q23-q24		X			
SLAIN motif family, member 1	SLAIN1	-6,301788	1,0535654	chr13q22.3					X
keratin 15	KRT15	-6,145492	1,1357817	chr17q21.2			X		
baculoviral IAP repeat-containing 3	BIRC3	-6,133067	1,274101	chr11q22	X	X			
podoplanin	PDPN	-6,117213	1,3051181	chr1p36.21	X		X		
tissue factor pathway inhibitor 2	TFPI2	-6,02203	1,3868429	chr7q22	X	X	X		
chemokine (C-X-C motif) ligand 3	CXCL3	-5,685529	0,6806859	chr4q21	X	X	X		
interleukin 7	IL7	-5,619633	0,9712535	chr8q12-q13	X	X	X		

phosphatidylinositol 3,4,5-trisphosphate-dependent RAC exchanger 1	PREX1	-5,467587	1,1150486	chr20q13.13			X		
epithelial membrane protein 1	EMP1	-5,466603	1,7039171	chr12p12.3	X	X			
sorbin and SH3 domain containing 1	SORBS1	-5,363524	1,274101	chr10q23.3-q24.1				X	

Name	Symbol			Location					
neurotrimin	HNT	-5,311195	1,0115994	chr11q25					X
absent in melanoma 1	AIM1	-5,183018	1,0785793	chr6q21				X	
signal-regulatory protein beta 1	SIRPB1	-5,174008	1,2489996	chr20p13					X
thrombomodulin	THBD	-5,131474	0,3785939	chr20p11.2	X		X		
Rho GDP dissociation inhibitor (GDI) beta	ARHGDIB	-4,985514	1,1532563	chr12p12.3	X		X		
G0/G1switch 2	G0S2	-4,87667	1,1846237	chr1q32.2-q41				X	
solute carrier family 7 (cationic amino acid transporter, y+ system), member 7	SLC7A7	-4,806772	0,8504901	chr14q11.2	X				
carbohydrate (keratan sulfate Gal-6) sulfotransferase 1	CHST1	-4,765183	1,2897028	chr11p11.2-p11.1			X		
metastasis suppressor 1	MTSS1	-4,70774	0,6027714	chr8p22			X		
olfactomedin-like 2B	OLFML2B	-4,608608	0,4041452	chr1q23.3					X
lysosomal associated multispanning membrane protein 5	LAPTM5	-4,54608	1,1846237	chr1p34	X				
ChaC, cation transport regulator homolog 1 (E. coli)	CHAC1	-4,488007	0,9539392	chr15q15.1					X
WD repeat domain 16	WDR16	-4,46431	0,5291503	chr17p13.1					X
N-deacetylase/N-sulfotransferase (heparan glucosaminyl) 2	NDST2	-4,447715	1,1150486	chr10q22				X	
potassium channel tetramerisation domain containing 12	KCTD12	-4,345765	0,9291573	chr13q22.3					X
WD repeat domain 66	WDR66	-4,310515	1,1135529	chr12q24.31					X
frizzled homolog 8 (Drosophila)	FZD8	-4,264583	0,9451631	chr10p11.21				X	
Friend leukemia virus integration 1	FLI1	-4,181213	0,9539392	chr11q24.1-q24.3	X	X			
stanniocalcin 1	STC1	-4,119437	1,0016653	chr8p21-p11.2	X	X	X		
neuromedin U	NMU	-4,040515	0,4932883	chr4q12			X		
sine oculis binding protein homolog (Drosophila)	SOBP	-4,039766	0,7937254	chr6q21					X
secretory leukocyte peptidase inhibitor	SLPI	-4,039766	0,7937254	chr20q12	X	X	X		
FOS-like antigen 1	FOSL1	-4,025425	0,6658328	chr11q13	X	X	X		
HOP homeobox	HOPX	-4,000069	0,7549834	chr4q11-q12	X				
roundabout homolog 4, magic roundabout (Drosophila)	ROBO4	-3,998551	0,6027714	chr11q24.2			X		
interleukin 27 receptor, alpha	IL27RA	-3,976065	0,7	chr19p13.11	X	X	X		
protein tyrosine phosphatase, receptor type, N polypeptide 2	PTPRN2	-3,940634	0,6557439	chr7q36		X			
interleukin 7 receptor	IL7R	-3,93157	0,8504901	chr5p13	X	X			
coronin, actin binding protein, 2B	CORO2B	-3,902654	1,0692677	chr15q23					X
sprouty homolog 4 (Drosophila)	SPRY4	-3,8868	0,8386497	chr5q31.3	X				
pentraxin-related gene, rapidly induced by IL-1 beta	PTX3	-3,847034	0,6429101	chr3q25	X		X		

Description	Symbol			Chr						
sema domain, immunoglobulin domain (Ig), transmembrane domain (TM) and short cytoplasmic domain, (semaphorin) 4B	SEMA4B	-3,83427	0,7767453	chr15q25						X
glycine dehydrogenase (decarboxylating)	GLDC	-3,818011	0,6027714	chr9p22						X
cystin 1	CYS1	-3,805593	0,5686241	chr2p25.1					X	
cortactin	CTTN	-3,765608	1,040833	chr11q13		X	X			
leucine rich repeat neuronal 3	LRRN3	-3,624993	0,321455	chr7q31.1					X	
spen homolog, transcriptional regulator (Drosophila)	SPEN	-3,612935	0,9643651	chr1p36.33-p36.11					X	
v-maf musculoaponeurotic fibrosarcoma oncogene homolog F (avian)	MAFF	-3,608241	0,9539392	chr22q13.1	X					
methylenetetrahydrofolate dehydrogenase (NADP+ dependent) 2-like	MTHFD2L	-3,591564	0,8504901	chr4q13.3						X
Solute carrier family 20 (phosphate transporter), member 1	SLC20A1	-3,446013	0,305505	chr2q11-q14	X	X				
coiled-coil domain containing 4	CCDC4	-3,436091	0,5507571	chr4p13						X
laminin, gamma 2	LAMC2	-3,420203	0,8326664	chr1q25-q31			X			
six transmembrane epithelial antigen of the prostate 1	STEAP1	-3,368923	0,6	chr7q21	X					
G protein-coupled receptor 92	GPR92	-3,313847	0,4582576	chr12p13.31						X
nuclear receptor interacting protein 3	NRIP3	-3,299529	0,6658328	chr11p15.3						X
ATP synthase mitochondrial F1 complex assembly factor 2	ATPAF2	-3,209763	0,6110101	chr17p11.2						X
Rho GTPase activating protein 22	ARHGAP22	-3,181882	0,5507571	chr10q11.22	X		X			
transmembrane protein 163	TMEM163	-3,180937	0,7211103	chr2q21.3						X
calmin (calponin-like, transmembrane)	CLMN	-3,16568	0,4932883	chr14q32.13						X
phytoceramidase, alkaline	PHCA	-3,155785	0,8144528	chr11q13.5						X
high mobility group AT-hook 1	HMGA1	-3,144861	0,6557439	chr6p21	X	X	X			
tumor necrosis factor (TNF superfamily, member 2)	TNF	-3,139666	0,4163332	chr6p21.3	X	X	X			
cation channel, sperm associated 1	CATSPER1	-3,129744	0,6082763	chr11q12.1			X			
leupaxin	LPXN	-3,103904	0,5567764	chr11q12.1					X	
ras-related C3 botulinum toxin substrate 2 (rho family, small GTP binding protein Rac2)	RAC2	-3,07007	0,4582576	chr22q13.1	X	X	X			
cystatin F (leukocystatin)	CST7	-3,064678	0,4358899	chr20p11.21					X	
C-type lectin domain family 11, member A	CLEC11A	-3,040406	0,3464102	chr19q13.3	X	X	X			
CD44 molecule (Indian blood group)	CD44	-2,954289	0,5773503	chr11p13	X	X	X			
dedicator of cytokinesis 4	DOCK4	-2,925812	0,6928203	chr7q31.1	X		X			
cytochrome P450, family 2, subfamily J, polypeptide 2	CYP2J2	-2,922883	0,4932883	chr1p31.3-p31.2	X	X	X			
glycerophosphodiester phosphodiesterase domain containing 5	GDPD5	-2,892167	0,4041452	chr11q13.4-q13.5	X					

Description	Gene	Value 1	Value 2	Location						
fumarylacetoacetate hydrolase (fumarylacetoacetase)	FAH	-2,891815	0,6244998	chr15q23-q25	X	X				
cyclin D1	CCND1	-2,887121	0,6082763	chr11q13	X	X	X			
eukaryotic translation initiation factor 3, subunit M	EIF3M	-2,881357	0,3511885	chr11p13						X
coiled-coil and C2 domain containing 2A	CC2D2A	-2,862656	0,2516611	chr4p15.33						X
kynureninase (L-kynurenine hydrolase)	KYNU	-2,86091	0,7234178	chr2q22.2					X	
interleukin-1 receptor-associated kinase 2	IRAK2	-2,831444	0,4582576	chr3p25.3					X	
arrestin, beta 1	ARRB1	-2,831444	0,4582576	chr11q13	X	X	X			
EH-domain containing 1	EHD1	-2,831444	0,4582576	chr11q13		X	X			
SPC24, NDC80 kinetochore complex component, homolog (S. cerevisiae)	SPC24	-2,829027	0,6658328	chr19p13.2					X	
axin 2 (conductin, axil)	AXIN2	-2,814189	0,4	chr17q23-q24	X	X				
UDP-N-acetyl-alpha-D-galactosamine:polypeptide N-acetylgalactosaminyltransferase 12 (GalNAc-T12)	GALNT12	-2,804475	0,7767453	chr9q22.33						X
Protocadherin alpha cluster	PCDHA	-2,80387	0,3605551	chr5q31						X
serine/threonine kinase 17b	STK17B	-2,80387	0,3605551	chr2q32.3	X	X				
microtubule associated serine/threonine kinase family member 4	MAST4	-2,798123	0,7571878	chr5q12.3						X
Tetraspanin 18	TSPAN18	-2,79306	0,3	chr11p11.2						X
tumor necrosis factor (ligand) superfamily, member 9	TNFSF9	-2,766542	0,5033223	chr19p13.3	X	X	X			
FERM domain containing 4A	FRMD4A	-2,759245	0,4725816	chr10p13						X
EGF, latrophilin and seven transmembrane domain containing 1	ELTD1	-2,755052	0,6658328	chr1p33-p32						X
sorting nexin 8	SNX8	-2,739201	0,4041452	chr7p22.2						X
tribbles homolog 3 (Drosophila)	TRIB3	-2,733221	0,781025	chr20p13-p12.2		X				
antigen p97 (melanoma associated) identified by monoclonal antibodies 133.2 and 96.5	MFI2	-2,721217	0,5859465	chr3q28-q29				X		
glucuronidase, beta pseudogene 1	GUSBP1	-2,694067	0,1154701	chr5q13.2						X
unc-5 homolog B (C. elegans)	UNC5B	-2,689649	0,4932883	chr10q22.1	X	X	X			
cytochrome P450, family 2, subfamily R, polypeptide 1	CYP2R1	-2,667002	0,4163332	chr11p15.2					X	
AHNAK nucleoprotein	AHNAK	-2,645873	0,321455	chr11q12.2	X					
progestin and adipoQ receptor family member VIII	PAQR8	-2,621869	0,1527525	chr6p12.1						X
adaptor-related protein complex 1, sigma 2 subunit	AP1S2	-2,602101	0,4582576	chrXp22.2						X
oligonucleotide/oligosaccharide-binding fold containing 1	OBFC1	-2,597406	0,4358899	chr10q24.33					X	
UDP-GlcNAc:betaGal beta-1,3-N-acetylglucosaminyltransferase-like 1	B3GNTL1	-2,576374	0,3605551	chr17q25.3						X

Description	Symbol			Location						
zinc finger CCCH-type containing 12C	ZC3H12C	-2,576277	0,3464102	chr11q22.3					X	
SH3-domain binding protein 5 (BTK-associated)	SH3BP5	-2,557579	0,5507571	chr3p24.3		X				
abhydrolase domain containing 2	ABHD2	-2,557579	0,5507571	chr15q26.1			X			
adenylate kinase 5	AK5	-2,54967	0,1732051	chr1p31		X				
glycine-N-acyltransferase-like 1	GLYATL1	-2,543891	0,1	chr11q12.1						X
Rho GTPase activating protein 18	ARHGAP18	-2,513586	0,4041452	chr6q22.33		X				
OTU domain, ubiquitin aldehyde binding 2	OTUB2	-2,509109	0,4163332	chr14q32.13						X
RAB38, member RAS oncogene family	RAB38	-2,444207	0,3785939	chr11q14					X	
ventricular zone expressed PH domain homolog 1 (zebrafish)	VEPH1	-2,420203	0,305505	chr3q24-q25						X
dysbindin (dystrobrevin binding protein 1) domain containing 2 /// SYS1-DBNDD2	DBNDD2 /// SYS1-DBNDD2	-2,407127	0,2081666	chr20q13.12						X
carbonyl reductase 4	CBR4	-2,377039	0,4358899	chr4q32.3						X
pleckstrin homology-like domain, family A, member 1	PHLDA1	-2,377039	0,4358899	chr12q15	X	X				
dihydropyrimidinase-like 3	DPYSL3	-2,377039	0,4358899	chr5q32		X	X			
popeye domain containing 3	POPDC3	-2,366399	0,4	chr6q21						X
oxysterol binding protein-like 6	OSBPL6	-2,35959	0,3605551	chr2q31-q32.1						X
UV radiation resistance associated gene	UVRAG	-2,348004	0,3	chr11q13.5					X	
serpin peptidase inhibitor, clade A (alpha-1 antiproteinase, antitrypsin), member 1	SERPINA1	-2,342225	0,2645751	chr14q32.1	X	X	X			
osteoclast associated, immunoglobulin-like receptor	OSCAR	-2,334928	0,2	chr19q13.42		X				
reelin	RELN	-2,327107	0,1	chr7q22					X	
rho/rac guanine nucleotide exchange factor (GEF) 2	ARHGEF2	-2,314252	0,4725816	chr1q21-q22	X					
CDC42 effector protein (Rho GTPase binding) 4	CDC42EP4	-2,292423	0,3785939	chr17q24-q25					X	
ERO1-like beta (S. cerevisiae)	ERO1LB	-2,278408	0,305505	chr1q42.2-q43						X
differentially expressed in FDCP 6 homolog (mouse)	DEF6	-2,265332	0,2081666	chr6p21.33-p21.1	X	X				
proteasome (prosome, macropain) subunit, beta type, 9 (large multifunctional peptidase 2)	PSMB9	-2,25994	0,1527525	chr6p21.3					X	
CD82 molecule	CD82	-2,24935	0,4932883	chr11p11.2	X	X	X			
protein kinase (cAMP-dependent, catalytic) inhibitor alpha	PKIA	-2,229635	0,4163332	chr8q21.12					X	
family with sequence similarity 131, member A	FAM131A	-2,229635	0,4163332	chr3q27.1						X
centaurin, delta 2	CENTD2	-2,21562	0,3511885	chr11q13.4						X
citron (rho-interacting, serine/threonine kinase 21)	CIT	-2,21124	0,321455	chr12q24	X	X	X			
jun dimerization protein 2	JDP2	-2,207238	0,305505	chr14q24.3	X	X				

Description	Symbol	Value	Value2	Location	C1	C2	C3	C4	C5
HIV-1 Tat interactive protein 2, 30kDa	HTATIP2	-2,204449	0,2886751	chr11p15.1		X	X		
integrin-linked kinase	ILK	-2,20043	0,2516611	chr11p15.5-p15.4	X	X	X		
nuclear factor of kappa light polypeptide gene enhancer in B-cells inhibitor, alpha	NFKBIA	-2,20043	0,2516611	chr14q13	X	X	X		
endothelin converting enzyme 1	ECE1	-2,20043	0,2516611	chr1p36.1		X			
t-complex 11 (mouse)-like 1	TCP11L1	-2,195038	0,2081666	chr11p13					X
transforming growth factor beta regulator 1	TBRG1	-2,195038	0,2081666	chr11q24.2	X				
zinc finger protein 91 homolog (mouse)	ZFP91	-2,148453	0,3605551	chr11q12					X
fibrillin 2 (congenital contractural arachnodactyly)	FBN2	-2,148453	0,3605551	chr5q23-q31	X	X			
extra spindle pole bodies homolog 1 (S. cerevisiae)	ESPL1	-2,137642	0,3	chr12q	X	X			
tumor necrosis factor receptor superfamily, member 11a, NFKB activator	TNFRSF11A	-2,137642	0,3	chr18q22.1	X	X			
family with sequence similarity 149, member A	FAM149A	-2,133262	0,2645751	chr4q35.2					X
fatty acid desaturase 1	FADS1	-2,13225	0,2645751	chr11q12.2-q13.1	X				
amyloid beta (A4) precursor-like protein 2	APLP2	-2,13225	0,2645751	chr11q23-q25|11q24			X		
hydroxymethylbilane synthase	HMBS	-2,125442	0,2	chr11q23.3					X
CD40 molecule, TNF receptor superfamily member 5	CD40	-2,122839	0,1732051	chr20q12-q13.2	X	X	X		
moesin	MSN	-2,076827	0,1732051	chrXq11.2-q12		X	X		
deformed epidermal autoregulatory factor 1 (Drosophila)	DEAF1	-2,070475	0,305505	chr11p15.5					X
LysM, putative peptidoglycan-binding, domain containing 2	LYSMD2	-2,070475	0,305505	chr15q21.2					X
cysteinyl-tRNA synthetase	CARS	-2,022735	0,4163332	chr11p15.5		X			
solute carrier family 39 (zinc transporter), member 8	SLC39A8	-2,020763	0,4041452	chr4q22-q24				X	
6-pyruvoyltetrahydropterin synthase	PTS	-2,001839	0,305505	chr11q22.3-q23.3					X
CHK1 checkpoint homolog (S. pombe)	CHEK1	-1,999236	0,2886751	chr11q24-q24	X	X			
transmembrane protein 41B	TMEM41B	-1,995486	0,2516611	chr11p15.4					X
Cas-Br-M (murine) ecotropic retroviral transforming sequence	CBL	-1,995486	0,2516611	chr11q23.3	X	X	X		
ring finger and FYVE-like domain containing 1	RFFL	-1,995486	0,2516611	chr17q12	X				
ring finger protein 26	RNF26	-1,993372	0,2309401	chr11q23					X
transmembrane protein 179B	TMEM179B	-1,993372	0,2309401	chr11q12.3					X
TRAF-interacting protein with a forkhead-associated domain	TIFA	-1,993372	0,2309401	chr4q25	X				

Name	Symbol			Location					
interferon induced transmembrane protein 2 (1-8D)	IFITM2	-1,990455	0,2081666	chr11p15.5				X	
HIRA interacting protein 3	HIRIP3	-1,990455	0,2081666	chr16p11.2					X
proteasome (prosome, macropain) 26S subunit, non-ATPase, 13	PSMD13	-1,990455	0,2081666	chr11p15.5					X
apolipoprotein B mRNA editing enzyme, catalytic polypeptide-like 3B	APOBEC3B	-1,986075	0,1527525	chr22q13.1-q13.2				X	
ribosomal protein S6 kinase, 90kDa, polypeptide 5	RPS6KA5	-1,986075	0,1527525	chr14q31-q32.1	X	X	X		
centaurin, delta 3	CENTD3	-1,986075	0,1527525	chr5q31.3		X	X		
myosin phosphatase-Rho interacting protein	M-RIP	-1,986075	0,1527525	chr17p11.2		X			
paired-like homeodomain 1	PITX1	-1,981381	0,057735	chr5q31				X	
multiple C2 domains, transmembrane 2	MCTP2	-1,981381	0,057735	chr15q26.2					X
mitogen-activated protein kinase kinase kinase kinase 4	MAP4K4	-1,930584	0,2645751	chr2q11.2-q12	X		X		
Rho GTPase activating protein 5	ARHGAP5	-1,930584	0,2645751	chr14q12	X		X		
transmembrane emp24-like trafficking protein 10 (yeast)	TMED10	-1,930584	0,2645751	chr14q24.3		X			
TMEM9 domain family, member B	TMEM9B	-1,923288	0,2	chr11p15.3					X
fibroblast growth factor (acidic) intracellular binding protein	FIBP	-1,921174	0,1732051	chr11q13.1					X
WD repeat domain 33	WDR33	-1,921174	0,1732051	chr2q14.3					X
mediator complex subunit 19	MED19	-1,920859	0,1732051	chr11q12.1				X	
DIX domain containing 1	DIXDC1	-1,916479	0,1	---				X	
coiled-coil domain containing 15	CCDC15	-1,916479	0,1	chr11q24.2					X
dehydrogenase/reductase (SDR family) member 1	DHRS1	-1,916479	0,1	chr14q12					X
ATP binding domain 4	ATPBD4	-1,914214	0	chr15q14					X
cannabinoid receptor interacting protein 1	CNRIP1	-1,862472	0,2516611	chr2p14				X	
CD59 molecule, complement regulatory protein	CD59	-1,862472	0,2516611	chr11p13	X	X	X		
ribonucleotide reductase M1 polypeptide	RRM1	-1,862472	0,2516611	chr11p15.5	X	X			
CDK2-associated protein 2	CDK2AP2	-1,853692	0,1527525	chr11q13				X	
twinfilin, actin-binding protein, homolog 2 (Drosophila)	TWF2	-1,851577	0,1154701	chr3p21.1				X	
ataxia telangiectasia mutated	ATM	-1,849312	0,057735	chr11q22-q23	X	X	X		
Sin3A-associated protein, 30kDa	SAP30	-1,792876	0,2081666	chr4q34.1					X
poly(A) polymerase alpha	PAPOLA	-1,78879	0,1527525	chr14q32.31				X	
calcium/calmodulin-dependent protein kinase IV	CAMK4	-1,78879	0,1527525	chr5q21.3	X	X	X		
peroxiredoxin 5	PRDX5	-1,78879	0,1527525	chr11q13		X			
glucosidase, alpha; neutral AB	GANAB	-1,786524	0,1154701	chr11q12.3					X
trafficking protein particle complex 4	TRAPPC4	-1,725708	0,1732051	chr11q23.3				X	

Name	Symbol			Location					
protein phosphatase 2 (formerly 2A), regulatory subunit B'', gamma	PPP2R3C	-1,721622	0,1	chr14q13.2					X
growth arrest-specific 2 like 1	GAS2L1	-1,721622	0,1	chr22q12.2	X				
cofilin 1 (non-muscle)	CFL1	-1,665186	0,2081666	chr11q13	X	X	X		
microsomal glutathione S-transferase 2	MGST2	-1,658834	0,1154701	chr4q28.3				X	
metastasis associated lung adenocarcinoma transcript 1 (non-protein coding)	MALAT1	-1,65672	0,057735	chr11q13.1				X	
cyclic AMP phosphoprotein, 19 kD	ARPP-19	-1,533117	0,1	chr15q21.2					X
calmodulin 1 (phosphorylase kinase, delta)	CALM1	-1,533117	0,1	chr14q24-q31	X	X			
epithelial membrane protein 3	EMP3	-1,533117	0,1	chr19q13.3	X	X			

Supplemental Table 4: List of top 16 up-regulated genes.

Gene	Fold Change	Molecular and Cellular Bio Function
HS6ST2	10.28	Cellular Growth and Proliferation
COL1A1	7.22	Cellular growth and Proliferation/ Cell Death and Survival/ Cellular Movement
GFRA1	6.91	Cellular growth and Proliferation/ Cell Death and Survival/ Cellular Movement
KRT7	5.56	Cellular growth and Proliferation/ Cellular Movement
VANGL2	5.48	Cellular Assembly and Organization/ Cellular Function and Maintenance
MXRA8	5.41	Cancer
PKP2	5.33	Cellular Assembly and Organization
F2RL1	5.31	Cellular growth and Proliferation/ Cell Death and Survival/ Cellular Movement
LEPREL1	4.99	Cellular Growth and Proliferation
THRB	4.88	Cellular growth and Proliferation/ Cellular Movement
ZBED2	4.59	Not Classified
ADAMTS5	4.36	Cancer
ID4	4.33	Cellular growth and Proliferation/ Cell Death and Survival
RHOB	4.13	Cellular Growth and Proliferation/ Cell Death and Survival/ Cellular Movement
PDZK1	3.99	Cellular Growth and Proliferation/ Cell Death and Survival
PDZK1IP1	2.90	Cellular Growth and Proliferation

Supplemental Table 5: List of the primers used in the Q-RT-PCR.

Gene	Forward Primer	Reverse Primer
HS6ST2	5'-tgcgatcttctccaagattttc-3'	5'-cgatcacggcaaataggaag-3'
COL1A1	5'-atgttcagctttgtggacctc-3'	5'-ctgtacgcaggtgattggtg-3'
KRT7	5'-caggctgagatcgacaacatc-3'	5'-cttggcacgagcatcctt-3'
VANGL2	5'-gccagccgcttctacaac-3'	5'-tctccaggatccacactgc-3'
PKP2	5'-tgtcagaggaaccattgcag-3'	5'-ggttatgaagaatgcacacacaa-3'
F2RL1	5'-tgctagcagcctctctctcc-3'	5'-aggcttcttcctttagaggatctatt-3'
LEPREL1	5'-tgcagattgcttaattccttga-3'	5'-ctcagggttagccacgaaaa-3'
THRB	5'-gggcactggtaatttggcta-3'	5'-cagaaggaaatcgcagatcc-3'
ZBED2	5'-gagagaagtccagagccttgc-3'	5'-aagcagctcaccatactccac-3'
ADAMTS5	5'-taagccctggtccaaatgc-3'	5'-aggtccagcaaacagttacca-3'
ID4	5'-tgcagtgcgatatgaacgac-3'	5'-gcaggatctccactttgctg-3'
RHOB	5'-tatgtggccgacattgagg-3'	5'-gcggtcgtagtcctcctg-3'
PDZK1	5'-ccggctctgctatctcgt-3'	5'-tcatgtacaccccctttttacc-3'
PDZK1IP1	5'-gcagtcaaccacttctggtg-3'	5'-gacggtcaggatcatgtgtg-3'
RNApol	5'-gcgatgagaacaagatgcaa-3'	5'-cgcaggaagacatcatcatc-3'
Twist1	5'-gctcagctacgccttctc-3'	5'-ccttctctggaaacaatgacattct-3'

Supplemental Table 6: LEPREL1 expression by immunohistochemistry in thyroid samples (n=86).

Tissue*	LEPREL1 positivity Percentage of positive samples (positive/total samples)		
NT	0% (0/27)		
PTC	26% (5/19)	+ [a]	0% (0/19)
		++ [b]	26% (5/19)
		+++ [c]	0% (0/19)
ATC	67% (27/40)	+ [a]	12.5% (5/40)
		++ [b]	12.5% (5/40)
		+++ [c]	42% (17/40)

* NT= normal thyroid, PTC= papillary thyroid carcinoma, ATC= anaplastic thyroid carcinoma.

[a] +:   >10–≤30% of positive cells.
[b] ++:   >30–≤60% of positive cells.
[c] +++:   >60% of positive cells.

Supplementary Fig. S1

Top Bio Functions

Diseases and Disorders

Name	p-value	# Genes
Cancer	7,23E-11 - 2,65E-03	200
Reproductive System Disease	9,36E-08 - 2,15E-03	115
Skeletal and Muscular Disorders	1,39E-05 - 2,65E-03	13
Inflammatory Response	3,09E-05 - 2,49E-03	60
Endocrine System Disorders	6,39E-05 - 1,46E-04	31

Molecular and Cellular Functions

Name	p-value	# Genes
Cellular Movement	7,73E-09 - 2,49E-03	115
Cellular Growth and Proliferation	2,05E-08 - 2,65E-03	160
Cell Death and Survival	3,01E-08 - 2,65E-03	155
Cellular Assembly and Organization	4,00E-07 - 2,65E-03	88
Cellular Function and Maintenance	4,00E-07 - 2,65E-03	141

Physiological System Development and Function

Name	p-value	# Genes
Tissue Development	4,00E-07 - 2,65E-03	94
Tumor Morphology	4,54E-07 - 2,65E-03	49
Cardiovascular System Development and Function	4,89E-06 - 2,65E-03	70
Lymphoid Tissue Structure and Development	8,26E-06 - 2,27E-03	40
Tissue Morphology	8,26E-06 - 2,65E-03	65

INGENUITY
S Y S T E M S

Supplementary Figure S1. Summary of Ingenuity Pathway Analysis. List of Top Bio Functions is divided in three different categories: Disease and Disorders, Molecular and Cellular Function, Physiological System Development and Function. The number of genes in each category and p-values corresponding to each single function are indicated on the right side.

Supplementary Fig. S2
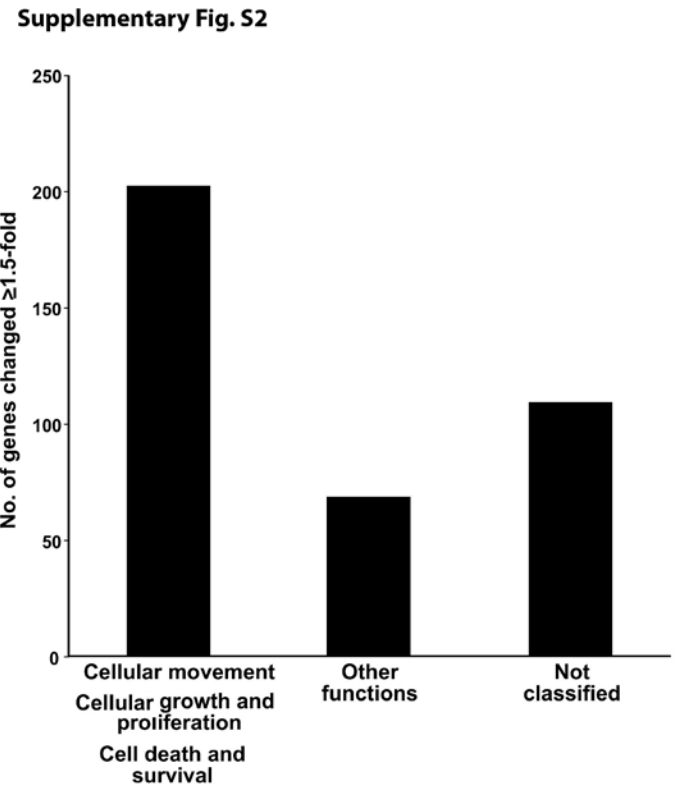
Supplementary Figure S2. Graphic representation of Ingenuity Pathway Analysis classification.

The number of the genes for each category is reported on *y* axis.
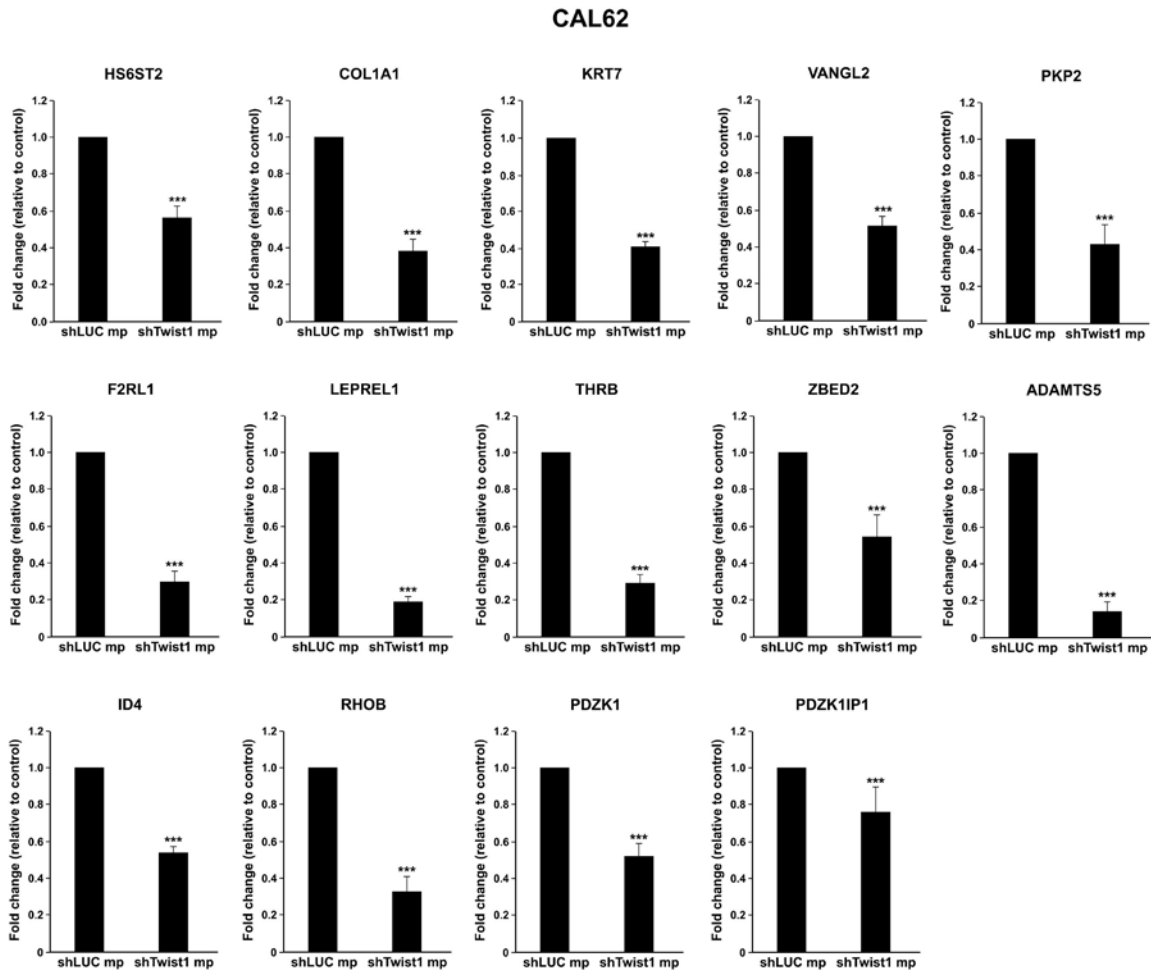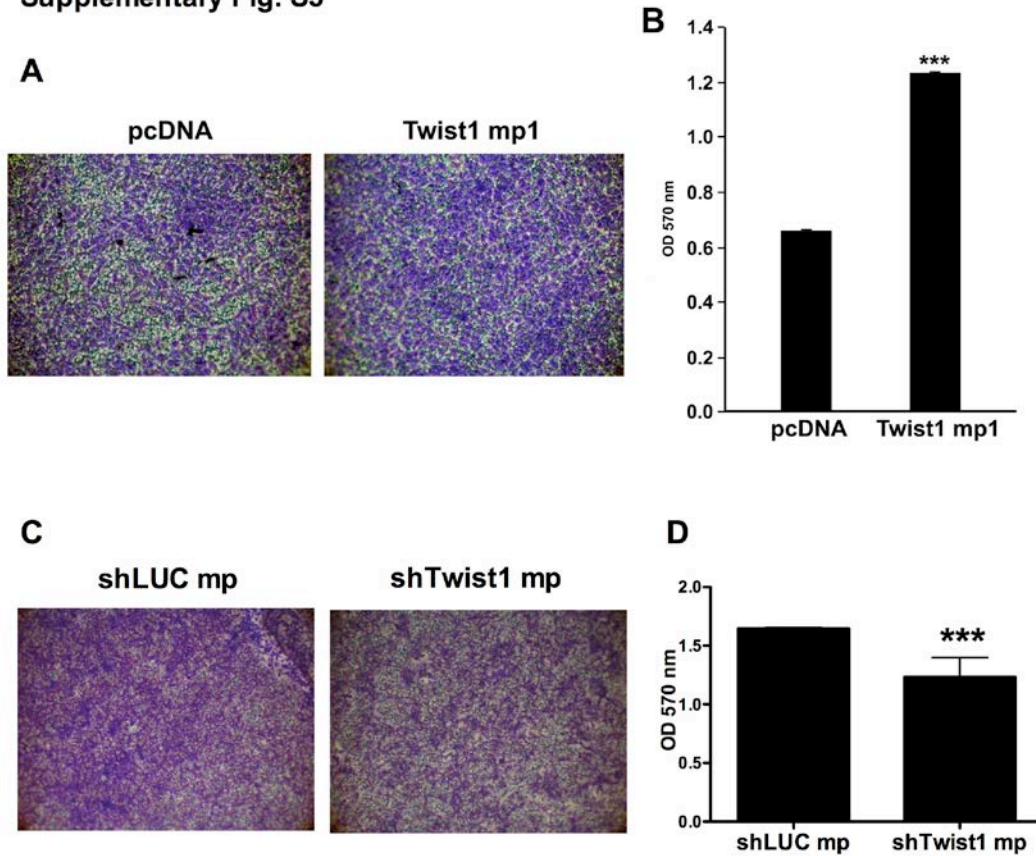
Supplementary Fig. S3
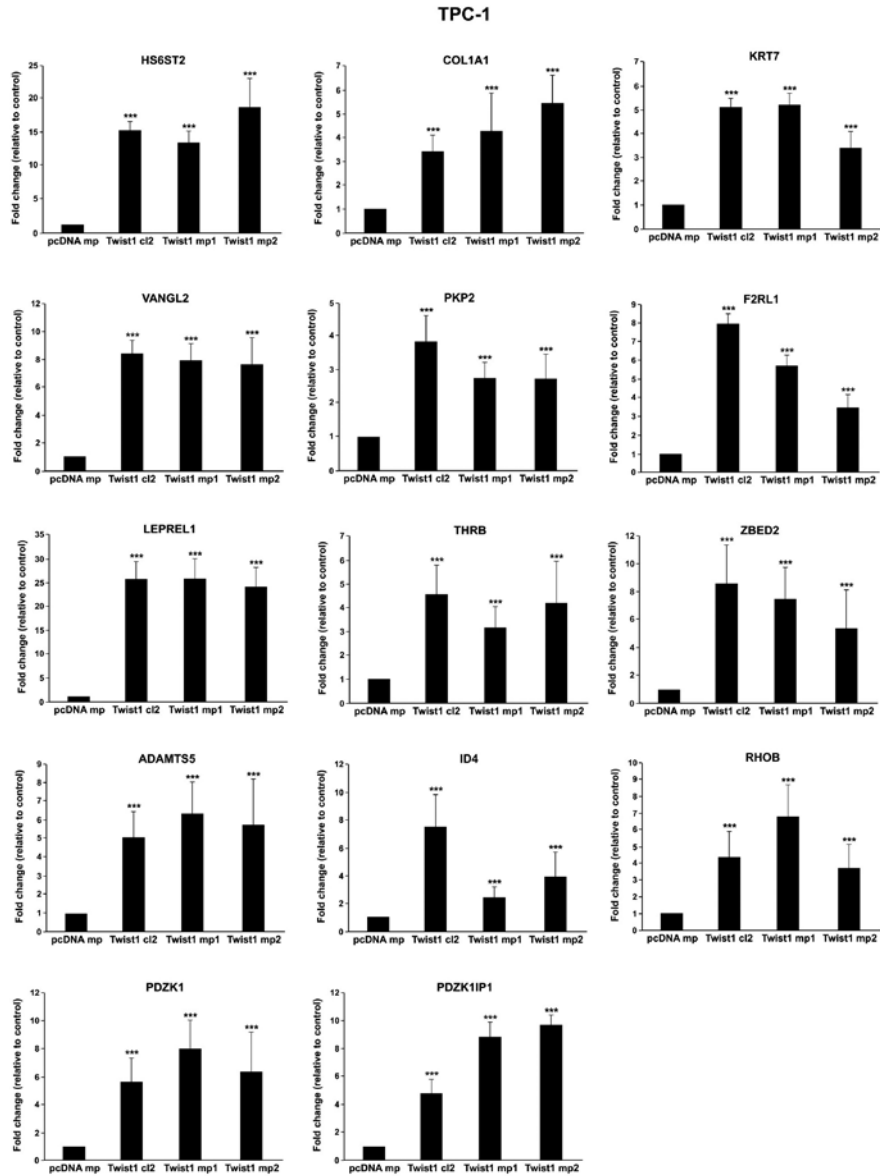
Supplementary Figure S3. Expression levels of Twist1 targets in TPC transfected cells. Q-RT-PCR of the indicated genes in TPC-Twist1 cells in comparison to vector control cells (pcDNA mp). Values represent the average of triplicate experiments ± standard deviations. Asterisks indicate $p < 0.001$ (***).

Supplementary Fig. S4



Supplementary Figure S4. Expression levels of Twist1 targets in CAL62 transfected cells. Q-RT-PCR of Twist1 in CAL62 shTwist1 mp cells in comparison to vector control cells (shLUC mp). Values represent the average of triplicate experiments $\pm$ standard deviations. Asterisks indicate $p < 0.001$ (***).
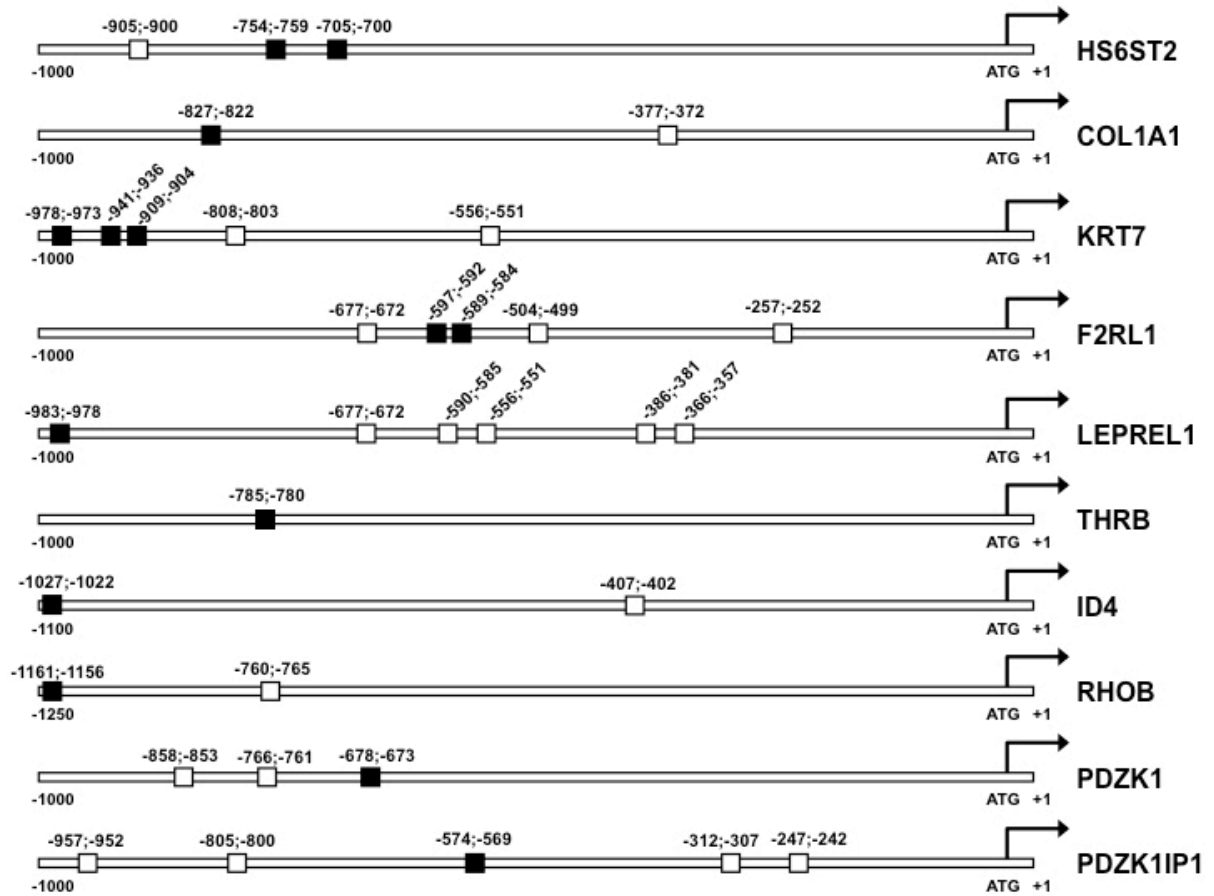
Supplementary Fig. S5

Supplementary Figure S5. Twist1 affects the ability of TPC and CAL62 cells to migrate in Collagen I matrix. **A-C.** TPC (**A**) and CAL62 (**C**) transfected cells were seeded onto the insert and incubated for 24h and 48h respectively. Then cells were stained and photographed. **B-D.** Migration ability was expressed as absorbance at OD 570 nm. Values represent the average of triplicate experiments ± standard deviations. Asterisks indicate $p < 0.001$ (***).
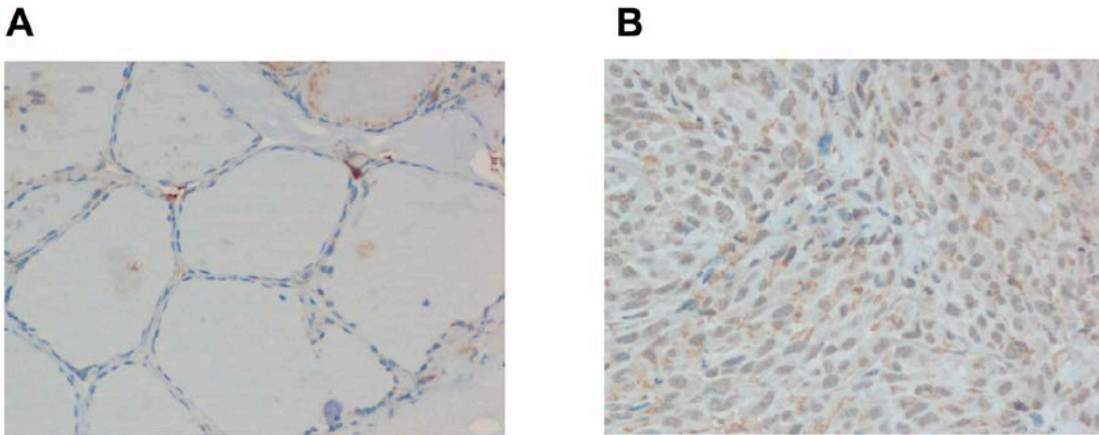
Supplementary Fig. S6

A

pcDNA   Twist1 mp1

B

C

shLUC mp   shTwist1 mp

D
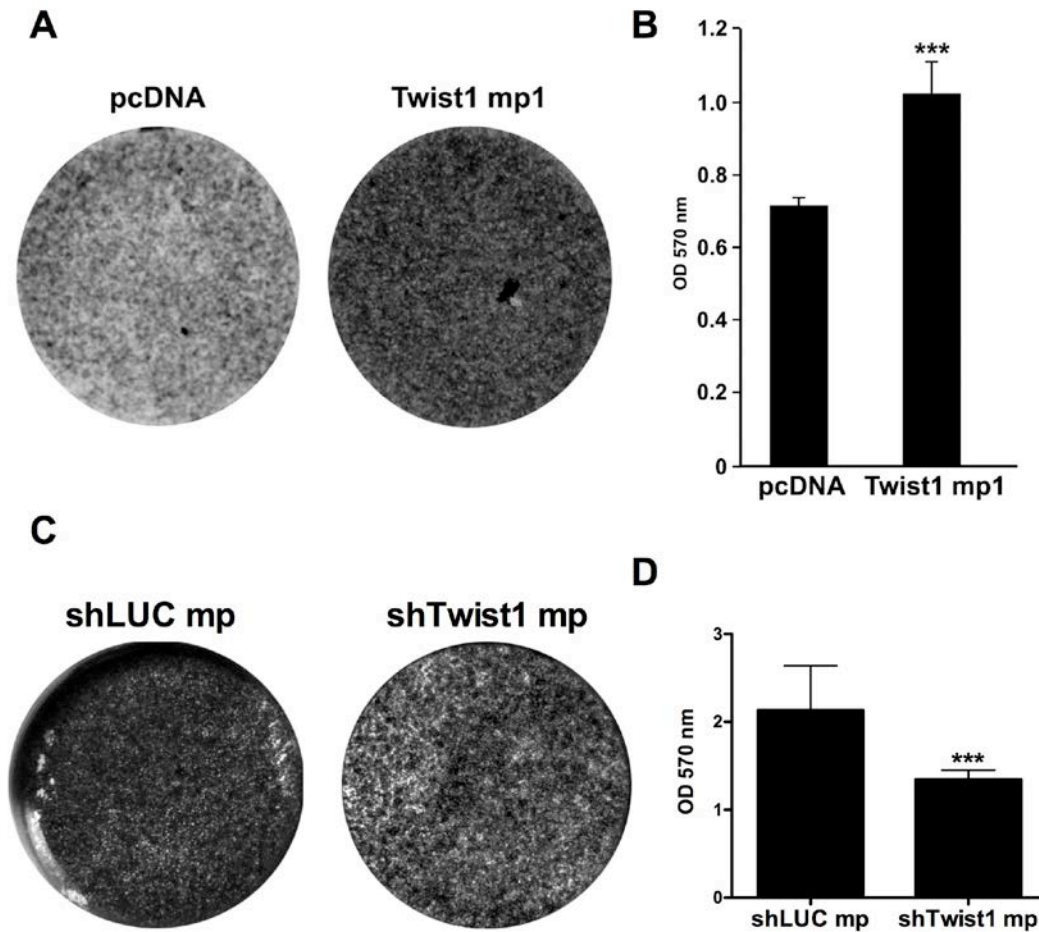
Supplementary Figure S6. Twist1 affects the ability of TPC and CAL62 cells to invade the Collagen I matrix. **A-C.** TPC (**A**) and CAL62 (**C**) transfected cells were seeded on insert and allowed to invade for 24h and 48h respectively. **B-D.** Invasive ability was expressed as absorbance at OD 570 nm. Values represent the average of triplicate experiments $\pm$ standard deviations. Asterisks indicate $p < 0.001$ (***).

Supplementary Fig. S7

A

pcDNA   Twist1 mp1   HUVEC only

B

C

shLUC mp   shTwist1 mp

D
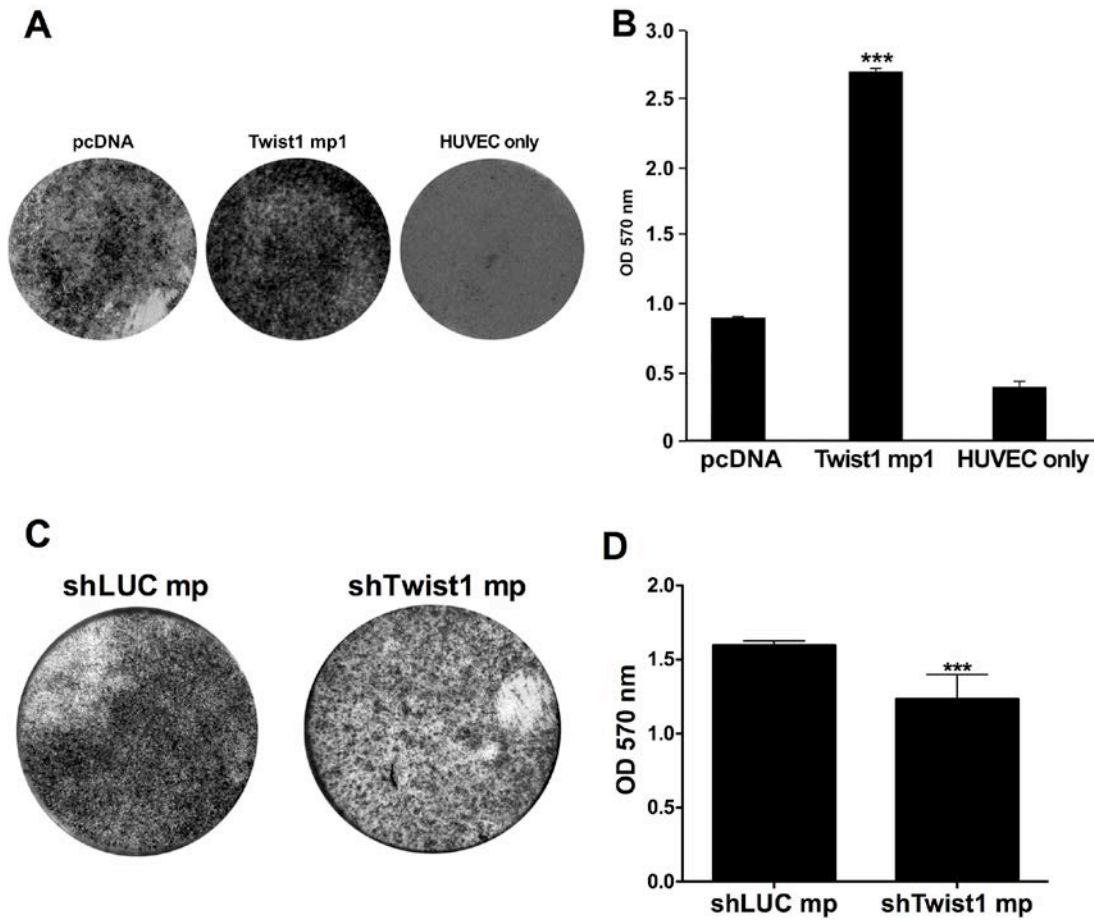
Supplementary Figure S7. Twist1 affects the ability of TPC and CAL62 cells to migrate through endothelium cells. **A-C.** TPC and CAL62 transfected cells were seeded on confluent monolayer of endothelial HUVEC cells and incubated for 24h and 48h respectively. Then cells were stained and photographed. HUVEC only was used as negative control. **B-D.** Quantification of the assay, migration ability was expressed as absorbance at OD 570 nm. Values represent the average of triplicate experiments ± standard deviations. Asterisks indicate $p < 0.001$ (***).

Supplementary Fig. S8: Twist1 directly binds the promoter of the indicated genes. Schematic representation of the E-box consensus sequences (CANNTG) in the promoter regions of the top ten up-regulated genes. In black are reported the E-box amplified in ChIP assay.

Supplementary Fig S9

Supplementary Fig. S9 Immunohistochemical analysis of LEPREL1 protein expression in normal and malignant thyroid tissues. **A**. Representative histological sections from normal thyroid (NT; 20X magnification) and anaplastic thyroid carcinoma (**B**) (ATC; 20X magnifications) stained with anti LEPREL1 antibody are shown.

Attached Manuscript # II

Di Maro G, Salerno P, Unger K, **Orlandella FM**, Monaco M, Chiappetta G, Thomas G, Oczko-Wojciechowska M, Masullo M, Jarzab B, Santoro M, Salvatore G.

MOLECULAR CANCER

Anterior gradient protein 2 promotes survival, migration and invasion of papillary thyroid carcinoma cells

Gennaro Di Maro[1], Paolo Salerno[1], Kristian Unger[2], Francesca Maria Orlandella[1], Mario Monaco[3], Gennaro Chiappetta[3], Gerry Thomas[2], Malgorzata Oczko-Wojciechowska[4], Mariorosario Masullo[5], Barbara Jarzab[4], Massimo Santoro[1] and Giuliana Salvatore[5*]

Abstract

Background: Through a transcriptome microarray analysis, we have isolated Anterior gradient protein 2 (AGR2) as a gene up-regulated in papillary thyroid carcinoma (PTC). AGR2 is a disulfide isomerase over-expressed in several human carcinomas and recently linked to endoplasmic reticulum (ER) stress. Here, we analyzed the expression of AGR2 in PTC and its functional role.

Methods: Expression of AGR2 was studied by immunohistochemistry and real time PCR in normal thyroids and in PTC samples. The function of AGR2 was studied by knockdown in PTC cells and by ectopic expression in non-transformed thyroid cells. The role of AGR2 in the ER stress was analyzed upon treatment of cells, expressing or not AGR2, with Bortezomib and analyzing by Western blot the expression levels of GADD153.

Results: PTC over-expressed AGR2 at mRNA and protein levels. Knockdown of AGR2 in PTC cells induced apoptosis and decreased migration and invasion. Ectopic expression of AGR2 in non-transformed human thyroid cells increased migration and invasion and protected cells from ER stress induced by Bortezomib.

Conclusions: AGR2 is a novel marker of PTC and plays a role in thyroid cancer cell survival, migration, invasion and protection from ER stress.

Keywords: Thyroid cancer, AGR2, Endoplasmic reticulum stress, Survival, Migration and invasion

Background

Thyroid carcinomas arising from thyroid follicular cells include papillary thyroid carcinoma (PTC), follicular thyroid carcinoma as well as the less common anaplastic thyroid carcinoma [1-3]. PTC is a well-differentiated, slow growing and treatable tumor. The tumor is usually removed by surgery and treated by iodine 131-radiation therapy, however a few PTC carriers develop recurrences and distant metastases [4,5].

To look for genes potentially involved in the neoplastic transformation of the thyroid gland, we conducted a transcriptome microarray screening [6]. Among the genes highly up-regulated in PTC, we focused on Anterior

gradient protein 2 (AGR2). AGR2, also known as hAG-2 or Gob-4, is the human orthologue of the *Xenopus laevis* protein XAG-2. In the frog embryo XAG-2 induces cement gland differentiation [7,8]. Several studies have shown a significant function for AGR2 in biological pathways including cell migration and transformation [9,10]. AGR2 protein is up-regulated in several human carcinomas, including breast, pancreatic, ovarian, lung and prostate ones, and is associated with a metastatic phenotype and poor prognosis [11-16].

AGR2 was found up-regulated in several published PTC microarrays [17-21]. Delys and colleagues produced a list of genes modulated in PTC, by comparing their data sets with two independent PTC microarray data sets, and AGR2 scored as one of the genes commonly up-regulated in PTC [19].

* Correspondence: giuliana.salvatore@uniparthenope.it
[5]Dipartimento di Scienze Motorie e del Benessere, Universita' "Parthenope", Via Medina 40, Naples 80133, Italy
Full list of author information is available at the end of the article

Over-expression or suppression of AGR2, in different cancer model systems, affects cell proliferation, invasion, survival and metastasis [9,10].

Recently, AGR2 has been shown to have structural characteristics of the protein disulfide isomerase (PDI) family, including a carboxyl-terminal endoplasmic reticulum (ER) retention signal (KTEL) and a single thioredoxin-like domain with a CXXS motif [22]. PDI proteins catalyze formation, reduction, and isomerization of disulfide bonds, thereby facilitating the maturation of proteins in the ER and ensure correct folding and multimerization of proteins [23,24].

During tumorigenesis, the high proliferation rate of cancer cells requires increased ER protein folding, assembly, and transport, a condition that can induce ER stress [25,26]. Importantly, AGR2 knock out mice showed elevated ER stress [27]. AGR2 expression is induced by ER stress, and siRNA-mediated knockdown of AGR2 increased ER stress response [27,28]. It has been shown that AGR2 exists in monomer/dimer equilibrium and that intermolecular salt bridges involving glutamic acid 60 or cysteine 81 (in the thioredoxin domain of AGR2) stabilize the dimer [29-31]. Importantly, it was demonstrated that dimerization of AGR2 is crucial in mediating the ER stress signaling pathway [29]. AGR2 localizes in the ER of normal intestinal epithelial cells and is essential for *in vivo* production of mucus [32,33]. Indeed, AGR2 mediates processing of the intestinal MUC2 through formation of mixed disulfide bonds [33].

In this work, we analyzed the expression of AGR2 in PTC and its functional role.

Results
AGR2 is up-regulated in human PTC samples
We measured AGR2 expression by immunohistochemistry with an anti-AGR2 monoclonal antibody in 64 samples including 25 normal thyroid (NT) samples and 39 PTC samples. Representative immunohistochemical staining is shown in Figure 1A, and the entire dataset is reported in Table 1. AGR2 was expressed at low levels in normal thyroid glands (Figure 1A, inset 1). In contrast, several PTC samples (PTC classical variant: 23 out of 28 samples; PTC follicular variant: 5 out of 11 samples) were strongly positive for AGR2 expression, and positivity was confined to tumor cells (Table 1 and Figure 1A, inset 2). No staining was observed in the absence of the primary antibody (Figure 1A, inset 3). Normal colon mucosa was used as positive control (Figure 1A, inset 4).

To determine whether up-regulation occurred also at RNA level, we verified AGR2 expression levels in a DNA array dataset of 15 normal human thyroid (NT) and 43 PTC samples. As shown in Figure 1B, PTC samples showed significantly increased AGR2 levels compared to normal thyroid tissues ($P < 0.0001$). These findings were

further confirmed by quantitative RT-PCR analysis of an independent set of PTC samples (Figure 1C).

### Knockdown of AGR2 induces apoptosis of TPC-1 cells
We evaluated the expression level of AGR2 in the papillary thyroid cancer cell line TPC-1 in comparison to non-transformed thyroid cells Nthy-ori 3–1. As shown in Figure 2A, AGR2 is over-expressed in TPC-1 cells. We evaluated the effects of AGR2 ablation in TPC-1 cells by RNA interference. TPC-1 cells were transfected with AGR2 siRNA or with scrambled siRNA, counted and lysed at different time points. Forty-eight hours after transfection TPC-1 cells transfected with scrambled siRNA numbered 192×10^3, whereas those transfected with AGR2 siRNA numbered 146×10^3 ($P = 0.0492$). Seventy–two hours after transfection, TPC-1 cells transfected with scrambled siRNA numbered 413×10^3, whereas those transfected with AGR2 siRNA numbered 279×10^3 ($P = 0.0045$) (Figure 2B). Accordingly, the fraction of trypan blue excluding (viable) cells of TPC-1 transfected with AGR2 siRNA, was reduced with respect to scrambled control, at 48 and 72 hours post transfection ($P < 0.0001$) (Figure 2C).

Knockdown of AGR2 reduces migration and invasion of TPC-1 cells
We evaluated migration (by a wound-closure assay) and invasion (by a Matrigel invasion assay) ability of AGR2 siRNA-transfected cells. A scraped wound was introduced on a confluent monolayer of TPC-1 cells transfected with AGR2 siRNA or scrambled siRNA. Figure 2D and E show that TPC-1 transfected with the scrambled control efficiently migrated into the wound; in contrast, cells transfected with AGR2 siRNA had a reduced migrating ability both at 12 and 24 hours ($P < 0.0001$). Moreover, cells transfected with AGR2 siRNA showed a reduced ability to invade Matrigel compared to control cells ($P < 0.0001$) (Figure 2F and G). The efficiency of AGR2 knockdown at the different time points examined is shown in Figure 2H.

Ectopic AGR2 promotes migration and invasion of Nthy-ori 3–1 cells
We transfected the non-transformed thyroid cells, Nthy-ori 3–1, with the empty vector (pcDNA), AGR2 wild type, AGR2-carrying the cysteine 81 to serine mutation AGR2 (C → S), or AGR2 carrying the glutamic acid 60 to alanine mutation AGR2 (E → A) (Figure 3A). Wild type AGR2, after treatment with disuccinimidyl suberate (DSS), is dimeric (Additional file 1: Figure S1). The C81S mutation targets the thioredoxin domain of AGR2 and impairs its catalytic activity and dimer formation, while the E60A mutation impairs AGR2 dimer formation [29-31]. Nthy-ori 3–1 AGR2, AGR2 (C → S), AGR2 (E → A) and pcDNA cells showed comparable growth rates (Figure 3B).
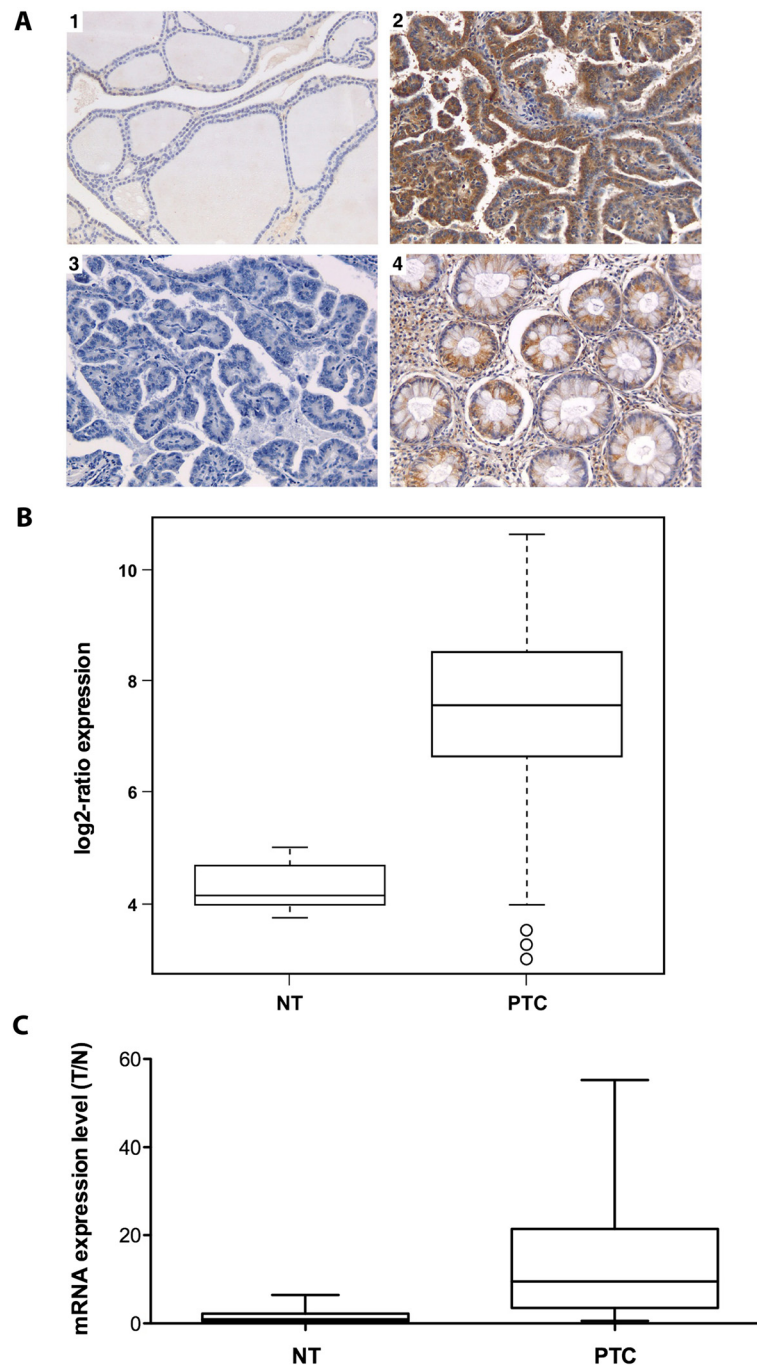
Figure 1 AGR2 expression in human thyroid tissue samples. A) Representative images (at 200x magnification) of normal thyroid (NT) (inset 1), papillary thyroid carcinoma (PTC) (inset 2), normal colon sample (inset 4) (used as positive control) stained with a mouse monoclonal anti-AGR2 antibody. PTC shows a strong immunoreactivity for AGR2, whereas NT is negative. Inset 3, shows a PTC sample incubated only with secondary antibody as negative control. **B)** Expression of AGR2 in DNA array of 15 normal thyroid (NT) samples and 43 PTC. The box plot of AGR2 shows a significant up-regulation of this gene in tumor tissues. **C)** Quantitative RT-PCR showing increased levels of AGR2 in PTC samples (n = 10) in comparison to normal thyroid controls (n = 10). The level of AGR2 expression in each sample was measured by comparing its fluorescence threshold with the average fluorescence threshold of the NT samples.

A scraped wound was introduced on the confluent monolayer and cell migration into the wound was monitored after 12 hours. As shown in Figure 3C and D, migration rate was larger in AGR2-transfected cells compared to control vector (pcDNA), AGR2 (C → S) and AGR2 (E → A) cells. Then we seeded AGR2, AGR2 (C → S) and vector

Table 1 AGR2 expression in thyroid samples (n = 64)

Tissue*	Number of samples**	AGR2 (score***)			
		Negative	Positive		
		0	1+	2+	3+
NT	25	4	21		
PTC	28 (PTC CV)	1	2	2	23
	11 (PTC FV)	2	1	3	5

*NT = normal thyroid; PTC = papillary thyroid carcinoma.
**PTC CV = papillary thyroid carcinoma, classical variant; PTC FV = papillary thyroid carcinoma, follicular variant.
***0 = < 10% of positive cells; 1 = 10-50% of positive cells; 2 = 51-75% of positive cells; 3 = 76-100% of positive cells.

control (pcDNA) cells into the top chamber of transwells and evaluated their ability to invade Matrigel. AGR2 over-expression increased the invasive ability of Nthy-ori 3–1 cells in comparison to vector control ($P < 0.0001$) and AGR2 (C → S) cells ($P < 0.0001$) (Figure 3E and F).

Ectopic AGR2 promotes cell migration and invasion of TPC-1 cells

To confirm these findings, we over-expressed AGR2 in TPC-1 cells. Cells were transfected with AGR2, AGR2 (C → S), AGR2 (E → A) or with the empty vector (pcDNA). Mass populations were selected in G418 (Additional file 1: Figure S2A). Growth rates of TPC-1 AGR2, AGR2 (C → S), AGR2 (E → A) and control (pcDNA) cell lines were similar (Additional file 1: Figure S2B). We studied cell migration using the wound closure assay. As shown in Additional file 1: Figure S2C, migration rate was larger in TPC-1 AGR2 cells compared to AGR2 (C → S), AGR2 (E → A) cells and to vector control (pcDNA) cells. We next seeded TPC-1 AGR2, AGR2 (C → S), and pcDNA control cells into the top chamber of transwells and evaluated their ability to invade Matrigel. AGR2 over-expression increased TPC-1 invasiveness in comparison to AGR2 (C → S) cells and control vector (Additional file 1: Figure S2D).

Nthy-ori 3–1 AGR2 cells have an increased disulfide isomerase activity

AGR2 has been identified as a protein disulfide isomerase, playing a role in the endoplasmic reticulum (ER) stress response [22-33]. Protein disulfide isomerases catalyze the formation (oxidation), breakage (reduction) and rearrangement (isomerization) of disulfide bonds between cysteine residues within proteins during their folding process. To determine whether AGR2 had a disulfide isomerase activity in thyroid cells we performed an insulin-reduction assay. In this assay, insulin reduction catalyzed by protein disulfide isomerases in the presence of dithiothreitol (DTT) results in the aggregation of its β chains that can be spectrophotometrically revealed at 650 nm [34]. As shown in Figure 4A, Nthy-ori 3–1 AGR2 cells showed an increased rate of insulin reduction compared to AGR2 (C → S) or vector control cells.

To confirm these findings, we measured the levels of oxidized (GSSG) and of reduced (GSH) glutathione in Nthy-ori 3–1 AGR2, AGR2 (C → S) and vector control cells. As shown in Figure 4B and C, levels of GSSG and GSH were increased in Nthy-ori 3–1 AGR2 cells compared to AGR2 (C → S) and to vector control cells. Finally, as shown in Figure 4D Nthy-ori 3–1 AGR2 cells displayed a decreased level of H_2O_2 compared to vector control and to AGR2 (C → S) cells ($P < 0.001$).

### AGR2 protects non-transformed thyroid Nthy-ori 3–1 cells from endoplasmic reticulum stress

It was shown that AGR2 has a role in the endoplasmic reticulum (ER) stress response [27-30]. Thus, we studied the effects of ectopic AGR2 expression in the ER stress pathway upon treatment with Bortezomib. Bortezomib is a potent and selective inhibitor of the proteasome that causes an accumulation of unfolded proteins in the ER [35-37]. Nthy-ori 3–1 cells transfected with AGR2, AGR2 (C → S), or vector (pcDNA) were treated for 24 hours with 100 nM Bortezomib. After treatment, cells were counted. As shown in Figure 5A, AGR2 protected Nthy-ori 3–1 cells from reduced viability caused by Bortezomib in comparison to AGR2 (C → S) and to control (pcDNA) cells.

Then, we determined by Western blot the expression level of GADD153 (also named Chop), a well-characterized biomarker of ER stress [37], in Nthy-ori 3–1 AGR2, AGR2 (C → S) or empty vector (pcDNA) cells treated with Bortezomib (100 nM) for 24 hours. As shown in Figure 5B, Nthy-ori 3–1 AGR2 cells presented a blunted increase of GADD153 upon Bortezomib treatment compared to pcDNA and to AGR2 (C → S) cells. These data suggest that ectopic AGR2 expression protects non-transformed thyroid cells from ER stress induced by Bortezomib.

Discussion

AGR2 is a protein disulfide isomerase that is over-expressed in several human carcinomas and stimulates cancer cell proliferation, survival, invasion, and metastasis [9,10]. In the present study, we demonstrated that AGR2 is over-expressed in PTC. Our data are in agreement with thyroid carcinoma microarray screenings that isolated AGR2 as a gene up-regulated in PTC [17-21].
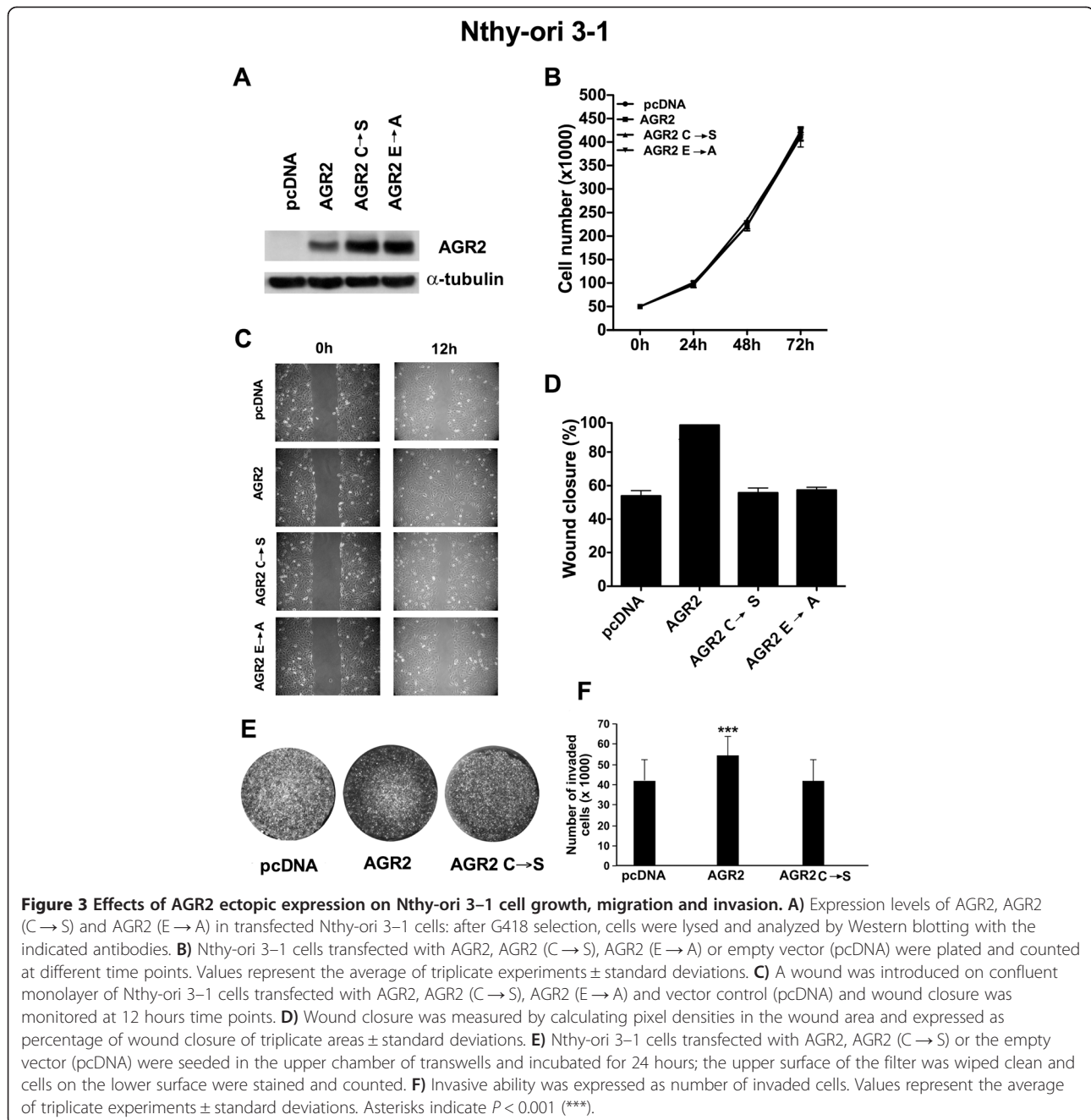
We investigated the functional role of AGR2 using gain and loss-of-function approaches. Knockdown of AGR2 in PTC cells decreased cell survival, migration and invasion. On the other hand, forced AGR2 expression in non-transformed thyroid Nthy-ori 3–1 cells, resulted in increased cell migration and invasion and protection from ER stress.
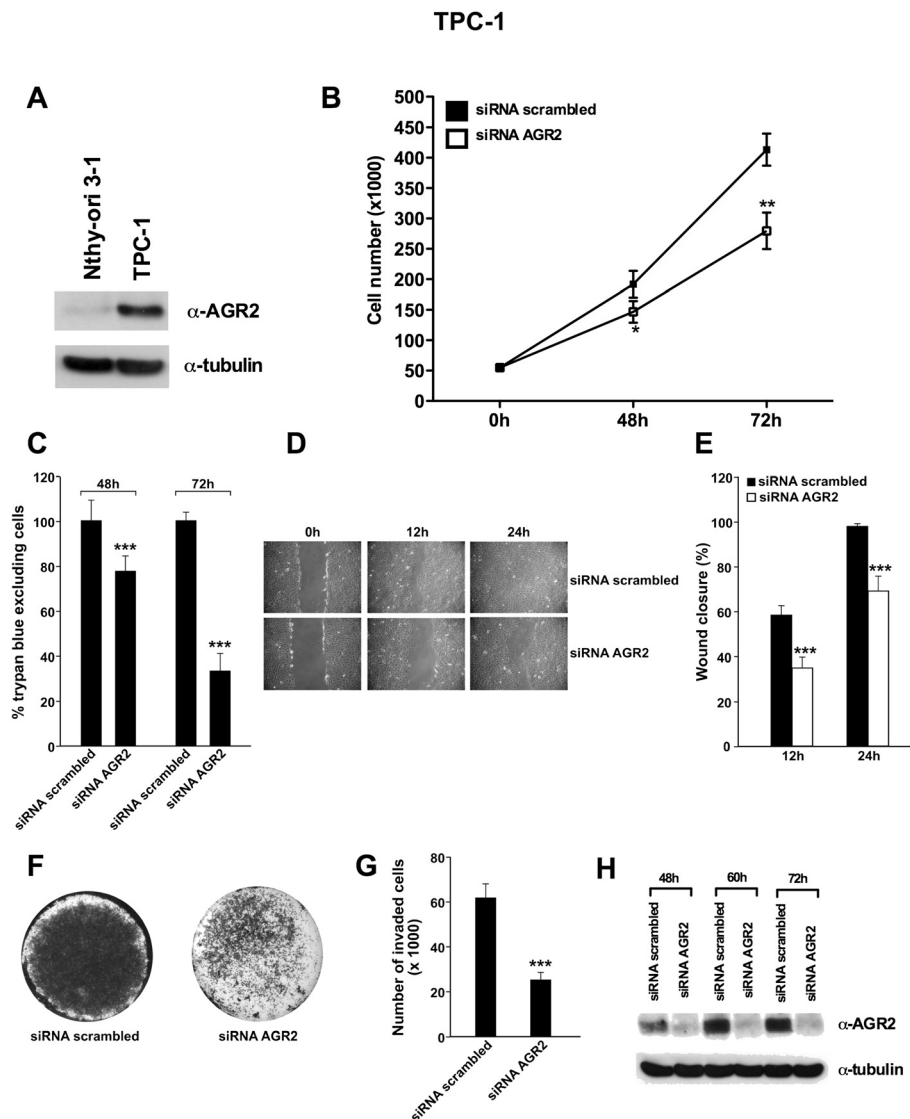
Figure 2 Effects of AGR2 knockdown on TPC-1 cell growth, migration and invasion. A) Expression levels of AGR2 in Nthy-ori 3–1 and TPC-1 cells. Cells were lysed and analyzed by Western blotting with the indicated antibodies. **B)** TPC-1 cells were transfected with AGR2 siRNA or with scrambled siRNA and counted at different time points. Values represent the average of triplicate experiments ± standard deviations. **C)** TPC-1 cells were transfected with AGR2 siRNA or with scrambled siRNA; after 48 and 72 hours cells were collected by trypsinization, stained for 10 minutes with trypan-blue and counted in triplicate. The percentage of trypan blue excluding cells compared to cells transfected with scrambled siRNA is reported ± standard deviations. **D)** TPC-1 cells were transfected with AGR2 siRNA or with scrambled siRNA; after 48 hours a wound was introduced and cell migration into the wound was monitored at 12 and 24 hours. **E)** Wound closure was measured by calculating pixel densities in the wound area and expressed as percentage of wound closure of triplicate areas ± standard deviations. **F)** TPC-1 (1×10^5) cells were transfected with AGR2 siRNA or with scrambled siRNA; 48 hours after transfection, cells were seeded in the upper chamber of transwells and incubated for 24 hours; the upper surface of the filter was wiped clean and cells on the lower surface were stained, photographed and counted. This figure is representative of three independent experiments. **G)** Invasive ability is expressed as number of invaded cells. Values represent the average of triplicate experiments ± standard deviations. **H)** TPC-1 cells were transfected with AGR2 siRNA or with scrambled siRNA. Cells were harvested at different time points and protein lysates were subjected to immunoblotting with the indicated antibodies. Asterisks indicate $P < 0.05$ (*), $P < 0.01$ (**) and $P < 0.001$ (***).

Proteins that fail to fold properly are retained in the ER and their accumulation may constitute a form of stress to the cell. Several signaling pathways, collectively known as unfolded protein response (UPR), have evolved to detect the accumulation of misfolded proteins in the ER and activate a cellular response to maintain homeostasis [25,26]. As a member of the protein disulfide isomerase family, AGR2 aids protein folding and assembly by catalyzing the formation, reduction, and isomerization of disulfide bonds, thereby stabilizing intermediate conformations during protein maturation in the ER.
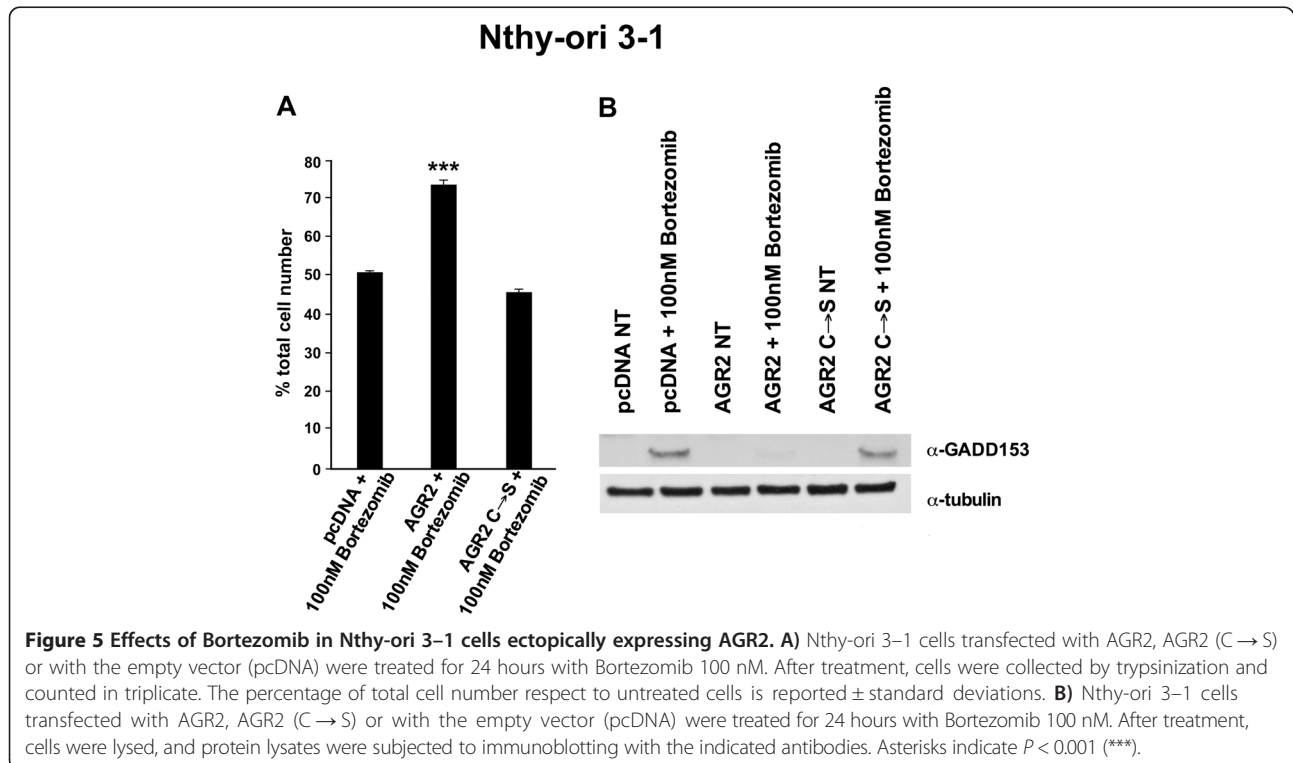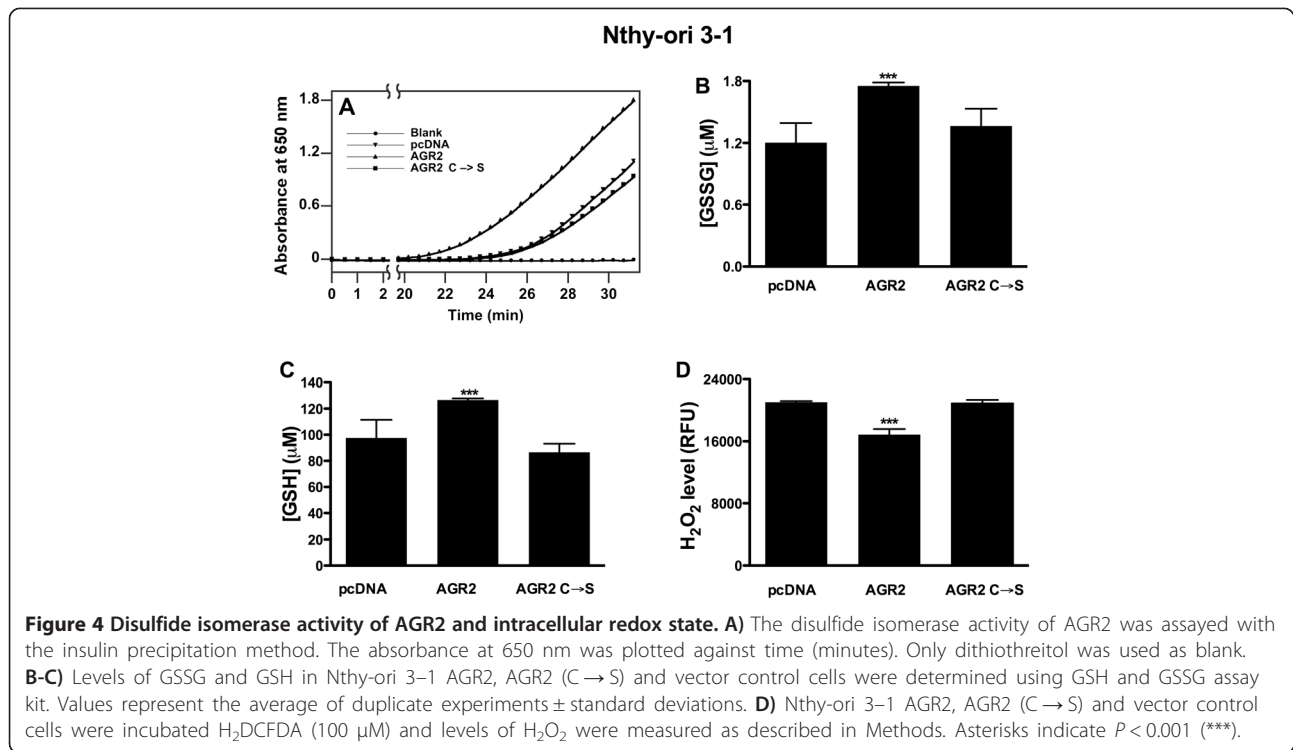
Figure 3 Effects of AGR2 ectopic expression on Nthy-ori 3–1 cell growth, migration and invasion. A) Expression levels of AGR2, AGR2 (C → S) and AGR2 (E → A) in transfected Nthy-ori 3–1 cells: after G418 selection, cells were lysed and analyzed by Western blotting with the indicated antibodies. **B)** Nthy-ori 3–1 cells transfected with AGR2, AGR2 (C → S), AGR2 (E → A) or empty vector (pcDNA) were plated and counted at different time points. Values represent the average of triplicate experiments ± standard deviations. **C)** A wound was introduced on confluent monolayer of Nthy-ori 3–1 cells transfected with AGR2, AGR2 (C → S), AGR2 (E → A) and vector control (pcDNA) and wound closure was monitored at 12 hours time points. **D)** Wound closure was measured by calculating pixel densities in the wound area and expressed as percentage of wound closure of triplicate areas ± standard deviations. **E)** Nthy-ori 3–1 cells transfected with AGR2, AGR2 (C → S) or the empty vector (pcDNA) were seeded in the upper chamber of transwells and incubated for 24 hours; the upper surface of the filter was wiped clean and cells on the lower surface were stained and counted. **F)** Invasive ability was expressed as number of invaded cells. Values represent the average of triplicate experiments ± standard deviations. Asterisks indicate $P < 0.001$ (***).

Accordingly, here we demonstrated *in vitro* that AGR2 acts as a disulfide isomerase in Nthy-ori 3–1 cells. By evaluating the aggregation of insulin as a result of reduction of disulfide bonds catalyzed by protein disulfide isomerase, we demonstrated that AGR2 over-expressing cells have an increased disulfide isomerase activity compared to control cells, an increased levels of GSSG and GSH and a decreased level of H_2O_2.

Further, we showed that wild type AGR2 is dimeric in transfected Nthy-ori 3–1 cells treated with DSS. Interestingly, it was recently demonstrated that dimerization of AGR2 attenuates ER stress-induced cell death through the association with BiP/GRP78 [29-31].

Increased expression of the UPR components, including GADD153 has been detected in breast, lung, gastric, and esophageal carcinomas [38-40]. In this context, our hypothesis is that AGR2 is up-regulated by PTC cells to cope with the ER stress. Thus, as shown for other ER resident proteins [25,26], increased AGR2 expression in PTC could enhance ER folding capacity and allow cancer cells to cope with increased protein production and secretion [41,42].

Figure 4 Disulfide isomerase activity of AGR2 and intracellular redox state. A) The disulfide isomerase activity of AGR2 was assayed with the insulin precipitation method. The absorbance at 650 nm was plotted against time (minutes). Only dithiothreitol was used as blank. **B-C)** Levels of GSSG and GSH in Nthy-ori 3–1 AGR2, AGR2 (C → S) and vector control cells were determined using GSH and GSSG assay kit. Values represent the average of duplicate experiments ± standard deviations. **D)** Nthy-ori 3–1 AGR2, AGR2 (C → S) and vector control cells were incubated H_2DCFDA (100 μM) and levels of H_2O_2 were measured as described in Methods. Asterisks indicate $P < 0.001$ (***).

Figure 5 Effects of Bortezomib in Nthy-ori 3–1 cells ectopically expressing AGR2. A) Nthy-ori 3–1 cells transfected with AGR2, AGR2 (C → S) or with the empty vector (pcDNA) were treated for 24 hours with Bortezomib 100 nM. After treatment, cells were collected by trypsinization and counted in triplicate. The percentage of total cell number respect to untreated cells is reported ± standard deviations. **B)** Nthy-ori 3–1 cells transfected with AGR2, AGR2 (C → S) or with the empty vector (pcDNA) were treated for 24 hours with Bortezomib 100 nM. After treatment, cells were lysed, and protein lysates were subjected to immunoblotting with the indicated antibodies. Asterisks indicate $P < 0.001$ (***).

Conclusions

Here, we demonstrated that AGR2 plays a key role in thyroid cancer cell survival, migration, invasion and protection from ER stress. AGR2 may be one of the pro-survival factors used by cancer cells to overcome stress due to excess protein production and to assist protein folding, degradation or both. These findings suggest that AGR2 could be exploited as a molecular marker of PTC.

Methods

Tissue samples

Tumor (n = 39) and normal (n = 25) thyroid tissue samples for immunohistochemical analysis were retrieved from the Pathology Department of the Istituto Pascale, Naples, Italy. In addition, RNA from frozen tissues of 10 PTC cases and 10 normal matched thyroid controls was obtained from the Chernobyl Tissue Bank (http://www.chernobyltissuebank.com) [43]. A set of 43 PTC and 15 normal thyroid tissues, also obtained from Chernobyl Tissue Bank, was used in the DNA array study (HG-U133 Plus 2.0, Handkiewicz Junak et al., manuscript submitted for publication) carried out in MSC Memorial Cancer Center and Institute of Oncology, Gliwice, Poland. In all cases, the respective Institutional review boards approved the study. The samples were classified according to the diagnostic criteria required for the identification of PTC [44].

Immunohistochemical staining

Sections of paraffin-embedded samples were stained with hematoxylin and eosin for histological examination [44]. For immunohistochemistry, 2 μm paraffin sections were deparaffinized and placed in a solution of 0.3% hydrogen peroxide in absolute methanol for 30 minutes and then washed in phosphate buffered saline (PBS) before immunoperoxidase staining. The slides were then incubated overnight at 4°C in a humidified chamber with mouse monoclonal antibody against AGR2 (PO1, Abnova, Taipei City, Taiwan) diluted 1:100 in PBS. The slides were subsequently incubated with biotinylated goat anti-mouse IgG for 20 minutes (Vectostain ABC kits, Vector Laboratories) and then with premixed reagent ABC (Vector) for 20 minutes. The immunostaining was performed by incubating the slides in diaminobenzidine (DAB, DAKO) solution containing 0.06 mM DAB and 2 mM hydrogen peroxide in 0.05% PBS, pH 7.6, for 5 minutes, and after chromogen development, the slides were washed, dehydrated with alcohol and xylene and mounted with coverslips using a permanent mounting medium (Permount). Micrographs were taken on Kodak Ektachrome film with a Zeiss system. Negative controls were performed in each case by incubating tissue slides with secondary antibody only. The expression of AGR2 was categorized as positive (staining of ≥10% of the tumor cells) or negative (staining of < 10% of the tumor cells). The staining intensity was further graded in: score 1 (10-50% of positive cells), score 2 (51-75% of positive cells) and score 3 (76-100% of positive cells). Score values were independently assigned by two blinded investigators (G.C. and M.M.) and a consensus was reached on all scores used for computation.

Cell cultures

Human papillary thyroid cancer cell line TPC-1 was obtained from M. Nagao (Carcinogenesis Division, National Cancer Center Research Institute, Tokyo, Japan) and identified based on the presence of the RET/PTC1 rearrangement. TPC-1 cell line was grown Dulbecco's modified Eagle's medium (DMEM) (Invitrogen) supplemented with 10% fetal bovine serum (FBS), L-glutamine and penicillin/streptomycin (Invitrogen). Nthy-ori 3–1 cells are non-transformed human thyrocytes immortalized by the Large T of SV40 and were obtained from the European Tissue Culture collection (Sigma Aldrich, St. Louis, MO, USA). Nthy-ori 3–1 cell line was grown in Roswell Park Memorial Institute (RPMI) 1640 medium supplemented with 10% fetal bovine serum (FBS), L-glutamine and penicillin/streptomycin (Invitrogen, Carlsbad, California, USA).

Reagents

Bortezomib was obtained from Millenium (Cambridge, MA, USA). Human insulin, disuccinimidyl suberate (DSS) and dithiothreitol (DTT) were from Sigma Aldrich (St. Louis, MO, USA). Glutathione reduced and oxidized assay kit was obtained from Bioassay Systems (Hayward, CA, USA).

Cell viability

For cell viability determination, cells were collected by trypsinization stained for 10 minutes with 0.4% trypan-blue (Sigma Aldrich) according to manufacturer's instructions, and counted in triplicate.

Chemoinvasion

Cell invasion was examined using a reconstituted extracellular matrix (Matrigel, BD Biosciences, San Jose, CA). The cell suspension (1×10^5 cells per well) was added to the upper chamber of transwell cell culture chambers on a prehydrated polycarbonate membrane filter of 8 μm pore size (Costar, Cambridge, MA) coated with 35 μg of Matrigel (BD Biosciences). The lower chamber was filled with 10% medium. After incubation at 37°C, non-migrating cells on the upper side of the filter were wiped-off. Invading cells were mounted on glass slides using mounting medium and stained with Hoechst (Sigma Aldrich). Cell migration was quantified by counting the number of stained nuclei in three individual fields in each transwell membrane, by fluorescence microscopy, in duplicate.

Wound closure assay

A wound was introduced on the confluent monolayer cells using a micropipette tip. Photographs were taken at 40 X magnification using phase-contrast microscopy immediately after wound incision and at selected time-points. Wound closure was measured by calculating pixel densities in the wound area by Cell[a] software (Olympus Biosystem Gmb, Hamburg, Germany) and expressed as percentage of wound closure of triplicate areas ± SD.

RNA silencing

A pool of 4 small inhibitor duplex RNAs (ON-*TARGETplus* siRNA SMARTpool) targeting human AGR2 (#L-0036 26-00), and a non-targeting pool (ON-*TARGETplus* Non-Targeting Pool) control (#D 001810-10-20) were purchased from Dharmacon RNAi Technologies (Dharmacon Inc., Chicago, IL, USA). Cells were grown under standard conditions. TPC-1 cells were plated in 60-mm dishes in complete medium without antibiotics and electroporated using MicroPorator (MP-100, Digital Bio, Euroclone, Milan, Italy) according to the manufacturer's instructions. Cells were harvested at different time points after transfection, counted and analyzed for protein expression.

Protein studies

Immunoblotting was carried out according to standard procedures. Anti-AGR2 (PO1) monoclonal antibody was from Abnova (Taipei City, Taiwan); anti-GADD153 (B-3, sc-7351) and anti-α-tubulin monoclonal antibody was from Sigma-Aldrich. Secondary anti-mouse and anti-rabbit antibodies coupled to horseradish peroxidase were from Santa Cruz Biotechnology.

Generation of stable AGR2 transfectants

cDNA containing the complete coding sequence of human AGR2 was produced by reverse transcription of RNA from HT29 colon adenocarcinoma cells (American Type Culture Collection, Rockville, MD, USA) using the following primers:

AGR2 Cl For: 5′-ATCCTCGAGCGATCATGGAGA AAATTCCA-3′;

AGR2 Cl Rev: 5′-ATCGGATCCCAATTCAGTCTTC AGCAA-3′ (annealing temperature: 60℃).

AGR2 cDNA was cloned into pcDNA3.1 (named pcDNA) (Invitrogen) by using BamHI and XhoI restriction enzymes and verified by sequencing.

Point mutations in AGR2 that changed the cysteine at position 81 to serine (C → S) and glutamic acid at position 60 to alanine (E → A) were introduced in the pcDNA-AGR2 plasmid by the Stratagene QuikChange site-directed mutagenesis kit (Agilent Technologies, Inc. Life Sciences and Chemical Analysis Group, Santa Clara, CA, USA).

The following oligonucleotides were used:

AGR2 C81S For: 5′- CATCACTTGGATGAGTCCCC ACACAGTCAAGC-3′;

AGR2 C81S Rev: 5′-GCTTGACTGTGTGGGGACT CATCCAAGTGATG-3′ (annealing temperature: 55℃).

AGR2 E60A For: 5′- CTGGACTCAGACATATGAA GCAGCTCTATATAAATCCAAGAC-3′;

AGR2 E60A Rev: 5′-GTCTTGGATTTATATAGAGCT GCTTCTTCATATGTGTCCAG-3′ (annealing temperature: 55℃).

The Nthy-ori 3–1 and the TPC-1 cells were transfected with pcDNA-AGR2, AGR2 (C → S), AGR2 (E → A) or the empty vector (pcDNA) using the Lipofectamine Reagent (Invitrogen) according to the instructions of the manufacturer. Two days later, G418 (Invitrogen) was added at concentration of 0.3 mg/ml (Nthy-ori 3–1) or of 1.2 mg/ml (TPC-1). Several clones and mass populations of transfectants were isolated, expanded and screened for AGR2 expression by Western blotting.

Chemical crosslinking

Nthy-ori 3–1 AGR2 transfected cells were treated with 1 mM disuccinimidyl suberate (DSS). Cells were harvested and washed 3 times with ice-cold PBS. The cross-linked cells were incubated for 60 minutes with mild shaking at room temperature, and then quenched by quenching buffer (1 M Tris, pH 7.5) to a final concentration of 10 mM for 15 min at room temperature to stop the chemical reaction. The chemically cross-linked cells were subjected to Western blotting analysis.

Evaluation of GSSG, GSH and H_2O_2 levels

To measure the oxidized glutathione (GSSG) and reduced glutathione (GSH), the EnzyChrom™ GSH and GSSG Assay Kit (EGTT-100) (Bioassay Systems, Hayward, CA, USA) was used according to manufacturer's instructions. Intracellular hydrogen peroxide levels were determined using the cell-permeable probe 2′,7′-dichlorodihydrofluorescein diacetate (H_2DCFDA) that upon cleavage of the acetate groups by intracellular esterases and oxidation is converted to 2′,7′-dichlorofluorescein (DCF) (Invitrogen, Carlsbad, CA). DCF is a highly fluorescent compound that can be detected by fluorescence spectroscopy using excitation and emission wavelength of 485 nm and 538 nm, respectively. Cells were incubated with H_2DCFDA (100 μM) in complete media for 1 hour at 37℃. After that, cells were washed twice in PBS and fluorescence intensity was quantified by microplate reader (Perkin-Elmer Envision 2103 multilabel reader).

Insulin reduction assay

The disulfide isomerase activity was measured by the reduction of disulfide bonds in human insulin in the presence of DTT, giving rise to the aggregation of its β chain, a process that can be followed by turbidimetry [32]. The

assay mixture was prepared in a cuvette by addition of 60 µl of insulin (10 mg/ml) to cell lysates in a buffer containing 100 mM sodium EDTA pH7 and 100 mM sodium phosphate pH 7 to give a final volume of 500 µl. The reaction started with the addition of 2 mM DTT and was followed kinetically by the increase of absorbance at 650 nm, due to insulin β chain precipitation. The absorbance at 650 nm was plotted.

RNA extraction and expression studies
Total RNA was isolated with the RNeasy Kit (Qiagen, Crawley, West Sussex, UK). The quality of the RNAs was verified by the 2100 Bioanalyzer (Agilent Technologies, Waldbronn, Germany); only samples with RNA integrity number (RIN) value > 7 were used for further analysis. One µg of RNA from each sample was reverse-transcribed with the QuantiTect® Reverse Transcription (Qiagen).

Quantitative RT-PCR
Quantitative RT-PCR was applied to study AGR2 expression in PTC samples (n = 10) and normal thyroid control (n = 10). RNA from each sample was reverse-transcribed with the QuantiTect® Reverse Transcription (Qiagen). For quantitative RT-PCR, we used the Human ProbeLibray™ system (Roche). AGR2 and RNA polymerase 2 primers sequences were:

AGR2 For: 5′-CTG GCC AGA GAT ACC ACA GTC-3′;
AGR2 Rev: 5′-AGT TGG TCA CCC CAA CCT C-3′;
RNA pol-For: 5′-GCGATGAGAACAAGATGCAA-3′;
RNA pol-Rev: 5′-CGCAGGAAGACATCATCATC-3′.

PCR reactions were performed in triplicate and fold changes were calculated with the formula: $2^{-(\text{sample 1 } \Delta Ct - \text{sample 2 } \Delta Ct)}$, where ΔCt is the difference between the amplification fluorescent thresholds of the mRNA of interest and the mRNA of RNA polymerase 2 used as an internal reference. Sample 1 represented each single PTC sample, and sample 2 was the average of all (n = 10) normal thyroid samples.

Statistical analysis
Data are presented as mean ± standard deviations. Two-tailed unpaired Student's t test was used for all statistical analysis. Mann–Whitney U test was used only for DNA array data analysis. $P < 0.05$ was considered statistically significant. Statistical analyses were carried out using the Graph Pad InStat (version 3.1a, La Jolla, CA, USA).

Additional file

Additional file 1: Figure S1. The chemical crosslinker DSS was added to Nthy-ori 3-1 AGR2 cell suspension at final concentration of 1 mM. Monomeric and dimeric AGR2 were detected by Western blotting with AGR2 antibody. Tubulin levels were used for normalization. **Figure S2.** Effects of AGR2 ectopic expression on TPC-1 cell growth, migration and

invasion. A) Expression levels of transfected AGR2, AGR2 (C→S) and AGR2 (E→A) in TPC-1 cells: after G418 selection, cells were lysed and blotted with the indicated antibodies. Levels of exogenous AGR2 are shown.
B) TPC-1 cells transfected with AGR2, AGR2 (C→S), AGR2 (E→A) or empty vector (pcDNA) were plated and counted at different time points. Values represent the average of triplicate experiments ± standard deviations.
C) A wound was introduced on confluent monolayer of TPC-1 cells transfected with AGR2, AGR2 (C→S), AGR2 (E→A) or vector control (pcDNA) and wound closure was monitored at 24 hours time point.
D) TPC-1 cells transfected with AGR2, AGR2 (C→S) or the empty vector (pcDNA) were seeded in the upper chamber of transwells and incubated for 24 hours; the upper surface of the filter was wiped clean and cells on the lower surface were stained.

Abbreviations
AGR2: Anterior gradient protein 2; DCF: 2′,7′-dichlorofluorescein; DSS: Disuccinimidyl suberate; DTNB: 5,5′-dithiobis (2-nitrobenzoic) acid; DTT: Dithiothreitol; ER: Endoplasmic reticulum; GSH: Reduced glutathione; GSSG: Oxidized glutathione; H_2DCFDA: 2′,7′-dichlorodihyfluorescein diacetate; NT: Normal thyroid; PDI: Protein disulfide isomerase; PTC: Papillary thyroid carcinoma; UPR: Unfolded protein response.

Author details
[1]Dipartimento di Medicina Molecolare e Biotecnologie Mediche, Università di Napoli "Federico II", Napoli, Italy. [2]Department of Surgery and Cancer, Hammersmith Hospital, Imperial College London, London, UK. [3]UOC Genomica Funzionale, Dipartimento Ricerca, Istituto Nazionale Tumori Fondazione G. Pascale- IRCCS, Napoli, Italia. [4]MSC Memorial Cancer Center and Institute of Oncology, Gliwice, Poland. [5]Dipartimento di Scienze Motorie e del Benessere, Universita' "Parthenope", Via Medina 40, Naples 80133, Italy.

References
1. Siegel R, Naishadham D, Jemal A: **Cancer statistics 2013.** *CA Cancer J Clin* 2013, **63:**11–30.
2. Kondo T, Ezzat S, Asa SL: **Pathogenetic mechanisms in thyroid follicular-cell neoplasia.** *Nat Rev Cancer* 2006, **6:**292–306.
3. Nikiforov YE, Nikiforova MN: **Molecular genetics and diagnosis of thyroid cancer.** *Nat Rev Endocrinol* 2011, **7:**569–580.
4. Xing M, Haugen BR, Schlumberger M: **Progress in molecular-based management of differentiated thyroid cancer.** *Lancet* 2013, **381:**1058–1069.
5. Xing M: **Molecular pathogenesis and mechanisms of thyroid cancer.** *Nat Rev Cancer* 2013, **13:**184–199.
6. Salvatore G, Nappi TC, Salerno P, Jiang Y, Garbi C, Ugolini C, Miccoli P, Basolo F, Castellone MD, Cirafici AM, Melillo RM, Fusco A, Bittner ML, Santoro M: **A cell proliferation and chromosomal instability signature in anaplastic thyroid carcinoma.** *Cancer Res* 2007, **67:**10148–10158.

7.   Aberger F, Weidinger G, Grunz H, Richter K: **Anterior specification of embryonic ectoderm: the role of the Xenopus cement gland-specific gene XAG-2.** *Mech Dev* 1998, **72:**115–130.

8.   KomiyaT TY, Hirohashi S: **Cloning of the gene gob-4, which is expressed in intestinal goblet cells in mice.** *Biochim Biophys Acta* 1999, **1444:**434–438.

9.   Brychtova V, Vojtesek B, Hrstka R: **Anterior gradient 2: a novel player in tumor cell biology.** *Cancer Lett* 2011, **304:**1–7.

10. Chevet E, Fessart D, Delom F, Mulot A, Vojtesek B, Hrstka R, Murray E, Gray T, Hupp T: **Emerging roles for the pro-oncogenic anterior gradient-2 in cancer development.** *Oncogene* 2012, **6:**2499–2509.

11. Fritzsche FR, Dahl E, Pahl S, Burkhardt M, Luo J, Mayordomo E, Gansukh T, Dankof A, Knuechel R, Denkert C, Winzer KJ, Dietel M, Kristiansen G: **Prognostic relevance of AGR2 expression in breast cancer.** *Clin Cancer Res* 2006, **12:**1728–1734.

12. Ramachandran V, Arumugam T, Wang H, Logsdon CD: **Anterior gradient 2 is expressed and secreted during the development of pancreatic cancer and promotes cancer cell survival.** *Cancer Res* 2008, **68:**7811–7818.

13. Chen R, Pan S, Duan X, Nelson BH, Sahota RA, de Rham S, Kozarek RA, McIntosh M, Brentnall TA: **Elevated level of anterior gradient-2 in pancreatic juice from patients with pre-malignant pancreatic neoplasia.** *Mol Cancer* 2010, **9:**149.

14. Park K, Chung YJ, So H, Kim K, Park J, Oh M, Jo M, Choi K, Lee EJ, Choi YL, Song SY, Bae DS, Kim BG, Lee JH: **AGR2, a mucinous ovarian cancer marker, promotes cell proliferation and migration.** *Exp Mol Med* 2011, **43:**91–100.

15. Fritzsche FR, Dahl E, Dankof A, Burkhardt M, Pahl S, Petersen I, Dietel M, Kristiansen G: **Expression of AGR2 in non small cell lung cancer.** *Histol Histopathol* 2007, **22:**703–708.

16. Zhang JS, Gong A, Cheville JC, Smith DI, Young CY: **AGR2, an androgen-inducible secretory protein over-expressed in prostate cancer.** *Genes Chromosomes Cancer* 2005, **43:**249–259.

17. Giordano TJ, Kuick R, Thomas DG, Misek DE, Vinco M, Sanders D, Zhu Z, Ciampi R, Roh M, Shedden K, Gauger P, Doherty G, Thompson NW, Hanash S, Koenig RJ, Nikiforov YE: **Molecular classification of papillary thyroid carcinoma: distinct BRAF, RAS, and RET/PTC mutation-specific gene expression profiles discovered by DNA microarray analysis.** *Oncogene* 2005, **24:**6646–6656.

18. Hébrant A, Dom G, Dewaele M, Andry G, Trésallet C, Leteurtre E, Dumont JE, Maenhaut C: **mRNA expression in papillary and anaplastic thyroid carcinoma: molecular anatomy of a killing switch.** *PLoS One* 2012, **7:**e37807.

19. Delys L, Detours V, Franc B, Thomas G, Bogdanova T, Tronko M, Libert F, Dumont JE, Maenhaut C: **Gene expression and the biological phenotype of papillary thyroid carcinomas.** *Oncogene* 2007, **26:**7894–7903.

20. Jarzab B, Wiench M, Fujarewicz K, Simek K, Jarzab M, Oczko-Wojciechowska M, Wloch J, Czarniecka A, Chmielik E, Lange D, Pawlaczek A, Szpak S, Gubala E, Swierniak A: **Gene expression profile of papillary thyroid cancer: sources of variability and diagnostic implications.** *Cancer Res* 2005, **65:**1587–1597.

21. Huang Y, Prasad M, Lemon WJ, Hampel H, Wright FA, Kornacker K, LiVolsi V, Frankel W, Kloos RT, Eng C, Pellegata NS, de la Chapelle A: **Gene expression in papillary thyroid carcinoma reveals highly consistent profiles.** *Proc Natl Acad Sci U S A* 2001, **98:**15044–15049.

22. Persson S, Rosenquist M, Knoblach B, Khosravi-Far R, Sommarin M, Michalak M: **Diversity of the protein disulfide isomerase family: identification of breast tumor induced Hag2 and Hag3 as novel members of the protein family.** *Mol Phylogenet Evol* 2005, **36:**734–740.

23. Benham AM: **The protein disulfide isomerase family key players in health and disease.** *Antioxid Redox Signal* 2012, **16:**781–789.

24. Kozlov G, Määttänen P, Thomas DY, Gehring K: **A structural overview of the PDI family of proteins.** *FEBS J* 2010, **277:**3924–3936.

25. Ma Y, Hendershot LM: **The role of the unfolded protein response in tumour development: friend or foe?** *Nat Rev Cancer* 2004, **4:**966–977.

26. Moenner M, Pluquet O, Bouchecareilh M, Chevet E: **Integrated endoplasmic reticulum stress responses in cancer.** *Cancer Res* 2007, **67:**10631–10634.

27. Zhao F, Edwards R, Dizon D, Afrasiabi K, Mastroianni JR, Geyfman M, Ouellette AJ, Andersen B, Lipkin SM: **Disruption of Paneth and goblet cell homeostasis and increased endoplasmic reticulum stress inAgr2–/–mice.** *DevBiol* 2010, **338:**270–272.

28. Higa A, Mulot A, Delom F, Bouchecareilh M, Nguyên DT, Boismenu D, Wise MJ, Chevet E: **Role of pro-oncogenic protein disulfide isomerase (PDI) family member anterior gradient 2 (AGR2) in the control of endoplasmic reticulum homeostasis.** *J Biol Chem* 2011, **286:**44855–44868.

29. Ryu J, Park SG, Lee PY, Cho S, Lee do H, Kim GH, Kim JH, Park BC: **Dimerization of pro-oncogenic protein Anterior Gradient 2 is required for the interaction with BiP/GRP78.** *Biochem Biophys Res Commun* 2013, **430:**610–615.

30. Patel P, Clarke C, Barraclough DL, Jowitt TA, Rudland PS, Barraclough R, Lian LY: **Metastasis-promoting anterior gradient 2 protein has a dimeric thioredoxin fold structure and a role in cell adhesion.** *J Mol Biol* 2013, **425:**929–943.

31. Gray TA, Murray E, Nowicki MW, Remnant L, Scherl A, Muller P, Vojtesek B, Hupp TR: **Development of a fluorescent monoclonal antibody-based assay to measure the allosteric effects of synthetic peptides on self-oligomerization of AGR2 protein.** *Protein Sci* 2013, **9:**1266–1278.

32. Gupta A, Dong A, Lowe AW: **AGR2 gene function requires a unique endoplasmic reticulum localization motif.** *J Biol Chem* 2012, **287:**4773–4782.

33. Park SW, Zhen G, Verhaeghe C, Nakagami Y, Nguyenvu LT, Barczak AJ, Killeen N, Erle DJ: **The protein disulfide isomerase AGR2 is essential for production of intestinal mucus.** *Proc Natl Acad Sci U S A* 2009, **106:**6950–6955.

34. Holmgren A: **Thioredoxin catalyzes the reduction of insulin disulfides by dithiothreitol and dihydrolipoamide.** *J Biol Chem* 1979, **254:**9627–9632.

35. Mujtaba T, Dou QP: **Advances in the understanding of mechanisms and therapeutic use of bortezomib.** *Discov Med* 2011, **12:**471–480.

36. Mitsiades CS, McMillin D, Kotoula V, Poulaki V, McMullan C, Negri J, Fanourakis G, Tseleni-Balafouta S, Ain KB, Mitsiades N: **Antitumor effects of the proteasome inhibitor bortezomib in medullary and anaplastic thyroid carcinoma cells in vitro.** *J Clin Endocrinol Metab* 2006, **91:**4013–4021.

37. Schönthal AH: **Pharmacological targeting of endoplasmic reticulum stress signaling in cancer.** *Biochem Pharmacol* 2013, **85:**653–666.

38. Lee CY, Lee MG, Choi KC, Kang HM, Chang YS: **Clinical significance of GADD153 expression in stage I non-small cell lung cancer.** *Oncol Lett* 2012, **4:**408–412.

39. Wang S, Kaufman RJ: **The impact of the unfolded protein response on human disease.** *J Cell Biol* 2012, **197:**857–867.

40. Luo B, Lee AS: **The critical roles of endoplasmic reticulum chaperones and unfolded protein response in tumorigenesis and anticancer therapies.** *Oncogene* 2013, **32:**805–818.

41. Lovat PE, Corazzari M, Armstrong JL, Martin S, Pagliarini V, Hill D, Brown AM, Piacentini M, Birch- Machin MA, Redfern CP: **Increasing melanoma cell death using inhibitors of protein disulfide isomerases to abrogate survival responses to endoplasmic reticulum stress.** *Cancer Res* 2008, **68:**5363–5369.

42. Goplen D, Wang J, Enger PØ, Tysnes BB, Terzis AJ, Laerum OD, Bjerkvig R: **Protein disulfide isomerase expression is related to the invasive properties of malignant glioma.** *Cancer Res* 2006, **66:**9895–9902.

43. Thomas GA: **The Chernobyl Tissue Bank: integrating research on radiation-induced thyroid cancer.** *J Radiol Prot* 2012, **32:**77–80.

44. Hedinger C, Williams ED, Sobin LH: **The WHO histological classification of thyroid tumors: a commentary on the second edition.** *Cancer* 1989, **63:**908–911.

Anterior gradient protein 2 promotes survival, migration and invasion of papillary thyroid carcinoma cells

Gennaro Di Maro[1], Paolo Salerno[1], Kristian Unger[2], Francesca Maria Orlandella[1], Mario Monaco[3], Gennaro Chiappetta[3], Gerry Thomas[2], Malgorzata Oczko-Wojciechowska[4], Mariorosario Masullo[5], Barbara Jarzab[4], Massimo Santoro[1], Giuliana Salvatore[5]

[1] Dipartimento di Medicina Molecolare e Biotecnologie Mediche, Università di Napoli "Federico II", Italy.

[2] Department of Surgery and Cancer, Hammersmith Hospital, Imperial College London, London, UK.

[3] UOC Genomica Funzionale, Dipartimento Ricerca, Istituto Nazionale Tumori Fondazione G. Pascale- IRCCS, Napoli, Italia.

[4] MSC Memorial Cancer Center and Institute of Oncology, Gliwice, Poland.

[5] Dipartimento di Scienze Motorie e del Benessere, Universita' "Parthenope", Naples, Italy.

Corresponding author: Giuliana Salvatore, Dipartimento di Scienze Motorie e del Benessere, Universita' "Parthenope", Naples, Via Medina 40, 80133 Naples, Italy. Ph: + 39-081-7463847, Fax: +39-081-74634581. E-mail: giuliana.salvatore@uniparthenope.it.
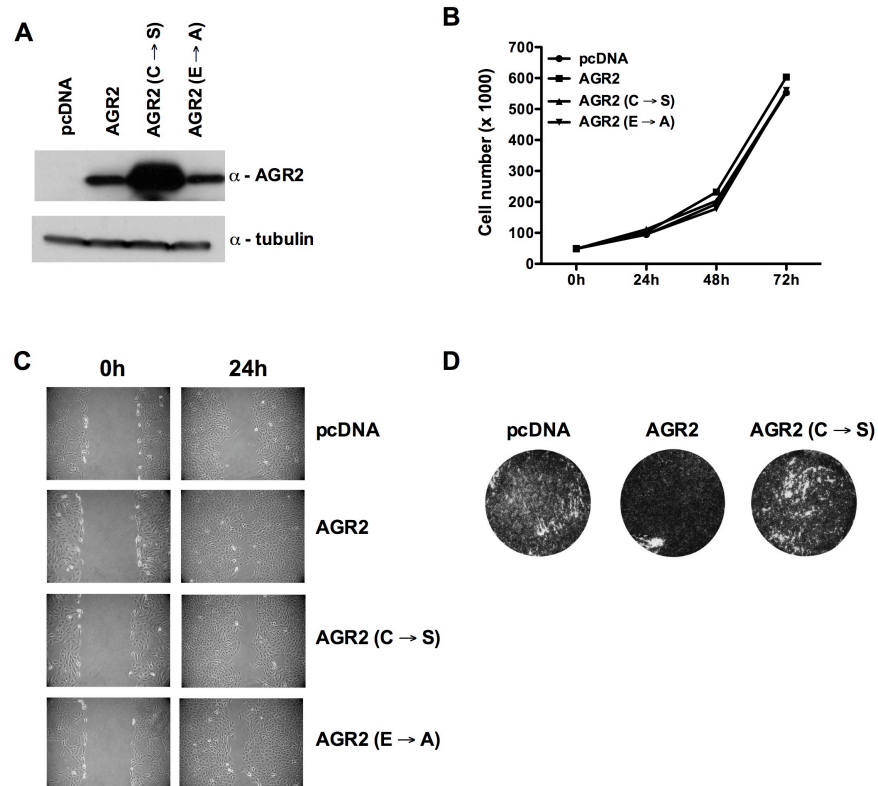
Supplementary Informations

Supplemental Figure 1
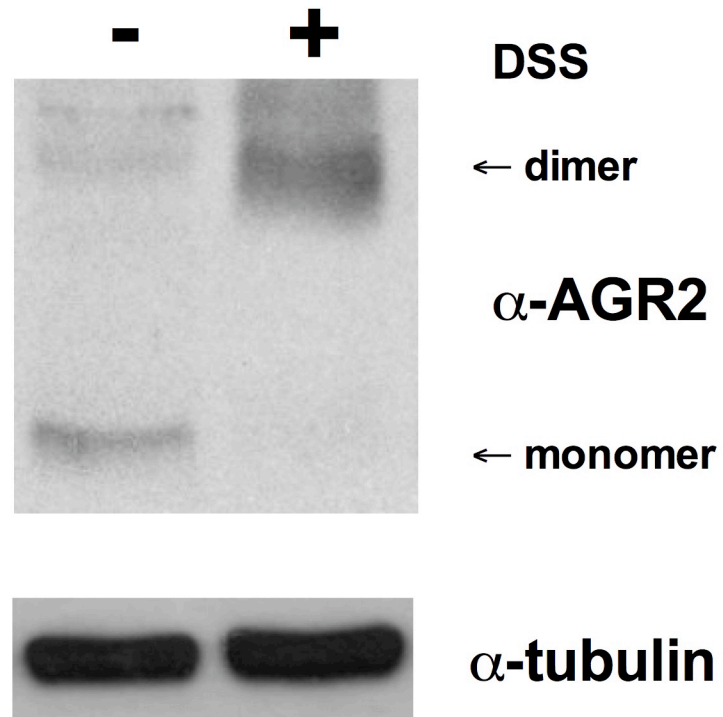
Supplemental Figure 1: The chemical crosslinker DSS was added to Nthy-ori 3-1 AGR2 cell

suspension at final concentration of 1 mM. Monomeric and dimeric AGR2 were detected by

Western blotting with AGR2 antibody. Tubulin levels were used for normalization.

Supplemental Figure 2

TPC-1

Supplemental Figure 2: **Effects of AGR2 ectopic expression on TPC-1 cell growth, migration and invasion**.

A) Expression levels of transfected AGR2, AGR2 (C→S) and AGR2 (E→A) in TPC-1 cells: after G418 selection, cells were lysed and blotted with the indicated antibodies. Levels of exogenous AGR2 are shown. **B)** TPC-1 cells transfected with AGR2, AGR2 (C→S), AGR2

(E→A) or empty vector (pcDNA) were plated and counted at different time points. Values represent the average of triplicate experiments ± standard deviations. **C)** A wound was introduced on confluent monolayer of TPC-1 cells transfected with AGR2, AGR2 (C→S), AGR2 (E→A) or vector control (pcDNA) and wound closure was monitored at 24 hours time point. **D)** TPC-1 cells transfected with AGR2, AGR2 (C→S) or the empty vector (pcDNA) were seeded in the upper chamber of transwells and incubated for 24 hours; the upper surface of the filter was wiped clean and cells on the lower surface were stained.